GEOLOGY, GEOCHEMISTRY AND PALAEOENVIRONMENT OF DEPOSITION OF BANDED IRON FORMATION OF THE KUSHTAGI SCHIST BELT KARNATAKA NUCLEUS, INDIA

Thesis Submitted in Partial Fulfilment of the Requirement
For the Award of the Degree of

Doctor of Philosophy

IN GEOLOGY

BY

RIYAZ MD. KAMARUDDIN KHAN

FACULTY OF SCIENCE
DEPARTMENT OF GEOLOGY
ALIGARH MUSLIM UNIVERSITY
ALIGARH

1993

DEDICATED TO MY FATHER

CERTIFICATE

We certify that this work is the original research work carried out by **Mr. RIYAZ MD. KAMARUDDIN KHAN** under our joint supervision at National Geophysical Research Institute, Hyderabad. It has not been submitted before either in parts or in full, to any University for the award of any degree.

Supervisor

Syed M. Zainuddin

Dr. S.M. ZAINUDDIN,
Reader,
Department of Geology,
Aligarh Muslim University,
ALIGARH

Supervisor

2.7.93

Dr. S.M. NAQVI, FNA,
Scientist,
National Geophysical
Research Institute,
HYDERABAD

2/7/93

Dr. H.K. Gupta, FNA,
Director,
National Geophysical Research Institute,
HYDERABAD

CHAPTER III

SUMMARY OF THE GEOLOGY OF THE NORTHEASTERN PART OF KARNATAKA NUCLEUS AND ADJOINING SCHIST BELTS WITH SPECIAL REFERENCE TO KUSHTAGI SCHIST BELT

ACKNOWLEDGEMENTS

I thank Dr. S.M. Naqvi, FNA, National Geophysical Research Institute, Hyderabad and Dr. S.M. Zainuddin, Department of Geology, Aligarh Muslim University, Aligarh for their supervision, inspiration and help.

I am greatly indebted to Dr. H.K. Gupta, FNA, the Director, National Geophysical Research Institute, Hyderabad for his valuable guidance and encouragement, for providing all the facilities for successful completion of this work. Dr. B.P. Radhakrishna, FNA; Dr. Hari Narain, FNA; Prof. K. Naha, FNA; Prof. K. Gopalan, FNA; Dr. M. Ramakrishnan, Prof. C. Leelanandam, Prof. S.M. Casshyap and Prof. S.N. Bhalla, have been the source of inspiration throughout the work.

I am highly obliged to Dr. P. Rama Rao for critically reviewing the manuscript and to Dr. V.N. Vasudev for helping and guiding me during the field work.

I sincerely thank Dr. R. Srinivasan, Dr. V. Divakara Rao, Dr. B.L. Narayana, Dr. T.S.M. Hussain, Dr. Y.J. Bhaskar Rao and Dr. T.V. Sivaraman for constant encouragement, help and support extended to me during the preparation of this manuscript.

I sincerely thank Dr. P.K. Govil, Dr. V. Balaram, Shri R. Natarajan, Dr. D.S.N. Murthy, Dr. S. Das Sharma, Dr. S. Nirmal Charan, Dr. T. Gnaneshwar Rao, Dr. (Mrs.) C. Manikyamba, Shri D.J. Patil, Shri S.L. Ramesh and Shri K.V. Anjaiah for helping me immensely in carrying out analytical work at various laboratories of NGRI.

The cooperation and help received from all my colleagues in NGRI, particularly Dr. B. Uday Raj, Dr. D.V. Subba Rao, Shri N.N. Murthy and Dr. Syed Moeen have been invaluable to me. My special thanks are due to Dr. Mukesh Arora for constructive and helpful criticism during the preparation of the manuscript. I am extremely grateful to all my friends, especially Messers Ajai Manglik, Prantik Mondal, K. Sain, B. Sreenivas and Miss Rita Singh for their affection, help, support and encouragement throughout this work. Without their cooperation, completion of this work in a stipulated period was difficult.

I acknowledge the help rendered by authorities of Hiremagi-Ramthal and Aihole-Sulebhavi Iron Ore Mines for allowing to collect fresh samples from their open cast mine. I acknowledge the help rendered by staff of Maps and Drawing section, Photographic section, Rock Cutting section, Mrs. Nancy Rajan for flawless typing of the manuscript.

This work has been carried out under the DST grant on evolution of life (Grant No. SP/12/PC2/86) to Dr. S.M. Naqvi and CSIR Fellowship as JRF-CSIR and SRF (NET) (Fellowship No. 31/23/18/88-EMR-I).

CHAPTER - I

INTRODUCTION

1.1 A General Perspective

Geological history of the Early Earth can be unravelled through a systematic detailed study of the Archaean greenstone/schist belts (henceforth referred to as schist belts, following Radhakrishna and Naqvi, 1986), which have developed in all major cratons. With the accumulation of new data, it is now largely believed that the development of granite-greenstone terrains has taken place in a variety of tectonic environments (West, 1980; Condie, 1981; Goodwin, 1991) and is characterized by rock types representing platformal, MOR and active/destructive plate margin tectonic settings (Goodwin, 1977, 1991; Fyfe, 1980). Genesis and nature of continental crust has remained one of the most controversial and sought after aspects in the evolutionary history of the Earth (Rogers, 1986, 1990, 1992; Jacobsen, 1988; Dia et al., 1990; Feng and Kerrich, 1990; Naqvi, 1990; McLennan and Taylor, 1991; Kroner and Layer, 1992). One of the momentous events in the evolution of the Earth and a characteristic feature of the greenstone belts is the deposition of the "BANDED IRON FORMATIONS" (BIFs). The significance and importance of BIFs in the crustal evolution processes and the tectonic setting and development of greenstone belts has not been fully understood as yet. However, during the last few years, some BIFs of the Archaean greenstone belts have been studied in some detail (Barrett et al., 1988; Dymek and Klein, 1988; Jacobsen and

Pimental-Klose, 1988; Derry and Jacobsen, 1990; Khan et al., 1992; Gnaneshwar Rao and Naqvi, 1993; Manikyamba and Naqvi, 1993a; Manikyamba et al., 1993).

Inspite of the above studies BIF remains as one of the most important and enigmatic rocks of the Earth's geological past. They form an important component of Archaean schist belts all over the world and occupy a unique position in Archaean sedimentation history, as they have no modern analogue (Cloud, 1983; Dymek and Klein, 1988; Khan et al., 1992). The BIF deposition is restricted in time and space. Middle Archaean and early Proterozoic are two major peak periods for the deposition of BIF (Gole and Klein, 1981; James, 1983; Walker et al., 1983; Fig. 1.1 A and B). In addition to these two very prominent and widespread depositional events of BIF, other significant depositional episodes are recorded between 2600-2900 Ma as well as between 450-750 Ma. The oldest BIF is found in the Isua supracrustal rocks of Greenland which occurs interbedded with quartzite, one of the oldest rocks of supracrustal origin (Allaart, 1976; Appel, 1983; Dymek and Klein, 1988). The youngest BIF deposit is of the Altai region of western Siberia and eastern Kazakhstan, with an assigned age of about 380 Ma (Kalugin, 1973). BIF of early Palaeozoic age has also been reported from Nepal and elsewhere (O'Rourke, 1961).

Virtual confinement of BIFs in space and time has made them extremely useful for the understanding of the Precambrian exogenic processes and the atmospheric-environmental changes that occurred during the early history of the Earth. They have been extensively used to support the models of atmospheric and hydrospheric

Pimental-Klose, 1988; Derry and Jacobsen, 1990; Khan et al., 1992; Gnaneshwar Rao and Naqvi, 1993; Manikyamba and Naqvi, 1993a; Manikyamba et al., 1993).

Inspite of the above studies BIF remains as one of the most important and enigmatic rocks of the Earth's geological past. They form an important component of Archaean schist belts all over the world and occupy a unique position in Archaean sedimentation history, as they have no modern analogue (Cloud, 1983; Dymek and Klein, 1988; Khan et al., 1992). The BIF deposition is restricted in time and space. Middle Archaean and early Proterozoic are two major peak periods for the deposition of BIF (Gole and Klein, 1981; James, 1983; Walker et al., 1983; Fig. 1.1 A and B). In addition to these two very prominent and widespread depositional events of BIF, other significant depositional episodes are recorded between 2600-2900 Ma as well as between 450-750 Ma. The oldest BIF is found in the Isua supracrustal rocks of Greenland which occurs interbedded with quartzite, one of the oldest rocks of supracrustal origin (Allaart, 1976; Appel, 1983; Dymek and Klein, 1988). The youngest BIF deposit is of the Altai region of western Siberia and eastern Kazakhstan, with an assigned age of about 380 Ma (Kalugin, 1973). BIF of early Palaeozoic age has also been reported from Nepal and elsewhere (O'Rourke, 1961).

Virtual confinement of BIFs in space and time has made them extremely useful for the understanding of the Precambrian exogenic processes and the atmospheric-environmental changes that occurred during the early history of the Earth. They have been extensively used to support the models of atmospheric and hydrospheric

1.1A. Schematic diagram showing relative abundance of Precambrian BIFs against time. The sharp curve represents the BIF based on the concept that the major basin containing Proterozoic iron formations may have been approximately coeval. The broad, lower curve takes account of (a) recent isotopic age dates which indicate that the basins containing major iron-formation were not coeval, and (b) the number and extent of BIFs in the Archaean (after Gole and Klein, 1981).

1.1B. Estimated abundance of iron-formation deposited through time. Horizontal scale is non-linear, approximately logarithmic; range $0\text{-}15^{15}$ tonnes (after James, 1983).

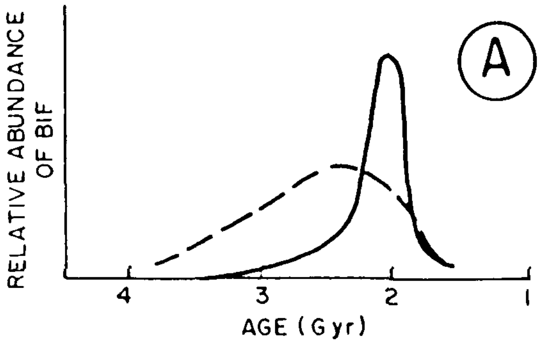
A
RELATIVE ABUNDANCE OF BIF
4
3
2
1
AGE (Gyr)

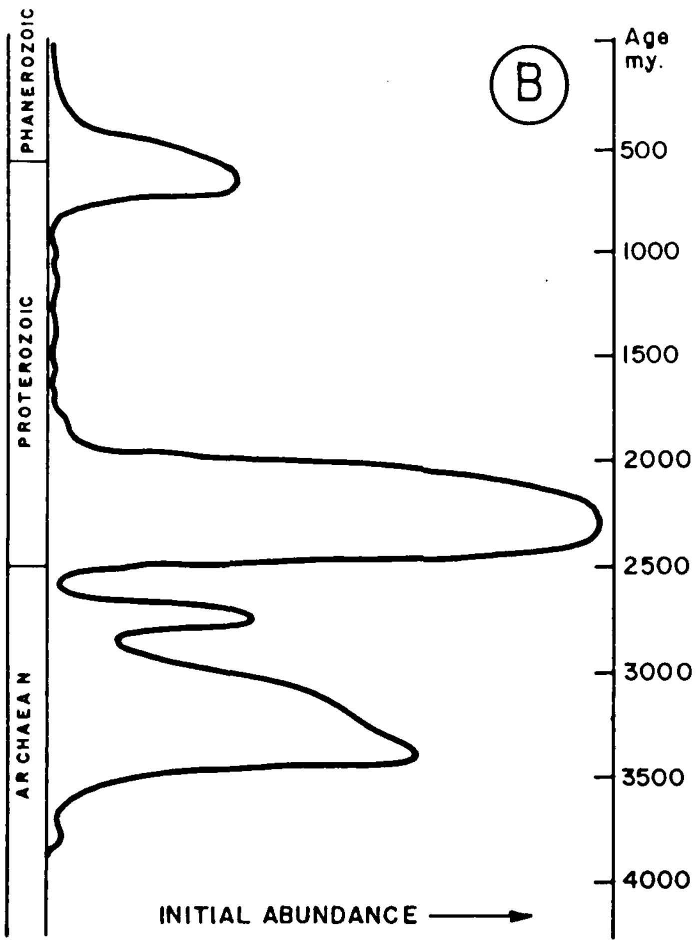
B
PHANEROZOIC
PROTEROZOIC
ARCHAEAN
Age my.
500
1000
1500
2000
2500
3000
3500
4000
INITIAL ABUNDANCE

evolution (Cloud, 1973, 1983; Nagy et al., 1983; Towe, 1983, 1990; Walker et al., 1983; Holland, 1984; Walker, 1987; Derry and Jacobsen, 1990; Kump and Holland, 1992; Alibert and McCulloch, 1993; Morris, 1993; Manikyamba et al., 1993).

1.2 Significance, Importance and Objective of the Problem

There are several major aspects related to the origin and evolution of BIF for which no satisfactory and generally agreed explanation is available, which has led to considerable debate and speculation (James, 1954, 1983; Trendall, 1968, 1983; Trendall and Blockly, 1970; Dimroth, 1977, 1986; Cloud, 1973, 1983; Goodwin, 1973; Holland, 1973, 1984; LaBerge, 1973, 1986; Gross, 1980, 1983; Beukes, 1983, 1984; Davy, 1983; Trendall and Morris, 1983; Goodwin et al., 1985; Dymek and Klein, 1988; Beukes and Klein, 1990; Beukes et al., 1990; Derry and Jacobsen, 1990; Carrigan and Cameron, 1991; Khan et al., 1992; Kump and Holland, 1992; Gnaneshwar Rao and Naqvi, 1993; Manikyamba et al., 1993; Morris, 1993). Continued research has only increased the number of hypotheses proposed for their origin. The discovery of microbiota in the cherts of Gunflint iron formation, Canada (Barghoorn and Tyler, 1965) and the availability of new tools for analysis of REE and isotopes of C,O,S and Nd in BIF have revolutionized scientific thought regarding its genesis and have provided an opportunity to test various conceptual models proposed from time to time (Jacobsen and Pimentel-Klose, 1988; Fralic et al., 1989; Kaufman et al., 1991). However, there is considerable debate regarding the sources of FeO, SiO_2 and O_2. It is still an enigma how the rhythmic banding and lamination in the BIFs are formed

(Morris, 1993) and whether it is due to the direct or indirect involvement of some bacteria (LaBerge, 1986; Nealson and Myers, 1990). It is not clear why the BIFs are mainly confined to rocks older than 1.9 Ga and why some anomalous occurrences of deposits younger than 1.9 Ga are found (Cloud, 1983). Despite the realization of their significance and consequent world-wide effort, understanding of major problems regarding the genesis of BIF remains extremely limited and the existing database is not adequate to arrive at a satisfactory explanation for its genesis. The exhalative model (Goodwin, 1956; Gross, 1986; Simonsen, 1985), the biological model (Cloud, 1973; LaBerge, 1973, 1986; Nealson and Myers, 1990), the continental weathering and leaching model (Cullen, 1963; Mel'nik, 1982), the ocean upwelling model (Holland, 1973; Morris, 1986, 1993), the evaporation model (Trendall and Blockley, 1970; Trendall, 1973; Garrels, 1987) the dust storm model (Carey, 1986) and the geochemical model (Drever, 1974) require reexamination of the field association, mineralogy, chemistry and lithology. REE and other geochemical data from the hydrothermal vents at the East Pacific Rise (EPR) and the Red Sea (RS) have provided a constraint on the source of FeO and SiO_2 (Barrett et al., 1988; Derry and Jacobsen, 1990). A few years ago neither microfossils nor stromatolites were found in Archaean BIFs. However, in recent years such structures have been recognised in BIF of Sandur (Naqvi et al., 1987), Transvaal (Klein et al., 1987) and Michipicoten (Hofmann et al., 1991) basins. Also, since large quantities of organic matter are often found to be interbedded with these rocks, it is believed that biogenic processes had played an important role in precipitating BIF. A close relationship exists between the photosynthetic generation of free O_2 by some microorganisms and BIF precipitation. However, two other abiotic sources of oxygen are also advocated. One of these is the photodissociation of water vapour by solar UV radiation (Canuto et al., 1983 and references therein), which is followed by atmospheric oxygen diffusion into primitive ocean waters. The second is that the early ocean had an intrinsic oxidizing capacity due to the radiolysis of water induced by ionizing radiation of potassium-40 (Draganic et al., 1991). But the oxygen production by these two abiotic processes is too small and is unable to explain the huge BIF deposits of Hamersley and Bababudan basins formed in a very short period.

Studies in India have mainly centred around the economic aspect of iron ores, while geochemical and genetic aspects of BIFs have seldom been attempted and the information is sporadic in nature (Majumder et al., 1984; Chakraborty and Majumder, 1986; Devaraju and Laajoki, 1986; Appel and Mahabaleswar, 1988; Basavanna and Mahabaleswar, 1988; Gnaneshwar Rao, 1992; Khan et al., 1992; Manikyamba et al., 1993). In India BIFs mainly occur in three different types of geological settings and associations; (1) BIF associated with platformal-arenite, stromatolitic-carbonate and Mn-formation formed mainly on shallow shelf (carbonate and oxide facies), (2) BIF of greywacke association formed in slightly deeper part of the basin (oxide facies), and (3) BIF of volcanic and volcaniclastic association deposited near hydrothermal vents (sulphide and carbonate facies).

The BIF of Kushtagi schist belt, one of the least metamorphosed belts in the Indian Peninsula, is different from the above mentioned settings and is of oxide facies associated with basic and acidic metavolcanics. Its northwestern part was once blanketed by Kaladgi rocks resulting in the BIFs being absolutely fresh. The study of least metamorphosed BIF along with underlying basic and acidic metavolcanics provides an excellent opportunity to analyse the chemical processes, as a basis for interpreting the palaeoenvironmental conditions of deposition and the origin of BIF in addition to a broad understanding of tectonic setting of late Archaean greenstone belts in general and evolution of Kushtagi schist belt in particular. Therefore, BIFs and associated volcanics of the Kushtagi schist belt have been studied to decipher the (1) source of FeO, SiO_2, O_2 (2) depositional environment and tectonic setting and (3) constraints of their geochemistry on the Archaean plate tectonic model.

1.3 Classification and Nomenclature of BIF

The classification and nomenclature of iron formations have been comprehensively summarized by Trendall (1983). In this connection, the classification schemes proposed by James (1954), Trendall (1968), Gross (1965), Beukes (1973) and Dimroth and Chauvel (1973) are of considerable importance. James (1954) proposed a four-fold subdivision of the BIF of the Lake Superior area on the basis of the dominant original iron mineral, viz., oxide, carbonate, sulphide and silicate. The relationship of the first three facies was shown to be gradational, deposited simultaneously in the shallow, intermediate and deep parts of the basin respectively. The different iron mineral characteristic of deposition at these different depths was related to parallel depth-related variation in Eh and pH. The silicate facies was believed to have a more complex and less precise depth related control (Trendall, 1983). He suggested the term "facies" to indicate the dominant iron bearing mineral present in a particular BIF without relating it to any stratigraphic or intergradational relationship between various BIFs. Gnaneshwar Rao (1992) has given a comprehensive account of facies variation within the BIFs of Chitradurga schist belt. There are certain basins in which the proportions of the end members of the facies are much larger leading to the concept of mixed facies (Dimroth, 1975). In another classification, known as type classification, the term Superior and Algoma types were introduced to differentiate between the kinds of associated rock in the depositional environment and geological settings for the various occurrences of BIFs (Gross, 1965). These two types, widely used in literature, do not have any time connotation. The Algoma type is characterised by banding and the absence of oolitic and granular textures, limited lateral extent and close association with volcanics and greywackes. The carbon and pyrite rich black shales are considered to be associated with it. The Superior type is closely associated with dolomite, quartzite and phyllite and is laterally very extensive. Recent studies, however, have exposed the difficulties in grouping iron formations into one or the other category. The late Archaean BIFs of Dharwar craton represent the characteristic of both Algoma and Superior types. Presence of rhythmic layers and other sedimentary structures have also helped in classifying them into Banded Iron Formation (BIF), Granular Iron Formation (GIF) and Peloidal Iron Formation (PIF) (Goode et al., 1983). With the identification of similarities between limestone and BIF, the terms like Fe-rhythmites, Fe-micrites etc. have been coined (Beukes, 1980).

1.4 Methodology

For a better understanding of the belt and to achieve the above mentioned objectives, sampling at various places in the belt and geological mapping on the available topographic map has been carried out in the central part of the belt on 1:50,000 scale. About 200 samples of BIFs and associated metavolcanics were collected. Out of these, 80 samples were analysed for 42 elements. Major elements and some trace elements (Cr, Ni, Zr) were determined by XRF while the remaining trace elements and REE were determined by ICP-MS. The oxygen isotopes of 4 pairs of hematite and chert were determined by VG Mass Spectrometer. Thin sections of the representative samples have been studied under both reflected and transmitted light and mineral composition of the constituent minerals has been determined by EPMA. The minerals present in Shaly Banded Iron Formation were determined by XRD method. The data obtained are presented in the following chapters and have been used to infer the evolution of Kushtagi schist belt and the process involved in the deposition of BIF.

1.5 Organization of the Thesis

The contents of the thesis are divided into 12 chapters and are organized as follows :

Chapter II contains a general review of the Archaean geology of the Karnataka Nucleus.

Chapter III summarises the geology of the northeastern Karnataka Nucleus and adjoining schist belts. Special emphasis has been given to the Kushtagi schist belt.

Chapter IV deals with the distribution of BIF in the Karnataka Nucleus.

Chapter V presents the summary of the available information and proposed models for the genesis of BIF and the environment in which these interesting rocks were laid down.

Chapter VI is concerned with the details of petrology and mineralogy of the constituent minerals of the BIF.

Chapter VII gives the details of petrological and mineralogical studies carried out on associated metavolcanics.

Chapter VIII provides the summary of the sampling details and the analytical techniques and procedure followed for chemical analysis.

Chapter IX presents the geochemistry of the BIF incorporating the variation in major, trace and rare earth element abundances. Different geochemical diagrams have been used to highlight the genetic aspects of BIF. It also deals with the oxygen isotopic study of the Kushtagi iron formation.

Chapter X deals with the geochemistry of metavolcanics of Kushtagi schist belt. The main aim of this chapter is to deduce the constraints for the basin evolution and determine its tectonic setting.

Chapter XI provides discussion and synthesis of the results presented in chapters 3 to 10 and reconstructs the palaeoenvironment of deposition and tectonic setting of BIF in the light of Archaean plate tectonics. A model has been proposed for the genesis of BIF of Kushtagi schist belt.

Chapter XII provides a summary of the entire work carried out and the conclusions arrived at.

The field investigation of Kushtagi schist belt suggests that this belt is a remnant of some Archaean orogenic belt. Part of the original belt is present as an enclave within a sea of gneisses and has been intruded by granites. The BIFs present in this belt directly overlie the metavolcanics. The basin appears to have started as a shallow water intracontinental basin which gradually opened up as rift ridge system. This Archaean Mid Oceanic Ridge (AMOR) provided FeO and SiO_2 content of the BIF, which, combined with O_2 produced by photosynthetic activity near shoreline and got precipitated below wave base and photic zone; the region of low organic productivity. Increased ridge length, high hydrothermal flux and its high exit temperature appear to be responsible for bringing such high quantity of FeO and SiO_2 to the Archaean oceans. The FeO and SiO_2 rich hydrothermal water from AMOR were transported to the shallow shelf region due to thermal and chemical potential differences. Simultaneously, along with the precipitation of iron and silica, terrigenous and volcaniclastic sedimentation also took place. The amount of clastic material is fairly high in SBIF, whereas it is negligible in CBIF. It suggests that the deposition of SBIF took place during regression above wave base and photic zone and during transgression CBIF got deposited below wave base and photic zone. The carbonate-BIF-chlorite schist and volcanic-BIF associations represent the opening stage (tensional) of the basin whereas low-Mg volcanic-rhyodacite association represent the closing stage (compressional). This change in tectonic regime is very well explained by application of mini plate model and shorter duration of Wilson Cycle for the evolution of granite-greenstone belts in general and that of the Kushtagi schist belt in particular.

CHAPTER - II

GENERAL GEOLOGY OF KARNATAKA NUCLEUS, DHARWAR CRATON

2.1 The Dharwar Craton

The Early Precambrian (Archaean) continental crust of South Indian Shield (SIS) is under constant investigation since the pioneering work of Newbold (1844) and Bruce Foote (1886). It is one of the well studied Precambrian cratonic blocks and probably represents a much more evolved stage of cratonization and evolution of related biosphere. Geologists with intimate knowledge about other Precambrian terrains of the world have been impressed with the complexity and variety exhibited by the Precambrian of SIS. With advancement in analytical techniques and the available knowledge of geochemical and isotopic characters through multi-disciplinary activities, we now have a better understanding of its geology. Comprehensive geological description of the area has appeared during the last few years and has been summarised by several workers (Naqvi, 1976, 1981; Swami Nath and Ramakrishnan, 1981; Divakara Rao and Rama Rao, 1982; Naqvi and Rogers, 1983, 1987; Pichamuthu and Srinivasan, 1983, 1984; Radhakrishna, 1983, 1987; Radhakrishna and Naqvi, 1986; Rogers, 1986; Chadwick et al., 1988; Radhakrishna and Ramakrishnan, 1988, 1990; Srinivasan and Naqvi, 1990; Naha et al., 1991).

The cratonized block of SIS which lies below the Narmada and Godavari lineament is known as "Dharwar Craton" (DC). On the western side it is bounded by Arabian Sea and in the east and south by the Middle Proterozoic Mobile Belt (MPMB) (Fig. 2.1). DC

2.1. Generalized geological map of Peninsular India. KN-Karnataka nucleus, SN-Singhbhum nucleus, JBN-Jeypore- Bastar nucleus, EPMB-Early Proterozoic Mobile Belt, MPMB- Middle Proterozoic Mobile Belt (after Radhakrishna and Naqvi, 1986).

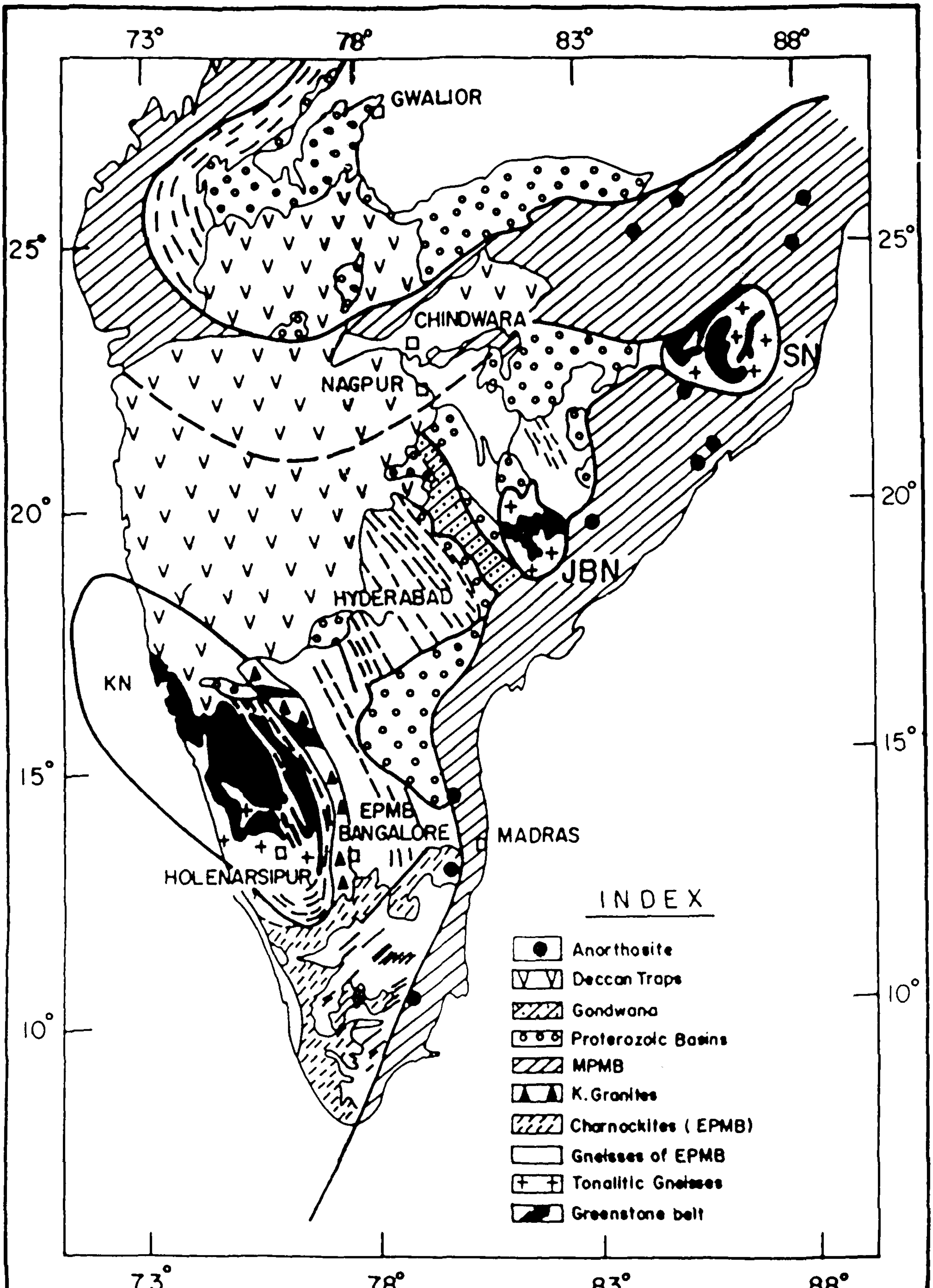

73°
78°
83°
88°
GWALIOR
CHINDWARA
NAGPUR
SN
JBN
HYDERABAD
KN
EPMB
BANGALORE
MADRAS
HOLENARSIPUR
25°
20°
15°
10°
INDEX
Anorthosite
Deccan Traps
Gondwana
Proterozoic Basins
MPMB
K. Granites
Charnockites (EPMB)
Gneisses of EPMB
Tonalitic Gneisses
Greenstone belt

forms a major portion of Dharwar-Singhbhum protocontinent (Radhakrishna and Naqvi, 1986). The Karnataka Nucleus (KN) and Singhbhum Nucleus (SN) of the Dharwar-Singhbhum protocontinent are reasonably well established as the oldest surviving parts of the Indian shield with rocks older than 2.5 Ga. A possibly similar Jeypore-Bastar Nucleus (JBN) has been identified based on the lithologies of the Bengpal, Sukma and Iron Ore Groups of the Jeypore-Bastar region (Crookshank, 1963), which are similar to those found in KN and SN, but JBN is yet to be established as no radiometric age data are available (Radhakrishna and Naqvi, 1986).

The difference in regional facies in terms of lithology, volcano-sedimentary environment, metamorphism of baric types and magmatism suggest a possible division of DC into a western and an eastern Dharwar craton separated possibly by Closepet Granite (Viswanatha and Ramakrishnan, 1975; Swami Nath et al., 1976; Rogers, 1986; Naqvi and Rogers, 1987), although the exact dividing line between these blocks is uncertain (Swami Nath and Ramakrishnan, 1981). The western Dharwar craton is synonymous with Karnataka nucleus.

The DC is essentially a granite-schist/greenstone province. It is composed of late Archaean low-grade supracrustal rocks, preserved in well defined small to large schist belts, and high-grade supracrustals of middle Archaean occurring as small schist belts and as inclusions in gneisses. Apart from schist belts, it also contains gneisses and granulites. The province passes through a transition zone to the high-grade granulite region in the southern part of the DC (Allen et al., 1983). The craton is partly covered by younger sedimentary and volcanic rocks, viz. Cuddapah,, Kaladgi and Bhima Group sediments, Deccan basalts, post Cretaceous laterites and Pliocene to Recent coastal and river alluvial deposits (Pichamuthu and Srinivasan, 1984).

2.2 A Brief Review of Archaean Geology of the Karnataka Nucleus

Karnataka nucleus is an elliptical area west of the Closepet Granite with a garland of K-rich granite plutons on at least two sides (Fig. 2.2). The eastern margin of KN is uncertain; apart from Closepet Granite forming its eastern margin, another possible margin is a major shear zone slightly west of the Closepet outcrop which has been recognized by Kaila et al. (1979), Drury and Holt (1980), Drury et al. (1984) and Naqvi and Rogers (1987). The northern extension of this nucleus is covered by Deccan Traps, whereas the western part is terminated at a passive continental margin developed at the time of the split of the Gondwana continent which resulted in the formation of Arabian Sea. Towards south, it is transitional into granulite facies assemblages.

KN is made up of four main rock units, namely, (1) Dharwar schist/greenstone/supracrustal suite, (2) Peninsular Gneiss, (3) intrusive granites and granodiorites and (4) layered igneous complexes. Besides these four main rock suites, undeformed sedimentary rocks of middle Proterozoic age, namely, Kaladgis and Bhimas are also found in KN.

2.2.1 Dharwar Schist/Greenstone/Supracrustal Suite

2.2.1.1 Definition and Historical Review

A few army officers of the British East India Company provided brief traverse notes on the geology of parts of

2.2. Geological map of Karnataka nucleus showing location and correlation of the schist belts (after Radhakrishna and Vasudev, 1977).

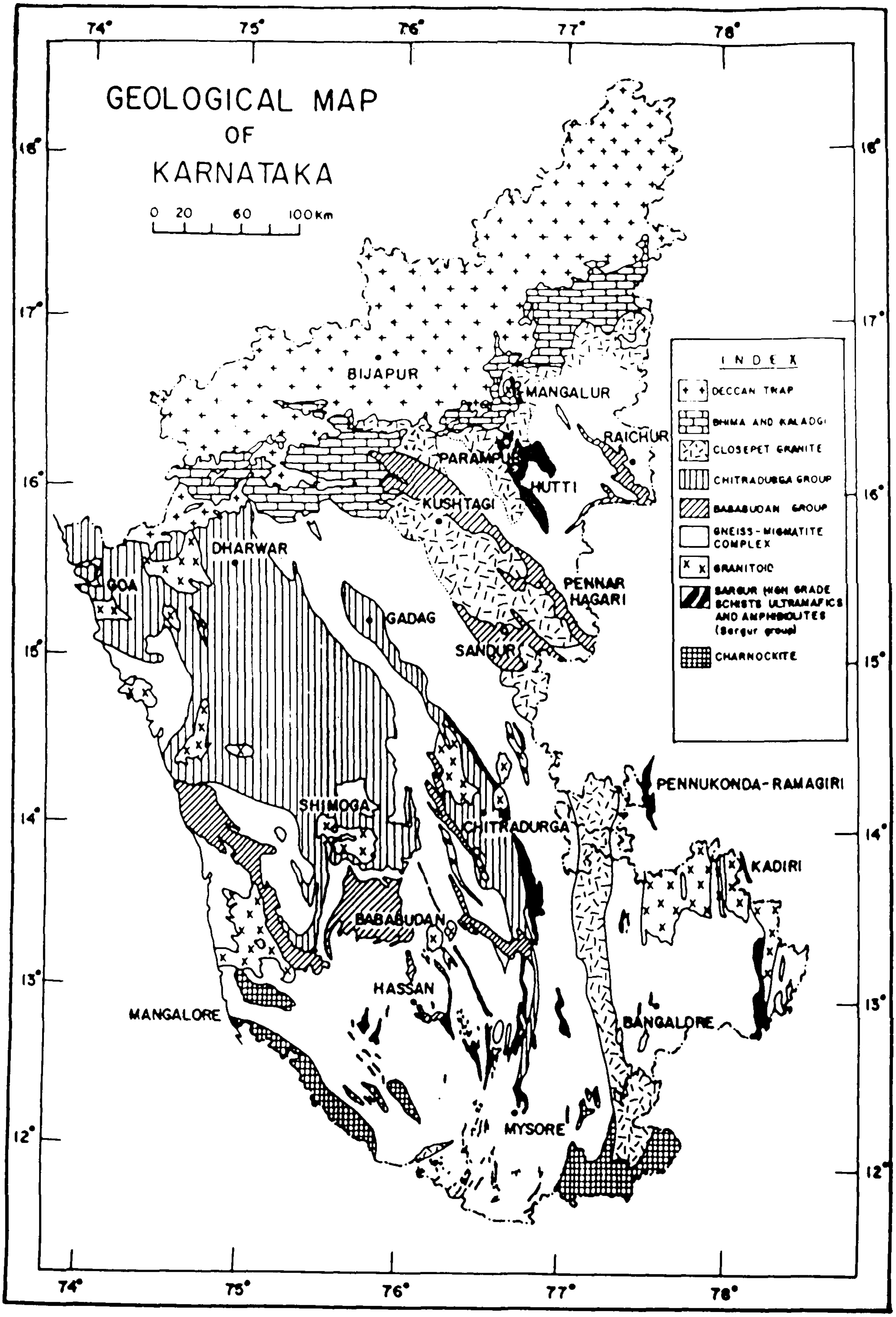

GEOLOGICAL MAP
OF
KARNATAKA
0 20 60 100Km
INDEX
DECCAN TRAP
BHIMA AND KALADGI
CLOSEPET GRANITE
CHITRADURGA GROUP
BABABUDAN GROUP
GNEISS-MIGMATITE COMPLEX
GRANITOID
SARGUR HIGH GRADE SCHISTS ULTRAMAFICS AND AMPHIBOLITES (Sargur group)
CHARNOCKITE
BIJAPUR
MANGALUR
RAICHUR
PARAMPUR
HUTTI
KUSHTAGI
DHARWAR
GOA
GADAG
PENNAR HAGARI
SANDUR
PENNUKONDA-RAMAGIRI
SHIMOGA
CHITRADURGA
KADIRI
BABABUDAN
HASSAN
MANGALORE
BANGALORE
MYSORE
74°
75°
76°
77°
78°
12°
13°
14°
15°
16°
17°
18°

Karnataka. Notable among them are Christie (1836) and Newbold (1844). Bruce Foote (1886) discovered schistose rocks near Dharwar in Karnataka state and called them "Dharwar System". The "Dharwar Schist" of the Dharwar System includes all the volcano-sedimentary schistose rocks and is mainly a lithological term. It neither indicates its origin nor its age. The gneissic complex with a host of small enclaves was termed as the "Fundamental Gneiss", in the belief that this group forms the basement on which the rocks of the Dharwar System occur unconformably (Bruce Foote, 1886). The term Fundamental Gneiss was later renamed as "Peninsular Gneiss" (Smeeth, 1916). Jayaram (1922), Rama Rao (1940), Ramakrishnan et al. (1976) and Swami Nath et al. (1976) believe that gneisses formed the basement for all the schistose rocks.

Smeeth (1916) was of the opinion that the Dharwar schists were intruded by four distinct epochs of granitic activity, namely Champion Gneiss, Peninsular Gneiss, Charnockite and Closepet Granite. He was the proponent of a strange theory that all the Dharwar schists were igneous in character and none was sedimentary and there are no rocks older than those in the Dharwar system of Karnataka. Sampat Iyengar (1905), based on extensive mapping of very large area of Bababudan, Chitradurga and some other belts was of different view. The mutual relationship between Dharwar schist and the engulfing gneisses is still beset with major controversies, (Radhakrishna and Ramakrishnan, 1990; Venkata Dasu et al., 1991).

The term Dharwar schists of Bruce Foote (1886) is synonymous with greenstone belt. However, some workers have emphasized the inadequacy of the term greenstone belt for characterizing the essentially schistose and metamorphic status of the supracrustal rocks of the Indian Archaean. The term "Supracrustals" includes all the meta-sedimentary and meta-igneous (volcanic and plutonic) rocks constituting the schist belts irrespective of their size and grade of metamorphism. Radhakrishna and Naqvi (1986) have suggested that the term "Schist Belt" should be used in place of greenstone belts for the Archaean volcano-sedimentary sequences in India, as it emphasizes the unique schistose character of these belts, whereas the terms greenstone belt, supracrustal association and supracrustals are inadequate in characterizing the essential schistose and metamorphic status of the supracrustal rocks in the Indian Archaean.

2.2.1.2 Classification and Correlation

The schist belts of KN are mainly unfossiliferous (no index fossil has been established as yet), deformed and metamorphosed to various grades. The absence of uniform distribution of primary sedimentary and volcanic structures, and scarcity of radiometric dates, have made the stratigraphic position of the Dharwar schist belts extremely controversial and debatable, thus making it difficult to establish an equally acceptable internal primary stratigraphy. Recent detailed investigations by several workers (Pichamuthu, 1967; Ramakrishnan et al., 1976; Swami Nath et al., 1976; Radhakrishna, 1983; Pichamuthu and Srinivasan, 1983, 1984; Radhakrishna and Naqvi, 1986; Srinivasan and Naqvi, 1990) have led to a variety of classifications. Thus, several stratigraphic columns have been proposed; some of these are given in Table 2.1.

Table 2.1 : Classification of supracrustal rocks in Dharwar Craton, Karnataka nucleus.

Swami Nath et al., (1976)

-------------UNCONFORMITY--------------------		
Dharwar	Chitradurga Group (2.3 - 2.5 Ga)	Greenstone belts
	---------Unconformity-----------	(Upper Archaean)
Supergroup	Bababudan Group (2.5 - 2.6 Ga)	
-------------UNCONFORMITY--------------------		
Peninsular Gneissic Complex	Migmatites, Gneisses and Granites	
Sargur Supergroup	Several unclassified groups of schist belts and enclaves	High grade schists (Lower Archaean)
------------UNCONFORMITY---------------------		
(?) Sialic	Basement (?)	(as yet undifferentiated from PGC)

Naqvi, 1981

CHITRADURGA GROUP	2.6 - 2.4 Ga Granitic activity. Chert, sericitic phyllite, metavolcanics, chlorite schist, Greywacke conglomerate (K.M. Kere) Greywacke Greywacke Conglomerate (Aimangala) Arkose-grit Greywacke Conglomerate (Talya)
BABABUDAN GROUP	Kaldurga Conglomerate Quartzite (BMQ) Argillite schist Mafic flows Mafic flows with interlayers amphibole-garnet schist Chlorite schist Orthoquartzite (fuchsitic at places) Basal Conglomerate
------------------------------UNCONFORMITY---------------------------	
JAVANAHALLI GROUP	Dykes Quartz veins Pegmatites, granites Fuchsite-quartzite Ultramafic-schist Ortho and para amphibolites interbedded with Carbonate, calcsilicates etc. Para-gneiss

(Tonalitic and Trondhjemitic activity (3.5 Ga))

	Dunite, fuchsite quartzite, high Al, Mg, sediments
HOLENARASIPUR GROUP	Hornblende schist, tremolite-actinolite schist, Serpentinite, Peridotite

? ? ? Basement ? ? ?

Swami Nath and Ramakrishnan (1981)

Kaladgi, Badami and Bhima Groups

--------UNCONFORMITY------------

DHARWAR SUPERGROUP	Chitradurga Group --Unconformity--- Bababudan Group

--------UNCONFORMITY------------

PENINSULAR GNEISS	Migmatites, gneisses, granitoids
SARGUR GROUP	Several unclassified associations of supracrustal rocks

B A S E M E N T N O T S E E N
(3.4 Ga Old Gneisses)

Pichamuthu and Srinivasan (1983)

Chitradurga Subgroup:	Greywackes, conglomerates, silicic volcanic rocks, banded iron formations
Dodguni Subgroup:	Quartz conglomerates and sandstones, metapelites, carbonates, manganese and iron formations
Bababudan Subgroup:	Quartz conglomerates and sandstones, basalts and rhyodacites, graphitic metapelites, banded iron formations
Nuggihalli Subgroup:	Quartzites, metapelites, ultramafic/anorthositic intrusive rocks

---

Radhakrishna (1983)

Younger greenstones (Dharwar type):	Quartzose clastic sediments, carbonates, cherts, iron formations, basalts and rhyolites; includes Shimoga, Chitradurga and Sandur basins

Ancient supracrustals (>3,000 m.y.):	Mafic/ultramafic igneous rocks, rare clastic sediments; sediments consist of volcanic debris or chemical precipitates; includes Holenarasipur, Nuggihalli, Krishnarajpet, etc. belts; Javanahalli belt is of same age but contains quartzose clastic sediments
Ancient supracrustals (Sargur type):	Occurs in transition zone to granulite facies at southern margin of craton; mafic/ultramafic/anorthositic suites, aluminous metapelites, fuchsite quartzites, iron and manganese cherts, graphitic schists

Radhakrishna and Naqvi (1986)

Date (M.Y.)	Event
	Late Archaean
	Invasion of younger granites (K-rich) bordering the nucleus.
2600	Granulite transformation of older crust along the margins of the nucleus.
3000-2600	Deposition of younger schist belts (Shimoga, Chitradurga, Sandur). Conglomerates, orthoquartzites, mafic and felsic volcanic sequences, banded iron formation, greywacke.
	Early Archaean
3000	Main development of migmatitic gneisses
3400	Emplacement of oldest tonalite-trondhjemite gneisses with enclaves of ancient supracrustal sequences.
>3400	Deposition of ancient supracrustal sequences, mafic-ultramafic volcanics and chemical sediments.
	Basement predominantly mafic crust.

The entire succession of the Dharwar schist belt shows interfingering stratigraphy with polyphase gneisses resulting in many controversies regarding the structure and stratigraphy of the belts. Several conflicting models of stratigraphy are proposed: 1) the schist belts represent a group of rocks younger than the Peninsular Gneisses and there exists an older Sargur Group which is older than the gneisses (Jayaram, 1922; Rama Rao, 1940; Ramakrishnan et al., 1976; Swami Nath et al., 1976; Chadwick et al., 1981b; Venkata Dasu et al., 1991; Nutman et al., 1992); 2) the Dharwar supracrustals and the Sargurs together represent one Supergroup which is regarded as pre or syn-Peninsular Gneisses (Pichamuthu and Srinivasan, 1984; Srinivasan, 1988; Gopal Rao et al., 1989) or post-gneiss (Drury et al., 1984) and 3) the Archaean supracrustals represent belts formed at different periods covering a span of at least 800 Ma (3400-2600 Ma), some older and some younger than the gneisses, which are themselves polyphase and polymetamorphic (Naqvi, 1981; Radhakrishna, 1983; Naqvi and Rogers, 1983, 1987).

With accumulation of new information and new thinking based on global analogies, it was gradually realised that all the Dharwar schist belts cannot represent one single system and that there are geological formations older than the Dharwar rocks (Radhakrishna, 1967). Based on detailed petrological and geochemical work on Chitradurga schist belt, Naqvi and Hussain (1972) opined that the Dharwar rocks of this belt are not the oldest in the KN, as was believed the then which was later substantiated and established by Viswanatha and Ramakrishnan

(1975). These older schistose rocks were designated by Swami Nath et al. (1976) as Sargur Supergroup. Since the rock units were not classified into different groups constituting a supergroup, the status of supergroup was abandoned and the units were called as "Sargur Schist Complex" (Viswanatha and Ramakrishnan, 1975). As this trinomial nomenclature was not in conformity with the provisions of stratigraphic codes, it was finally re-named as "Sargur Group" (Swami Nath and Ramakrishnan, 1981). Despite considerable uncertainity regarding the classification of schistose rocks of KN, they can be divided into two major divisions, namely, older and younger. Swami Nath et al. (1976) and Ramakrishnan et al. (1976) have designated the younger division as "Dharwar Supergroup" and the older pre-basement division as "Sargur Group". The unconformity at the base of the younger schist belt is a well established and documented phenomenon (Venkata Dasu et al., 1991). The "Peninsular Gneiss" together with older schist belts and enclaves forms the basement to the younger rocks overlying the basal unconformity, marked by the uraniferous and pyritiferous conglomerate (oligomictic) exposed in the Bababudan, Western Ghats, Chitradurga and Sigegudda belts (Arora, 1991). The Dharwar Supergroup is further divided into a lower volcanic-rich Bababudan Group and a upper shale-greywacke-rich Chitradurga Group (Swami Nath et al., 1976).

However, in spite of all these attempts to classify the Dharwar schist belts, a continuous history of tectonic evolution between a period of 800 Ma to 1000 Ma was recognized (Naqvi, 1981; Pichamuthu and Srinivasan, 1983; Srinivasan and Naqvi, 1990), which is substantiated by the same style and sequence of multiple deformation in various rock types of KN (Chadwick et al., 1978; Mukhopadhyay, 1986; Naha et al., 1986, 1991). Naqvi (1981) has proposed a genetic and sequential five fold classification of Dharwar schist belts in which Holenarasipur and Javanahalli Group are part of the older schist belts and Bababudan, Chitradurga and Ranibennur Group are part of the younger schsit belts. These different schistose groups have been intruded by precursors of gneisses at different times (Fig. 2.3) and the entire interfingering stratigraphic sequence developed through a period of 800 Ma, a concept substantiated by available geochronological data. It is evident from this model that Dharwar schist belts are of varying ages and the precursors of Peninsular Gniess have intruded the belts of different ages at different times. Hence, any individual belt may be younger than any particular gneiss and older than other group of gneisses.

Preliminary geochronological studies in the region show that a tonalite-trondhjemite crust was formed in this terrain between 3.3 and 3.5 Ga ago (Beckinsale et al., 1980; Dhoundial et al., 1987). Most of the schist belts post-dated this event. Although Naqvi (1976) has expressed the opinion that some older schist belts such as Holenarasipur, Nuggihalli and Sargur could be older than 3.4 Ga, unequivocal 3.4 Ga or older ages for the supracrustal rocks of these schist belts are yet to be obtained. However, it must be noted that the 3.3 to 3.4 Ga tonalite-trondhjemite gneisses (grey gneiss) which are found as pebbles in the polymictic conglomerates are characterized by REE patterns with

2.3. Interfingering sequence model of greenstone belts and acid plutons (including precursors of the Peninsular gneiss), showing that the Dharwar schist belts and acid plutons have formed in five successive stages. Indirect geochemical evidence preserved in the metasediments and meta-ultramafites of Holenarasipur Group leads to the speculation of a basic ultrabasic lunar type of crust as a starting point. Stages I to V indicate the development of basins for different successive greenstone belts and stage VI denotes the deposition of Kaladgi sediments. Curved lines indicate unconformities. A to E are indicative of successive emplacement of different acid plutons (after Naqvi, 1981).

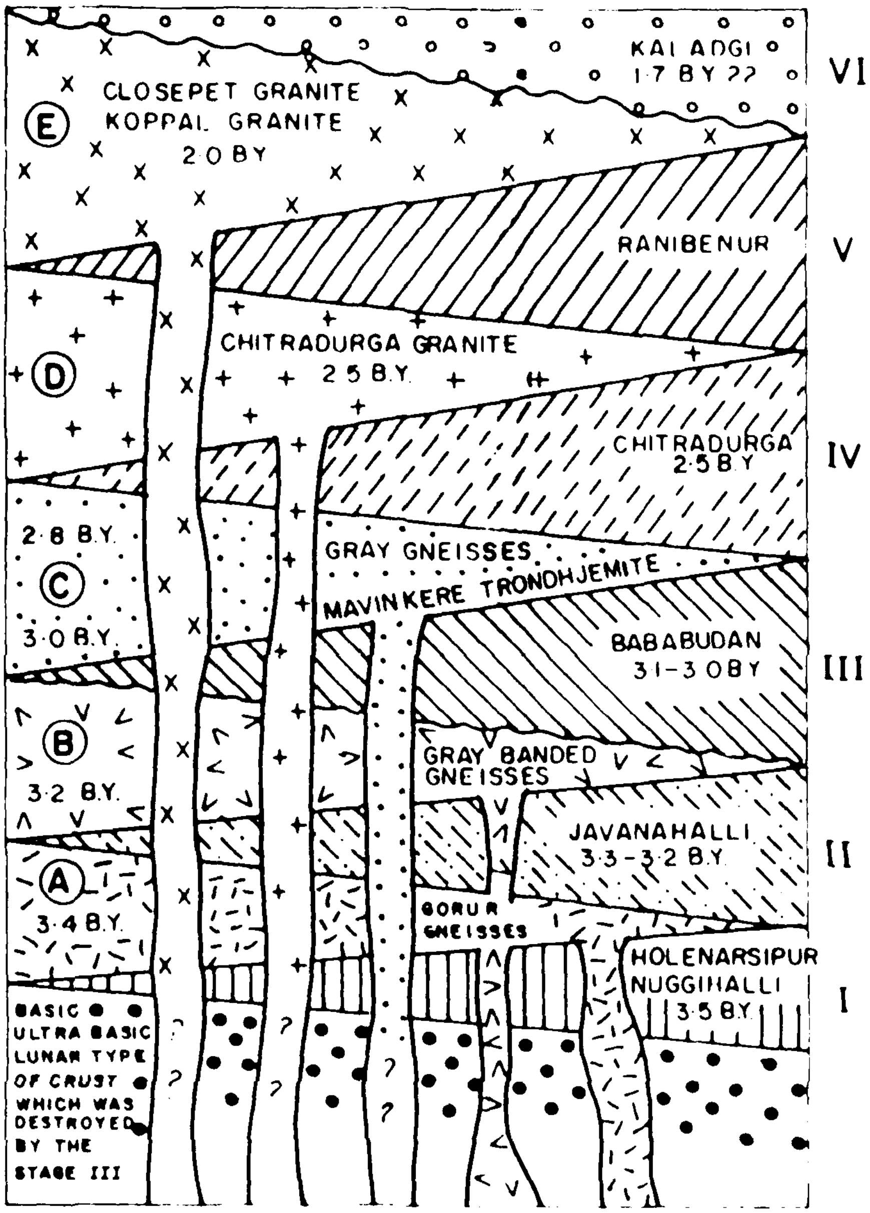

KALADGI
1·7 B.Y ??
VI
CLOSEPET GRANITE
KOPPAL GRANITE
2·0 B.Y
E
RANIBENUR
V
CHITRADURGA GRANITE
2·5 B.Y.
D
CHITRADURGA
2·5 B.Y
IV
2·8 B.Y.
C
3·0 B.Y.
GRAY GNEISSES
MAVINKERE TRONDHJEMITE
BABABUDAN
3·1–3·0 B.Y
III
B
3·2 B.Y.
GRAY BANDED
GNEISSES
JAVANAHALLI
3·3–3·2 B.Y.
II
A
3·4 B.Y.
GORUR
GNEISSES
HOLENARSIPUR
NUGGIHALLI
3·5 B.Y.
I
BASIC
ULTRA BASIC
LUNAR TYPE
OF CRUST
WHICH WAS
DESTROYED
BY THE
STAGE III

negative Eu anomaly, indicating metabasaltic amphibolite as the probable source rock, partial melting of which gave rise to tonalite- trondhjemite gneisses (Srinivasan, 1985). Recently, Nutman et al. (1992) have evaluated 3580 Ma as the upper age limit of Sargur Group.

The older schist belts, viz., Holenarasipur, Krishnarajpet, Nuggihalli, Nagamangala, Sargur and Parampur belts are mostly mafic, ultramafic flows consisting of komatiites to basalts, showing spinifex texture, and chemogenic argillaceous sediments. They are completely devoid of arenaceous sediments provided from a source area having free plutonic quartz. These belts contain only 1.3% siliceous sediments (fuchsite quartzite) having $\delta^{18}O = +12.5$ indicating that this siliceous material is, in fact, a metamorphosed chert (Naqvi et al., 1981). Conglomerates of true sedimentary origin are also absent in these belts. The Tattekere Conglomerate present in Holenarasipur schist belt is considered by Chadwick et al. (1978) to be a sedimentary basal conglomerate, while Glikson (1979), and Hussain and Naqvi (1983) advocated for its autoclastic nature. Rama Rao (1940) also considered it to be an autoclastic conglomerate.

In the absence of primary sedimentary structure and reliable radiometric dates, it is difficult to determine the internal primary stratigraphy of these belts. Based on tectonic and other considerations, Naqvi (1976) suggested that the mafic-ultramafic volcanic rocks are the basal members of this group and are overlain by sediments. In contrast, Ramakrishnan and Viswanatha (1981) considered the mafic-ultramafic rocks to be intrusive.

These older schist belts were intruded by 3.4 Ga old Gorur Gneisses near Katya in the western part of Holenarasipur schist belt (Beckinsale et al., 1980; Naqvi, 1981).

The basalt part of the younger schist belts/Dharwar Supergroup, designated as Bababudan Group represents stable platformal and shelf conditions indicated by quartz-pebble-conglomerate (QPC) at the base which is followed by mature quartzites exhibiting current-bedding and ripple-marks, with BIFs at top. These quartzites are interbedded with "within plate" and "MORB type" volcanic rocks (Bhaskar Rao, 1980; Arora, 1991). The upper part of the younger schist belts, designated as Chitradurga Group represents rocks deposited on an active continental margin. The common rock type occurring in this group are greywackes and greywacke type conglomerates, BIFs, cherts, shales and acid to basic volcanics. In this group Mn-formations and stromatolites are abundant. The division between Bababudan and Chitradurga Group is not unique. Ramakrishnan (1980) divided these two groups on the basis of Aimangla, Kaldurga and Talya Conglomerates, where as Chadwick et al. (1981a) separated them by a BIF horizon which they called as BIF-I. Naqvi (1981, 1983) was of the opinion that Chitradurga Group is intruded by 2.6 Ga granites while Bababudan Group is intruded by Halekote trondhjemite at Holenarasipur. Srinivasan and Sreenivas (1972) suggested the existance of Dodguni Group between Bababudan and Chitradurga Groups based on the occurrence of Mn-formations at some places and their absence at others. They (ibid) were of the opinion that Fe-and Mn-formations along with volcanic rocks and current bedded and other platformal strata represents the Dodguni Group. The platformal strata which do not contain Mn-formations is considered to represent Bababudan Group. Radhakrishna (1983) considered Bababudan and Chitradurga Groups to be coeval but this concept is no more valid with the accumulation of more geochronological data. Although in the absence of radiometric dates it is difficult to correlate the Kushtagi schist belt of northern Karnataka with any of those of southern Karnataka, based on lithological considerations, it is tentatively classified as Bababudan Group. Radhakrishna and Vasudev (1977, Fig. 2) have also classified it as Bababudan Group.

2.2.1.3 Distribution, Petrology and Geochemistry of the rock types present in the younger schist belts

Various type of metavolcanic rocks with minor anorthositic ultramafic suites, arenites, greywackes, conglomerates, BIFs, BMFs and stromatolites are the main constituents of the younger schist belts. They are discussed below :

2.2.1.3.1 Metavolcanic Associations

Although most of the volcanics are mafic, local occurrence of acid volcanics are also observed. Both columnar and pillow structures have been found in the different areas and eruption apparently occurred under a variety of conditions. These volcanics show characteristics of "within plate" basalts, "MORB" and also those which are produced at active plate margins. Volcanics interbedded with current bedded and ripple marked quartzites show "within plate" geochemical features, whereas volcanics found interlayered with greywackes exhibit characters of active plate margin (Manikyamba, 1992). The metabasalts now commonly consist of a mineral assemblage of amphibole and plagioclase, ±quartz ±garnet ±epidote as major mineral phases. Detailed geochemical work on these rocks has been carried out by Bhaskar Rao et al. (1992).

2.2.1.3.2 Quartzites

Quartzites being of sedimentary origin, are purely detrital and exhibit various primary sedimentary structures. They mainly consist of mono and poly crystalline quartz with some ferrous minerals, feldspars and a number of heavy minerals like zircon, rutile and garnet. Based on REE and other trace elements characteristics of the quartzites from Bababudan and Chitradurga schist belts, Srinivasan et al. (1992), inspite of enigmatic scarcity of granite-granodiorite pebbles in the Dharwar conglomerates, proposed the occurrence of a significant granodioritic upper crust in the Dharwar provenance. Arora (1991) from the study of the sediments of the Bababudan schist belt postulated that provenance of these sediments consisted of tonalite-trondhjemite-gneiss along with mafic/ultramafic rocks in significant amount which were subjected to intense chemical disintegration and strong hydrodynamic processes. The sediments thus produced were deposited at a shallow shelf or tidal flat environment.

2.2.1.3.3 Greywackes

Greywackes are the most abundant rock types present in younger schist belts. They were commonly deposited late in the evolutionary history of the basin and are highly immature sediments and were subjected to intense mechanical weathering, rapid transportation and less sedimentary differentiation. They were derived from a mixed provenance. Naqvi et al. (1988) have studied the geochemical characters of these sediments in detail. Their geochemical characters are similar to those of active plate margin turbidites.

2.2.1.3.4 Conglomerates

Both oligomictic and polymictic conglomerate are present in the younger schist belts. Oligomictic sedimentary conglomerates are rare and mainly consist of quartz pebbles only, with matrix of quartz and/or uraninite, gold and pyrite. The polymictic conglomerates have a clayey matrix and generally contain various sizes and shapes of fragments of all underlying rock types, viz., tonalite-trondhjemite gneiss, quartzite, BIF, carbonates, chert, vein quartz etc. (Naqvi et al., 1978; Arora et al., 1993).

2.2.1.3.5 Banded Iron and Manganese Formations

Iron formations are found in all the younger schist belts of KN, whereas Manganese formations are present in Chitradurga, Shimoga and Sandur schist belts only (Manikyamba, 1992). Extensive development of BIF is found in Kudremukh, Bababudan, Sandur and Kushtagi schist belts. Iron oxide and chert/quartz are the main constituent of BIF. At some places minerals like cummingtonite, grunerite, riebeckite and acmite are also found along with chert and iron oxides (Chadwick et al., 1986; Khan et al., 1992). In Kushtagi schist belt BIFs are found associated with metavolcanics.

2.2.1.3.6 Stromatolites

Stromatolites are organosedimentary structures produced by sediment trapping, binding and/or precipitation as a result of the growth and metabolic activity of micro-organisms, principally cyanophytes. They are mainly found in association with BIF and/or BMF (Srinivasan et al., 1989; Venkatachala et al., 1989). Non stromatolite carbonates and carbonate facies BIF pass into stromatolitic dolomite and limestone.

2.2.2 Peninsular Gneiss

The "Peninsular Gneiss" (grey gneiss) was believed to be the basement on which the supracrustal sequence now occurring as number of discrete linear belts was deposited. Bruce Foote (1886) called it as "Fundamental Gneiss" but Smeeth (1916) later renamed it as "Peninsular Gneiss". Basically, they are quartzo-feldspathic gneisses engulfing Dharwar schist belts. Recent work (Naqvi, 1981; Uday Raj, 1991) has revealed that these rocks have formed from atleast four or five events of emplacement 3.4 Ga to 2.6 Ga ago. They exhibit compositional range from tonalites/trondhjemites to diorites, granodiorites and granites showing light and dark coloured banding, ptygmatic folding and agmatitic structures (Naqvi et al., 1983). In addition to ortho (magmatic) gneisses, sedimentary precursors (paragneiss) of some of the gneisses at Javanahalli and Melukote have been identified (Naqvi et al., 1983; Uday Raj, 1991).

2.2.3 Granitoids

Granite is used as a geologic term in two ways. Strictly, for a plutonic igneous rock of very specific mineralogy and broadly for a group of plutonic igneous rocks with modal quartz, often referred to as granitic or granitoids. The granitoids comprise alkali feldspar granites, granites, granodiorites and tonalites. Tonalites are essentially composed of plagioclase ($An_{<50}$, generally 50-75 vol% of total) and mafic constituents including hornblende, biotite or augite with quartz >20%. Trondhjemite is a light coloured tonalite, containing oligoclase or andesine with little or no alkali-feldspar.

The granitoids range in size from small dykes and sills to plutons with diameters of many kilometers. Chickmagalur granodiorite is dated at ~3.1 Ga (Taylor et al., 1984). Other granitoids of similar age and character are Halekote trondhjemite and Sigegudda trondhjemite and (Stroh et al., 1983; Rama Rao et al., 1991).

The younger, K-rich granites are studied in detail by Divakara Rao et al. (1990), Friend and Nutman (1991) and Bhaskar Rao et al. (1992). The compositional and textural properties are discordant with surrounding rocks. Some of these granitic bodies are the Closepet, Arsikere, Banavar, Hosedurga and Chitradurga Granites. Most of these bodies are associated with 2.5-2.6 Ga orogeny. The Closepet Granite have been dated to be 2.4-2.6 Ga (Crawford, 1969; Taylor et al., 1984; Friend and Nutman, 1991; Bhaskar Rao et al., 1992). Divakara Rao et al. (1991) after a detailed work on a number of granitic bodies, concluded that most of the granites are formed by the partial melting of the continental crust.

2.2.4 Layered Igneous Complexes

The southern part of the KN contains a number of outcrops with ultramafic composition, including pyroxenites, norites, gabbros and anorthosites. Many of the rocks form layered igneous complexes or fragments of older complexes. Nuggihalli schist belt is one of the best examples of Archaean layered igneous complexes. This belt consists of economic concentrations of chrome spinel, which is rare in Archaean terrains outside gneiss-granulite provinces (Srinivasan and Naqvi, 1990). Layered igneous complexes constitute shallow level emplacements in stable tectonic environments (Jackson and Thayer, 1972). Therefore, presence of layered igneous complexes in KN indicates stable crustal conditions in the early part of earth's history of SIS.

2.3 Age and Structural-Stratigraphic Control of the Schist Belts

Compared to many other Archaean areas, reliable radiometric dates for the Archaeans of KN is scanty. Available age data have been summarized by Naqvi and Rogers (1987). The Peninsular Gneiss is accepted to be a polyphase complex, with available radiometric age data showing a range from 3.4 to 2.8 Ga (Beckinsale et al., 1980; Janardhan and Vidal, 1982; Taylor et al., 1988; Friend and Nutman, 1991). The whole-rock Rb-Sr and Pb-Pb isochron ages of ~3.15-3.0 Ga of the components of the basement gneisses proximal to the basal unconformities of the Bababudan Group (Taylor et al., 1984) and a Sm-Nd isochron age of 3030 $\pm$ 230 Ma (Drury et al., 1983) for the volcanic rocks in the Kudremukh schist belt imply an older limit to the age of deposition of the Bababudan Group at ~2.9 Ga. Lastly, Chitradurga, Closepet and several other late to post kinematic granitic intrusions into the Dharwar schist belts have furnished an age of about 2.6-2.5 Ga (Taylor et al., 1988; Friend and Nutman, 1991; Bhaskar Rao et al., 1992). This set the younger (or minimum) age at ~2.6 Ga for the Dharwar Supergroup. Available geochronological data indicate that the early Precambrian (Archaean) continental crust of SIS evolved in the time span between 3.4 and 2.6 Ga ago, approximately over a period of 800 Ma. Detrital zircon grains from a pelitic schist and quartzite from Sargur Group have yielded ages in the range of 3580-2960 Ma by U-Pb method (Nutman et al., 1992).

The structure of the KN has been investigated by various workers (Naqvi, 1973; Chadwick et al., 1981a,b; Roy and Biswas, 1983; Ghosh and Sengupta, 1985; Mukhopadhyay, 1986; Naha et al., 1986, 1991; Naha and Mukhopadhyay, 1990; Mukhopadhyay and Matin, 1993). Many of the conclusions drawn by investigators in individual areas are highly controversial (Naqvi and Rogers, 1987).

Naha et al. (1986, 1991) found out remarkable structural unity, traceable throughout the gneisses, older and younger schist belts. All the rock types of KN have been involved in the same style and sequence of superposed deformations irrespective of their primary age. The first generation folds (DF_1) are normally isoclinal with attenuated limbs as well as thickened hinges. These together with the axial planar cleavage have been affected by a near coaxial upright folding (DF_2) varying in tightness from open to isoclinal in selected sectors. On these earlier structures a set of open folds (DF_3) have been overprinted. All these structures of three generations are present in outcrop and in hand specimen as well. Due to this complexity in structure the BIFs are found to be repeated structurally at several places. This structural unity thus runs counter to the suggestion that two distinct groups of supracrustal rocks, namely, Dharwar Supergroup and Sargur Group are separated by an angular unconformity. Migmatization synkinematic with the first folding event in a large part of the PG also argues against the gneiss being the basement for the supracrustal rocks (Naha and Mukhopadhyay, 1990). There is no general agreement on the presence of pre-DF_1 structures on a regional scale in KN. Radhakrishna and Naqvi (1986) and Naqvi (1985) have presented evidence in support of a structural episode prior to the deposition of the Bababudan Group of rocks. They studied the Talya Conglomerate of Chitradurga schist belt and observed bent lineation in quartzite pebbles and folding and fracturing parallel to the main Dharwar compression direction in BIFs. These clearly indicate the existence of deformation and metamorphism before the deposition of the rocks of the Dharwar Supergroup (Naqvi and Hussain, 1972). The ages of deformation have not been resolved by Rb-Sr isotopic work. The spatial distribution of the Rb-Sr dates is intriguing. Despite all these attempts, available structural and geochronological data are not enough to resolve the problem of the evolution of KN. However, it appears that the interfingering model, suggested by Naqvi (1981), holds the key to this problem.

2.4 Metamorphism

In the northern and central portions of the KN, metamorphism of the schist belts ranges from lower greenschist to amphibolite facies while in the Southern region it varies from amphibolite to granulite grade. A typical assemblage in low-grade metapelites is chlorite-muscovite-biotite (-garnet) and, in basic volcanics, actinolite-plagioclase-chlorite-quartz (Seshadri et al., 1981). Along the eastern and western margins of several belts in the northern region, a localised metamorphism of higher grade has also been reported (Harris and Jayaram, 1982; Roy and Biswas, 1979). Sillimanite and kyanite bearing suites have been reported from Sandur and Chitradurga schist belt respectively (Swami Nath and Ramakrishnan, 1981; Seshadri et al., 1981). All along the margin of the Closepet Granite, remnants of higher grade metamorphic rocks have been found (Ramakrishnan and Viswanatha, 1981). The wide variation in the grade of metamorphism in DC has been investigated by Raase et al. (1986). The presence of high grade/older schist belts, earlier unknown in northern Karnataka, has indicated widespread development of ancient supracrustal rocks all over Karnataka. These supracrustals and their cofolded relations with the associated migmatites and gneisses refute the earlier belief that there is a progressive increase in the metamorphic grade from north to south in the KN (Roy, 1983).

2.5 Palaeobiological Activity in the Karnataka Nucleus

The Archaean schist belts of KN, composed of extensive deposits of carbonate rocks, banded iron formation and banded manganese formation, have the potential to preserve evidence of a large magnitude of biological activity (Srinivasan et al., 1989). These rocks are considered to act as a sink for oxygen, produced during the early part of the Earth's history (Cloud, 1976). During the last decade, a large number of horizons having stromatolites and a few cherty horizons containing permineralised filamentous structures resembling cyanobacteria have been discovered and have enriched our understanding of Archaean biosphere, hydrosphere and lithosphere. Although Pichamuthu (1945) recorded the presence of cyanobacterial filaments in cherts of the Dodguni area in Chitradurga schist belt, the evidence for its syngenecity and biogenecity was provided by Suresh (1982). Naqvi et al. (1987) have recorded unambiguous syngenetic silicified cyanobacteria-like microfossils in the black cherts of Donimalai in Sandur schist belt. From carbon isotopic data, Kumar et al. (1983) have suggested the presence of life during the formation of younger schist belts of KN. Murthy and Reddy (1984), Baral (1986), Mallikarjuna et al. (1987), Srinivasan et al. (1989, 1990), Vasudev et al. (1989) and Venkatachala et al. (1989, 1990) have recorded the occurrence of stromatolites in the carbonate rocks of the lower part of the Dharwar sequence. Evidence in favour of biological activity during the deposition of BIF in Chitradurga and Sandur schist belts have been provided by Gnaneshwar Rao (1992) and Manikyamba (1992).

2.6 Geophysical Characteristics of Dharwar Craton

Geophysical properties of Dharwar craton have been summarised by Narain and Subrahmanyam (1986) and Naqvi and Rogers (1987). The analysis of gravity field data and DSS results suggests that the Eastern Ghats is a mid Proterozoic collisional belt. The eastern margins of the Chitradurga schist belt and the Cuddapah basin are sites of crustal shortening during E-W compressions. DSS data indicate thick crustal blocks of about 40 km in the KN.

To a large extent seismotectonic activity is limited to the coastal regions along which continental break-up took place and seems to be associated with the fractures and faults cutting up the continental interior, particularly the rift zones in which much alkaline plutonic activity has been recorded (Udas et al., 1979). The higher heat flow along the eastern margin of the Cuddapah basin may indicate recurrent igneous activity along the faulted boundary, which probably was a collisonal front (Narain and Subrahmanyam, 1986).

The boundary between the eastern and the western Dharwar craton still remains an enigma. The gravity signatures over Chitradurga schist belt suggest that it may be a late Archaean continental rift and suture between two blocks of DC (Verma and Subrahmanyam, 1984), supporting the interpretation from field observations and deep seismic sounding.

2.7 Evolutionary Models and Constraints

It is now widely accepted that the plate tectonic regime, thickness of continental crust, distribution of radioactive elements and the thermal gradient during the Archaean times were not same, as they are now. Evidence for a higher thermal gradient in the early earth is accumulating. The time required for a "Wilson Cycle" to complete is getting shorter. All these factors have made the problem of evolution and origin of the continental crust more complex. Several models for the evolution of Precambrian Continental Crust through a study of volcanic and sedimentary rocks of the granite-greenstone/schist belts have been proposed (Naqvi, 1978, 1981, 1983; Fyfe, 1980; Shaw, 1980; West, 1980; Goodwin, 1981, 1991; Taylor and McLennan, 1985; Naqvi et al., 1988; Anhaeusser, 1990 and McLennan and Taylor, 1991).

The dichotomy in the conceptual models related to the evolution of DC has resulted in two widely accepted models : (a) The model proposed by Naqvi (1978, 1981, 1983) envisaging a uni-directional crustal evolution from a primordial basaltic crust and gradually transforming it into a sialic composition and (b) the model suggested by Ramakrishnan et al. (1976) and Chadwick et al. (1981a, b) that the oldest supracrustal rocks were laid down on a stable sialic crust. Arora et al. (1993) also came up with the conclusion that primordial continental crust was basic-ultrabasic in nature.

The Archaeans of KN have a spectrum of BIF bands of various facies and metamorphic grade but in all the models given for crustal evolution, BIF has not been considered with due importance. The iron and silica, which constitute the major portion of BIF, were probably provided from hydrothermal vents present near the oceanic ridges and deposited under stable conditions at shallow shelf region below wave base and photic zone. It offers unique insight into many aspects of crustal evolution. Understanding of the problem of crustal genesis taking into account the complexities shown by BIF is called for. In the present work, an attempt has been made to understand the early

Precambrian crustal evolution and state of hydrosphere and atmosphere during that time on the basis of detailed geological and geochemical investigation in the least metamorphosed Kushtagi schist belt of KN with special emphasis on BIF.

CHAPTER - III

SUMMARY OF THE GEOLOGY OF THE NORTHEASTERN PART OF KARNATAKA NUCLEUS AND ADJOINING SCHIST BELTS WITH SPECIAL REFERENCE TO KUSHTAGI SCHIST BELT

3.1 General Statement

The cratonic area of northeastern Karnataka and adjoining area of Andhra Pradesh comprises the low and high grade schist belts set in a vast mass of the Peninsular Gneiss Complex (Fig. 2.2). The Kushtagi and the Sandur schist belts which lie on the eastern margin of KN are intruded by Closepet Granite, and have intermediate character between the schist belts of western and eastern blocks of the Dharwar craton. The schist belts of the north-eastern block of the Dharwar craton are named as Gurgunta/Parampur, Hutti-Maski, Pennar-Hagari, Mangalur and Raichur schist belts.

Viswanatha and Ramakrishnan (1975) have inferred that the schist belts in the eastern block are dominated by volcanics, lack of shelf facies sediments, extensive granitic intrusion, localisation in a low pressure metamorphic terrain and gold mineralization. While in the western block the belts are marked by basal conglomerates and angular unconformities set in an intermediate pressure metamorphic terrain. Hence, they (ibid) have referred the schist belts as Dharwar type for the western block and Keewatin type for those of the eastern block. The following major differences between the lithologic assembiages of eastern and western Dharwar craton have been highlighted by Naqvi and Rogers (1987).

(a) Ultramafic/anorthositic suites, particularly layered complexes, have not been described in the eastern part of the craton, although they are abundant in the west. Komatiites are present in some of the eastern schist belts, but intrusive equivalents are absent or rare.

(b) Mafic to andesitic volcanic rocks are more abundant in the eastern schist belts compared to those to the west. The western schist belts are predominantly volcanosedimentary belts.

(c) The high Mg-Al sediments that characterize some of the older schist belts in the western block are absent in the eastern belts.

(d) Abundance of potassic Closepet type granites is much higher in the eastern part of the craton compared to the west.

Ramakrishnan et al. (1976) have found that the schist belts of the eastern block are in many respect similar to the classical greenstone belts of the world, but for the absence of the dominant ultramafic unit at the base. The Keewatin type of schist belts have evolved under a relatively unstable regime; whereas, a more stable regime witnessed the evolution of the Dharwar type of schist belts (Ramakrishnan et al., 1976).

3.2 Distribution of Rock Suites

Northeastern Karnataka and the adjoining areas of Andhra Pradesh are made up of four main lithotectonic elements, namely, (1) Peninsular Gneiss, (2) high grade mafic schists, (3) low grade mafic schists and (4) intrusive granites and granodiorites. Apart from these four main rock suites, undeformed sedimentary rocks of middle Proterozoic age, namely the Kaladgi and Bhima are also found, part of which are covered by Deccan Traps.

3.2.1 Peninsular Gneiss

The detailed study on the Peninsular Gneiss Complex of this area is yet to be taken up to separate the different components of the gneissic complex. From the available description, the gneisses are broadly divisible into (1) banded biotite and/or hornblende granodiorite/tonalite gneiss, (2) migmatites and (3) faintly foliated granitoid (Roy, 1983). Field, petrological and geochemical evidences suggest that gneisses of KN represent both para as well as ortho-gneiss (Uday Raj, 1991). In the adjacent areas the PG has been described as a group of composite gneisses, mostly banded or layered, formed as a result of migmatization of the older metasediments and metabasic rocks by a quartzo-feldspathic injection (Perraju and Natarajan, 1977; Sarvothaman and Leelanandam, 1992).

3.2.2 High Grade Mafic Schists

The high grade schists, mafic in character, generally occur as small enclaves within gneisses and migmatites (Roy, 1983). A high grade schist belt of fairly large aerial extent has been reported from northeastern Karnataka, which has been named as Gurgunta/Parampur schist belt (Narasimha and Hans, 1983; Jagannathachar and Madusudanan, 1989). It is characterized by amphibolite to lower granulite facies metamorphism and widespread migmatization. Apart from this well recognized belt some small patches of high grade schists have also been reported from Bellary, Raichur and Gulbarga districts (Roy, 1983). Intense deformation and disruption by the gneisses had made construction of a stratigraphic section of the high grade schists virtually impossible (Naqvi and Rogers, 1987). It is possible that some of the belts are considerably older and have been intruded by older members of the Peninsular Gneiss Complex. The discovery of the occurrence of these high grade schist belts in north Karnataka has indicated that geological activity was widespread and uniform in the entire KN and the directions of the dynamic force which resulted in the deformation of these belts was similar. However, it is yet to be seen whether they are of a single or polycyclic phenomena. The presence of these schist belts and their co-folded relations with the associated Peninsular Gneiss Complex refute the earlier belief of a progressive increase in the metamorphic grade from north to south in the DC (Roy, 1983).

3.2.3 Low Grade Mafic Schists

The low grade schist belts present in the area of interest, like other belts of southern Karnataka, occur as arcuate to linear, NW-SE trending belts engulfed in the sea of tonalite-trondhjemite gneiss. Only Sandur schist belt is not linear, instead it is boat shaped due to the geometry of the deformational structures (Matin and Mukhopadhyay, 1987; Mukhopadhyay and Matin, 1993). These belts are predominantly characterised by greenschist facies metamorphism but in some belts by amphibolite facies rocks.

The significant features of these belts are the total absence of sedimentary units to commence the succession, lack of shallow water platformal lithological association and absence of recognizable depositional contacts. So far, except from Sandur schist belt (Murthy and Reddy, 1984; Naqvi et al., 1987;

Manikyamba, 1992), neither stromatolites nor microfossils have been reported from any of the Archaean schist belts of northeastern KN.

All these belts are put into the category of unclassified schist belts. However, some tentative correlation has been proposed. Radhakrishna and Vasudev (1977) observed resemblance between Hutti-Muski, Ramagiri and Kolar schist belts and classified them as Sargur Group; Kushtagi, Sandur and Raichur schist belts were regarded as Bababudan Group. Rocks of Hutti-Maski and Mangalur schist belts have lithological affinity with the rocks of the Kolar schist belt. These belts pose problem in correlation with the Bababudan Group, as the typical orthoquartzite present in Bababudan Group is absent in these schist belts. In all these three belts, the western parts are incomplete and all the members seen on the eastern margin do not repeat themselves along the western limb of the fold, indicating that part of the succession has been cut off in the west (Iyengar, 1976). In general, all the low grade schit belts of northeastern KN are tentatively regarded as correlative with the Bababudan Group (Naqvi and Rogers, 1987).

3.2.4 Intrusive Granites and Granodiorites

Intrusive granites and granodiorites are the least studied rock type present in the northeastern KN. Kushtagi and Sandur schist belts are intruded by Closepet Granite. Apart from Closepet Granite, various other K-granite plutons are found in this region. They are discordant with the surrounding gneisses and schist belts. It is supposed that they were emplaced more or less at the same time in the geological history of the DC, around 2.6 Ga ago. Apart from these younger granites, some older granites are also present in the area. These older granites from Gulbarga, Raichur, Bellary and Shimoga districts have been dated by Venkatasubramanian and Narayanaswamy (1974) at 2990 ± 120 Ma.

3.3 Structures

Roy (1983) has made an attempt to correlate the deformation episodes in the schist belts of the northeastern KN (Fig. 3.1). Three main deformation episodes have been recognised. In the younging order they are, (1) the Sargur episode (SgD_1 in the high grade schist belts), (2) the Hutti episode (HuD_1 in the Hutti-Maski schist belt) and (3) the Dharwar episode (DhD_1 in the equivalents of Bababudan Group). SgD_1 is restricted to the high-grade schist belt, whereas HuD_1 (superposed on SgD_1) affected the Hutti-Maski schist belt and the high grade schist belts, DhD_1 is a regional event imprinted on all the belts (Roy, 1983).

The structural style, orientation and timing of different deformational phases relating to metamorphism in the schist belts of eastern and western blocks of DC are comparable and indicate their coeval development (Mukhopadhyay, 1986). Naha et al. (1986, 1991) have observed a remarkable structural unity in the Archaean terrain of Karnataka. The north-south orientation of structures has been attributed to east-west compression, implying a long term continuity of stress orientation over a very broad area (Naqvi and Rogers, 1987).

3.1. Schematic diagrams (not to scale) showing the structural patterns of different schist belts of north Karnataka. A = Gurgunta/Parampur schist belt, B = Hutti-Muski schist belt, C = Kushtagi schist belt, D = Dharwar-Shimoga-North Kanara-Goa schist belt, E = Gadag schist belt, F = Sandur schist belt (after Roy, 1983).

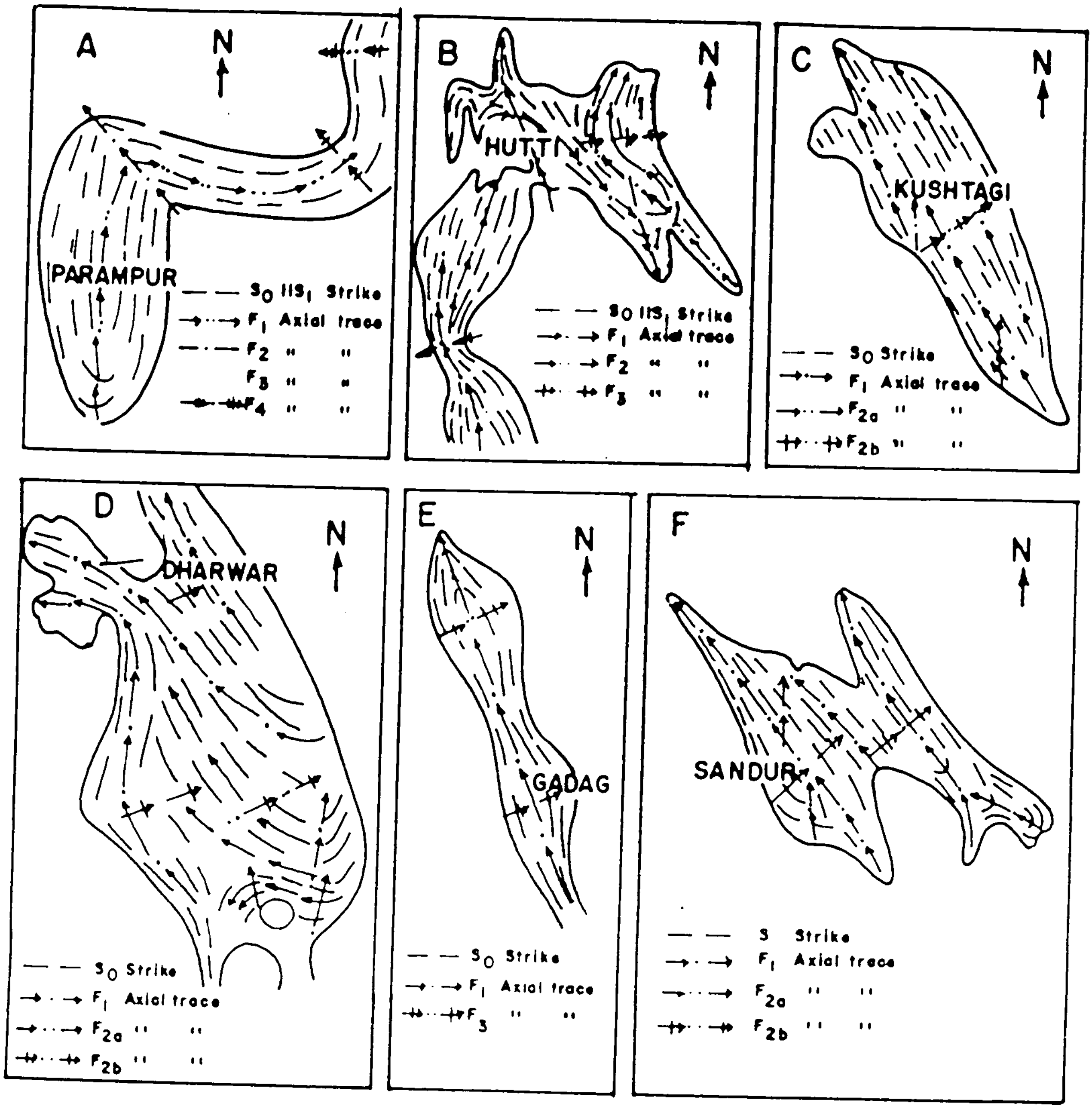

A
N
PARAMPUR
$S_0 \parallel S_1$ Strike
F_1 Axial trace
F_2 " "
F_3 " "
F_4 " "
B
N
HUTTI
$S_0 \parallel S_1$ Strike
F_1 Axial trace
F_2 " "
F_3 " "
C
N
KUSHTAGI
S_0 Strike
F_1 Axial trace
F_{2a} " "
F_{2b} " "
D
N
DHARWAR
S_0 Strike
F_1 Axial trace
F_{2a} " "
F_{2b} " "
E
N
GADAG
S_0 Strike
F_1 Axial trace
F_3 " "
F
N
SANDUR
S Strike
F_1 Axial trace
F_{2a} " "
F_{2b} " "

3.4 Age of the Schist Belts

There is a greater paucity of age data for the Archaean rocks of northeastern Karnataka and the adjoining areas of Andhra Pradesh compared to those of south Karnataka. Practically no age data are available for the rock formations in these localities. Venkatasubramanian and Narayanaswamy (1974) based on a reconnaissance study of north Karnataka granites, gave an age of 2990 ± 120 Ma with an initial ratio of $^{87}Sr/^{86}Sr = 0.707 \pm 004$. These ages are comparable with some of the gneisses of south Karnataka. However, further detailed study and data are called for to arrive at some satisfactory conclusion.

Venkatasubramanian et al. (1971) dated biotite from a pegmatite cutting into gneisses, close to the western margin of the Sandur schist belt. As metamorphic effects dominate the pattern of mica ages, they (ibid) found 2400 Ma age of biotites from Hospet, which is in accordance with the ages of Peninsular Gneiss from south Karnataka.

The general chronologic relationships are similar to those in the western block of the DC. Mafic schist belts have been invaded by younger potassic granites and perhaps also by suites commonly regarded as part of the PG. Relationships between old parts of the gneiss and the schist belts are unknown (Naqvi and Rogers, 1987).

3.5 Geology of the Schist Belts

In this section the geology of the schist belts present in the area are briefly discussed

3.5.1 Gurgunta/Parampur Schist Belt

Gurgunta/Parampur schist belt is situated about 18 km northwest of Hutti schist belt in Raichur district, Karnataka and is regarded as the high grade equivalent of Sargur schist belt (Narasimha and Hans, 1983; Roy, 1983; Jagannathachar and Madusudanan, 1989). This high grade schist belt has been referred to both as Gurgunta and Parampur schist belt (Narasimha and Hans, 1983; Roy, 1983; Jagannathacher and Madusudanan, 1989). The rocks of this belt occur as linear belts and enclaves in PG locally named as "Amareshwar Gneiss". Narasimha and Hans (1983) have mapped the area and proposed the following stratigraphic column for Gurgunta/Parampur schist belt

Younger Granite

Hutti Schist Belt

----------- Unconformity ------------

Peninsular Gneiss

---------- Unconformity -------------

	Meta-ultrabasics
Gurgunta/Parampur Schist Belt	Meta pelitic schists and quartzite
(Sargur Group)	Banded ironstone
	Amphibolite with thin acid volcanics

------------ Basement Unknown --------------

Gurgunta/Parampur schist belt occurs as remnant of a highly folded schist belt represented by metamorphosed gold-bearing ironstones (quartz-magnetite-grunerite-pyroxene+garnet), amphibolites (hornblende-calcic plagioclase+garnet) and calc-gneiss (diopside-epidote-zoisite-quartz) together with a few conformable bands of asbestos bearing metapyroxenite (talc-tremolite-schist), which show a low grade metamorphism within an amphibolite- granulite terrain (?) (Narasimha and Hans, 1983; Roy, 1983).

The area west of Amareshwar is intruded by a number of spodumene containing pegmatites which are essentially unzoned (Devaraju et al., 1990). The pegmatites contain variable amount of Li and it is still to be seen if they could be economically exploited.

Four distinct phases of deformation producing a complex structural pattern have been recognized in this schist belt (Roy, 1983). The first phase of deformation (SgD_1) is associated with the development of a penetrative S-fabric (schistosity-S_1) and some minor folds (f_1). The second phase of deformation (SgD_2) is associated with the development of large-scale (F_2) as well as small scale folds (f_2) on S_o and S_1. The migmatites and gneisses are cofolded during SgD_2 and the subsequent deformations. The third phase of deformation (SgD_3) produced large-scale (F_3) folds having NW-SE to WNW-ESE axial trace and crenulation and fracture cleavage. SgD_3 is also observed in associated cofolded gneisses. The fourth phase of deformation (SgD_4) is of mild intensity, producing only broad and open flexures having axial trace along ENE-WSW to E-W direction (Roy, 1983).

3.5.2 Hutti-Maski Schist Belt

The Hutti-Maski schist belt (H-M schist belt) well known for its gold mineralization is intensely deformed and metamorphosed to such an extent that it is difficult to establish its stratigraphy (Naqvi and Rogers, 1987). It is surrounded by intrusive granodiorite and granite and because of extensive younger granitic activity, its basement has not yet been properly identified (Roy, 1979). It has attained greenschist to amphibolite facies of regional metamorphism (Anantha Iyer et al., 1980).

H-M schist belt consists predominantly of volcanic suite of rocks (>90%) with subordinate amount of metasediments. Basaltic/ andesitic rocks predominate in the volcanic suite, and are followed by acid lava and quartz porphyry in order of abundance. Metasediments include banded ferruginous chert, quartzite, greywacke-argillite, garnetiferous mica schist, andalusite schist, garnet-cordierite gneiss and conglomerate known as "Palkanmaradi Conglomerate". Palkanmaradi Conglomerate contains well rounded water worn pebbles and boulders of granodiorite/tonalite (Roy, 1979).

The gold bearing quartz veins and lenses occur within narrow shear zones in the metamorphosed basic volcanics of H-M schist belt. Gold is in the native state and no tellurides are present (Vasudev and Naganna, 1973). Anantha Iyer et al. (1980) concluded that gold bearing volcanics of H-M schist belt indicate formation in a tectonic environment similar to that of a back arc spreading centre (marginal basin). The basaltic rocks are comparable with the oceanic tholeiites of the type generated at marginal basin tectonic environment (Anantha Iyer and Vasudev, 1979).

Menon et al. (1981) measured the $\delta^{34}S$ values of pyrrhotite and arsenopyrite samples from the gold bearing quartz-sulphide reefs of Hutti and found a narrow range of mantle-meteoritic values indicating that sulphides are of magmatic-hydrothermal origin. The famous gold deposits of Hutti mine are described by Curtis et al. (1990).

H-M schist belt shows evidence of three distinct phases of deformations (HuD_1, HuD_2, HuD_3) of which the first two phases are quite pronounced and the third phase (HuD_3) is of mild intensity (Roy, 1979). HuD_1 deformation is associated with the development of schistosity (S_1), mylonite banding (S_d) and minor folds in vein quartz and banded ferruginous chert. It has resulted in formation of a syncline accompanied by an anticline, which are recognized on the basis of pillow structures present in the metabasalts of the area. HuD_2 deformation is accompanied by the development of crenulation cleavages or fracture cleavage (S_2) and minor folds on S_1 or S_d. HuD_3 deformation is associated with the development of kink band or chevron folds and S_3 cleavages on S_1 (Roy, 1979). The regional Dharwar trend of NW-SE in the H-M schist belt is defined by the second generation folds (F_2) (Roy, 1983).

3.5.3 Sandur Schist Belt

The Sandur schist belt in Bellary district has a lithologic assemblage broadly similar to those of other low grade schist belts (Krishna Murthy, 1974; Manikyamba, 1992). Roy and Biswas

(1979) showed metamorphic conditions ranging from greenschist facies in the center of the belt to amphibolite facies on the margins. It displays lithostratigraphic characters intermediate between those of eastern and western block schist belts. Roy and Biswas (1979, 1983) have divided the stratigraphic sequence of the belt into (1) Yeshwanthanagar, (2) Deogiri, (3) Donimalai and (4) Nandihalli Formations. Yeshwanthanagar Formation consists of amphibolites, metapyroxenites, metagabbro, quartzite, quartz mica schist. Deogiri Formation is essentially a sedimentary sequence of manganiferous greywacke-argillite with bands of quartzite and arkoses with siliceous dolomite (stromatolitic) and BIF. Donimalai Formation is made up of oxide facies BIFs and metavolcanics ranging in composition from basic to acidic, metagabbros, greywackes, fuchsite quartzite, carbonaceous schists, metapelites and sulphide facies BIFs. The youngest Nandihalli Formation is characterized by the absence of BIF and is made up of metabasalts and metagabbros, acid volcanics and greywacke-argillite sequence (Roy and Biswas, 1983). Murthy and Reddy (1984) have reported the presence of stromatolites and Naqvi et al. (1987) have reported the presence of cyanobacteria from the cherts of Sandur schist belt.

Rocks of Sandur schist belt have undergone two phases (DhD_1 and DhD_2) of deformation, producing structures of two generation (Roy, 1983). This has resulted in folding of the belt into two NNW to NW trending regional synclines separated by a major central anticline. The regional synclines are doubly plunging and canoe-shaped (Mukhopadhyay, 1986). Roy and Biswas (1983) regard these folds, along with the axial plane schistosity, as first phase structures (F_1). A later deformation produced folds with ENE-WSW striking axial planes and crenulation cleavage (Mukhopadhyay, 1986).

3.5.4. Mangalur Schist Belt

Mangalur schist belt is situated in Shorapur taluk of Gulbarga district. Shorapur is about 45 km east of Mangalur. The belt is a volcanosedimentary pile extending for a length of about 25 km in a NNW-SSE direction (Jagannathachar and Madusudanan, 1989) and is similar to the H-M schist belt in tectonic setting, lithology, structural and metamorphic pattern and gold mineralization. These similarities might suggest that they are isolated remnants of a continuous schist belt, separated by subsequent igneous activity (Roy, 1983). A thick peridotite band is seen in this belt which appears to be pretectonic sheet-like intrusive body within the basaltic host rock (Roy, 1983).

Jagannathachar and Madusudanan (1989) have given the following lithological succession for Mangalur schist belt:

Post Dharwar Intrusives	
	Metarhyolite
Mangalur Schist	Metaultramafites and gabbro
Belt	Metabasalt
	Older metamorphite and migmatites

The metabasalt and acid volcanics are profusely intruded by tourmaline-bearing pegmatite along foliation plane. Pegmatites of two distinct generations have been noticed and are under investigation for exploitation of tin (Jagannathachar and Madusudanan, 1989).

3.5.5 Pennar-Hagari Schist Belt

The Pennar-Hagari schist belt has not been studied much in recent years. Bruce Foote (1886) considered it as the extension of Kushtagi schist belt, which was then known as Hunugunda schist band. The belt is located in Bellary and Anantapur districts. The major portion of this belt is occupied by black cotton soil and sandy soil and is under investigation for presence of diamond bearing kimberlite pipe (Rao, 1989). Main rock types present in this area are chlorite schist, hematite schist, hornblende schist and jaspery BIF (Bruce Foote, 1886).

3.6 Kushtagi Schist Belt

The Kushtagi schist belt is an elongated belt located in the northeastern part of the KN (Fig. 2.2). This belt has been referred as Hungund schist belt in geological literature (Bruce Foote, 1886; Viswanatha and Ramakrishnan, 1975; Iyengar, 1976). It has NW-SE strike direction and the sedimentary rocks dip at a high angle. Kushtagi schist belt is approximately 115 km in length and about 15 km in width, on an average.

It is bounded on either side by the Closepet Granite and on SE part of eastern flank by Peninsular Gneiss Complex. The northwestern tip of the belt is covered by the sediments of Kaladgi Group. The BIF present in the NW tip of the belt, once blanketed by the Kaladgi, now stands exposed after the erosion and subsequent removal of the overlying Kaladgi sediments. These BIFs in the mining area are absolutely fresh and are used in the present study for the understanding of BIF genesis.

This late Archaean volcano-sedimentary sequence is situated between N. Lat $15^{o}40'$-$16^{o}15'$ and E. Long $75^{o}40'$-$76^{o}35'$, occupies an area of about 1700 km^2, and is correlated with the basal part of the Dharwar Supergroup, i.e. Bababudan Group. The belt exposes one of the least metamorphosed geological section of the Bababudan Group. Radhakrishna and Vasudev (1977, Fig. 2) have also classified it as the Bababudan Group, where as Iyengar (1976) has considered the basal amphibolitic part as Bababudan Group and the upper chloritic part as Vanivilas Group. Roy (1983) has correlated Kushtagi schist belt with Sandur schist belt, which is classified as the Bababudan Group (Radhakrishna, 1983).

3.6.1 Distribution of Rock Types in Kushtagi Schist Belt

Though much attention has been paid on the Archaean rocks of southern Karnataka, the rocks of northern Karnataka including Kushtagi schist belt have not been studied in detail in any aspect. Even a detailed geological map of the belt has not been published. One obvious reason appears to be that this region was not a part of earstwhile Mysore State and thus Mysore Geology Department did not carry any geological studies here. Therefore the geological information regarding this belt is scanty. The results of the work of Geological Survey of India is given in its reports which are not generally available Some short reports have been published which form the basis of the information given here.

The rocks of this belt are broadly classified into three stratigraphic horizons. From bottom to top, these are (i) metabasalts with minor metaultramafics, (ii) metasediments with intercalated basic and acid metavolcanics and (iii) greywacke with intercalated banded iron formations (Roy, 1983). The schist belt rests on the gneisses with an unconformity and is intruded by younger granites in the central and as well as southern part. The distribution of the rock types is shown in the geological map of *central part of the belt (Fig. 3.2).*

3.6.1.1 Metabasalt

The metabasalts of the Kushtagi schist belt are now represented by amphibolite, amphibole-chlorite schist, hornblende-plagioclase schist and hornblende-actinolite-tremolite schist (Gera, 1989). Predominant metavolcanics (constituting >90% of the schist belt) are present as linear/ or persistant outcrops within the granite and gneisses and show concordant relationship. These metavolcanics probably represent the oldest and major lithounit of the area (Ananthanarayana et al., 1989). At some places the contacts of amphibolite are seen to be digested by granites which are throughly migmatised. The metabasalts are well foliated with schistosity along NW with moderate to steep dip in NE or SW direction. Schistosity is marked by the preferred orientation of flakes and needles of chlorite and actinolite. On the basis of textural studies, Ananthanarayana et al. (1989) have divided the metabasalts into three varieties, viz. (a) schistose metabasalt, (b) granular metabasalt and (c) massive metabasalt. Schistose variety occupies major part of the belt and occurs as small bands and lenses of varying lengths within the massive and granular varieties while the massive variety shows deformed pillow structures. The varieties grade from one to the other.

3.2 Geological map of central part of the Kushtagi schist belt.

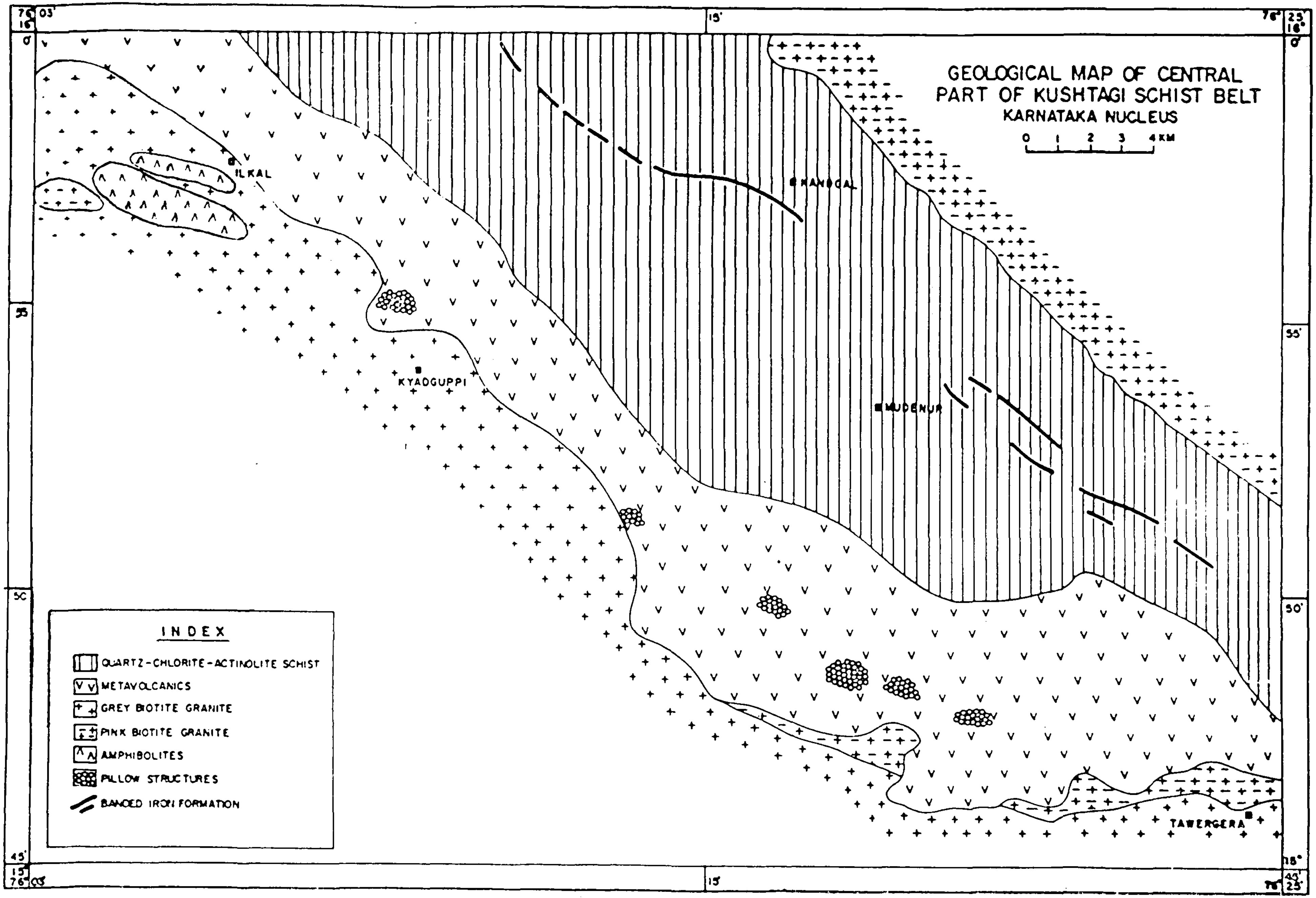
GEOLOGICAL MAP OF CENTRAL
PART OF KUSHTAGI SCHIST BELT
KARNATAKA NUCLEUS
0 1 2 3 4 KM
ILKAL
KANDGAL
KYADGUPPI
MUDENUR
TAWERGERA
INDEX
QUARTZ-CHLORITE-ACTINOLITE SCHIST
METAVOLCANICS
GREY BIOTITE GRANITE
PINK BIOTITE GRANITE
AMPHIBOLITES
PILLOW STRUCTURES
BANDED IRON FORMATION
76° 03'
16°
0'
15'
76° 25'
55'
50'
45'
15°

Pillow structures are noticed in the metabasalts which form an extensive portion of the Kushtagi schist belt (Fig. 3.3A). It has a width of about 2.5 km and runs parallel to the belt in its central portion on the western flank. The pillows often have thin crust consisting of cherty matter with the surface having vesicular structures. The mutual relationship of these pillow structures do not indicate any younging direction, as they are mostly distorted and nonoriented.

The schistose rocks are subjected to low grade greenschist facies of metamorphism characterised by the assemblage of albite, actinolite, chlorite and epidote. Small isolated bodies of ultramafics also occur within metabasalts, granites and gneisses. The exposures are lenticular and discontinuous bodies having sharp contact with the country rock. The ultramafics are traversed by quartzo-feldspathic and granitic veins. The ultramafic body having komatiitic affinity occuring west of Ilhal occurs within the metabasalts (Fig. 3.3B).

The Kushtagi schist belt like other gold bearing volcanic belts is characterised by profuse development of pillowed basalts and subordinate amount of felsic volcanics. Evidences of gold mineralization in the belt is found in the form of old workings in metabasalt, in the form of shaft and pits. Generally gold bearing volcanic belts have silicate to sulphide facies BIF associated with them. In this respect the Kushtagi schist belt is different. It is characterised by the development of oxide facies BIF only.

3.6.1.2 Acid Volcanics

Few bands of acid volcanics are found associated with metabasalts at places, showing sharp contacts (Fig. 3.3C). These acid volcanic bands are very prominent between Kalarhatti and Mulur. Megascopically, the rock is fine to medium grained, whitish grey, massive, hard and compact and exhibits weak foliation at places. They are characterised by the presence of opalescent quartz.

Acid volcanics are absent or insignificant in most of the Archaean schist belts. Mostly they are present as basalt-andesite-rhyolite association characteristic of orogenic belts. Eruption of acidic lavas can occur in a number of geotectonic environments but they are abundant at destructive plate margins.

The mafic and silicic volcanic rocks of the Bababudan schist belt have been studied by Bhaskar Rao and Naqvi (1978) and Bhaskar Rao and Drury (1982). These rocks show a flat HREE pattern and moderate LREE enrichment, probably indicating mantle source enriched in lithophile elements. The increase in negative Eu anomaly with increasing whole-rock SiO_2 content has been attributed to plagioclase fractionation in more siliceous melt (Naqvi and Rogers, 1987).

3.6.1.3 Metasediments

The metasediments occur interbanded with metavolcanics as small narrow bands and lenses. They are mainly chlorite schist and carbonaceous phyllite (Ananthanarayana et al., 1989). The schist belts of northeastern KN are dominated by volcanics and are

Figure 3.3A. Field photograph of basic volcanic rock showing pillow structures (Location - 2 kms NNW of village Kyadaguppi).

Figure 3.3B. Field photograph of ultramafic body (Location - 200 mts. west of village Ilhal).

Figure 3.3C. Field photograph showing sharp contact between acid volcanics and metabasalt (Location - 300 mts. south of village Kalarhatti on Mudgal-Tawergera road).

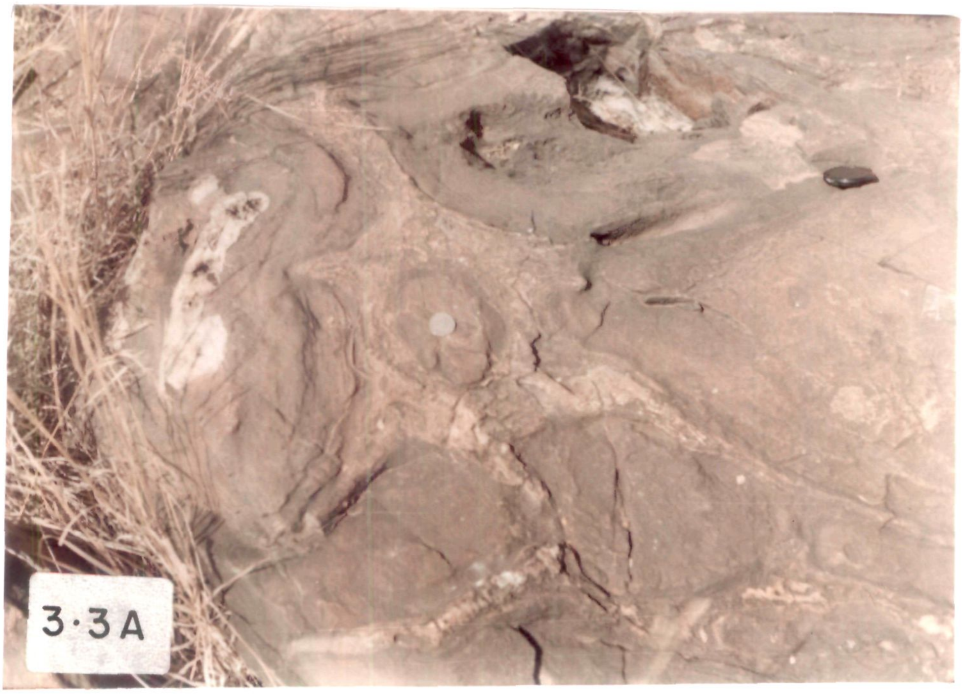

3·3A

3·3B

3·3C

devoid of shelf facies rocks (Viswanatha and Ramakrishnan, 1975). In the present study, author has not encountered occurrence of any clastic metasediment on a mappable scale, in the reconnaissance survey of the belt. However in the present work presence or absence of orthoquartzites has not been given much attention.

At number of places thin bands of dolomite/limestone is exposed as observed at south of Amrapur where it is associated with metabasalts. SW of Hire Bhergi and west of Chick Bhergi it is associated with chlorite schist and metabasalt as well (Fig. 3.4A & B) while 5 kms SW of Chandanhalli at the SW tip 499 mts. hill, it is associated with BIF. These carbonate bands can be recognized from a distance as they show perfect elephant skin like weathering (Fig. 3.4C); at places it contains quartz veins.

3.6.1.4 <u>Banded Iron Formation</u>

BIF forms conspicious topographic feature of the terrain in the form of narrow rectilinear strip associated with ferruginous phyllites and shales, and passes through almost centre of the area. This ridge runs continuously in the northwesterly direction from SE of Chandanhalli through Jajad Gudda hillock, terminates abruptly at Benchmatti and reappears at Kandgal and runs in a terrain of arcuate chains upto Chick Sangangutti. A very conspicious ridge of BIF starts from Aihole Iron Ore Mines and goes upto Tummurmatti village in the northwestern tip of the belt, where Kaladgi sediments rest on the BIFs with distinct unconformity, through Haremagi Ramthal Iron Ore Mines with break in between them. Patches of BIFs are also present at the northwestern boundary of Hungund and east of Idlapur.

Figure 3.4A. Field photograph showing the presence of limestone/ dolomite in the Kushtagi schist belt. Here it is present in sharp contact with chlorite schist (Location - SW of village Hire Bhergi).

Figure 3.4B. Field photograph of limestone/dolomite band showing contact between carbonate and metabasalt (Location - West of village Chick Bhergi).

Figure 3.4C. Field photograph showing close view of carbonate band having perfect elephant skin like weathering (Location - West of village Chick Bhergi).


3·4A


3·4B


3·4C

The BIFs present in the northwestern tip of the belt, once blanketed by the Kaladgi rocks, now stand exposed after the erosion and subsequent removal of this cover, are absolutely fresh (Fig. 3.5A and B) and are the least metamorphosed BIF present in the Indian Peninsula. BIFs present in the NW tip of the belt are used in the present study for understanding the BIF genesis.

BIF present in the belt are of two types. The one which contains no or negligible amount of clastic contamination and consists entirely of iron oxide and silica is called Cherty BIF (Fig. 3.5C). In CBIF ribbon like jaspery material is also common (Fig. 3.6A). The other type which contains significant amount of clastic material is termed as Shaly BIF. Within the SBIF, absolutely fresh continent derived clayey material is present (Fig. 3.6B and C). The iron rich layers of BIF consists of densely packed platy hematite, while the magnetite occurrence is occasional. Colourless aggregates of sericite and tabular grains of dirty green tourmaline appear among other constituents (Viswanathiah and Sathyanarayan, 1968). These bands of chert and iron oxides are cut across by thin veins of silica.

The BIFs of Kushtagi schist belt show banding of various scales. However, in majority of cases microbanding with alternating silica and iron rich layers are predominant in the area. These alternating layers are often less than few mm. in thickness. These layers are integrately folded, which are considered as intraformational folds by Chadwick et al. (1981a) in case of Chitradurga schist belt. However, Naha et al. (1986) are

Figure 3.5A. Field photograph of absolutely fresh banded iron formation, exposed after the removal of overlying Kaladgi sediments. These BIFs are probably the least metamorphosed BIF present in Indian peninsula (Location - Near Aihole-Sulebhavi Iron Ore Mines).

Figure 3.5B. Field photograph showing close view of the previously shown BIF outcrop.

Figure 3.5C. Field photograph of Cherty Banded Iron Formation (CBIF), consisting entirely of hematite and chert bands (Location - Hiremagi-Ramthal Iron Ore Mines).


3·5A


3·5B

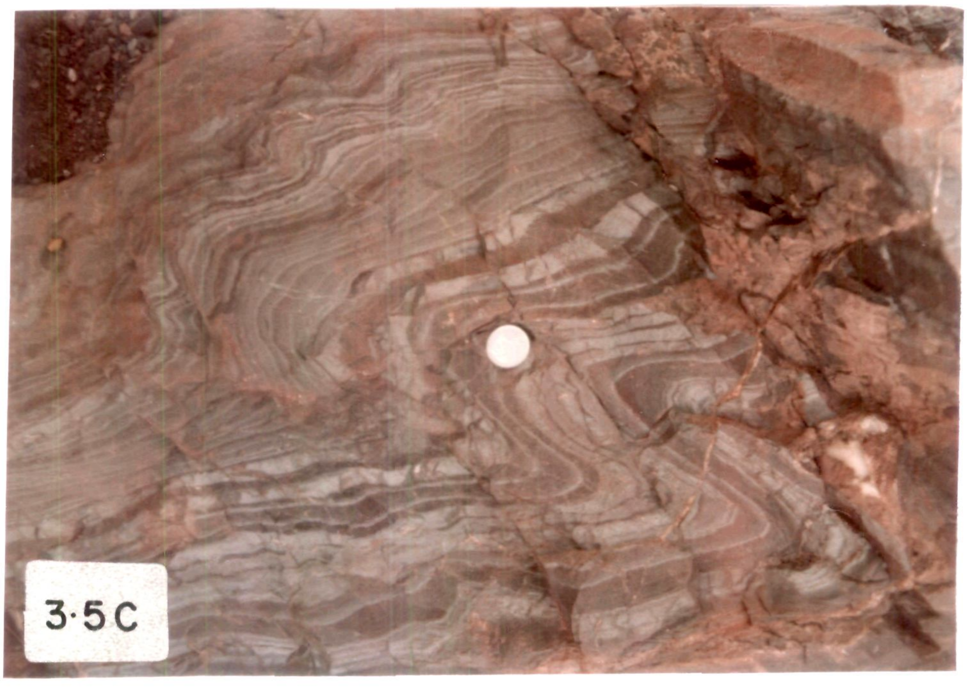
3·5C

Figure 3.6A. Field photograph of CBIF containing jasper (Location Hiremagi-Ramthal Iron Ore Mines).

Figure 3.6B. Field photograph of Shaly Banded Iron Formation (SBIF) containing absolutely fresh clayey material of about 15 cms in thickness (Location - Aihole-Sulebhavi Iron Ore Mines).

Figure 3.6C. Field photograph showing close view of the absolutely fresh clayey material present within SBIF (Location Aihole-Sulebhavi Iron Ore Mines).

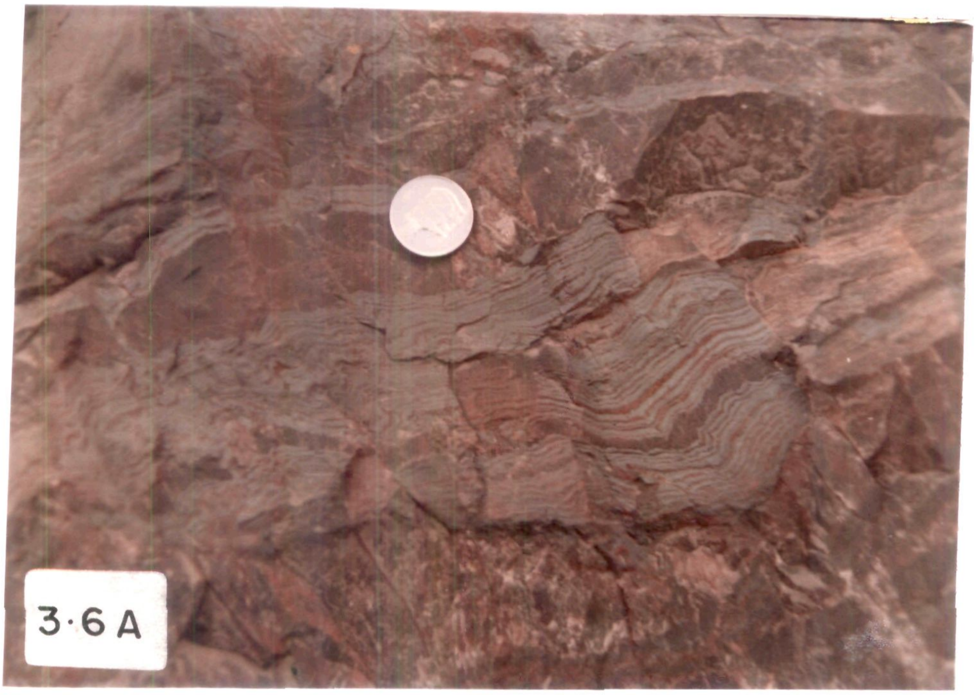
3·6A

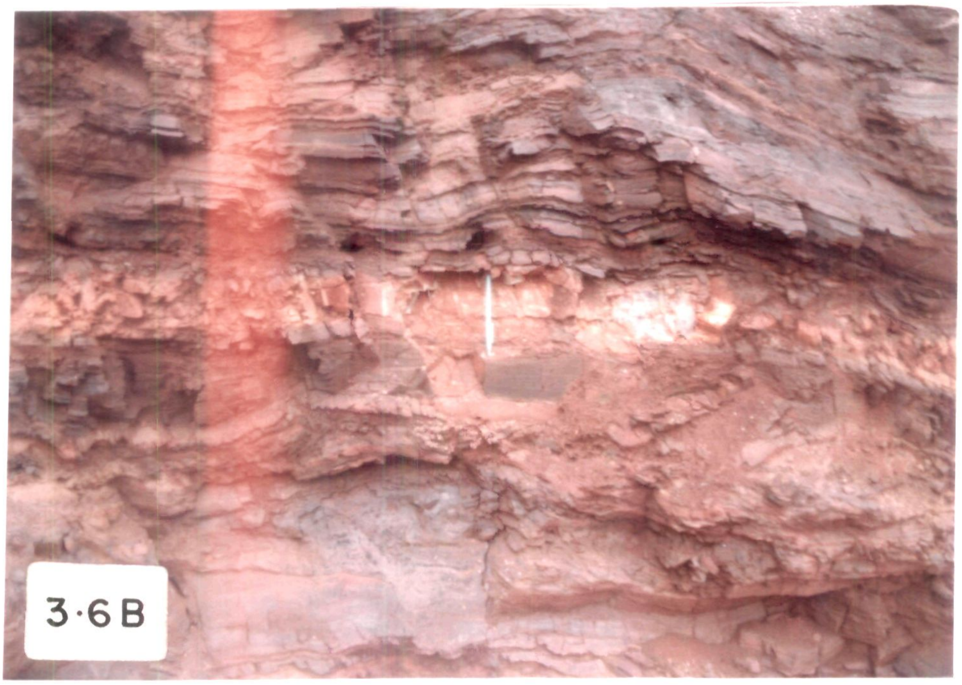
3·6B

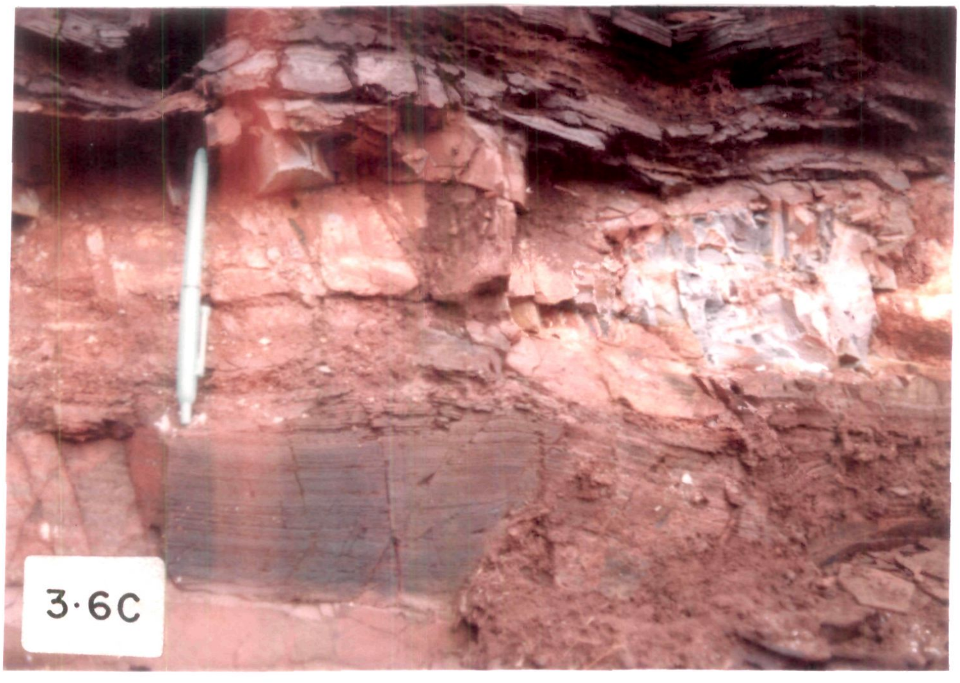
3·6C

of the view that these are the second generation folds produced during the ductile deformation of the strata (Fig. 3.7 A).

3.6.1.5 Granites

The Kushtagi schist belt is intruded by younger granites (Fig. 3.7 B) which constitutes about 60% of the belt in the form of scattered boulders and knolls, isolated outcrops and cluster of hillocks. Xenoliths, clots, rafts and enclaves of schistose rocks are seen within the granites (Gera, 1989). These granites show variation in colour, texture and mineral composition. Two type of granites are present in the belt; viz. grey biotite granite and pink granite, the latter being more abundant. In the west central part of the belt pink granite is present whereas in the eastern and southern parts grey biotite granite predominates. The pink granite ia nonfoliated and exhibits coarse porphyritic texture. It is light coloured and poor in ferromagnesian minerals. The granite consists of quartz, potash feldspar, sodic plagioclase, minor amount of biotite and occasional muscovite. Perthitic intergrowth is also noticed. At places biotite is found to alters into chlorite (Gururaja Rao and Devadu, 1975). The granite is intrusive into gneisses and grey biotite granite.

Gururaja Rao and Devadu (1975) have reported molybdenite mineralization associated with chalcopyrite and pyrite in the fine grained pink granite in Malatgud hillock, 8 km east of Kushtagi schist belt on Sindhanur-Tawargere road. The area around Malatgud consists of grey biotite-gneiss with inclusion of amphibolite, perhaps represents the Pre-Dharwarian rocks possibly equivalent to PG (Gururaja and Devadu, 1975).

Figure 3.7A. Field photograph showing integrately folded bands of iron oxide and silica. (Location - Aihole-Sulebhavi Iron Ore Mines).

Figure 3.7B. Field photograph of pink granite. These granites are intrusive into the Kushtagi schist belt and marks the culmination of geological activity in the area (Location - Granite quarry near village Hanamnal on Ilkal-Kushtagi road).

3·7A

3·7B

3.6.2 Structure

The structural study of the Kushtagi schist belt is in a very nascent stage and no detailed work on the structure of the schist belts northeastern KN has been taken up as yet. Roy (1983) has made an attempt to decipher the structural patterns of these belts and concluded that the structural style of Kushtagi schist belt is similar to that of Sandur schist belt. The rocks have undergone two phases of deformation (DhD_1 and DhD_2), producing structures of two generation in hand specimen and outcrop as well. The schistose rocks occur in the form of highly folded syncline and anticline with their fold axes trending NW-SE (F_1) and NNE-SSW (F_2) respectively indicating two deformational events (Ananthanarayana et al., 1989). The banded iron formation of Kushtagi schist belt has been intensely deformed near the northern end of the belt which is underlain by the Kaladgi. Some meso scale folds are suspected to be the first generation F_1 folds. The schistosity and the bedding in this belt is also parallel. However, at the hinges of the F_1 folds an angular-relationship between schistosity and bedding plane is observed (Fig. 3.8 A). The first generation folds are isoclinal and recumbent with vertical to steep plunge of the fold axis. They are extremely tight and the angular relationship between schistosity and bedding plane is observed only at the nose of such folds. Most of the meso- and micro-structure folds are of second generation developed on a subparallel bedding schistosity plane (Fig. 3.8 B). Along the hinges of these folds, a fracture cleavage has been observed (Fig. 3.9 A). The second generation folds are tight to open and are generally coaxial with F_1 and show

Figure 3.8A. Field photograph of suspected first generation F_1 fold in BIF, at hinges of the F_1 fold an angular relationship between schistosity and bedding plane is observed (Location - Hillock present NW of Hungund).

Figure 3.8B. Field photograph showing meso- and micro-structure folds of second generation developed on a subparallel bedding schistosity plane (Location - Hiremagi-Ramthal Iron Ore Mines).

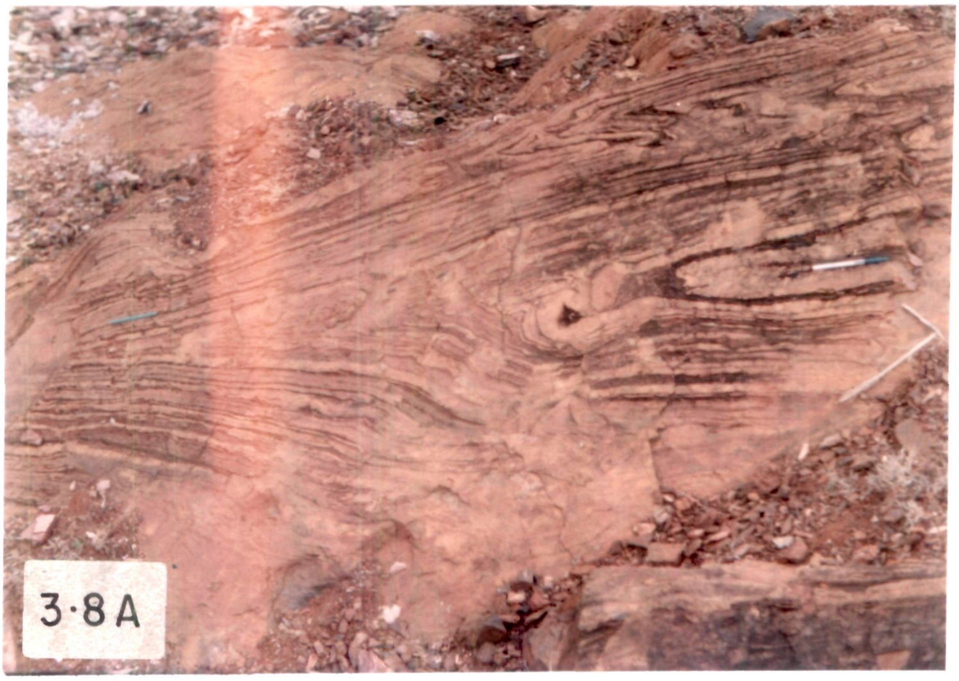
3·8A


3·8B

isoclinal nature. The nature and dimension of the second generation folds is highly variable and amplitude also varies greatly. Third generation fold appear to be large scale warping of the first generation fold arms. At many places the rheological differences between silica and iron rich layers has resulted in thickening of hematite rich layer at the hinges of the folds (Fig. 3.9 B). Since the major interest of the author is the study of the geochemical features of BIF and associated rocks, the detailed structural analysis has not been carried out. However, it appears that the structural behaviour of the Kushtagi schist belt is similar to the structural pattern of other belts of KN (Roy, 1983; Naha et al., 1986, 1991; Naqvi and Rogers, 1987; Naha and Mukhopadhyay, 1990; Mukhopadhyay and Matin, 1993). The structural unity proposed by Naha et al. (1986, 1991) and Naha and Mukhopadhyay (1990) appears to be applicable to this region also.

3.6.3 Metamorphism

The Kushtagi schist belt is one of the least metamorphosed schist belt present in the KN. It is subjected to low grade greenschist facies metamorphism characterized by the assemblage of albite, actinolite, chlorite and epidote (in the schistose rock). The older rock unit which occurs as enclaves within the migmatite show amphibolite facies metamorphism as evidenced by the presence of quartz, hornblende, relict pyroxene and andesine. The granitic rocks do not show any significant effect of metamorphism (Ananthanarayana et al., 1989). Although Kushtagi schist is considered to be the least metamorphosed schist belt present in KN, detailed work on metamorphism is yet to be carried out.

Figure 3.9A. Field photograph showing fracture cleavage along the hinges of F_2 folds (Location - Aihole-Sulebhavi Iron Ore Mines).

Figure 3.9B. Field photograph showing thickening of hematite rich layer at the hinges of the folds, formed due to rheological difference between silica and iron rich layers (Location - Hillock NW of Hungund).


3·9 A

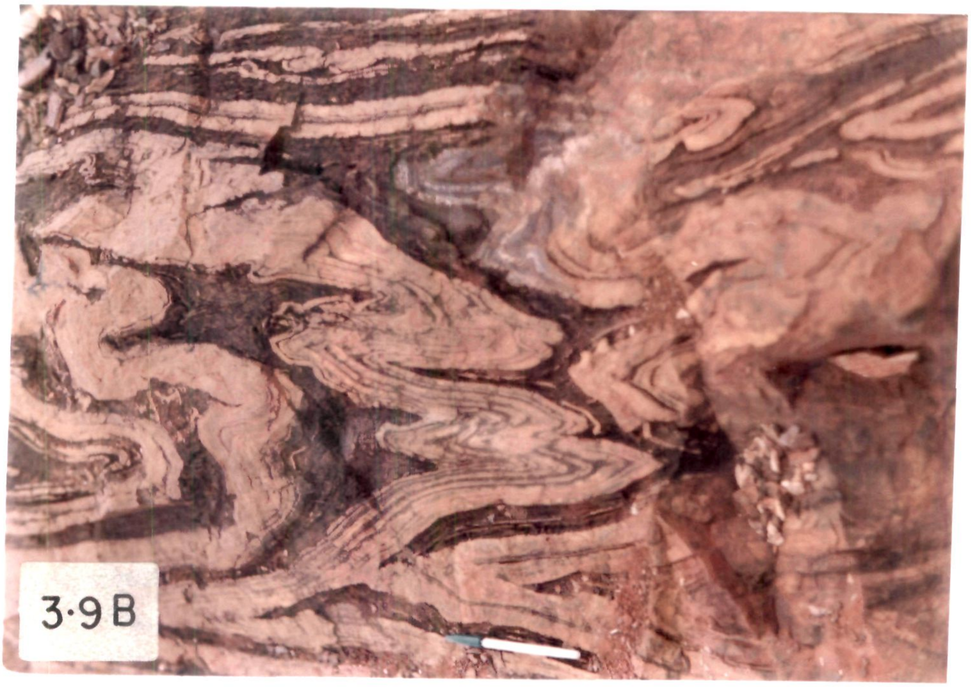
3·9 B

CHAPTER - IV

DISTRIBUTION OF BIF IN KARNATAKA NUCLEUS

4.1 Distribution of BIF in Indian Context

The maximum development of iron-formation in India is restricted to the Archaean (Pichamuthu, 1974; Radhakrishna and Naqvi, 1986; Naqvi and Rogers, 1987). The older of these (3500-3000 Ma) are represented by minor bands of complexly folded and metamorphosed iron rich beds confined to high grade regions like those of Tamil Nadu, Kerala and south Karnataka. They occur as remnants of an older group of sediments and volcanics (Sargur supracrustals) engulfed in a sea of tonalitic gneisses dated at 3305 $\pm$ 54 Ma by Beckinsale et al. (1980). These have been designated as Tamil Nadu type (Prasad et al., 1982) and are also found in Bihar, Madhya Pradesh and Rajasthan. Bulk of the iron formations of India, however, is confined to the Archaean cratonic nuclei (2900-2600 Ma) forming part of the greenstone sequence (Sarkar et al., 1969; Sarkar and Saha, 1977) and are found in Bihar and Orissa (Gurumahisani, Badampahar, Tomka-Daitery, Janda-Koira), Karnataka (Bababudan, Kudremukh, Bellary-Hospet, Sandur, Chitradurga, Shimoga, Kushtagi), Maharashtra (Ratnagiri), Madhya Pradesh (Bailadila, Rowghat, Dalli, Rajhara) and Goa. Mishra (1990) has given a beautiful account of the distribution of Archaean BIFs of Karnataka in space and time.

4.2 Distribution of BIF in KN

Iron formations are found in all the schist belts of KN (Fig. 4.1). In older greenstone belts, they are found within the

Figure 4.1. Geological map of Karnataka state showing the location and map pattern of BIF of different schist belts. (Modified from Manikyamba, 1992).

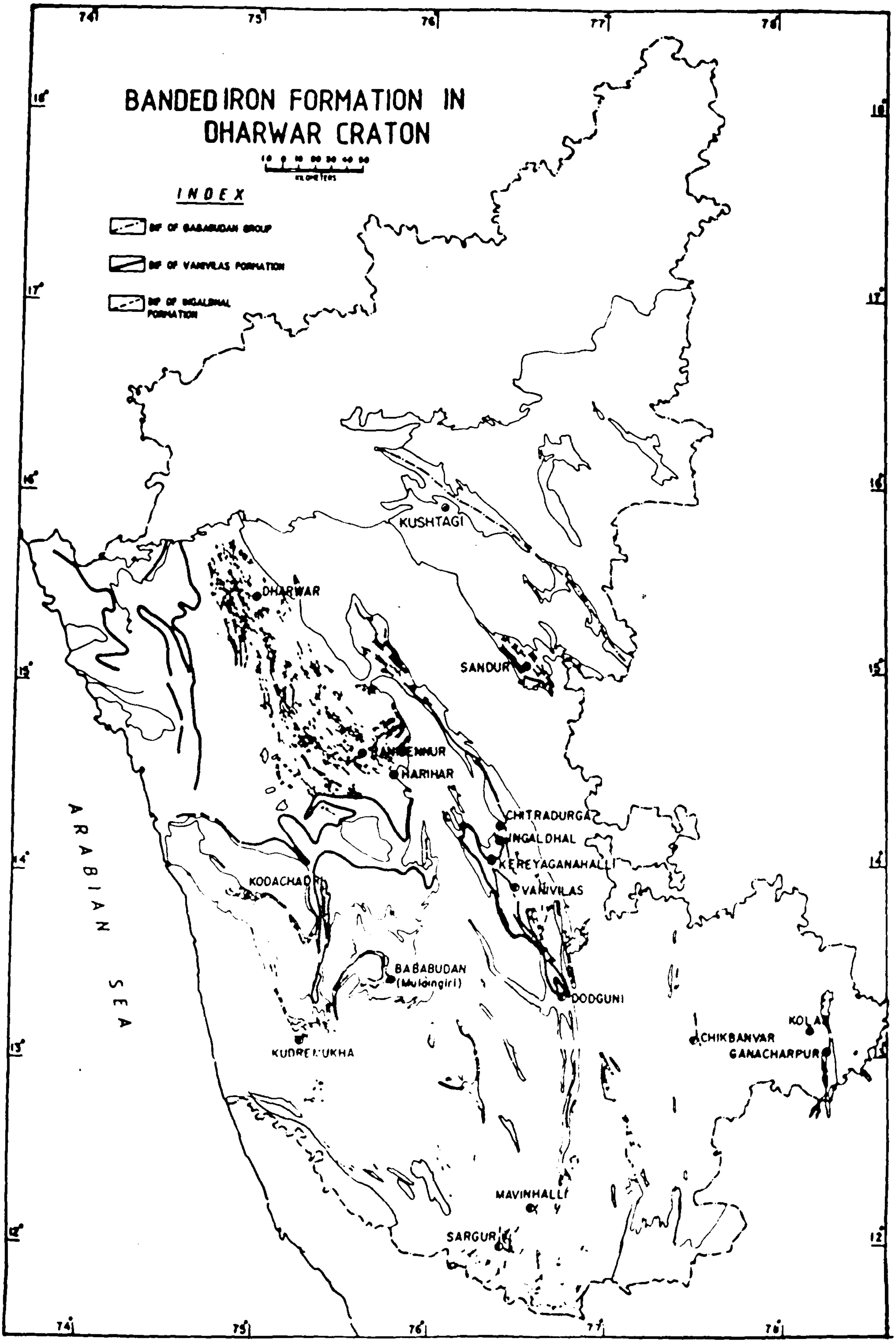
BANDED IRON FORMATION IN
DHARWAR CRATON
INDEX
KUSHTAGI
DHARWAR
SANDUR
HARIHAR
CHITRADURGA
INGALDHAL
KEREYAGANAHALLI
VANIVILAS
KODACHADRI
BABABUDAN
(Mulaingiri)
DODGUNI
KOLAR
CHIKBANVAR
GANACHARPUR
MAVINHALLI
SARGUR
ARABIAN SEA
74°
75°
76°
77°
78°
18°
17°
16°
15°
14°
13°
12°

mafic/ultramafic komatiites and amphibolites. Only a few bands of magnetite-garnet-grunerite-quartz are found in these rocks (Naqvi, 1981). Thickest and widest development of BIF is found in Kudremukh, Bababudan, Kushtagi and Sandur schist belts. In most of the schist belts of KN quartz-pebble-conglomerate (QPC) and quartzites are followed by a dolomitic horizon which at several places has preserved excellent exposures of stromatolites (Gnaneshwar Rao, 1992; Manikyamba et al., 1993). A transition from stromatolitic cherty carbonate to oxide facies BIF and shales through manganese carbonate shales and carbonate facies BIF has been observed at Shimoga (Kumsi) and Chitradurga belts (Gnaneshwar Rao, 1992).

4.3 Cyclicity of BIF deposition in KN

Naqvi et al. (1988) have identified five successive units or cycles of BIF precipitation in the schist belts of KN (Fig. 4.2) which have been designated as BIF_1, BIF_2, BIF_3, BIF_4 and BIF_5. Out of these five cycles, three have been studied in detail by Gnaneshwar Rao (1992). The BIF of Bababudan Group in Kudremukh schist belt has been studied by Khan et al. (1992) and in Sandur schist belt by Manikyamba et al. (1993). First cycle of BIF deposition (BIF_1), as a very thin horizon of only 1-2 meters thickness is found in older greenstone belts. The second cycle of BIF precipitation (BIF_2) took place in Javanahalli Group in between the amphibolites. The BIF_3 cycle of around 3000 Ma in the Bababudan Group is most extensively developed and well preserved in Bababudan, Kudremukh and Sandur schist belts. In Bababudan Group of Kudremukh schist belt mostly cherty and shaly mixed oxide

Figure 4.2. Model stratigraphic sequence of schist belts of Karnataka nucleus, showing five successive cycles of BIF deposition in the older and younger schist belts (after Naqvi et al., 1988).

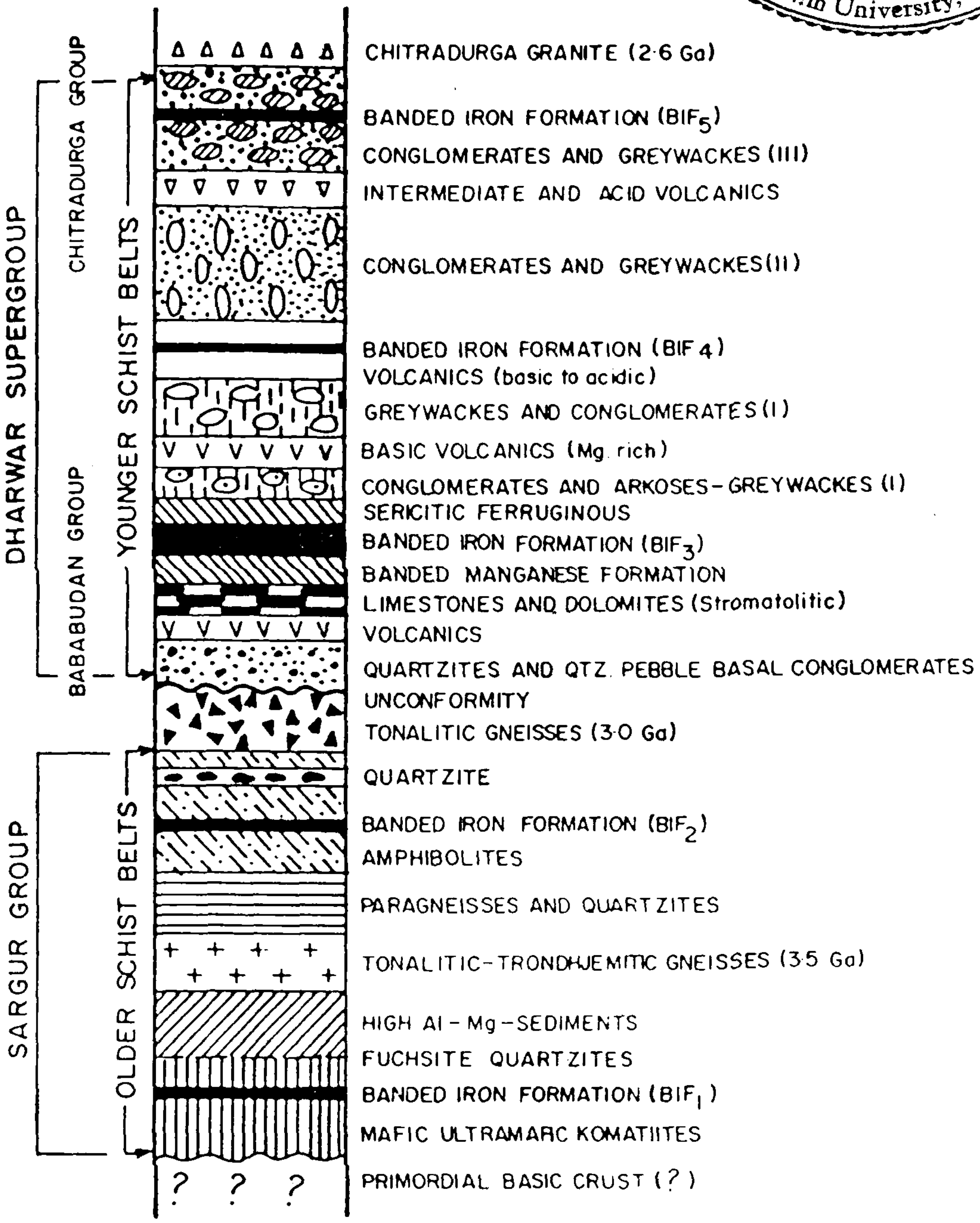
DHARWAR SUPERGROUP
CHITRADURGA GROUP
BABABUDAN GROUP
YOUNGER SCHIST BELTS
SARGUR GROUP
OLDER SCHIST BELTS
CHITRADURGA GRANITE (2·6 Ga)
BANDED IRON FORMATION (BIF_5)
CONGLOMERATES AND GREYWACKES (III)
INTERMEDIATE AND ACID VOLCANICS
CONGLOMERATES AND GREYWACKES (II)
BANDED IRON FORMATION (BIF_4)
VOLCANICS (basic to acidic)
GREYWACKES AND CONGLOMERATES (I)
BASIC VOLCANICS (Mg rich)
CONGLOMERATES AND ARKOSES-GREYWACKES (I)
SERICITIC FERRUGINOUS
BANDED IRON FORMATION (BIF_3)
BANDED MANGANESE FORMATION
LIMESTONES AND DOLOMITES (Stromatolitic)
VOLCANICS
QUARTZITES AND QTZ. PEBBLE BASAL CONGLOMERATES
UNCONFORMITY
TONALITIC GNEISSES (3·0 Ga)
QUARTZITE
BANDED IRON FORMATION (BIF_2)
AMPHIBOLITES
PARAGNEISSES AND QUARTZITES
TONALITIC-TRONDHJEMITIC GNEISSES (3·5 Ga)
HIGH Al - Mg - SEDIMENTS
FUCHSITE QUARTZITES
BANDED IRON FORMATION (BIF_1)
MAFIC ULTRAMAFIC KOMATIITES
PRIMORDIAL BASIC CRUST (?)

sulphide carbonate facies BIF are found. BIF_4 is found in the Chitradurga schist belt where occurrence of oxide, carbonate, as well as sulphide facies BIF is found (Gnaneshwar Rao, 1992). The fifth and last cycle is a thin uneconomic zone of cherty and shaly BIF associated with greywackes. All the five cycles of BIF precipitation are well preserved in Chitradurga schist belt. In the Archaean greenstone belts, BIFs are found in three associations namely with (1) arenites-stromatolitic-carbonate-Mn formations-argillite suite (2) volcanogenetic-volcaniclastic suite and (3) greywacke-argillite suite. In Kushtagi schist belt of Bababudan Group BIF_3 is mostly of cherty and shaly oxide facies and is associated with volcanics.

4.4 Restriction of BIF in Archaean Schist Belts

BIFs are very well developed in India and are present in all the schist belts of Archaean age. However, while in Australia, Canada, Greenland and South Africa the BIFs are very well developed in early Proterozoic basins, in India they are mainly confined to Archaean schist belts and are not found in early Proterozoic basins. The middle Proterozoic basins like Cuddapah are devoid of BIF and its sedimentation is confined to Archaean schist belts (Radhakrishna et al., 1986). In KN they are mostly developed in 3.0 to 2.8 Ga old Bababudan Group (Manikyamba et al., 1993). Therefore, these BIFs have a special significance in the history of crustal evolution and probably represent a much more advanced stage of evolution of the DC and related biosphere, as such a thick BIF development has not taken place in the Archaean Greenstone belts of other shield areas (Goodwin, 1973, 1991).

CHAPTER - V

PROBLEMS AND QUESTIONS RELATED TO BIF : STATUS OF INFORMATION AVAILABLE

5.1 The Debate

The genesis of BIFs of the Precambrian is highly debated and is a controversial aspect of geology. Limited work carried out during last few years has only sharpened the differences within the proposed models. This work has led to atleast one conclusion that palaeo-climatic and environmental conditions have played a very significant role in deposition of BIFs. The debate is regarding the type of climatic and environmental conditions which gave rise to BIFs. Most probably and according to several models the climatic condition during the early history of the Earth was entirely different from that of today (Kasting, 1993). The climatic and environmental conditions are likely to have affected the origin and evolution of early life; which in turn appears to have been responsible for the change from anoxic to oxic atmosphere and the redox potential of the ocean waters. These changes are probably preserved in the stable isotopic composition of sedimentary rocks. The factors that must have affected the Precambrian climate include enhanced rotation rate of the Earth, reduced solar luminosity, decreased exposed land area, presence of enormous amount of CO_2, absence of UV radiation protective covering, high rate of heat flow from the Earth, and the absence of vegetation on Earth's surface. Cloud cover is also a major uncertainty.

One of the major problems still debated is the source of iron, silica and oxygen in the BIFs (Khan et al., 1992; Kump and Holland, 1992; Alibert and McCulloch, 1993; Manikyamba et al., 1993; Morris, 1993; Widdel et al., 1993). The rhythmic layers of BIF clearly indicate that the deposition of iron rich and iron poor layers is an episodic phenomena (Morris, 1993). Majority of present day workers believe that BIFs are of marine origin (Jacobsen and Pimentel-Klose, 1988; Derry and Jacobsen, 1990; Khan et al., 1992; Manikyamba et al., 1993; Morris, 1993), but some workers still favour a fresh water origin (Hough, 1958; Haase, personal communication to Garrels, 1987). Some authors believe that their deposition took place in restricted environments (Eugster and Chou, 1973; Garrels, 1987), while others in the open sea environments (Jacobsen and Pimentel-Klose, 1988). In general, it is assumed that they formed under low oxic conditions in a basin which has an enormous amount of soluble Fe^{2+}, but the source of Fe^{2+} and SiO_2 is highly debated.

5.1.1 Source of FeO and SiO_2

Since BIFs of Archaean greenstone belts contain very large quantity of iron, the source should be able to provide huge quantities of FeO. The same source is also expected to supply the equally huge amount of SiO_2 present in BIFs. The rate of supply of FeO and SiO_2 should also be consistent with the estimated mass and deposition time interval (Jacobsen and Pimentel-Klose, 1988).

There are three models proposed for the source of iron and silica; (a) hydrothermal solutions enriched in iron and silica are believed to have added FeO and SiO_2 to the ambient ocean water

(Barrett et al., 1988; Dymek and Klein, 1988; Jacobsen and Pimentel-Klose, 1988; Derry and Jacobsen, 1990; Khan et al., 1992; Alibert and McCulloch, 1993; Gnaneshwar Rao and Naqvi, 1993; Manikyamba et al., 1993), (b) iron was carried in solution by the rivers into restricted basins (Garrels, 1987); iron was transported into the basin by aeolian storms (Carey, 1986) and (c) FeO and SiO_2 were leached out from the detrital sediments after deposition in the deeper and reducing portion of the ocean Holland, 1973; 1984). Presence of low concentration of ΣREE, flat REE to slightly enriched HREE pattern with positive Eu anomaly have completely ruled out the possibility of continental material being the only source of FeO and SiO_2. Most of the models proposed for the source of FeO and SiO_2 argue for one source or the other, but the recent work by Khan et al. (1992), Gnaneshwar Rao and Naqvi (1993), Manikyamba et al. (1993) and Morris (1993) has indicated the irregular dominance of one or the other source. Presence of clayey material in BIF clearly indicates that there has been some contribution from landward side during the chemical precipitation of FeO and SiO_2 (Khan et al., 1992, 1993; Manikyamba et al., 1993). Thus the contribution of FeO and SiO_2 from continental debris cannot be completely ruled out, although the amount of contribution may be very little. The deep ocean water saturated with iron and silica was suggested as another alternative (Holland, 1973, 1984) source. Simonsen (1985) has tested the various source models and concluded that only basinward source of iron can explain the observed sedimentological facts. Based on recent studies of REE and Nd isotopic data the hydrothermal source of FeO and SiO_2 seems to be more convincing (Alibert and McCulloch, 1993).

Nd isotopic data and REE patterns of the BIFs indicate that FeO, SiO_2 and REEs of BIFs have been provided by the hydrothermal solutions generated at the Mid Oceanic Ridges (Barrett et al., 1988; Dymek and Klein, 1988; Jacobsen and Pimental-Klose, 1988; Beukes and Klein, 1990; Derry and Jacobsen, 1990; Khan et al., 1992; Alibert and McCulloch, 1993; Gnaneshwar Rao and Naqvi, 1993; Manikyamba et al., 1993). The hydrothermal flux during Archaean would have been greater if hydrothermal circulation through the ridges was more intense due to higher thermal regime prevailing at that time. The ridges today release only about 4 x 10^{10} moles of Fe annually; this rate is less than 15% of the probable rate of deposition of Fe in the BIF of Hamersley basin (Holland, 1984). In terms of redox equivalents, it represents only 0.1% of the total oxygen consumption in the present day exogenic cycle (Kump and Holland, 1992). Arguments based on heat flow calculations suggest that either the flow of water through the ridges were higher or concentration of Fe in hydrothermal waters were higher or both were higher in the Archaean if the main source of Fe was hydrothermal water (Jacobsen and Pimentel-Klose, 1988). Higher heat production in the Archaean Earth almost certainly implies a higher Archaean surface heat flow which in turn should result in high sea-floor production rates. A substantial proportion of the Earth's heat flow is dissipated by the passage of sea water through ocean ridges. Seyfried and Janecky (1985) have found that the concentration of Fe in hydrothermal fluids is temperature sensitive between 350 and 425°C; at 425°C the Fe content of their experimental fluid was approximately a hundred fold greater than at 350°C. If MOR hydrothermal fluids were significantly warmer in the Archaean than today, Fe fluxes might have been substantially greater, probably sufficient for the deposition of enormous amount of BIF.

Enormous amount of silica precipitation has taken place along with iron in the absence of silica secreting bacteria during Archaean times, deposition of large quanity of SiO_2 is also an unresolved problem. Precipitation of silica is also difficult to explain because alkaline environment is needed to bring silica into solution and to precipitate it, acidic environment is essential (Mel'nik, 1982). In view of this difficulty, LaBerge (1973, 1986) and Walsh (1992) believe that even silica has been precipitated by biological process. Cherts precipitated by biogenic processes during Phanerozoic (Rangin et al., 1981) are characterized by the presence of a strong negative Ce and absence of positive Eu anomalies. Their REE pattern resembles that of the Modern Oceanic Water, whereas cherts and ferruginous cherts within, and associated with, BIF have depleted ΣREE, flat patterns with significant positive Eu anomalies (Khan et al., 1992; Gnaneshwar Rao and Naqvi, 1993; Manikyamba et al., 1993). These characteristics indcate that the SiO_2 of cherts is also supplied by the hydrothermal solutions.

5.1.2 Source of O_2

As the source of FeO and SiO_2 should be capable of providing huge quantity of dissolved FeO and SiO_2, the source of O_2 also must be consistent with the rate of oxidation of FeO to Fe_2O_3 within a short time. Archaean atmosphere is generally believed to be anoxic (Cloud, 1973, 1983; Walker et al., 1983; Kasting, 1987, 1993; Walker, 1987; Morris, 1993). However, other models of oxic atmosphere at an early stage are also suggested (Dimroth and Kimberley, 1976; Towe, 1983, 1990). Anoxic atmosphere at or around 3.0 Ga, is evidenced by detrital pyrite and uraninite bearing conglomerate at the base of Dharwar Supergroup and some other sequences of Archaean cratons (Swami Nath and Ramakrishnan, 1981; Walker et al., 1983; Arora and Naqvi, 1993). Thus, a source of oxygen is needed not only to precipitate FeO into Fe_2O_3 but also to gradually change the anoxic to oxic atmosphere by 2.0 Ga ago.

There are three possible ways by which required O_2 can be produced; one of them is biotic and the other two are abiotic. Abiotic sources of oxygen includes photodissociation of water vapour by solar UV radiation (Berkner and Marshall, 1965; Towe, 1978, 1988; Canuto et al., 1983) and by radiolysis of water induced by ionizing radiation of potassium-40 (Draganic et al., 1991). The third process of oxygen generation is biotic, known as photosynthesis. At variance with abiotic sources of oxygen in the early hydrosphere, the photosynthetic generation of oxygen seems to be more appropriate. It merits more attention than given in the studies of the oxidation state of the Archaean ocean. If abiotic processes were instrumental in oxygen production for the oxidation of Fe^{2+} into Fe^{3+} in basins like the Hamersley or Animikie, the slow rate of oxygen production would require five billion years at least for the precipitation of all the iron present in these basins. On the other hand it is estimated that the BIFs of Dales Gorge Member of the Hamersley basin were deposited within 2.0 Ma (Trendall, 1983; Morris, 1993). In view of the close association of microbial forms, stromatolites and the organic carbon, the biotic source of O_2 explains many observed facts in the BIFs (Cloud, 1973, 1983; Chapman and Schopf, 1983; Schopf, 1983; Schopf and Walter, 1983; Walter and Hofmann, 1983; Klein et al., 1987; Naqvi et al., 1987; Towe, 1988; Srinivasan et al., 1989, 1990; Vasudev et al., 1989; Venkatachala et al., 1989; Hofmann et al., 1991; Manikyamba et al., 1993). Occurrence of sulphide facies BIF in most of the BIF basins along with oxide and carbonate facies indicate that probably the ocean water was stratified as far as the dissolved amount of CO_2 and O_2 are concerned (Klein and Beukes, 1989). In some of the greenstone belts of India the O_2 level was high enough to allow MnO_2 precipitation, which is associated with organic matter, stromatolites and a few bands of cherts containing cyanobacteria (Manikyamba and Naqvi, 1993a). Microfossils and pseudo microfossils are found in Chitradurga schist belt (Suresh, 1982) and the $\delta^{13}C$ values (-16.5%. MSW) of the carbon present in it provide the basic data to infer the relationship between the deposition of BIF and biogenic activity (Gnaneshwar Rao and Naqvi, 1993). Schopf (1993) has described eleven taxa of cellularly preserved filamentous microbes from bedded chert unit of approximately 3465 Ma old Apex basalt of Western Australia; suggesting that oxygen-producing photoautotrophy may have already evolved by this early stage in biotic history. Therefore, the most probable source of O_2 appears to be photosynthesis which has been advocated by a large number of workers (Cloud, 1983; Schidlowski, 1989, 1990; Walker, 1987; Kasting, 1993; Morris, 1993; Schopf, 1993). However, Widdel et al. (1993) on the basis of their experimental studies, have demonstrated that oxygen-independent biological iron oxidation was possible before the evolution of oxygenic photosynthesis and thus have questioned the assumption that the appearance of Fe (III) oxides in BIFs is always an indicator of the appearance of free oxygen.

5.1.3 Banding in BIF

The rhythmic bands of iron and chert in BIF is also one of the major problems awaiting satisfactory explanation. Trendall (1983) and Garrels (1987) have proposed that the BIFs were deposited in basins, where evaporation exceeded the rate of annual addition of iron rich and silica rich solutions and resulted in varved like nature of the BIFs. Morris (1993) has advocated the formation of bands by interaction of two major oceanic supply systems : (1) surface currents and (2) convective upwelling from MOR or hot-spot activity. These supply systems are modified by varied input of pyroclastic material. The chert rich band was formed under seasonal meterological influence by precipitation of silica from the surface currents, saturated with silica, whereas, the iron rich band precipitated from convection driven upwelling of high iron solutions from MOR or hot-spot activity. Thus, silica was deposited from saturated solution mainly by evaporative concentration, and iron by oxidation due to photolysis and photosynthetically produced oxygen. This model given by Morris (1993) does not seem to be consistent with the REE and Nd isotopic data as discussed in previous sections and subsequent chapters as source for FeO and SiO_2 has to be the same.

Cloud (1973, 1983) believes that discontinuous availability of O_2 and Fe^{2+} or both have resulted in the deposition and microbanding of BIF. LaBerge (1973, 1986) and Nealson and Myers (1990) have invoked direct role of iron and silica secreting and iron reducing bacteria for the formation of chemical banding observed in the BIFs. Iron oxides and hydroxides were formed by reaction between FeO and photosynthetically generated O_2.

5.2 <u>The Present Status</u>

The present status regarding the BIFs seems to be that no single model is able to explain all the characteristics of BIF of different basins. For example, in the early Proterozoic, the Earth acquired a fairly stable condition from an unstable regime. These tectonic changes lowered volcanic activity and the input of iron and reduced gases [H_2, CH_4 (methane), NH_3 (ammonia)] into the ocean. Two Proterozoic BIF bearing basins of Australia i.e the Hamersley and the Nebburu basin show different modes of origin of BIF. In Hamersley basin the BIFs are flat and their deposition as varves seems plausible, (Trendall, 1983; Garrels, 1987; Morris, 1993) but in Nebburu basin deposition of BIF has been related to a time of maximum transgression (Goode et al., 1983). In DC the BIFs have been found to be of two different association (Manikyamba et al., 1993). Chitradurga, Shimoga and Sandur schist belts are associated with stromatolites, manganese formation and carbon phyllites whereas Bababudan, Kushtagi and Kudremukh belts are devoid of these associations. All these factors clearly indicate that the deposition of BIF cannot be related to a single process. There are BIFs of different nature, type, tectonic setting and depositional history and are products of a complex interplay between hydrosphere, biosphere, atmosphere and lithosphere. Interaction between depositional environment, tectonic setting, biogeochemical processes and the chemical characteristics of the ocean basins have all played their role to generate these most interesting rock suites (Khan et al., 1992; Gnaneshwar Rao and Naqvi, 1993; Manikyamba et al., 1993). In view of all these facts, in the present work, fresh and least metamorphosed BIF present along with the associated metavolcanics in DC have been studied to provide new information on BIF genesis.

CHAPTER - VI

MINERALOGY AND PETROLOGY OF BANDED IRON FORMATION

6.1 General Statement

BIFs are characterised by great diversity of environment of deposition, lithological association and composition. Consequently, these rocks show varying mineral associations having different degrees of oxidation and different oxidation-reduction capacities, different original contents of water O_2, CO_2 and S and uneven distribution of corresponding minerals (e.g. carbonates and silicates) (Mel'nik, 1982) resulting in formation of different facies of one or two dominant mineral either oxides, carbonates, sulphides or silicates (James, 1954). Recent studies on BIFs indicate that three processes namely, hydrothermal/fumarolic activity, volcaniclastic debris settling and terrigenous sedimentation simultaneously along with chemical precipitation have contributed to the formation of BIFs (Gnaneshwar Rao, 1992; Khan et al., 1992; Manikyamba et al., 1993) and have given rise to the formation of various types of silicates and carbonates in otherwise pure chemical sediments. Although there have been numerous mineralogic and petrologic studies on BIFs (Ayres, 1972; Dimroth and Chauvel, 1973; Immage and Klein, 1976; Floran and Papike, 1978; Majumdar and Chakraborty, 1979; Klein and Gole, 1981; Haase, 1982; Klein, 1983; Chadwick et al., 1986; Dymek and Klein, 1988; Laajoki and Devaraju, 1989; Stanton, 1989; Khan et al., 1993), still the original primary mineralogy of BIF is highly debated. It is almost impossible to obtain first-hand information on the primary mineralogy of the BIF even if it is in diagenetic stage (Klein, 1983). Only inference can be made about original mineralogy, based on laboratory evidence of the crystallization of siliceous gels and the behaviour of Fe-oxides and hydroxides at low temperatures and pressures (25^{o}C and atmospheric pressure) and on theoretical evaluations. Such inferences are possible only if one accepts the BIFs as chemical precipitates (e.g. James, 1954). If the mineralogical assemblages are considered to be the result of some earlier replacement processes (e.g. Dimroth, 1977), such assemblages provide very few, if any, chemical or mineralogical clues about the precursor materials (Klein, 1983).

The essential mineral present in an oxide facies BIF is chert/quartz, magnetite and/or hematite. Different views have been expressed concerning the formation of iron oxides in BIFs. While some authors advocate that it is a diagenetic or metamorphic product of primary precipitates (Cloud, 1983; Klein, 1983; Stanton, 1989), other have argued in favour of its production due to bacterial activity (LaBerge, 1986). Cloud (1983) proposed the hypothesis of "microbial oxygen balance". It suggests deposition of Fe^{2+} as ferric hydroxides, a chemical byproduct of the local and temporary presence of photosynthetic O_2. LaBerge (1973, 1986) believes that iron was precipitated by iron secreting bacterias. The intial mineralogy was metastable siderite-hematite-chert, which results in widespread development of magnetite and/or iron-silicates on subsequent metamorphism. Klein (1973) believes that the type of materials that could have been the precursors of the presently observed magnetite/hematite would have been hydromagnetite ($Fe_3O_4.nH_2O$) or mixtures of iron hydroxides [$Fe(OH_3)$ and $Fe(OH)_2$]. Hackett and Bischoff (1973) observe that iron oxides in the sediment appears to form directly from a precursor, may be limonite, and develops during sedimentation and diagenesis. Limonite is the precursor to goethite, goethite to hematite and hematite to magnetite (Stanton, 1989). Manikyamba (1992) has given the evidence for the biogenic nature of hematite, based on the presence of coccoids in the CBIF of Sandur schist belt. This interpretation is very similar to the one given by LaBerge (1986) for the formation of iron oxides. However, similar structures from Sokoman Iron Formation near Labrador and the nanospheres of hematite found in Marrambaba BIF of the Hamersley basin, Australia, have been considered to be due to colloidal precipitation unrelated to biogenic activity (Lesher, 1978; Ahn and Buseck, 1990; Heaney and Veblen, 1991).

A current, strongly held view is that the silica-secreting organisms were largely responsible for the deposition of chert in Archaean time. Walsh (1992) has reported widespread textural evidence for microbial activity in the cherts of the early Archaean Onverwacht Group in the form of layers with fine carbonaceous laminations resembling fossil microbial mats and filamentous microfossils. LaBerge (1973, 1986) has also advocated that the deposition of silica is biologically controlled. Presumably silica may have been precipitated largely by *Eosphaera tyleri* (double walled photosynthetic microfossil) in a periodic fashion (LaBerge, 1986).

hydromagnetite ($Fe_3O_4.nH_2O$) or mixtures of iron hydroxides [$Fe(OH_3)$ and $Fe(OH)_2$]. Hackett and Bischoff (1973) observe that iron oxides in the sediment appears to form directly from a precursor, may be limonite, and develops during sedimentation and diagenesis. Limonite is the precursor to goethite, goethite to hematite and hematite to magnetite (Stanton, 1989). Manikyamba (1992) has given the evidence for the biogenic nature of hematite, based on the presence of coccoids in the CBIF of Sandur schist belt. This interpretation is very similar to the one given by LaBerge (1986) for the formation of iron oxides. However, similar structures from Sokoman Iron Formation near Labrador and the nanospheres of hematite found in Marrambaba BIF of the Hamersley basin, Australia, have been considered to be due to colloidal precipitation unrelated to biogenic activity (Lesher, 1978; Ahn and Buseck, 1990; Heaney and Veblen, 1991).

A current, strongly held view is that the silica-secreting organisms were largely responsible for the deposition of chert in Archaean time. Walsh (1992) has reported widespread textural evidence for microbial activity in the cherts of the early Archaean Onverwacht Group in the form of layers with fine carbonaceous laminations resembling fossil microbial mats and filamentous microfossils. LaBerge (1973, 1986) has also advocated that the deposition of silica is biologically controlled. Presumably silica may have been precipitated largely by *Eosphaera tyleri* (double walled photosynthetic microfossil) in a periodic fashion (LaBerge, 1986).

Dimroth and Chauvel (1973) worked on the BIF of Sokoman Iron Formation and found close similarity between the sedimentary textures of BIF and limestone. They (ibid) applied Folk's (1962) classification of limestone to the iron formation and recognized following textural elements : (a) femicrite (a matrix of iron silicate and carbonate) and matrix chert, both analogous to micrite; (b) cement chert and carbonatic cements; (c) aggregated particles, comparable to Folk's allochems : pellets, intraclasts, ooliths and pisolites. Beukes (1980) proposed a comprehensive nomenclature of BIF, based on Dimroth and Chauvel's (1973) earlier suggestion that carbonate rock nomenclature provides the best model for application to iron-formation. Beukes (1980) extended these nomenclature to cover the full range of banded, granular and intermediate textural types present in BIF of the Transvaal Supergroup, South Africa.

Dimroth and Chauvel (1973) were of the view that atleast four types of particles have been precipitated from sea water: siderite, an iron silicate of unknown mineralogy ("precursor silicate"), silica-gel, and silica-gel with adsorbed iron-oxide hydrate. The iron-oxide hydrate is precipitated under oxidizing conditions and siderite is precipitated if the electron potential is below the "hematite-siderite fence". Precipitation of siderite furthermore depends on the CO_2 content of sea water but the physicochemical conditions of the precipitation of the "precursor silicate" are unknown. Iron and silica were co-precipitated as mixed gels under oxidizing conditions. The precipitated particles accumulated as femicrites and as matrix cherts. Pellets are invariably present in matrix chert. The first-cycle rocks (femicrite and matrix chert) were fragmented to form intraclasts. Ooliths and pisolites accreted at the surface of objects that were kept in suspension in a turbulent environment. The intraclasts, ooliths, and pisolites were transported and deposited to form second-cycle rocks. Repetition of these processes leads to the formation of intraclasts and ooliths with complex internal textures (Dimroth and Chauvel,1973).

Archaean BIFs of India have usually been metamorphosed to varying grades which has altered their primary mineral composition. Reconstruction of depositional facies of iron formation, therefore, requires reconstruction of primary assemblage, through an understanding of the diagenetic/metamorphic reactions which have given rise to the observed mineral assemblages. Mineralogical details of the BIF of DC have been rarely studied except at a few places (Devaraju and Laajoki, 1986; Chadwick et al., 1986; Devaraju et al., 1986; Mahabaleswar, 1986; Laajoki and Devaraju, 1989; Khan et al., 1993). The BIF of Kushtagi schist belt is one among the least metamorphosed BIFs of Archaean age therefore it gives the mineral content of BIF which may be near to primary mineral composition.

BIFs of Kushtagi schist belt have relatively simple mineralogy; the meso-bands and micro-bands are mainly composed of hematite and chert. BIF present in the belt are of two types. One which contains no or negligible amount of clastic contamination and consists entirely of iron oxide and silica is termed as Cherty Banded Iron Formation (CBIF). The other type which contains significant amount of clastic material is termed as Shaly Banded Iron Formation (SBIF). In CBIF ribbon like jaspery material is also common. The mineralogy of CBIF is very simple, whereas the same of the SBIF is slightly complex. The mineralogy of BIF indicates that most of the BIFs in this schist belt have been metamorphosed to lower greenschist facies. Exact condition of metamorphism in this belt have been estimated on the basis of the study of $\delta^{18}O$ on BIF and will be discussed in Chapter IX (Table 9.3).

6.2 <u>Cherty Banded Iron Formation</u>

CBIF mainly consists of alternating bands of crypto-crystalline to micro-crystalline chert (Fig. 6.1A) and anhedral hematite with occassional minute grains of muscovite (Fig. 6.1B). The thickness of iron-rich layers and the concentration of hematite in different layers is extremely variable. The layers show abrupt changes from a silica rich to an iron rich nature. On the other hand in some cases the quantity of hematite grains gradually diminishes into a chert rich layer. In many thin sections hematite microbands consisting of chain of hematite crystals are seen. In pure chert band hematite is also present as disseminated grains (Fig. 6.1C) or as very minute bands consisting of a chain of one or few grains of hematite (Fig. 6.1A). The folding observed on outcrop section (Chapter III) is also observed at micro levels (Fig. 6.2A and 6.2B). The bottom of microfolds shows closed structure which gradually opens up towards the top. It may be due to differential stress acting on BIF. This differential stress is reflected in the size of grains

Figure 6.1A. Photomicrograph of CBIF showing the rhythmic layering of hematite and chert. Ewen within pure chert band minute bands of hematite are observed (X 35).

Figure 6.1B. Photomicrograph showing presence of occassional grains of muscovite in CBIF (X 100).

Figure 6.1C. Photomicrograph showing presence of disseminated hematite grain within pure chert band (X 100).

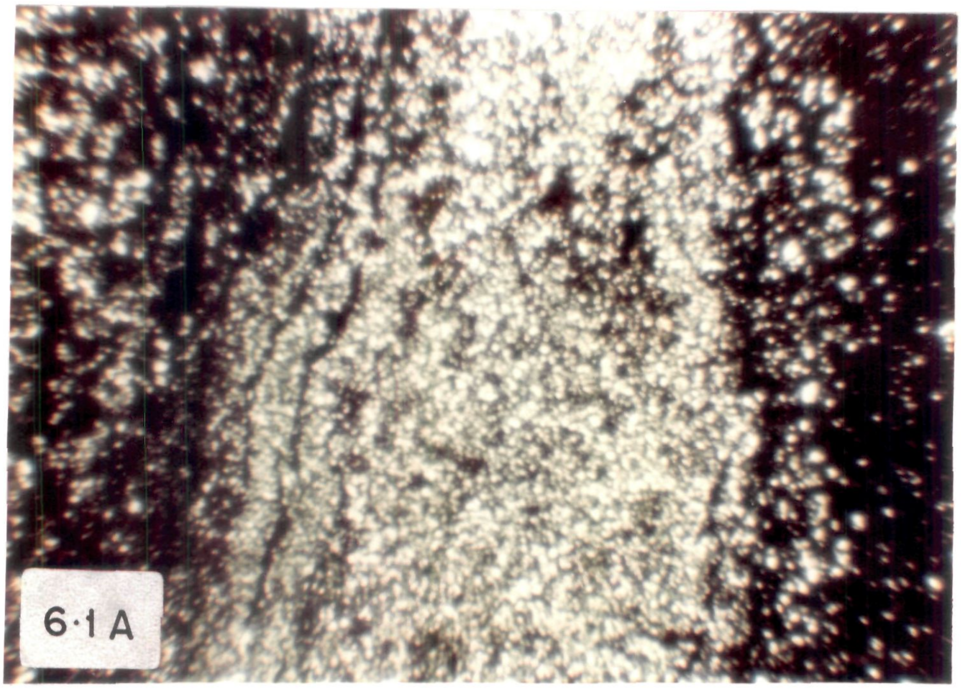
6·1A

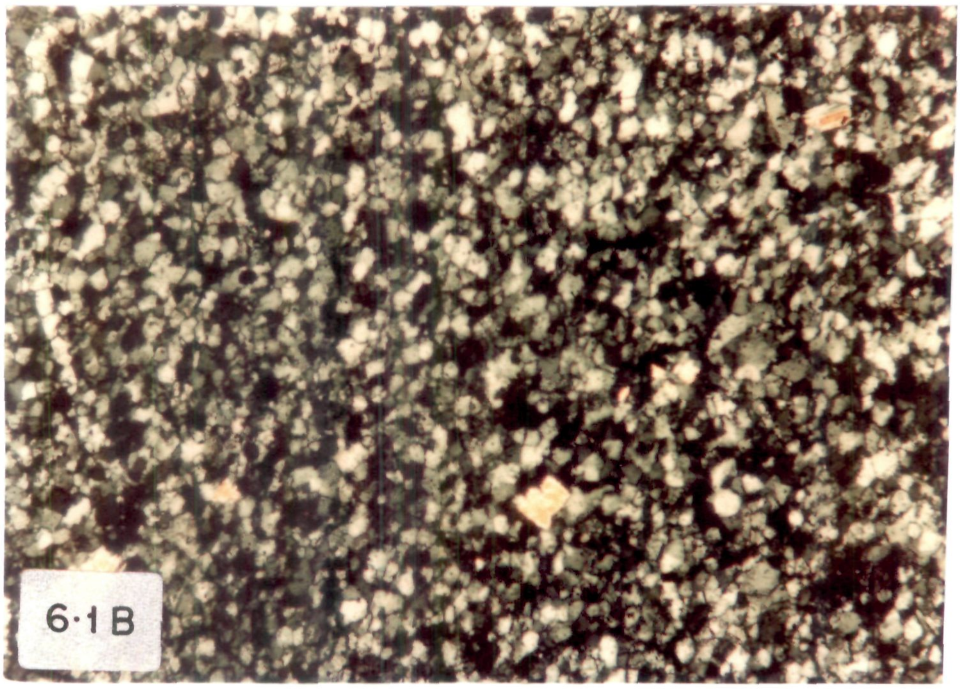
6·1B

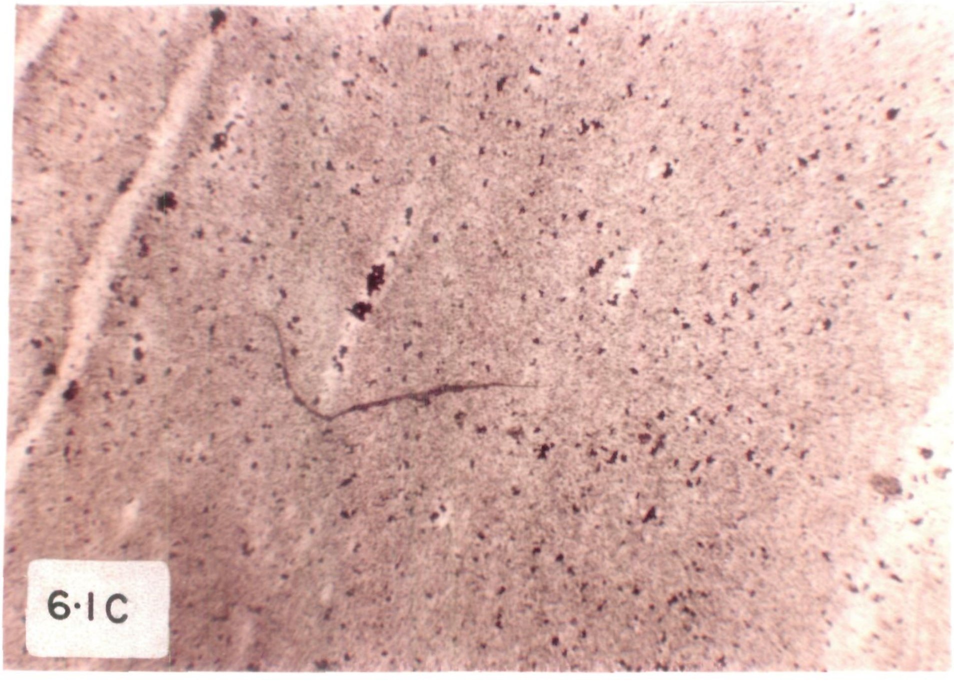
6·1C

in a single band also. In a single chert band, minute layering of chert grains of three different sizes is observed (Fig. 6.2C). Clustering of minute dust (hematite?) to form the microbands is observed at certain places and the alignment of these microbands sometimes gives the impression of a filamentous structure (Fig. 6.3A and 6.3B).

Apart from hematite and chert sporadic occurrence of muscovite is also observed in CBIF of Kushtagi schist belt (Fig. 6.1B). The abundance of muscovite is more in SBIF.

6.2.1 Hematite

Hematite is observed to be present in the form of chains. At places it is present as anhedral disseminated grains. Cleavage is not observed under reflected light. It shows pure white colour (Fig. 6.3C). It is anisotropic under crossed nicols, with no internal reflections being observed. Hematite does not contain any inclusion of ilmenite or any other mineral as shown by its composition (Table 6.1).

6.2.2 Chert

Chert is the most abundant mineral, other than hematite, in the Kushtagi Iron Formation. It is cryptocrystalline to slightly crystalline and is extremely fine grained. Recrystallization in certain layers has resulted in the formation of coarse grained quartz. At places due to coating by iron oxide, the cherts have become jasper, showing red tint.

6.2.3 Muscovite

Muscovite is present as minute detrital grains within chert band. The occurrence of muscovite in CBIF is occassional. It is

Figure 6.2A. Photomicrograph showing folding in BIF at micro level (X 35).

Figure 6.2B. Photomicrograph showing folding in BIF at micro level (X 35).

Figure 6.2C. Photomicrograph showing presence of chert bands of three different sizes in a single chert band (X 35).

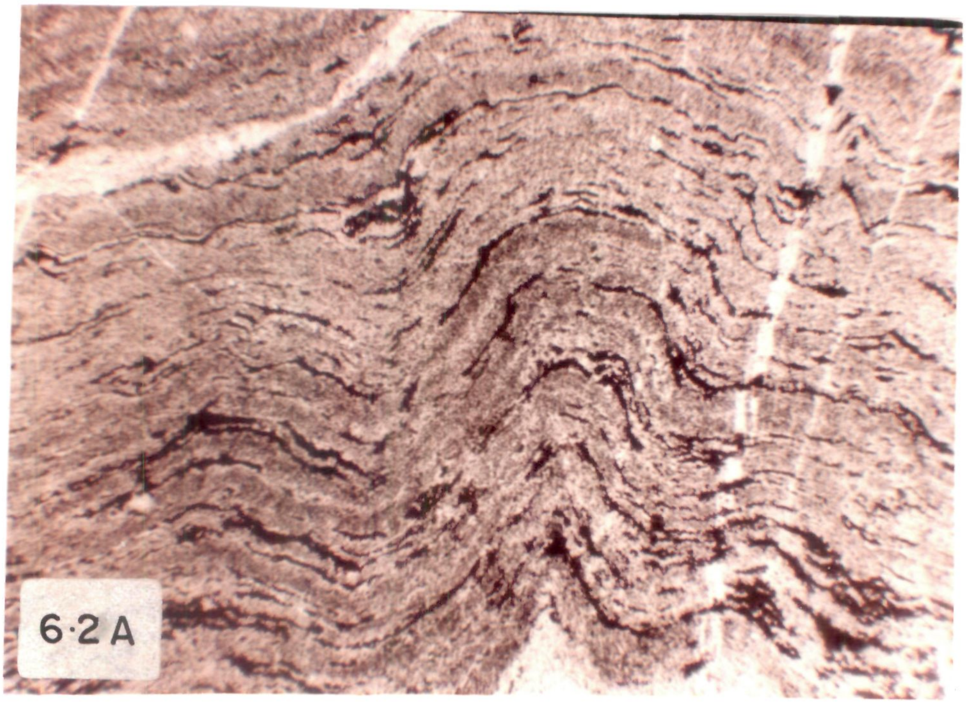
6·2A

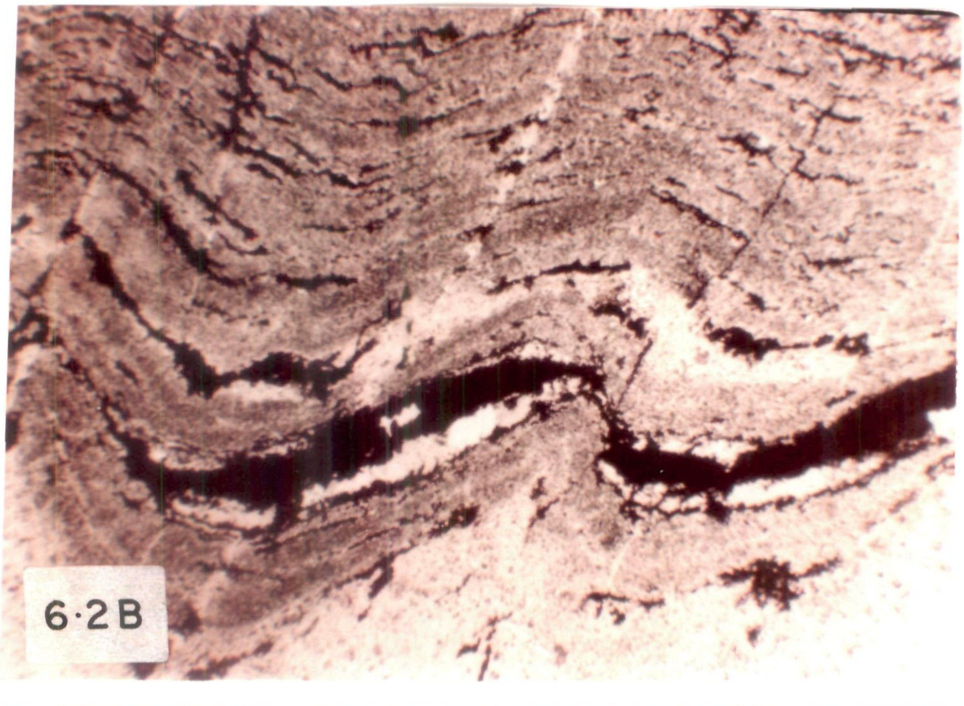
6·2B

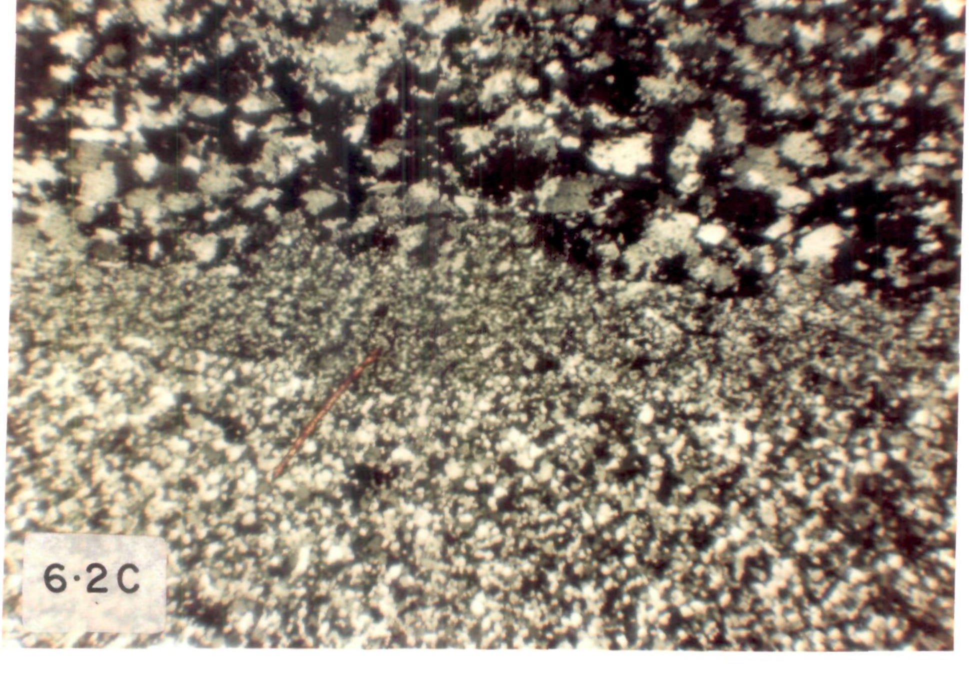
6·2C

Figure 6.3A. Photomicrograph showing clustering of minute dust (hematite ?) which gives the impression of a filamentous structure (X 400).

Figure 6.3B. Photomicrograph showing alignment of clusters of minute dust (hematite?) in form of microbands, giving the impression of filamentous structure (X 100).

Figure 6.3C. Photomicrograph of CBIF under reflected light showing disseminated grains of hematite (X 400).

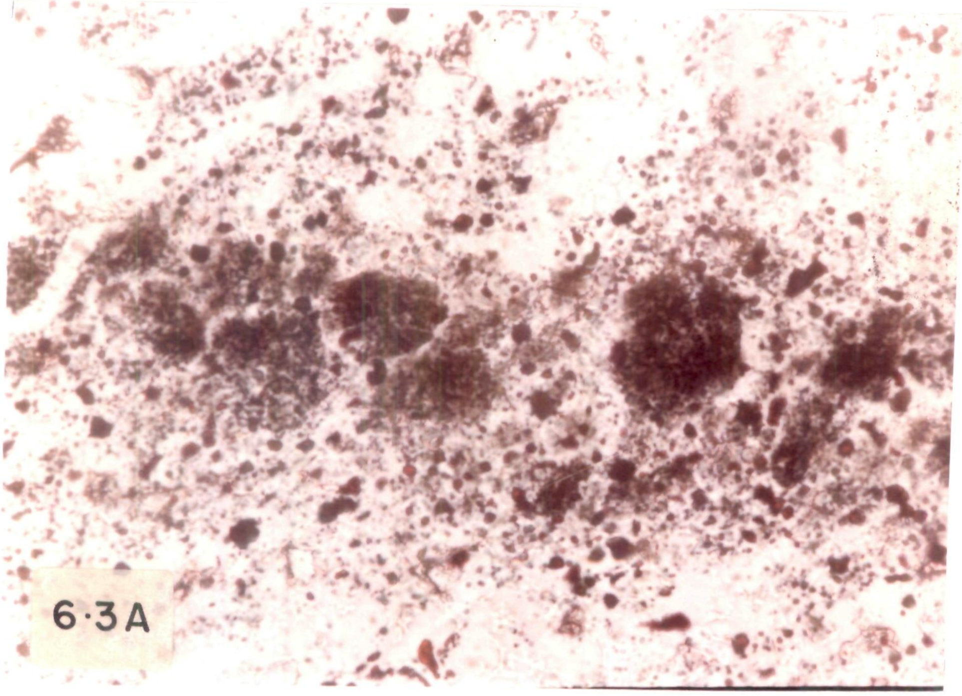

6·3A

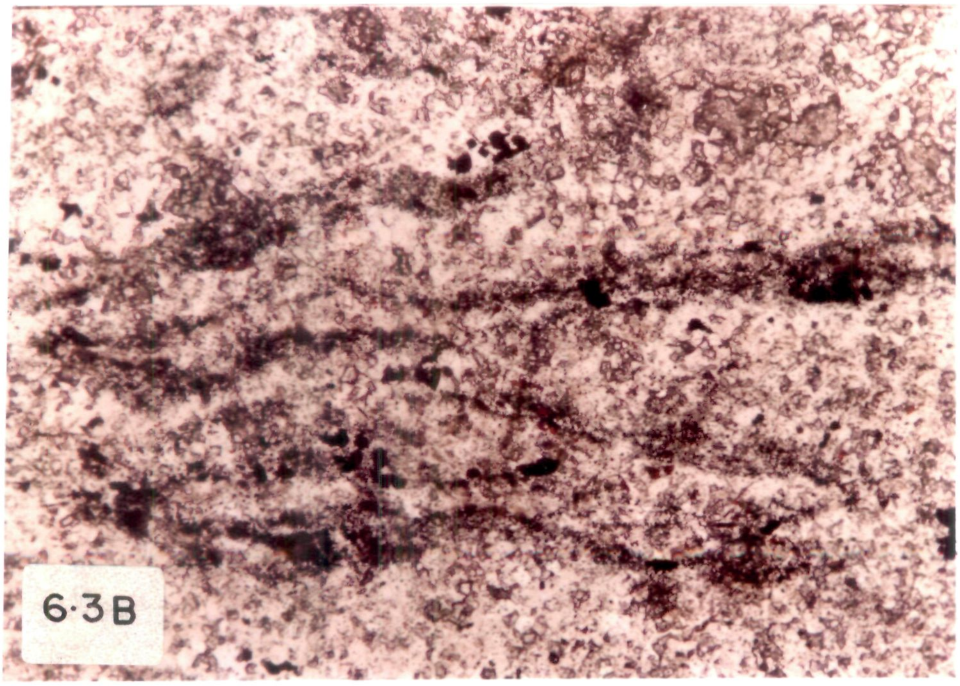

6·3B

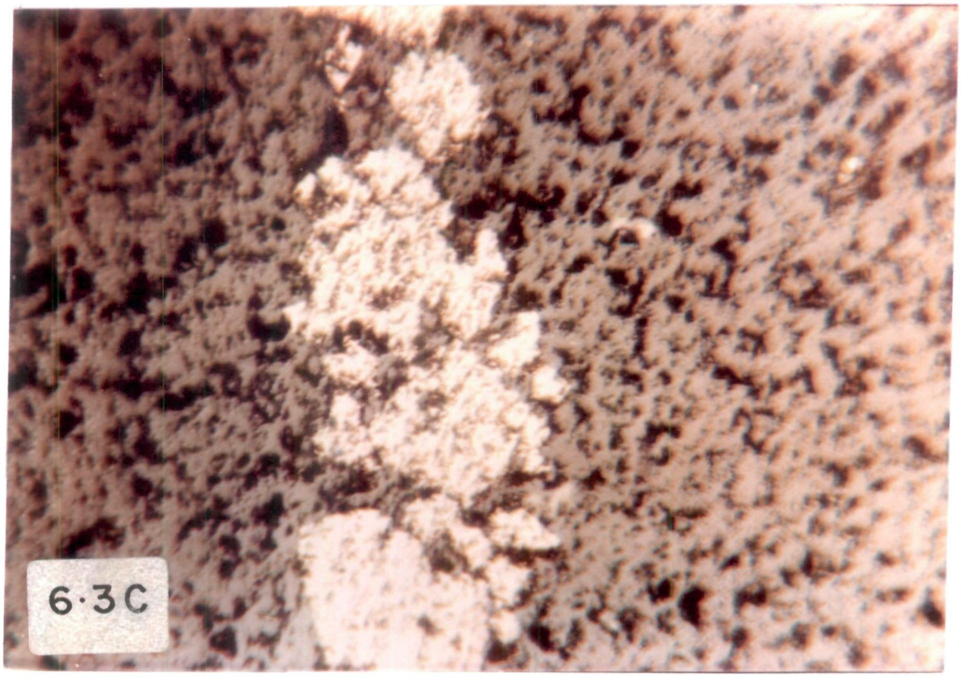

6·3C

TABLE 6.1 REPRESENTATIVE ELECTRON MICROPROBE ANALYSES OF MUSCOVITE

N	3	1	2	3	4
SiO_2	49.18	49.66	52.11	48.34	49.94
Al_2O_3	28.42	27.28	25.57	27.28	26.20
TiO_2	0.01	-	0.05	0.01	0.03
FeO^*	4.93	4.80	4.75	5.28	5.25
MgO	2.62	2.92	2.72	2.73	2.74
Na_2O	0.31	0.30	0.51	0.49	0.33
K_2O	11.15	12.05	10.67	11.25	11.01
Total	**96.62**	**97.01**	**96.38**	**95.38**	**95.50**
Cation based on 22 oxygen					
Si	6.594	6.666	6.955	6.602	6.779
Al^{IV}	1.406	1.334	1.045	1.398	1.221
Al^{VI}	3.087	2.983	2.978	2.995	2.972
Ti	0.001	-	0.005	0.001	0.003
Fe^{2+}	0.553	0.539	0.530	0.603	0.596
Mg	0.524	0.534	0.541	0.556	0.554
Na	0.081	0.078	0.132	0.130	0.087
K	1.907	2.063	1.817	1.960	1.907
Total	14.153	14.197	14.003	14.245	14.119

* Total Fe reported as FeO
N = Number of spots analysed on an individual grain

REPRESENTATIVE ELECTRON MICROPROBE ANALYSES OF HEMATITE

SiO_2	0.65	0.34	0.09	0.15	1.29
Al_2O_3	0.28	0.26	0.06	0.15	0.08
TiO_2	0.06	0.11	-	0.07	-
FeO^*	90.40	91.10	90.94	89.99	88.37
MnO	0.05	-	-	-	0.01
MgO	0.04	-	-	0.05	-
CaO	0.04	0.08	0.06	0.03	0.06
Na_2O	-	0.20	0.12	0.22	0.34
K_2O	0.04	0.09	0.06	0.06	0.07
NiO	-	0.01	0.05	0.12	-
Cr_2O_3	0.05	0.04	0.03	0.03	-
Total	91.61	92.23	91.41	90.87	90.22

colourless in plane polarized light. Chemical composition of muscovite is given in Table 6.1. Ti content is extremely low.

6.3 Shaly Banded Iron Formation

Interbedded with CBIF, SBIF is found at several places. SBIF has a variable mineralogical composition. It has extremely thin silica, iron and clay-mineral rich layers. Under the microscope identification of minerals present is almost impossible because of their fine grained nature. XRD analysis of fifteen SBIF samples has indicated the presence of kaolinite and muscovite besides hematite and chert in them. This mineralogy of BIF is different from the mineralogy of BIFs in other parts of DC. The CBIF of Kudremukh, Bababudan and Sandur have been reported to contain different types of amphiboles, carbonates and some other minerals (Chadwick et al., 1986; Manikyamba, 1992; Khan et al., 1993). Presence of kaolinite and detrital muscovite with low Ti content indicates that the BIFs of Kushtagi schist belt has been metamorphosed upto lower greenschist facies. All kaolinite minerals decompose at approximately 400^{o}C, throughout the range of pressures 2500 to 25,000 lb/in^2 (Deer et al., 1979). Thus it seems that BIFs of the studied area has not been subjected to even a temperature of 400^{o}C, at a moderate pressure.

CHAPTER - VII

MINERALOGY AND PETROGRAPHY OF ASSOCIATED VOLCANICS

7.1 Introduction

The Kushtagi schist belt consist acidic and basic types of metavolcanics. The volcanics of the belt, in general, show a reconstituted mineralogy. The metabasalts are massive as well as schistose. The massive variety shows deformed pillow structures, whereas the schistose variety are represented by actinolite-chlorite schist, actinolite-plagioclase schist and actinolite-tremolite schist. The varieties grade from one to the other. In metabasalt both massive and schistose varieties have been studied. The massive variety is fine grained whereas schistose variety is medium grained. The planar arrangement of actinolite and chlorite defines the schistosity. The most common minerals present in basic volcanic are green to yellow actinolite (fibrous and prismatic) and plagioclase. Poikiloblasts of plagioclase carry the inclusions of chlorite, actinolite and epidote. Though chlorite and sphene form an important component, calcite and ilmenite are also present in significant amount.

The acidic metavolcanics are leucocratic-light grey in colour, porphyritic in hand specimen and in thin sections with phenocrysts of albite and quartz. The ground mass consists of muscovite, albite, chlorite, quartz, ilmenite, magnetite and calcite. Muscovite is present within plagioclase grains also.

7.2 Textures and Microstructures

The rocks under study display a complex interplay of grain growth, deformation and hydration reactions. Often rocks have escaped metamorphism and as a result, relict primary structures and textures are preserved. Relict porphyritic textures with large palimpset plagioclase in various stages of degradation are common (Fig. 7.1A and B). Palimpset olivines or pyroxenes were not observed in metavolcanics from Kushtagi schist belt. The massive metabasalts with pillow structures, show accicular aggregates consisting of elongated grains of actinolite, chlorite and plagioclase (Fig. 7.1C and D).

The acid volcanics show typical porphyritic texture with microcrystalline ground mass and porphyroblasts made up of plagioclase and quartz (Fig. 7.2A and B). Plagioclase and quartz are present in ground mass along with fibrous muscovite and chlorite. The sheet silicates define schistosity which is deflected around quartz phenocrysts (Fig. 7.2C). Ilmenite and magnetite are the accessory phases present in ground mass. Calcite occurs in small quantity as a replacement mineral (Fig. 7.2D). Plagioclase is found to alter (Fig. 7.2B).

7.3 Mineralogy of Volcanics

Four sections, two of mafic (sample No. RN-17 and RKY-10) and two of acid (Sample No. RKL-16 and 44) volcanics were selected for EPMA study. Following mineral association are present in them:

1) RN 17 - quartz + actinolite + chlorite + albite + sphene + calcite + ilmenite + epidote

Figure 7.1A. Photomicrograph showing relict porphyritic texture in schistose metabasalt with large palimpset plagioclase (X 100).

Figure 7.1B. Photomicrograph showing relict porphyritic texture in pillow basalt with degraded plagioclase (X 35).

Figure 7.1C. Photomicrogaph of pillow basalt showing extremely fine grained accicular aggregates of actinolite, chlorite and plagioclase (X 35).

Figure 7.1D. Photomicrograph of pillow basalt showing accicular aggregates of actinolite, chlorite and plagioclase (X 35).

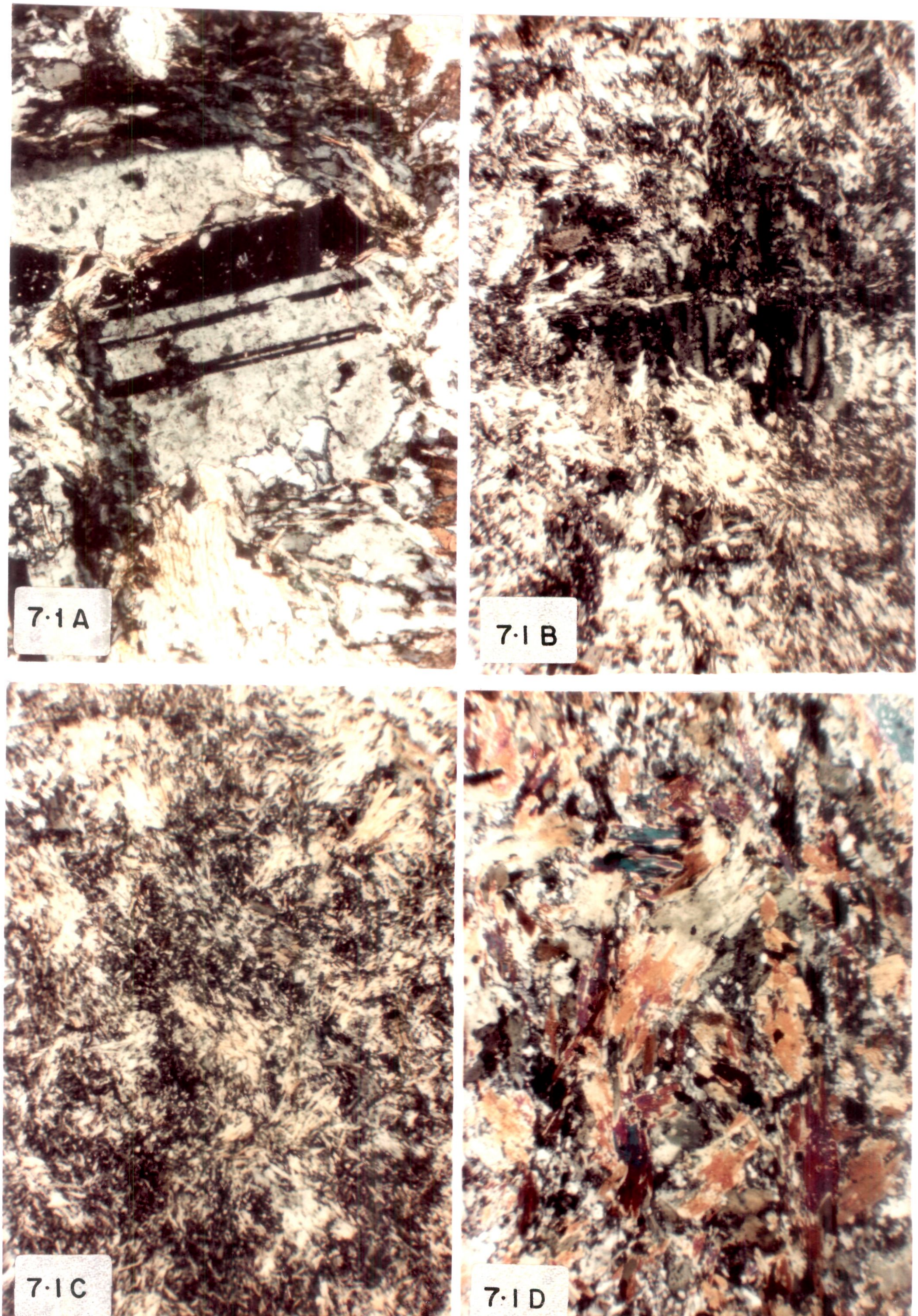
7·1A
7·1B
7·1C
7·1D

Figure 7.2A. Photomicrograph of acid volcanic showing typical porphyritic texture with microcrystalline groundmass and porphyroblast of plagioclase (X 100).

Figure 7.2B. Photomicrograph showing altered plagioclase prophyroblast in acid volcanic (X 35).

Figure 7.2C. Photomicrograph showing development of schistosity in acid volcanic. Sheet silicates may be noticed deflected around quartz phenocryst (X 100).

Figure 7.2D. Photomicrograph showing presence of calcite as a replacement mineral in acid volcanic (X 100).

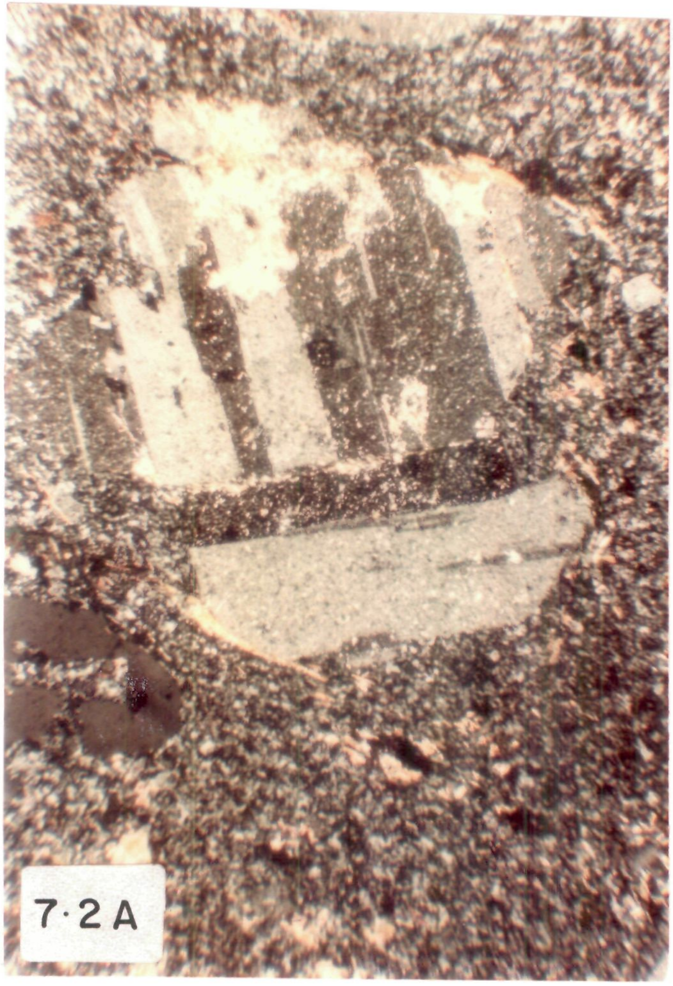
7·2 A

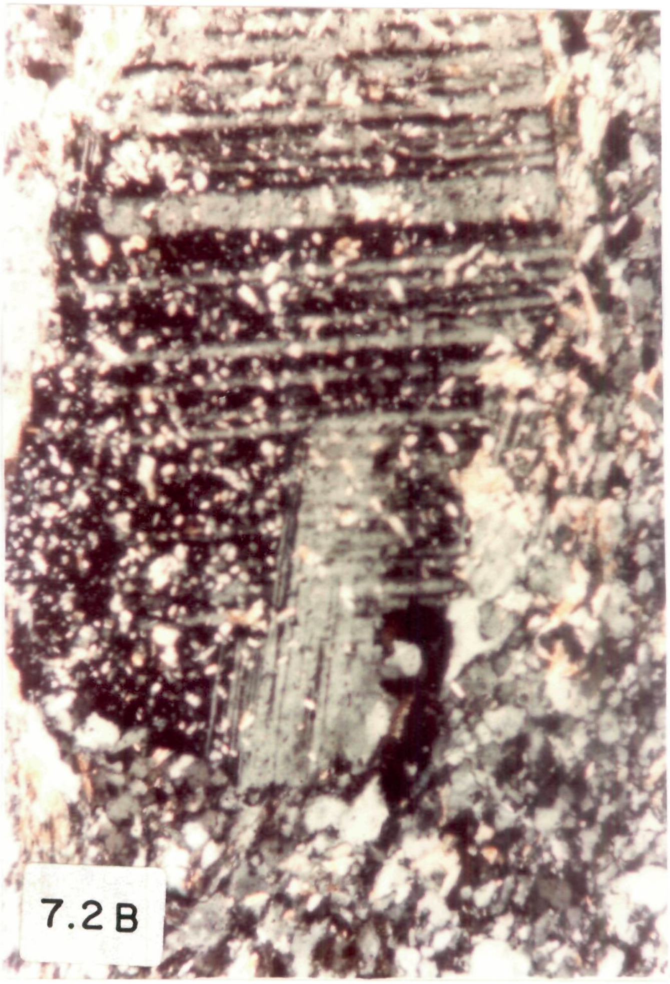
7.2 B

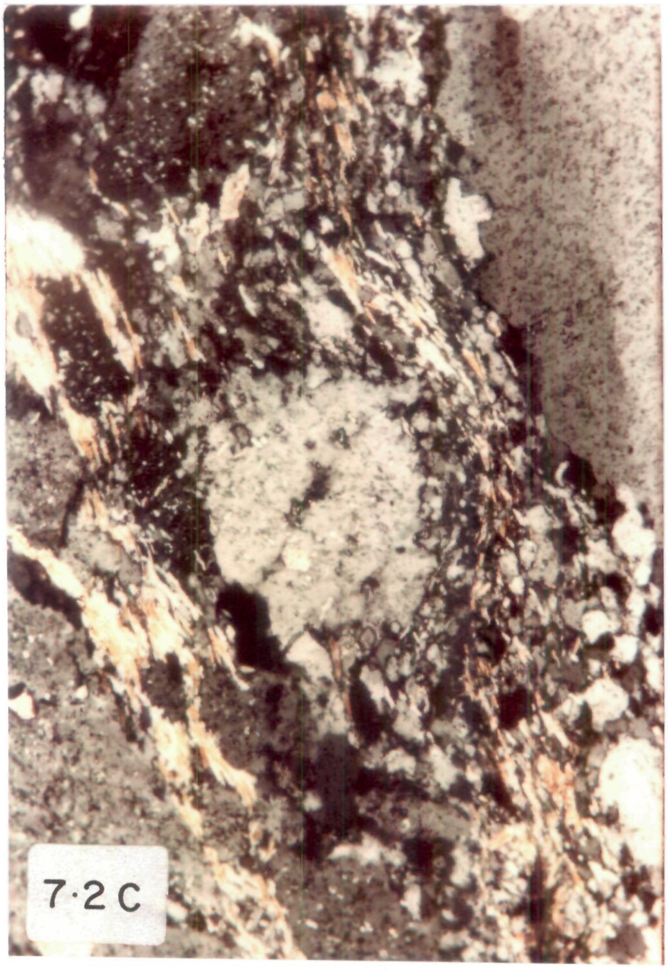
7·2 C

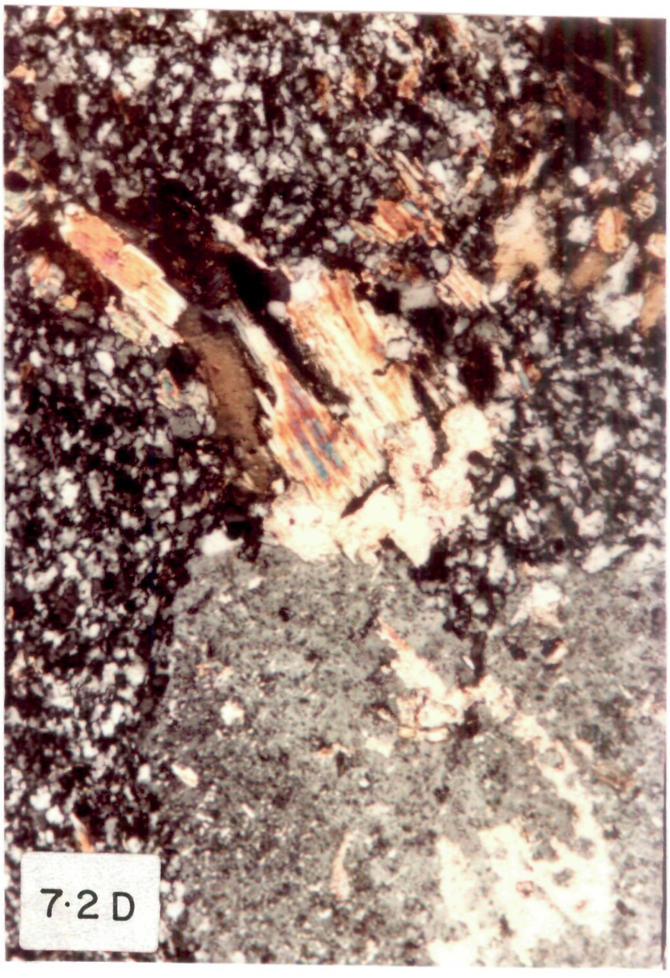
7·2 D

2) RKY 10 - quartz + actinolite + chlorite + albite + sphene + calcite + ilmenite + epidote

3) RKL 16 - quartz + albite + chlorite + muscovite + calcite + ilmenite + magnetite

4) RKL 44 - quartz + albite + chlorite + muscovite + calcite + ilmenite + magnetite

The electron probe microanalysis of the volcanic rocks from Kushtagi schist belt is given in Table No. 7.1 and 7.2.

7.3.1 Actinolite

Actinolite is one of the most abundant silicate present in metabasalts of Kushtagi schist belt. It is absent in acid volcanics. It is generally euhedral to subhedral, fibrous to columnar in form, pleochroic from pale yellow to green, showing typical cleavages of amphiboles (Fig. 7.3A). The extinction angle varies from 10° to 21°. The chemical composition is given in Table 7.1. According to the classification of Hawthorne (1981), it is ferro-actinolitic hornblende with X_{Mg} around 4.2 (Table 7.1).

7.3.2 Albite

Albite is present in both acid (Fig. 7.2A and B) and basic (Fig. 7.1A and B) volcanics and shows similar optical characters. It is colourless and exhibits repeated twinning on the albite law. The extinction angle ranges from 0° to 10°. In basic volcanics, it is minor in amount and occurs as euhedral phenocrysts and in prismatic form, whereas in acid volcanics, it is present in substantial amount in the form of phenocrysts of coarse to medium

TABLE 7.1 REPRESENTATIVE ELECTRON MICROPROBE ANALYSES OF SAMPLE No. RN-17

	1	2	3	4	5	6	7
N	3	4	2	3	2	4	2
SiO_2	25.84	48.54	0.09	31.12	0.03	65.58	38.84
Al_2O_3	20.76	5.47	0.04	1.29	0.15	20.49	24.63
TiO_2	0.06	0.18	0.03	37.52	64.57	0.09	0.09
FeO^*	34.30	22.04	0.53	0.63	31.56	0.18	11.41
MnO	0.35	0.31	0.37	0.02	2.09	0.01	0.13
MgO	10.02	8.86	0.01	0.02	0.04	-	0.02
CaO	0.14	12.19	55.40	28.95	0.07	0.83	24.29
Na_2O	0.08	0.69	-	0.06	0.07	11.65	-
K_2O	0.12	0.29	0.05	0.08	0.08	0.09	0.03
Total	91.67	98.57	56.52	99.69	98.66	98.92	99.44
Oxygens	28	23	6	20	6	32	13
Si	5.452	7.305	0.009	4.077	0.001	11.663	3.214
Al^{IV}	2.548	0.695	0.005	0.199	0.008	4.296	2.403
Al^{VI}	2.616	0.275	-	-	-	-	-
Ti	0.010	0.020	0.002	3.697	2.315	0.012	0.006
Fe^{2+}	6.053	2.774	0.044	0.069	1.258	0.027	0.790
Mn	0.063	0.040	0.031	0.002	0.084	0.002	0.009
Mg	3.151	1.987	0.001	0.004	0.003	-	0.002
Ca	0.032	1.966	5.891	4.064	0.004	0.158	2.154
Na	0.033	0.201	-	0.015	0.006	4.017	-
K	0.032	0.056	0.006	0.013	0.005	0.020	0.003
Total	19.989	15.318	5.990	12.141	3.685	20.196	8.581
X_{Mg}	0.34	0.42	-	-	-	-	-
X_{Fe}	0.66	-	-	-	-	-	-
Ab Mol.%	-	-	-	-	-	95.76	-
An	-	-	-	-	-	3.77	-
Or	-	-	-	-	-	0.48	-

* Total Fe reported as FeO

N : Number of spots analysed on an individual grain

X_{Mg} = Mg/(Mg+Fe)

X_{Fe} = Fe/(Fe+Mg)

1 = Chlorite; 2 = Actinolite; 3 = Calcite; 4 = Sphene;
5 = Ilmenite; 6 = Albite; 7 = Epidote

TABLE 7.1 (Contd...) SAMPLE No. RKY-10

	1	2	3	4	5	6	7
N	3	3	4	3	3	2	2
SiO_2	48.73	26.59	31.20	64.97	0.05	39.35	0.04
Al_2O_3	4.79	20.83	1.18	21.13	-	23.95	-
TiO_2	0.16	0.05	38.49	0.04	52.17	0.14	0.01
FeO^*	21.74	33.32	0.85	0.06	43.56	11.47	0.75
MnO	0.34	0.42	0.06	0.02	3.64	0.20	0.62
MgO	9.19	10.51	0.05	0.01	0.01	-	0.09
CaO	12.56	0.10	28.72	0.54	0.28	23.24	57.10
Na_2O	0.63	0.05	0.04	12.72	0.13	0.34	0.03
K_2O	0.24	0.05	0.08	0.12	0.05	0.04	0.03
Total	98.38	91.92	100.67	99.61	99.89	98.73	58.67
Oxygens	23	28	20	32	6	13	6
Si	7.347	5.549	4.050	11.522	0.003	3.273	0.004
Al^{IV}	0.653	2.451	0.181	4.418	-	2.349	-
Al^{VI}	0.198	2.674	-	-	-	-	-
Ti	0.018	0.008	3.757	0.005	1.986	0.009	0.001
Fe^{2+}	2.741	5.816	0.092	0.009	1.844	0.798	0.060
Mn	0.043	0.074	0.007	0.003	0.156	0.014	0.050
Mg	2.065	3.269	0.010	0.003	0.001	-	0.013
Ca	2.029	0.022	3.994	0.103	0.015	2.071	5.863
Na	0.184	0.020	0.010	4.374	0.013	0.055	0.006
K	0.046	0.013	0.013	0.027	0.003	0.004	0.004
Total	15.325	19.897	12.114	20.464	4.020	8.573	6.000
X_{Mg}	0.43	0.36	-	-	-	-	-
X_{Fe}	-	0.64	-	-	-	-	-
Ab Mol.%	-	-	-	97.11	-	-	-
An	-	-	-	2.29	-	-	-
Or	-	-	-	0.60	-	-	-

* Total Fe reported as FeO

N = Number of spots analysed on an individual grain

X_{Mg} = Mg/(Mg+Fe)

X_{Fe} = Fe/(Fe+Mg)

1 = Actinolite; 2 = Chlorite; 3 = Sphene; 4 = Albite;
5 = Ilmenite; 6 = Epidote; 7 = Calcite

TABLE 7.2 REPRESENTATIVE ELECTRON MICROPROBE ANALYSES OF SAMPLE NO. RKL-16

	1	2	3	4	5	6	7	8
SiO_2	64.00	63.82	26.40	28.88	46.50	0.89	0.47	0.32
Al_2O_3	21.66	23.51	24.26	19.17	30.71	0.13	-	0.34
TiO_2	0.02	-	0.10	0.57	0.20	53.89	-	-
FeO^*	0.03	0.04	23.84	23.63	4.17	40.33	90.55	0.67
MnO	-	0.03	0.32	0.18	0.05	2.71	-	0.60
MgO	-	0.02	13.88	14.64	1.47	0.12	0.30	0.58
CaO	3.56	2.37	0.05	0.29	-	0.72	0.58	50.99
Na_2O	10.28	10.53	-	0.01	0.40	0.44	0.26	-
K_2O	0.11	0.36	0.05	0.63	11.24	0.11	0.10	0.08
NiO	-	-	0.04	0.04	-	-	0.02	-
Cr_2O_3	-	-	-	0.09	0.01	0.02	0.02	0.04
Total	**99.66**	**100.68**	**88.94**	**88.13**	**94.75**	**99.36**	**92.30**	**53.62**
Oxygens	32	32	28	28	22	6	32	6
Si	11.365	11.204	5.402	5.986	6.358	0.044	0.193	0.033
Al^{IV}	4.534	4.866	2.598	2.014	1.642	0.008	-	0.042
Al^{VI}	-	-	3.254	2.670	3.308	-	-	-
Ti	0.003	-	0.015	0.089	0.021	2.017	-	-
Fe^{2+}	0.004	0.006	4.079	4.096	0.477	1.679	31.035	0.058
Mn	-	0.004	0.055	0.032	0.006	0.114	-	0.053
Mg	-	0.005	4.232	4.522	0.300	0.009	0.183	0.090
Ca	0.677	0.446	0.011	0.064	-	0.038	0.255	5.661
Na	3.540	3.584	-	0.004	0.106	0.042	0.207	-
K	0.025	0.081	0.013	0.167	1.961	0.007	0.052	0.011
Ni	-	-	0.003	0.003	-	-	0.003	-
Cr	-	-	-	0.015	0.001	0.001	0.006	0.003
Total	**20.148**	**20.196**	**19.664**	**19.661**	**14.179**	**3.959**	**31.934**	**5.950**
X_{Mg}	-	-	0.51	0.53	-	-	-	-
X_{Fe}	-	-	0.49	0.48	-	-	-	-
Ab Mol.%	83.45	87.18	-	-	-	-	-	-
An	15.96	10.85	-	-	-	-	-	-
Or	0.59	1.97	-	-	-	-	-	-

* Total Fe reported as FeO

X_{Mg} = Mg/(Mg+Fe)

X_{Fe} = Fe/(Fe+Mg)

1 = Albite (coarse grained); 2 = Albite (medium grained);
3 = Chlorite (coarse grained); 4 = Chlorite (fine grained);
5 = Muscovite; 6 = Ilmenite; 7 = Magnetite; 8 = Calcite

TABLE 7.2 (Contd...) SAMPLE NO. RKL-44

	1	2	3	4	5	6	7	8	9
SiO_2	65.61	65.74	47.38	26.91	26.77	0.89	0.21	0.20	0.04
Al_2O_3	20.76	21.70	31.66	23.09	21.91	0.22	-	0.08	-
TiO_2	-	0.06	0.10	0.10	0.13	56.39	51.43	-	0.01
FeO^*	-	0.03	3.08	25.72	28.17	38.05	43.39	91.70	0.14
MnO	-	-	0.02	0.50	0.35	2.68	3.26	0.02	0.55
MgO	0.01	-	1.68	12.12	10.59	0.33	0.01	-	0.02
CaO	1.04	0.56	-	0.07	0.11	0.72	0.20	-	56.14
Na_2O	11.86	11.38	0.26	-	0.11	0.22	0.01	0.04	0.15
K_2O	0.33	0.11	11.01	0.05	0.07	0.13	0.12	0.01	0.06
NiO	-	-	-	0.10	-	0.01	0.08	0.10	0.03
Cr_2O_3	0.10	0.03	-	0.07	-	-	0.15	0.08	0.01
Total	99.71	99.61	95.19	88.73	88.21	99.64	98.86	92.23	57.15
Oxygens	32	32	22	28	28	6	6	32	6
Si	11.607	11.577	6.384	5.580	5.662	0.044	0.011	0.083	0.004
Al^{IV}	4.330	4.505	1.616	2.420	2.338	0.013	-	0.039	-
Al^{VI}	-	-	3.413	3.225	3.125	-	-	-	-
Ti	-	0.008	0.010	0.016	0.021	2.075	1.978	-	0.001
Fe^{2+}	-	0.004	0.347	4.460	4.983	1.557	1.855	31.695	0.012
Mn	-	-	0.002	0.088	0.063	0.111	0.141	0.007	0.046
Mg	0.003	-	0.337	3.746	3.338	0.024	0.001	-	0.003
Ca	0.197	0.106	-	0.016	0.025	0.038	0.011	-	5.910
Na	4.068	3.886	0.068	-	0.045	0.021	0.001	0.032	0.029
K	0.074	0.025	1.893	0.013	0.019	0.008	0.008	0.005	0.008
Ni	-	-	-	0.008	-	-	0.002	0.016	0.001
Cr	0.014	0.004	-	0.011	-	-	0.006	0.026	0.001
Total	20.283	20.115	14.071	19.583	19.618	3.890	4.013	31.903	6.013
X_{Mg}	-	-	-	0.46	0.40	-	-	-	-
X_{Fe}	-	-	-	0.54	0.60	-	-	-	-
Ab Mol.%	93.75	96.74	-	-	-	-	-	-	-
An	4.54	2.64	-	-	-	-	-	-	-
Or	1.71	0.62	-	-	-	-	-	-	-

* Total Fe reported as FeO

X_{Mg} = Mg/(Mg+Fe)

X_{Fe} = Fe/(Fe+Mg)

1 = Albite (medium grained); 2 = Albite (coarse grained);
3 = Muscovite; 4 = Chlorite (medium grained);
5 = Chlorite (coarse grained); 6 = Ilmenite;
7 = Ilmenite; 8 = Magnetite; 9 = Calcite

grain size and are usually euhedral in shape. It is also present in ground mass.

The albite mol. % in acid volcanics is lower, having slight affinity towards oligoclase; ranges from 83% to 97%, whereas, it is always high (>95%) in basic volcanics. The Na-rich plagioclase appears to be a product of crystallization from magma containing unusually large amount of volatiles, notably water (Deer et al,. 1979). As with the outset of metamorphism the composition of plagioclase changes from low An content to higher An content; the composition of plagioclase in metamorphic rock is generally related to the grade of the host rock. Albite is the stable plagioclase in the zones of low grade of regional metamorphism (Winkler, 1976). The low An content of plagioclase in metavolcanics of Kushtagi schist belt indicate greenschist facies of metamorphism.

7.3.3 Chlorite

Chlorite occurs in all sections of both acid and basic volcanics. It is light green in colour and shows pleochroism. Chlorite is abundant in low grade metamorphic rocks, and it is the most characteristic mineral of the greenschist facies. It is generally formed from ferromagnesian minerals. According to the classification of Hey (1954), they are ripidolite in the basic volcanics and the composition varies from ripidolite to pycnochlorite and brunsvigite in acidic volcanics. They are rich in Al but are poor in Mg. The association of Mg-poor chlorite with albite, actinolite and epidote indicates that chlorite is a product of low grade of metamorphism.

7.3.4 Muscovite

Muscovite is present in small quantity only in acid volcanics and occurs in accicular or tabular form. It is colourless to light brownish. High Fe content of muscovite (Table 7.2) is probably the cause for this body colour. The Ti content in muscovite increases with grade of metamorphism (Guidotti, 1984), therefore, the low Ti content of muscovites in the present study indicates a low grade of metamorphism.

7.3.5 Epidote

Epidote shows high refractive index, slight pleochroism and is present in the basic volcanics of the Kushtagi schist belt. It is absent in the acid volcanics of the region. Epidote grains are equigranular and subhedral (Fig. 7.3B).

7.3.6 Sphene

Sphene is present only in basic volcanics in a very large amount (5% approx) (Fig. 7.3B). The TiO_2 content of sphene is around 38% and CaO content is around 29% (Table 7.1). The presence of such large amount of sphene along with ilmenite in basic volcanics is consistent with the high TiO_2 content upto 3.19% of whole rock composition (Table 10.1).

7.3.7 Magnetite and Ilmenite

Magnetite is present only in acid volcanics (Fig. 7.3C). It is medium grained showing different shapes. Ilmenite is present in both types of volcanics and shows similar chemical composition. Magnetite and ilmenite have been distinguished on the basis of their chemical composition, as determined by EPMA. The Ti content of magnetite is below detection limit, whereas, that of ilmenite

Figure 7.3A. Photomicrograph of actinolite in metabasalt showing typical cleavages of amphibole (X 100).

Figure 7.3B. Photomicrograph of basic volcanic showing presence of sphene in a very large amount. Presence of equigranular and subhedral epidote grains may be noticed (X 35).

Figure 7.3C. Photomicrograph showing presence of magnetite in acid volcanics (X 100).

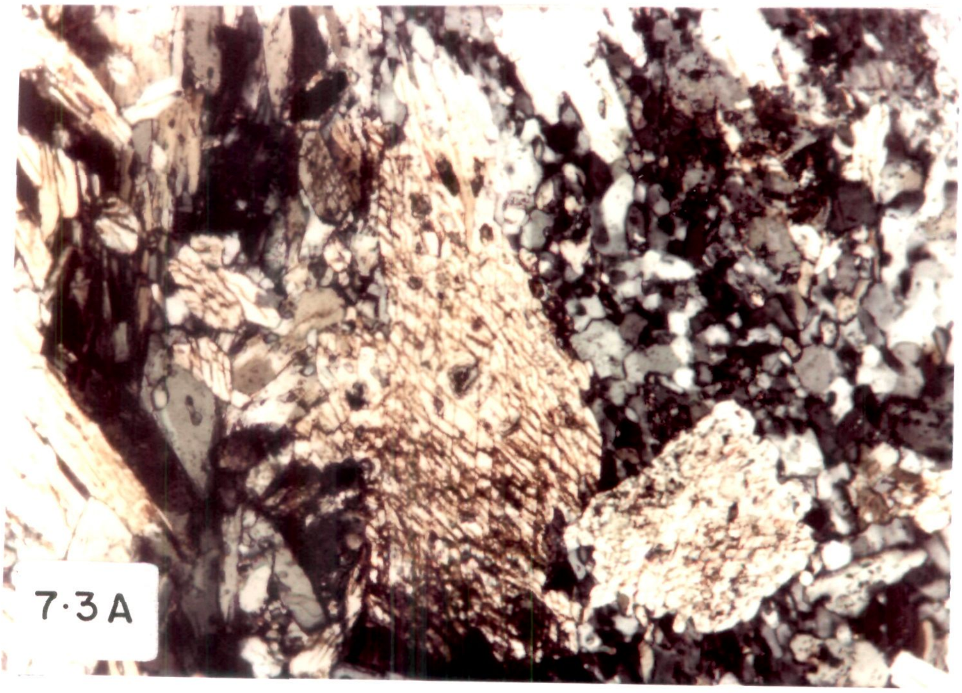
7·3A

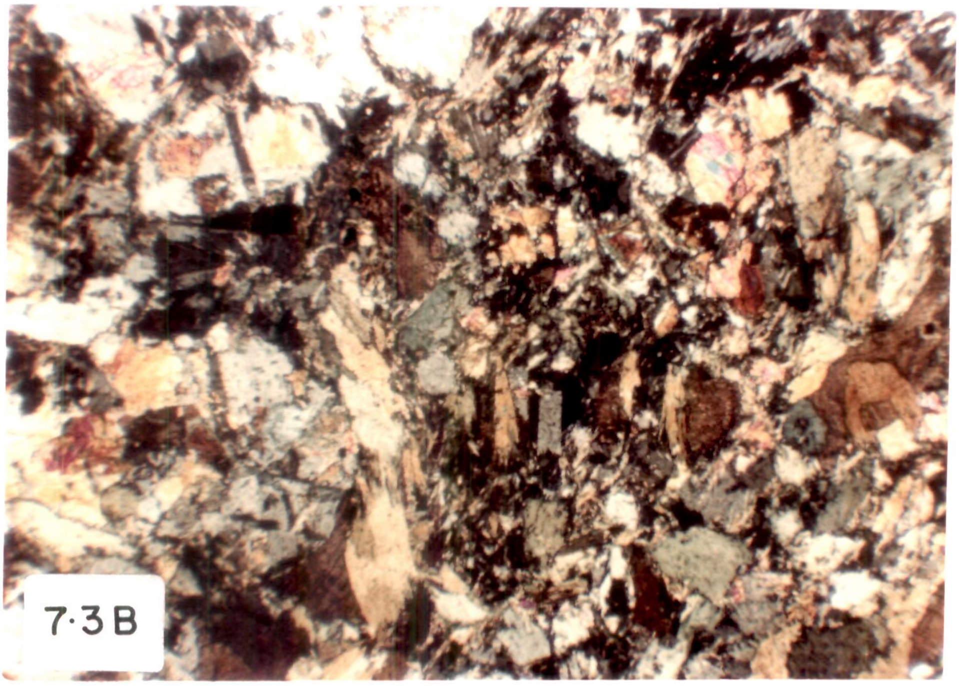
7·3B

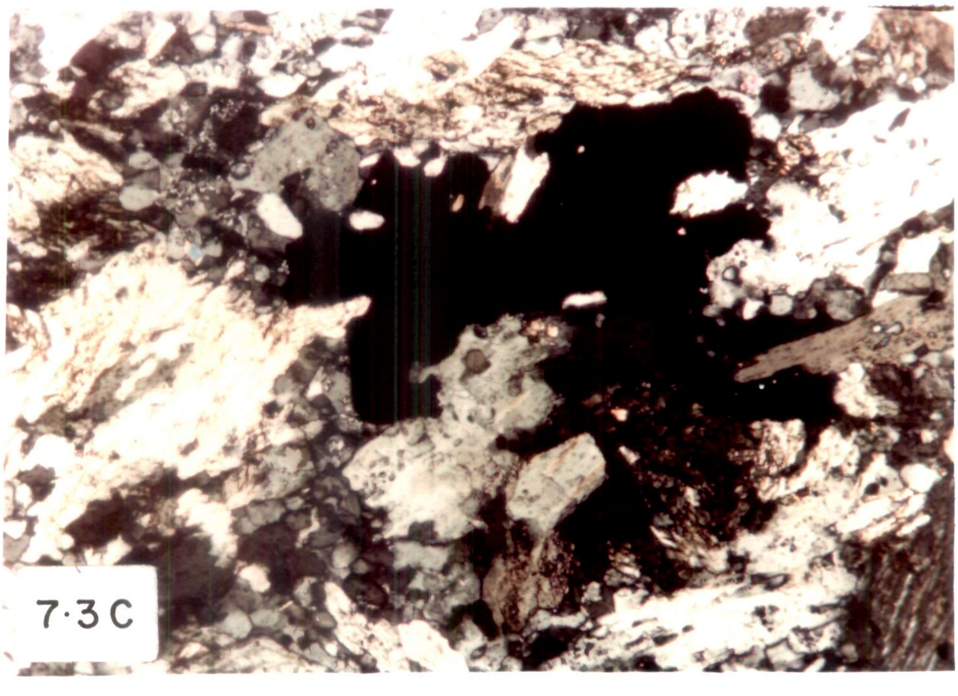
7·3C

ranges from 51.43% to 65.57%. Apart from Ti and Fe, ilmenite also contains substantial amount of Mn ($\simeq$ 2% ; Table 7.1 and 7.2).

7.4 Metamorphism

As no coexisting mineral pair is suitable for geothermobarometry, only a broad generalization of the metamorphic grade of the lithologies is possible in the present study. The characteristic mineral assemblage of basic volcanics viz. albite $\pm$ actinolite $\pm$ Mg-poor chlorite $\pm$ epidote and absence of Ca-plagioclase, hornblende, biotite and garnet suggests low grade regional metamorphism for these rocks (Winkler, 1976). The mineral assemblage present in the basic volcanics of Kushtagi schist belt is characteristic of lower greenschist facies of metamorphism. Further the following chemical characteristics are also indicative of lower greenschist facies;

(1) An content being in the range of An_2 to An_{11}, is indicative of greenschist facies (Winkler, 1976).

(2) Presence of Mg-poor chlorite, as chlorite becomes rich in Mg with grade of metamorphism (Winkler, 1976).

(3) Low Ti content of muscovite is in harmony with Ti content of muscovite of greenschist facies.

Therefore, based on mineral assemblages, a low grade of greenschist facies of metamorphism is inferred for Kushtagi schist belt. The oxygen isotopic data discussed in the subsequent chapter substantiates this inference.

CHAPTER - VIII

ANALYTICAL TECHNIQUES

8.1 Sampling and Sample Selection

Sampling of BIF was mainly dependent on the availability of the open cast mines, exploration pits and fresh outcrops. Total 200 samples of BIF, basic and acid volcanics were collected from various localities for geochemical studies. Absolutely fresh BIF samples were collected from Hiremagi-Ramthal and Aihole-Sulebhavi Iron Ore Mines. Basic volcanics were collected from the hill tops near Kyadaguppi and Mulur. Acid volcanics were collected from road cuttings and nearby exposures around Kalarhatti and Mulur.

8.2 Sample Preparation and Analytical Techniques

Sample preparation and geochemical analysis of the samples were carried out at the Geochemical Laboratories of the National Geophysical Research Institute, Hyderabad. For chemical analysis, about 1000 gm of each rock sample was crushed into gravel-size bits using a hammer. A coarse fraction of about 250 gm was obtained by coning and quartering. These fractions were then crushed to -200 mesh size using a Herzog Swing-Grinding Mill with grinding tools made up of tungsten carbide. For BIF, stainless steel grinding tools were used. Special care was taken in cleaning the jaw crusher and the tungsten carbide/stainless steel mortar by using high purity silica sand followed by crushing a dummy sample to avoid contamination. For determination of oxygen isotopes in BIF, the iron oxide and chert band were slowly chipped off, and from each iron oxide and chert rich fraction, iron oxide and chert were hand picked and their degree of purity was confirmed by examining each grain under Leitz binocular microscope. Iron oxide and chert were powdered in agate mortar. Due to the fine grained nature of hematite absolutely pure chert could not be obtained. The Fe_2O_3 impurities in chert layers were also estimated by XRF.

The major and a few selected trace elements were estimated by X-ray Fluorescence Spectrometer (XRF). The trace element analysis was carried out on Atomic Absorption Spectrometer (AAS) and Inductively Coupled Plasma Mass Spectrometer (ICP-MS) while rare earth concentrations were determined by ICP-MS. Mineral compositions of coexisting phases were determined by Electron Probe Micro analyser (EPMA). Mineralogical study of SBIF was done on XRD. Oxygen isotopic study was carried out on a VG Mass Spectrometer. FeO was determined by titration method.

8.3 Inductively Coupled Plasma-Mass Spectrometer (ICP-MS)

8.3.1 Sample Preparation

0.1 gm of the sample powder was weighed accurately and placed in Teflon beakers with light lids. To each sample, 3 ml concentrated nitric acid (HNO_3) and 7 ml Hydrofluoric acid (HF) were added. The teflon beakers were placed in an oven for four hours at 40°C. Then the lids were removed and the beakers were placed on hot plate at a temperature of 110°C till the solution evaporated to dryness. The residue was dissolved in 10 ml of nitric acid and double distilled water (1:1). Then, 0.1% rock solutions were prepared with an overall concentration of 100 gm/ml of indium, which serves as an internal standard. This solution was used for estimation of all 18 trace elements (including Th and U) and REE concentration.

8.3.2 Instrumentation

The instrument consists mainly of a standard inductively coupled plasma torch (Fassel-type), a quadrupole mass filter and an interface unit consisting of two water cooled nickel cones.

After minimising the signal on ^{115}In in the single ion mode, the system is operated on a mass scanning mode in the mass range m/z 45-228 covering 18 trace elements (including Th and U), all the 14 REE and the internal standard (indium). Detection limit is calculated using the count rate obtained on the 0.1% solution of the standards.

Operating conditions are as follows :

1. Plasma :

Power	= 1.35 KW
Nebulizer gas	= 0.75 lit/min
Aux. flow rate	= 0.75 lit/min
Coolant flow rate	= 13 lit/min
Sample intake rate	= 1 ml/min

2. MS Conditions :

Vacuum stage 1	- <2.5 m bar
Vacuum stage 2	- $<10^{-4}$ m bar
Vacuum stage 3	- $<2.10^{-6}$ m bar

3. Scan Conditions :

Mass range	= 113-179 amu
Number of scans	= 120

Dwell time/channel = 500 μs

Number of channels used = 2048

8.3.3 Operating Conditions

Sample solutions were introduced into the ICP with the help of a nebulizer at the rate of 1 ml/min, where the sample is heated to 8000 K and the dissolved solids are vapourised, atomised as well as ionised with a fraction of the ions getting pumped through the interface. While passing through the interface the gases expand adiabatically and are then introduced into the quadrupole mass filters, where an ion beam passes through the skimmer cones as well as a number of plates at appropriate potentials. Electrostatic fields created by these plates focus the ion beam into a form suitable for transmission through the mass filters. There is a linear relationship between the ion beam and the concentration of elements and the resultant signals are converted into concentrations by using an online IBM PC/XT microcomputer.

Elemental concentration for the standard reference rocks such as FER-1, FER-2, FER-3, FER-4, IF-G, GSR-5, SCo-1, JR-1, JR-2, JG-2, BR and JB-1a are in good agreement with reported values. Precision is better than 5% RSD (Relative Standard Deviation). For detailed procedure and accuracy, see Balaram et al. (1988, 1990).

8.4 X-Ray Fluorescence

8.4.1 Sample Preparation

Two types of sample pellets in the form of (A) fused beads and (B) pressed discs were prepared. The procedure adopted are as follows :

(A) Fused Pellet (beads)

0.5 gm of -200 mesh sample powder was thoroughly mixed with 2.5 gm of flux (lithium tetraborate + lithium metaborate + lanthanum oxide in the ratio of 6:3:1) in a platinum gold crucible (Pt : Au :: 95:5) and heated for about 20 minutes in a Herzog automatic fusion machine (HAG 12/1500) at 1200°C. The crucible containing the sample and flux was tilted bothways with the help of a built in rocking device for 10 minutes, while heating was on, in the fusion chamber (a) to remove air bubbles and (b) also to obtain a homogenous melt. The crucible containing the melt was cooled gradually by exposing it to a flow of filtered air and vacuum suction simultaneously. The resultant pellet was of 31 mm diameter. Pellets prepared by this fusion technique were used to estimate the major elements in the samples except for Na_2O because lanthanum oxide present in the flux interferes with Na_2O. Therefore pressed pellets were used to estimate the sodium content, flux to sample ratio was changed from 1:2 in acidic samples to 1:5 in basic samples.

(B) Pressed Pellet

Collapsible aluminium cups were filled with 9 gm of boric acid which acts as binding material. 1 gm of -200 mesh sample powder was sprayed on it, uniformly covering the boric acid and about 15 tonnes of pressure was applied using a Herzog hydraulic press (H/100) to obtain a 40 mm diameter pellet. Such pellets were used to estimate Na_2O as well as the trace elements Zr, Y, Sr, Rb, Ba and V.

8.4.2 <u>Instrumentation</u>

Philips PW 1400 microprocessor controlled wavelength dispersive, sequential X-ray fluorescence spectrometer (Philips, Holland) with 100 KvA X-ray generator was used for analysis. It also incorporates a 72 position automatic sample changer for loading and unloading of sample pellets and has a four position internal sample turret, in which four samples can be loaded at a time. A Philips model P851 on line, dedicated computer was used to prepare calibration curves relating the concentration and intensity levels in standards as well as the unknown samples after due matrix corrections.

Software available in the computer is able to take care of dead time, background and line overlap corrections giving the output directly as concentration in oxide weight percentages or in ppm as required, after converting the counts into concentration with the help of the calibration curves. There is also a provision for calculating correction factors such as the intensity based corrections on the Lucas-Tooth-Pyne model and concentration based corrections on the DeJong and Resberry-Heinrich models. Reference iron ore standards prepared by the Geological Survey of Canada samples analysed by different methods at the Kudremukh Iron Company, Karnataka were used to prepare calibration curves for major element data of BIF. JR-1, JG-2, JG-1a, GSR-4, Cr-1a, CT-1A, JB-1a, JB-2, JA-1, JGb-1, GSR-3, GSR-5 and JB-3 standards were used to calibrate the major elements data for acid volcanics granites, basic volcanics and shales. For trace element analysis a series of synthetic standards were prepared besides using reference standards from Canada to build the calibration curves (Govil and Gnaneshwar Rao, 1991). The major element data estimated by XRF are reproducible with a precision range of ± 1% and for the trace elements it is ± 5% (Govil, 1985).

8.4.3 Operating Conditions

A spinner was used to spin the samples inside the spectrometer while measuring, to obtain uniform counts. Certain elements were analysed by using a Rhodium target X-ray tube while Na, Al and Mg were estimated by a Chromium X-ray target tube since the concentration levels of these elements were very low. P_{10} (90% Ar + 10% CH_4) gas was pumped in the flow proportional counter for ionisation and a polypropylene counter window of 1 µm was used. All the elements were estimated under vacuum media (20 pascal units).

8.5 Electron Probe Micro Analysis

8.5.1 Slide Preparation

Doubly polished sample thin sections of 0.03 mm thickness were prepared on 46 mm long glass slides without the cover slip by grinding and polishing moderately thin slabs of the rock samples using chromium and aluminium oxide powders on a glass plate as well as a metal disc covered with chamois leather. Carbon coating of 150°A units thickness was given to the sample by the carbon evaporation technique in a Hindivac Shadow Casting Unit at 10^{-6} Torr vacuum for obtaining uniform electrical conductivity.

8.5.2 Instrumentation

To determine the composition of minerals and estimation of P-T-t conditions, "CAMEBAX-MICRO" (Cameca, France) electron probe was used. The electron microprobe consists of three fully focussing spectrometers (two vertical and one inclined). It has a central gun column housing the inverted 'V' shaped tungsten filament (source of the electron beam) and the Wehnelt, the anode and the electromagnetic lenses which control the size and the shape of the electron bean on its way to the sample surface. There is a co-axial binocular microscope to bring the sample into the field of view. A sample chamber with a movable stage which can take samples either as thin sections or as mounted discs is an integral part of this instrument.

8.5.3 Operating Conditions

The operating conditions were 15 KV accelerating voltage 4.2 nA sample current, 20 seconds counting time with a beam diameter of 1-3 μm. The corrections, using the method of Henoc and Maurice (1978) were applied with the help of the PDP 11/03 computer. Analytical concentrations in the form of oxide wt.% were derived by applying intensity data of samples to a calibration curve established from intensity data of the standards. Precision was of the order of ± 0.5 - 2.0% of the amount for major constituents.

Following elemental and synthetic standards were used for corresponding elemental analysis at suitable wavelengths :

Elements	Standards	Wavelength	Crystal
Na_2O	Albite	46363	TAP
K_2O	Orthoclase	42765	PET

CaO	Wollastonite	38387	PET
SiO_2	Wollastonite	27737	TAP
MgO	MgO*	38499	TAP
Al_2O_3	Al_2O_3*	32463	TAP
Cr_2O_3	Cr_2O_3*	56866	LIF
MnO	$MnTiO_3$*	52200	LIF
TiO_2	$MnTiO_3$*	31416	PET
$FeO^{(t)}$	Fe_2O_3	48083	LIF
BaO	Barite	31730	PET

* = Synthetic standards

8.6 X-Ray Diffraction Analysis (XRD)

XRD study of SBIF was carried out at Indian Institute of Chemical Technology, Hyderabad. Minerals were analysed on a Phillips X-ray diffractometer (PW 1730/PW-1390) with a proportional counter using Ni-filtered Cu-Kα radiation (= 1.5416°A) with 40 KV and 20 mA. The chart speed was 1-2 cm/min and the goniometer speed was 1°/minute.

8.7 Stable Isotope Mass Spectrometry

The fluorinating line for extraction of oxygen from silicates and oxides is similar to that designed by Clayton and Mayeda (1963) with a minor modifications (Das Sharma et al., 1993). A typical sample run is made as follows : Previously deccicated sample is weighed (3-8 mg) and loaded quickly in the nickel reaction vessel in an atmosphere of argon. The argon present in the vessel prevents any contamination of atmospheric oxygen or moisture during sample loading. The line is evacuated slowly with rotary and diffusion pump combination. The loaded sample is heated to about 150-200°C for two hours during pumping. This ensures expulsion of absorbed moisture by the sample and a vacuum of the order of 10^{-5} torr is obtained. An aliquot of twice distilled BrF_5 is expanded in the known volume (usually in the ratio 5:1) and is transferred to the nickel reaction vessel using liquid nitrogen. The valve of the reaction vessel is closed. The sample is then heated to about 550°C (chert) and 625°C (hematite) for 12-20 hours to liberate oxygen. The liberated oxygen is converted to CO_2, measured manometrically for its yield and collected in the sample collection bottle. After every 4 or 5 sample runs, usually the reaction vessel is dismantled from the line and cleaned. Two blank runs (without sample) are performed in which the first blank yield is more because of exposure of the reaction vessel to the atmosphere and the second blank is usually less than 0.5μmole. Following the second blank run, the reaction vessel is ready for next batch of sample run.

The CO_2 obtained is analysed by VG Mass Spectrometer having triple collector and updated to computer control using SIRA software. The sample and reference gases are alternately led into the ion source by a changeover valve. While one gas is being analysed the other gas is pumped away through the bleed pump. The gas to be analysed is ionized by bombarding with electrons emitted from a filament. The positively charged ions are then accelerated by applying an accelerating voltage of a few Kv and the beam is directed towards a magnetic field which acts in a direction perpendicular to the ion beam. Ions of different masses are separated based on the m/e ration, and collected by the Farady cup collectors for final ration calculations by using the online computer. This is the molecular ratio of masses 44, 46 which are to be corrected to get the real isotopic ratio i.e. $^{18}O/^{16}O$. Different correction as recommended by Mook (1968) and changeover valve leakage correction as suggested by the manufacturers were applied.

The $\delta^{18}O$ is reported in %. with respect to the Standard Reference Material (SMOW). The δ values are calculated on the basis of the following equation.

$$\delta^{18}O = \frac{R_{(sample)} - R_{standard)}}{R_{standard)}} \times 10^3$$

where, $R_{(sample)}$ = $^{18}O/^{16}O$ ratio in the sample

$R_{(standard)}$ = $^{18}O/^{16}O$ ratio in the standard

During the course of the analysis of the present samples, two NBS 28 quartz standard gave $\delta^{18}O$ = 9.7 and 9.9%. as against reported value of 9.64%. relative to SMOW.

CHAPTER - IX

GEOCHEMISTRY OF BIF

9.1 General Statement

The major, trace and rare earth elements (REEs) characteristics of the BIFs from Kushtagi schist belt are discussed in this chapter. The chemical data (Tables 9.1 and 9.2), are plotted on different geochemical variation diagrams and the North American Shale Composite (NASC) normalized REEs are plotted on Masuda-Coryl diagram to understand the genesis of the banded iron formation from the studied area. BIFs are essentially chemical sediments and mainly consists of Fe_2O_3(T) and SiO_2 but they are drastically affected by clastic input.

9.2 Behaviour of Major Elements

Major element composition of BIF show significant variation in iron and silica content depending upon the thickness of rhythmic bands and also on the type of the minerals present in these bands. The data show considerable amount of enrichment in Fe_2O_3, SiO_2 and Al_2O_3 and depletion in all other major oxides (Table 9.1 and 9.2). On the basis of Al_2O_3 content the samples are grouped as Cherty Banded Iron Formation (CBIF) and Shaly Banded Iron Formation (SBIF). CBIF contain more than 15% Fe_2O_3 and rest is SiO_2, SBIF contains Fe_2O_3 more than 15% and Al_2O_3 more than 3%. Gnaneshwar Rao and Naqvi (1993) and Manikyamba et al. (1993) have given Al_2O_3 content of 5% as dividing line between CBIF and SBIF. Generally, all BIFs show decrease in their iron content with the increase in silica content (Fig. 9.1) and the

TABLE 9.1 CHEMICAL COMPOSITION OF THE CHERTY BANDED IRON FORMATION

Element	RHR-1	RHR-2	RHR-3	RHR-4	RHR-5	RHR-6	RHR-7	RHR-8	RHR-9	RHR-10
SiO_2 (Wt.%)	18.69	29.61	30.64	55.01	51.32	40.24	50.01	71.80	46.82	41.52
TiO_2	0.04	0.06	0.04	-	-	0.03	-	0.03	-	0.04
Al_2O_3	0.46	0.54	0.62	0.37	0.39	0.40	0.48	0.31	-	0.20
Fe_2O_3	80.88	70.02	68.78	44.91	48.26	58.32	48.41	26.71	51.08	58.08
FeO	-	0.04	0.04	0.12	0.16	-	-	-	0.04	0.04
MnO	-	-	-	-	-	-	-	-	-	-
MgO	0.04	0.01	-	0.02	0.01	-	0.05	0.03	0.05	-
CaO	-	0.03	0.02	0.01	0.02	-	0.03	-	0.01	-
Na_2O	0.01	-	-	-	0.03	0.02	0.01	0.04	0.02	0.02
K_2O	-	0.01	0.03	0.02	0.01	0.03	-	0.01	0.02	0.01
P_2O_5	-	-	0.02	0.02	-	0.01	0.03	0.03	0.02	0.03
LOI	1.00	1.00	-	-	-	0.50	-	1.00	1.00	0.50
Total	**101.12**	**101.32**	**100.19**	**100.48**	**100.20**	**99.55**	**99.02**	**99.96**	**99.06**	**100.44**
Sc (ppm)	1.11	0.90	0.87	0.68	0.93	0.64	1.55	0.85	0.79	0.77
V	9.53	10.34	6.68	7.62	8.30	6.50	7.14	9.55	7.79	8.21
Cr	137.98	149.86	187.91	172.58	169.83	138.76	135.85	164.26	211.04	145.26
Co	1.45	1.68	1.47	1.59	1.51	1.44	1.35	2.08	1.31	1.26
Ni	8.21	8.96	7.07	7.19	6.34	8.83	6.55	7.48	7.23	4.59
Cu	98.61	116.54	2.05	162.55	124.88	2.46	4.12	166.09	82.57	147.53
Zn	7.06	7.59	-	6.20	1.98	-	-	1.73	1.54	3.70
Ga	1.87	1.27	1.37	1.26	1.36	1.35	1.24	0.87	0.77	0.72
Rb	0.83	0.69	0.37	0.59	0.41	0.19	0.18	0.28	0.16	0.18
Sr	16.24	8.41	5.76	20.82	28.66	14.10	21.77	38.39	5.09	5.33
Y	8.47	4.09	4.74	3.71	21.32	6.58	5.59	4.94	2.09	1.85
Zr	10.24	4.77	8.56	3.93	6.16	6.57	4.75	4.93	2.32	1.73
Nb	0.76	0.25	0.44	0.17	0.39	0.36	0.22	0.31	0.08	0.10
Ba	10.69	23.44	1.05	9.93	38.01	8.86	15.62	43.41	5.72	2.94
Hf	0.25	0.14	0.19	0.11	0.25	0.21	0.18	0.18	0.09	0.06
Ta	0.06	0.01	0.01	-	0.02	0.02	0.02	0.02	-	0.01
Th	1.45	0.89	0.75	0.67	0.51	0.45	0.31	0.41	0.18	0.22
U	1.05	1.02	0.50	0.71	0.62	0.19	0.16	0.74	0.57	0.49
La	6.84	3.51	2.32	3.88	6.82	9.44	1.68	5.83	3.14	1.62
Ce	11.52	4.82	4.32	6.50	11.61	11.06	3.49	10.04	4.14	2.34
Pr	1.08	0.43	0.43	0.59	1.26	0.95	0.35	0.98	0.45	0.23
Nd	3.98	1.91	1.62	2.40	4.73	3.19	1.80	3.81	1.50	0.92
Sm	0.69	0.35	0.29	0.60	1.19	0.39	0.64	1.03	0.34	0.31
Eu	0.63	0.31	0.31	0.36	0.61	0.43	0.50	0.70	0.20	0.17
Gd	0.94	0.65	0.44	0.63	1.16	0.63	0.58	1.01	0.32	0.36
Tb	0.14	0.09	0.08	0.10	0.22	0.11	0.09	0.14	0.05	0.06
Dy	0.99	0.60	0.60	0.63	1.68	0.80	0.63	0.84	0.34	0.38
Ho	0.18	0.09	0.11	0.11	0.34	0.15	0.11	0.13	0.06	0.07
Er	0.47	0.27	0.41	0.34	1.28	0.53	0.36	0.38	0.19	0.21
Tm	0.08	0.03	0.07	0.05	0.22	0.08	0.05	0.05	0.03	0.03
Yb	0.51	0.19	0.46	0.28	1.51	0.54	0.32	0.27	0.16	0.18
Lu	0.08	0.04	0.07	0.03	0.22	0.05	0.05	0.05	0.03	0.03
SiO_2/Fe_2O_3	0.23	0.42	0.46	1.23	1.06	0.69	1.03	2.87	0.92	0.72
Zr/Hf	40.96	34.07	45.05	35.73	24.64	31.29	26.39	27.39	25.78	28.83
$Nd_{(N)}/Yb_{(N)}$	0.73	0.95	0.33	0.81	0.29	0.56	0.53	1.33	0.89	0.48
$L_{(N)}/HREE_{(N)}$	0.57	0.49	0.30	0.58	0.31	0.65	0.37	0.71	0.69	0.38
Eu/Eu^*	2.33	1.94	2.58	1.71	1.53	2.53	2.38	2.06	1.82	1.55
ΣREE	28.13	13.34	11.53	16.50	32.85	28.35	10.65	25.26	10.95	6.91

Element	RHR-11	RHR-12	RHR-13	RHR-14	RHR-15	RHR-16	RHR-17	RHR-18	RHR-19	RHR-20
SiO_2 (Wt.%)	53.85	85.30	27.20	70.56	83.60	49.82	83.82	83.02	82.33	52.38
TiO_2	0.03	0.01	0.09	0.01	0.01	0.03	0.01	0.01	0.01	0.04
Al_2O_3	0.19	-	0.80	0.08	-	-	-	0.10	0.02	0.10
Fe_2O_3	45.99	14.28	71.65	28.96	14.98	50.06	15.01	15.68	16.11	46.26
FeO	-	-	-	0.08	0.04	-	0.08	-	0.04	0.24
MnO	-	-	-	-	-	-	-	-	-	-
MgO	0.05	0.01	0.04	0.03	0.05	0.02	0.04	0.03	0.04	-
CaO	0.01	0.02	0.02	0.03	0.01	-	0.02	0.02	0.01	0.04
Na_2O	-	0.02	0.02	0.02	0.01	0.03	0.04	0.04	0.03	0.02
K_2O	-	0.03	0.03	0.01	0.02	0.02	0.01	0.01	0.02	0.01
P_2O_5	0.02	-	0.02	0.02	0.01	0.01	0.01	0.02	0.02	0.03
LOI	-	-	-	0.50	1.00	0.50	0.50	0.50	1.00	0.50
Total	**100.14**	**99.67**	**99.87**	**100.30**	**99.73**	**100.49**	**99.54**	**99.43**	**99.63**	**99.62**
Sc (ppm)	0.85	0.33	1.79	0.36	0.26	0.99	0.35	0.33	0.40	0.91
V	6.79	3.09	12.17	3.72	3.71	4.83	1.34	2.06	3.47	3.77
Cr	143.76	214.76	109.09	208.69	277.13	159.27	234.41	220.57	239.87	171.77
Co	1.67	2.10	1.84	1.50	1.70	1.53	1.39	1.36	1.87	1.34
Ni	8.29	5.72	7.74	5.33	7.53	5.85	6.40	6.76	6.71	5.65
Cu	104.56	5.21	95.99	1.77	8.43	17.45	4.65	4.75	3.65	3.21
Zn	10.37	-	10.74	-	-	-	-	-	-	-
Ga	1.09	0.45	1.72	0.95	0.33	1.13	0.54	0.35	0.47	1.03
Rb	0.18	0.06	0.39	0.30	0.86	0.71	0.10	0.07	0.63	0.15
Sr	7.72	5.97	20.35	20.98	0.86	8.51	1.33	1.57	7.01	5.50
Y	3.87	3.25	6.71	10.78	0.20	5.31	1.98	1.01	1.59	3.54
Zr	4.81	2.82	16.01	3.38	0.96	9.87	1.57	1.04	2.39	2.91
Nb	0.28	0.12	0.82	0.22	0.12	9.04	0.04	0.04	0.09	0.24
Ba	5.56	-	10.84	29.34	43.63	2.76	-	1.95	4.00	2.00
Hf	0.16	0.11	0.48	0.12	0.04	0.28	0.04	0.03	0.07	0.11
Ta	0.01	-	0.09	0.02	-	0.28	-	-	-	0.03
Th	0.54	0.09	1.16	0.18	0.20	0.85	0.04	0.05	0.11	0.17
U	0.40	0.18	1.18	0.24	0.17	0.49	0.01	0.07	0.20	0.20
La	5.86	0.37	10.45	7.77	0.20	4.34	0.81	2.06	1.51	3.22
Ce	8.79	0.64	15.17	12.94	0.57	7.12	1.23	2.93	1.40	4.42
Pr	0.83	0.06	1.05	1.19	0.07	0.73	0.13	0.41	0.14	0.42
Nd	3.10	0.35	3.55	4.48	0.31	2.89	0.58	1.61	0.56	1.79
Sm	0.69	0.11	0.65	0.73	0.80	0.67	0.11	0.23	0.09	0.39
Eu	0.48	0.07	0.40	0.39	0.03	0.47	0.09	0.19	0.08	0.33
Gd	0.73	0.11	1.02	0.92	0.12	0.73	0.11	0.24	0.15	0.56
Tb	0.11	0.02	0.17	0.14	0.02	0.12	0.02	0.03	0.03	0.09
Dy	0.70	0.21	1.16	0.95	0.12	0.79	0.12	0.21	0.21	0.60
Ho	0.12	0.05	0.21	0.21	0.02	0.14	0.02	0.03	0.04	0.10
Er	0.35	0.22	0.69	0.70	0.06	0.45	0.07	0.11	0.16	0.32
Tm	0.05	0.04	0.10	0.10	0.01	0.06	0.01	0.01	0.03	0.05
Yb	0.28	0.34	0.65	0.61	0.05	0.40	0.07	0.08	0.18	0.27
Lu	0.05	0.05	0.09	0.10	0.01	0.06	0.02	0.01	0.03	0.02
SiO_2/Fe_2O_3	1.17	5.97	0.38	2.44	5.58	1.00	5.58	5.30	5.11	1.13
Zr/Hf	30.06	25.64	33.35	28.17	24.00	35.25	39.25	34.67	34.14	26.46
$Nd_{(N)}/Yb_{(N)}$	1.04	0.10	0.51	0.69	0.56	0.68	0.78	1.89	0.29	0.62
$L_{(N)}/HREE_{(N)}$	0.70	0.12	0.55	0.56	0.31	0.50	0.50	0.93	0.33	0.46
Eu/Eu^*	2.00	1.75	1.43	1.39	0.27	1.96	2.25	2.38	2.00	2.06
ΣREE	22.14	2.64	35.36	31.23	2.56	18.97	3.39	8.15	4.61	12.58

Element	RHR-21	RHR-22	RHR-23	RHR-24	RHR-25	RHR-26	RHR-27	RHR-28	RHR-29	RHR-30
SiO_2 (Wt.%)	75.44	77.34	50.54	67.90	37.89	82.97	54.36	37.08	51.33	83.68
TiO_2	-	0.02	0.03	-	0.03	-	0.04	0.03	0.03	0.01
Al_2O_3	0.48	0.52	0.28	0.32	0.45	0.65	0.56	0.03	0.52	0.09
Fe_2O_3	25.70	21.32	48.82	32.78	61.66	15.59	46.04	61.83	48.08	15.01
FeO	0.04	-	0.16	-	0.04	0.04	0.08	-	-	-
MnO	-	-	-	-	-	-	-	-	-	-
MgO	0.03	0.02	0.02	-	-	0.06	0.04	0.02	0.05	0.03
CaO	-	-	0.03	0.01	0.01	-	0.03	-	-	0.02
Na_2O	0.02	0.01	-	-	0.02	-	0.02	0.03	-	-
K_2O	0.01	0.02	0.03	0.01	-	-	-	0.02	0.02	0.01
P_2O_5	-	0.03	0.04	0.02	0.01	0.01	-	0.05	0.02	0.03
LOI	-	-	0.50	1.00	1.00	0.50	1.00	1.00	0.50	0.50
Total	**101.72**	**99.28**	**100.45**	**102.04**	**101.11**	**99.82**	**102.17**	**100.09**	**100.55**	**99.38**
Sc (ppm)	0.71	1.18	1.30	0.59	0.82	0.70	0.87	0.83	0.99	0.47
V	7.85	5.03	7.74	5.90	11.60	4.21	8.06	10.04	10.92	4.01
Cr	225.96	181.55	160.77	260.38	168.07	249.88	27.83	175.08	200.62	228.46
Co	1.70	1.74	1.75	1.69	2.05	1.62	83.90	2.08	2.43	1.39
Ni	12.20	8.26	8.45	10.22	12.44	12.29	4.82	14.30	8.19	9.18
Cu	5.11	3.54	5.20	6.91	5.85	14.32	5.72	4.12	118.17	7.44
Zn	7.56	7.06	2.34	3.04	6.79	7.72	7.17	5.02	18.21	5.14
Ga	1.05	0.60	1.85	0.78	1.44	0.89	0.75	1.00	1.32	0.56
Rb	0.31	0.34	0.22	0.29	0.19	0.14	0.19	0.27	0.56	0.10
Sr	21.08	5.09	16.73	2.22	4.39	3.23	3.27	4.40	12.54	4.69
Y	4.72	3.26	6.18	1.89	6.76	1.24	2.38	3.13	5.74	1.81
Zr	2.53	2.33	8.48	2.51	6.29	2.23	3.90	2.95	7.85	1.79
Nb	0.27	0.17	0.54	0.24	0.52	0.23	0.30	0.18	0.51	0.19
Ba	25.68	13.76	22.35	5.42	16.70	5.94	5.60	26.04	14.83	14.18
Hf	0.06	0.07	0.12	0.04	0.18	0.04	0.08	0.08	0.21	0.05
Ta	0.01	0.01	0.02	-	0.03	-	0.46	-	0.04	-
Th	0.13	0.11	0.20	0.08	0.26	0.09	0.11	0.16	0.47	0.09
U	0.49	0.36	0.19	0.07	0.56	0.45	0.46	1.17	0.70	0.29
La	2.36	1.06	2.71	2.47	2.14	1.67	3.73	3.77	5.19	0.67
Ce	5.79	2.09	5.83	4.21	3.90	0.83	4.50	6.56	8.58	1.59
Pr	0.41	0.22	0.63	0.37	0.82	0.15	0.49	0.74	0.85	0.18
Nd	1.96	1.44	2.96	1.55	4.76	0.73	1.87	2.92	3.22	0.83
Sm	0.37	0.35	0.65	0.25	0.91	0.18	0.42	0.74	0.65	0.27
Eu	0.25	0.25	0.43	0.22	0.43	0.04	0.27	0.44	0.30	0.12
Gd	0.53	0.52	0.86	0.25	0.95	0.14	0.39	0.59	0.70	0.25
Tb	0.08	0.08	0.13	0.04	0.15	0.02	0.06	0.09	0.11	0.04
Dy	0.51	0.43	0.87	0.30	0.94	0.17	0.36	0.52	0.75	0.27
Ho	0.08	0.08	0.15	0.06	0.16	0.03	0.06	0.08	0.13	0.05
Er	0.25	0.25	0.47	0.19	0.50	0.11	0.18	0.23	0.42	0.15
Tm	0.03	0.03	0.07	0.03	0.07	0.02	0.02	0.03	0.06	0.02
Yb	0.19	0.19	0.39	0.19	0.41	0.11	0.14	0.16	0.38	0.13
Lu	0.04	0.04	0.08	0.03	0.09	0.02	0.04	0.03	0.05	0.03
SiO_2/Fe_2O_3	2.94	3.63	1.04	2.07	0.61	5.32	1.18	0.60	1.07	5.58
Zr/Hf	42.17	33.29	70.67	62.75	34.94	55.75	48.75	36.88	37.38	35.80
$Nd_{(N)}/Yb_{(N)}$	0.97	0.72	0.71	0.77	1.09	0.61	1.27	1.71	0.80	0.60
$L_{(N)}/HREE_{(N)}$	0.51	0.30	0.38	0.62	0.39	0.53	0.76	0.83	0.60	0.36
Eu/Eu^*	1.67	1.79	1.72	2.44	1.39	0.80	1.93	2.00	1.30	1.33
ΣREE	12.85	7.03	10.16	10.16	16.23	4.22	12.53	16.90	21.39	4.60

Element	RHR-31	RHR-32	RHR-33	RHR-34	RHR-35	RHR-36	RHR-37	RHR-38	RHR-39	RHR-40
SiO_2 (Wt.%)	40.88	82.67	30.55	53.58	75.02	49.62	84.60	61.28	49.95	58.78
TiO_2	0.06	-	0.04	-	0.01	-	-	0.04	0.02	0.03
Al_2O_3	0.73	0.58	0.62	0.33	-	0.27	0.31	-	0.59	0.48
Fe_2O_3	57.17	16.37	69.23	46.20	24.39	49.73	15.03	38.05	49.44	40.38
FeO	-	0.04	-	0.04	0.12	0.20	0.12	0.08	-	-
MnO	-	-	-	-	-	-	-	-	-	-
MgO	0.01	0.05	0.05	-	-	0.05	-	0.03	0.05	0.04
CaO	-	-	-	-	0.01	-	-	0.02	0.14	-
Na_2O	-	-	0.04	0.07	0.06	0.06	0.03	-	0.05	0.06
K_2O	-	-	-	-	0.02	-	-	0.01	-	0.03
P_2O_5	-	0.01	0.03	-	0.01	0.03	-	-	0.07	0.01
LOI	1.00	0.50	1.00	1.00	0.50	1.00	-	-	0.50	-
Total	**99.85**	**100.22**	**101.56**	**101.22**	**100.14**	**100.96**	**100.00**	**99.51**	**100.81**	**99.81**
Sc (ppm)	1.54	0.85	1.36	1.24	0.32	0.40	0.30	0.65	0.81	0.55
V	16.81	9.55	9.38	8.03	4.35	4.18	3.93	8.07	8.74	4.91
Cr	138.85	227.24	99.97	171.68	156.32	183.31	270.13	217.11	137.10	220.91
Co	2.75	1.51	1.34	1.38	1.53	1.93	1.37	1.63	2.45	1.61
Ni	11.65	9.12	12.56	7.92	5.61	6.70	10.27	9.16	6.27	7.45
Cu	9.28	144.32	18.01	3.29	1.87	2.12	3.26	136.37	4.71	4.79
Zn	20.71	14.86	7.22	5.61	7.54	6.48	4.53	9.47	5.26	8.34
Ga	2.18	0.93	2.16	1.02	0.45	0.87	0.48	0.68	1.63	0.85
Rb	0.26	0.06	0.14	0.03	0.11	0.05	0.03	0.10	0.21	0.04
Sr	14.58	4.68	8.38	4.86	3.42	7.42	3.33	7.00	4.88	9.90
Y	17.88	2.00	6.65	3.11	1.46	3.54	1.31	2.50	5.92	5.22
Zr	10.60	3.63	7.70	2.81	0.79	1.51	1.11	1.59	11.62	3.26
Nb	0.70	0.31	0.68	0.34	0.11	0.22	0.09	0.12	0.55	0.28
Ba	34.46	4.71	8.70	11.21	9.83	8.29	4.15	9.99	7.38	13.86
Hf	0.28	0.11	0.23	0.08	0.02	0.06	0.04	0.03	0.31	0.11
Ta	0.04	0.01	0.05	0.01	-	0.03	-	0.01	0.04	0.01
Th	0.41	0.20	0.30	0.11	0.06	0.06	0.04	0.07	0.64	0.20
U	0.48	0.74	0.73	0.46	0.52	0.38	0.47	0.57	0.24	0.40
La	2.55	1.05	3.58	1.72	2.95	1.41	0.69	1.45	4.34	0.89
Ce	5.21	1.93	7.61	3.66	4.98	2.70	1.17	2.36	7.82	1.86
Pr	0.56	0.20	0.85	0.38	0.38	0.26	0.14	0.27	0.81	0.23
Nd	2.49	0.71	4.04	1.68	1.28	1.29	0.51	1.24	3.32	0.97
Sm	0.68	0.18	0.89	0.46	0.35	0.50	0.20	0.33	0.70	0.26
Eu	0.47	0.08	0.61	0.33	0.10	0.29	0.06	0.25	0.51	0.16
Gd	0.91	0.15	1.01	0.52	0.25	0.37	0.16	0.44	0.95	0.31
Tb	0.16	0.03	0.15	0.08	0.04	0.06	0.03	0.06	0.14	0.05
Dy	1.22	0.20	0.97	0.54	0.24	0.42	0.20	0.38	0.92	0.35
Ho	0.24	0.04	0.16	0.09	0.04	0.08	0.04	0.06	0.16	0.06
Er	0.88	0.14	0.14	0.30	0.12	0.26	0.12	0.16	0.48	0.21
Tm	0.14	0.02	0.07	0.04	0.02	0.04	0.02	0.02	0.07	0.03
Yb	0.99	0.19	0.38	0.25	0.09	0.24	0.12	0.12	0.40	0.20
Lu	0.18	0.04	0.05	0.04	0.02	0.04	0.02	0.04	0.06	0.05
SiO_2/Fe_2O_3	0.72	5.05	0.44	1.16	3.08	1.00	5.63	1.61	1.01	1.46
Zr/Hf	37.86	33.00	33.48	35.13	39.50	25.17	27.75	53.00	37.48	29.64
$Nd_{(N)}/Yb_{(N)}$	0.24	0.36	0.99	0.63	1.35	0.51	0.41	0.97	0.78	0.45
$L_{(N)}/HREE_{(N)}$	0.20	0.37	0.50	0.40	0.99	0.40	0.37	0.41	0.48	0.29
Eu/Eu^*	1.74	1.33	1.91	1.94	1.00	1.93	1.00	1.92	1.82	1.60
ΣREE	16.68	4.96	20.51	10.09	10.86	7.96	3.48	7.18	20.68	5.63

Element	RHR-41	RHR-42	RHR-43	RHR-44	RHR-45	RHR-46	RHR-47	RHR-48	RHR-49	RHR-50
SiO_2 (Wt.%)	42.24	32.64	44.16	51.21	83.02	40.52	48.38	83.09	18.67	24.38
TiO_2	-	0.02	-	0.03	0.01	0.04	0.05	0.02	0.01	0.01
Al_2O_3	0.28	0.36	0.58	0.40	0.20	0.33	0.48	0.26	0.10	0.12
Fe_2O_3	57.69	66.79	53.78	47.63	15.93	58.69	50.12	15.98	80.09	75.24
FeO	-	-	0.04	0.04	0.08	0.32	-	0.20	0.04	0.08
MnO	-	-	-	-	-	-	-	-	-	-
MgO	-	0.02	0.30	-	0.02	0.06	0.03	0.02	0.02	0.03
CaO	-	-	0.05	-	-	-	0.01	0.02	-	0.01
Na_2O	0.07	0.08	-	0.07	0.03	0.03	-	0.01	-	-
K_2O	-	-	0.01	-	0.04	-	0.04	0.02	0.03	0.03
P_2O_5	0.02	0.02	0.06	0.02	-	0.05	0.03	-	0.01	0.02
LOI	0.50	1.00	0.50	0.50	0.50	-	0.50	1.00	1.00	0.50
Total	**100.80**	**100.93**	**99.48**	**99.90**	**99.83**	**100.04**	**99.64**	**100.62**	**100.06**	**100.42**
Sc (ppm)	0.75	0.86	0.54	0.58	0.24	1.00	0.66	1.11	1.32	1.19
V	4.66	13.35	7.90	9.22	2.49	12.25	9.56	35.74	14.96	20.19
Cr	151.20	153.70	186.62	215.99	312.73	168.28	156.07	193.94	145.80	116.21
Co	1.46	2.13	1.61	2.05	1.90	1.63	1.71	2.17	1.60	2.16
Ni	6.77	6.78	7.11	7.86	7.62	7.09	4.55	11.49	6.10	5.99
Cu	5.04	6.23	3.56	5.01	5.34	1.81	3.14	81.91	132.13	83.08
Zn	6.47	12.74	3.66	4.31	3.53	3.62	5.74	15.13	15.91	21.90
Ga	0.93	1.11	1.68	0.96	0.23	1.59	1.15	0.84	1.64	1.41
Rb	0.06	0.22	0.20	0.14	-	0.17	0.28	3.58	0.29	0.30
Sr	9.03	7.58	10.32	2.80	2.76	7.68	16.22	8.68	8.67	21.68
Y	4.52	3.77	5.06	3.34	0.97	5.84	7.27	1.99	5.91	5.21
Zr	2.70	5.92	7.40	6.52	0.30	9.63	10.09	7.06	6.90	9.44
Nb	0.24	0.40	0.49	0.28	0.07	0.53	0.48	1.21	0.45	0.64
Ba	11.89	13.41	8.09	5.07	4.06	10.67	14.21	106.67	7.83	27.11
Hf	0.06	0.18	0.17	0.16	0.01	0.17	0.32	0.20	0.15	0.18
Ta	-	0.01	0.02	0.03	-	0.03	0.03	0.05	0.03	0.05
Th	0.11	0.25	0.31	0.24	0.03	0.22	0.51	0.84	0.30	0.31
U	0.46	0.89	0.19	0.27	0.41	0.17	0.22	1.33	0.58	0.55
La	1.94	3.98	5.43	3.81	1.40	4.80	4.95	4.73	3.31	2.81
Ce	4.43	5.71	10.09	5.51	1.62	8.43	8.39	8.22	6.13	5.77
Pr	0.42	0.49	0.95	0.65	0.19	0.71	0.82	0.97	0.67	0.58
Nd	2.01	2.07	3.93	2.52	0.62	3.04	3.60	4.11	2.89	2.58
Sm	0.55	0.44	0.76	0.63	0.16	0.55	0.86	0.77	0.79	0.48
Eu	0.34	0.30	0.44	0.32	0.04	0.38	0.55	0.17	0.51	0.49
Gd	0.65	0.55	0.72	0.52	0.12	0.63	0.93	0.52	0.78	0.61
Tb	0.10	0.09	0.11	0.09	0.02	0.11	0.14	0.08	0.12	0.10
Dy	0.63	0.55	0.68	0.57	0.12	0.75	0.88	0.52	0.82	0.70
Ho	0.11	0.09	0.11	0.10	0.02	0.14	0.15	0.09	0.15	0.13
Er	0.32	0.28	0.34	0.33	0.07	0.46	0.44	0.27	0.46	0.42
Tm	0.04	0.04	0.05	0.05	0.01	0.07	0.06	0.04	0.07	0.06
Yb	0.25	0.22	0.26	0.29	0.06	0.45	0.35	0.22	0.40	0.40
Lu	0.06	0.04	0.04	0.05	0.01	0.07	0.07	0.03	0.07	0.07
SiO_2/Fe_2O_3	0.73	0.49	0.82	1.08	5.21	0.69	0.97	5.20	0.23	0.32
Zr/Hf	45.00	32.89	43.53	40.75	30.00	56.65	31.53	35.30	46.00	52.44
$Nd_{(N)}/Yb_{(N)}$	0.75	0.89	1.42	0.81	1.00	0.63	0.97	1.76	0.78	0.61
$L_{(N)}/HREE_{(N)}$	0.40	0.58	0.80	0.59	0.83	0.51	0.55	0.98	0.44	0.40
Eu/Eu*	1.70	1.77	1.76	1.68	0.80	1.90	1.83	0.81	1.96	2.72
ΣREE	11.85	14.85	23.91	15.44	4.46	20.59	22.19	20.74	17.17	15.20

TABLE 9.2 CHEMICAL COMPOSITION OF THE SHALY BANDED IRON FORMATION

Element	RA-1AS	RA-1BS	RA-2S	RA-3AS	RA-4S	RA-5S	RA-6S	RA-7AS	RA-8S	RA-9S
SiO_2 (Wt.%)	36.93	22.07	27.59	24.64	17.20	3.08	22.68	23.66	13.18	14.53
TiO_2	0.57	0.40	0.56	0.51	0.39	0.10	0.52	0.49	0.14	0.16
Al_2O_3	33.64	12.45	17.37	13.81	8.49	3.43	17.56	14.27	4.50	5.02
Fe_2O_3	15.51	56.12	46.02	51.41	69.19	89.99	50.94	53.13	80.50	78.88
FeO	0.08	0.12	0.12	1.10	0.12	0.08	0.08	-	-	-
MnO	-	-	-	-	0.01	-	-	-	-	-
MgO	-	-	-	-	-	2.00	-	-	1.00	1.50
CaO	0.28	0.19	0.12	0.10	0.07	0.07	0.23	0.12	0.05	0.05
Na_2O	0.67	0.88	0.88	0.90	0.90	-	0.64	0.60	-	-
K_2O	-	0.04	0.04	0.42	0.04	0.06	0.07	0.05	0.03	0.04
P_2O_5	0.05	0.12	0.10	0.16	0.12	0.08	0.08	0.05	0.06	0.06
LOI	13.00	7.50	7.50	6.00	4.00	0.50	7.50	7.50	0.50	0.50
Total	100.73	99.89	100.30	99.49	100.53	99.39	100.30	99.87	99.96	100.74
Sc (ppm)	7.45	14.37	16.59	12.89	11.76	4.88	10.65	11.90	4.44	8.89
V	14.19	42.27	41.45	36.04	199.04	20.62	36.79	42.52	35.00	41.13
Cr	23.68	62.90	52.10	40.98	11.32	11.55	30.35	55.11	12.47	33.33
Co	4.17	4.16	2.20	4.01	4.62	7.61	3.81	3.45	11.99	1.92
Ni	35.56	69.17	58.92	61.36	29.21	12.01	51.11	64.88	10.03	7.05
Cu	17.72	51.13	29.41	23.58	24.61	4.51	21.02	29.27	90.78	69.25
Zn	77.70	57.97	42.46	61.47	38.28	10.36	53.62	82.15	22.47	32.06
Ga	21.50	15.23	21.34	17.93	8.48	4.57	19.91	15.80	5.94	5.49
Rb	0.29	0.65	0.13	0.31	0.64	0.91	0.25	0.25	0.63	1.12
Sr	35.27	32.16	41.82	24.71	54.29	10.33	26.04	31.56	11.15	17.52
Y	14.25	15.33	21.33	16.59	30.45	5.33	13.66	17.73	8.38	7.90
Zr	160.02	152.60	168.66	176.99	151.44	16.97	136.19	114.25	64.20	41.83
Nb	4.83	4.42	5.64	5.11	5.69	1.26	4.03	4.23	2.77	1.04
Ba	8.77	10.44	18.44	28.79	75.16	21.60	23.70	16.54	16.07	24.77
Hf	6.58	4.54	5.91	5.39	3.83	0.35	4.33	3.08	1.31	0.85
Ta	0.67	0.53	0.63	0.46	0.75	0.10	0.40	0.43	0.20	0.14
Th	7.67	4.81	5.05	7.04	3.88	0.59	4.53	4.13	1.55	1.01
U	0.42	0.81	0.70	0.83	2.23	0.66	0.75	0.47	0.32	0.31
La	62.72	32.91	7.30	12.15	13.84	4.45	22.38	16.12	6.39	15.22
Ce	154.67	69.06	20.92	30.32	32.09	14.58	46.66	34.33	13.08	21.70
Pr	16.53	8.16	2.24	3.50	3.34	1.13	6.78	4.34	1.86	2.88
Nd	60.55	29.08	9.48	14.89	12.42	4.78	27.57	19.51	8.53	11.49
Sm	5.15	2.61	1.41	1.90	2.59	0.74	3.88	2.90	1.36	1.81
Eu	1.57	0.83	0.80	0.75	1.08	0.42	1.12	0.91	0.77	0.82
Gd	3.49	2.22	1.41	1.32	2.65	0.72	2.45	1.82	1.20	1.56
Tb	0.55	0.37	0.27	0.25	0.48	0.13	0.38	0.32	0.21	0.25
Dy	3.65	2.64	2.12	1.94	3.65	0.94	2.53	2.38	1.55	1.68
Ho	0.64	0.48	0.45	0.40	0.74	0.18	0.44	0.45	0.30	0.30
Er	2.07	1.62	1.67	1.53	2.65	0.65	1.39	1.60	1.07	0.95
Tm	0.30	0.25	0.29	0.25	0.43	0.10	0.20	0.26	0.17	0.14
Yb	1.83	1.55	2.10	1.82	3.00	0.69	1.21	1.74	1.13	0.85
Lu	0.28	0.22	0.30	0.25	0.49	0.07	0.29	0.27	0.21	0.12
SiO_2/Fe_2O_3	2.38	0.39	0.60	0.48	0.25	0.03	0.45	0.45	0.16	0.18
Zr/Hf	24.32	33.61	28.54	32.84	39.54	48.49	31.45	37.09	49.01	49.21
$Nd_{(N)}/Yb_{(N)}$	3.11	1.76	0.42	0.77	0.39	0.65	2.14	1.05	0.71	1.27
$L_{(N)}/HREE_{(N)}$	1.80	1.17	0.36	0.61	0.35	0.54	1.03	0.71	0.45	0.80
Eu/Eu^*	1.10	1.03	1.67	1.42	1.23	1.68	1.08	1.18	1.79	1.44
ΣREE	314.00	152.00	50.76	71.27	79.45	29.58	117.28	86.95	37.83	59.77

Element Wt.%	RH 17S	RH 20S	RH 21AS	RH 22AS	RHR 71AS	RHR 72S	RHR 73S	RHR 74S	RHR 75S	RHR 76S
SiO_2	35.63	50.11	28.09	42.23	6.72	41.14	4.70	3.92	5.01	18.64
TiO_2	0.42	0.65	0.25	0.61	0.09	0.32	0.09	0.16	0.14	0.34
Al_2O_3	13.15	19.25	11.38	21.63	4.79	6.42	4.51	3.75	4.40	13.44
Fe_2O_3	40.32	19.93	49.97	22.90	84.37	49.43	86.51	88.89	85.39	65.81
FeO	-	-	0.08	0.04	0.12	0.60	0.08	0.12	0.12	0.12
MnO	-	-	-	-	-	0.02	-	0.03	0.02	-
MgO	-	-	-	-	1.60	-	2.00	1.40	1.10	-
CaO	0.13	0.16	0.17	0.16	0.11	0.10	0.09	0.08	2.03	0.11
Na_2O	0.40	0.42	0.36	0.32	0.36	0.22	0.22	0.24	0.26	0.24
K_2O	2.20	2.47	1.03	3.91	0.06	0.06	0.05	0.06	0.07	0.06
P_2O_5	0.05	0.05	0.06	0.08	0.05	0.05	0.06	0.06	0.05	0.05
LOI	7.50	7.00	8.50	8.50	1.50	2.00	1.50	1.50	1.50	2.00
Total	99.80	100.04	99.89	100.38	99.77	100.36	99.81	100.21	100.09	100.81
Sc (ppm)	8.01	11.36	6.04	10.00	2.90	6.30	2.49	3.34	2.96	7.61
V	54.81	62.77	31.88	53.77	60.87	65.98	43.86	72.03	54.02	184.51
Cr	44.69	84.06	26.35	65.37	16.13	24.24	14.46	25.62	15.96	32.20
Co	11.14	6.09	5.23	9.42	9.66	17.20	12.93	6.10	8.47	6.77
Ni	43.38	63.77	39.90	54.08	9.65	26.67	7.53	6.53	8.90	57.75
Cu	70.07	5.40	3.43	7.78	82.78	16.17	78.97	4.68	55.01	59.41
Zn	23.88	18.21	28.92	22.82	19.74	36.04	19.86	8.21	16.30	47.88
Ga	15.55	20.89	17.61	28.62	6.16	4.85	6.23	5.31	5.97	15.75
Rb	128.65	152.96	58.88	233.08	0.33	0.78	0.67	0.33	0.75	0.22
Sr	36.00	53.31	23.54	78.58	58.64	8.24	37.92	16.33	31.21	14.69
Y	12.07	18.69	10.85	17.93	18.95	29.77	15.86	5.52	16.92	37.08
Zr	152.58	276.88	123.90	259.25	30.76	166.98	20.93	49.87	62.94	267.75
Nb	3.46	5.48	6.61	8.24	1.49	1.61	1.22	2.07	2.40	1.64
Ba	68.37	84.30	35.59	108.65	35.05	15.46	29.49	32.31	49.18	37.09
Hf	4.10	6.50	3.94	8.18	0.67	4.83	0.35	1.06	1.44	5.77
Ta	0.39	0.61	0.70	0.87	0.10	0.34	0.11	0.20	0.22	0.29
Th	6.36	9.24	21.26	12.50	0.72	3.66	0.86	1.28	1.70	4.40
U	2.39	2.23	2.32	2.02	1.71	1.85	1.34	1.14	0.99	2.77
La	5.65	17.62	5.85	21.52	6.15	4.58	8.68	20.18	20.68	10.26
Ce	6.67	16.04	9.26	28.06	12.03	7.11	14.96	26.35	13.39	20.45
Pr	1.51	4.10	1.86	4.16	1.70	1.36	1.78	3.35	4.64	1.99
Nd	6.97	16.08	6.89	17.56	8.75	6.80	6.62	12.60	20.19	8.87
Sm	1.25	2.43	1.56	3.30	1.67	1.63	1.29	1.92	3.64	2.30
Eu	0.51	0.92	0.46	0.96	1.09	0.96	1.07	0.93	1.48	1.53
Gd	1.34	2.90	1.31	2.36	2.18	1.95	1.73	2.04	3.20	3.09
Tb	0.23	0.44	0.23	0.39	0.33	0.37	0.26	0.34	0.52	0.58
Dy	1.68	2.94	1.74	2.70	2.03	3.10	1.58	2.36	3.42	4.61
Ho	0.32	0.50	0.35	0.49	0.33	0.66	0.26	0.43	0.60	0.84
Er	1.12	1.56	1.24	1.62	0.99	2.58	0.76	1.41	1.76	3.50
Tm	0.17	0.22	0.20	0.24	0.13	0.46	0.10	0.22	0.25	0.59
Yb	1.16	1.29	1.35	1.51	0.77	3.27	0.58	1.37	1.53	4.17
Lu	0.20	0.26	0.19	0.25	0.12	0.44	0.16	0.19	0.21	0.83
SiO_2/Fe_2O_3	0.88	2.51	0.56	1.84	0.08	0.83	0.05	0.04	0.06	0.28
Zr/Hf	37.22	42.60	31.45	31.69	45.91	34.57	59.80	47.05	43.71	46.40
$Nd_{(N)}/Yb_{(N)}$	0.56	1.17	0.50	1.09	1.07	0.20	1.08	0.86	1.24	0.20
$L_{(N)}/HREE_{(N)}$	0.34	0.56	0.38	0.71	0.45	0.16	0.54	0.65	0.61	0.19
Eu/Eu^*	1.16	1.02	0.96	1.02	1.70	1.60	2.14	1.39	1.29	1.70
ΣREE	28.78	67.30	32.49	85.12	38.27	35.27	39.83	73.69	75.51	63.61

Fe_2O_3/SiO_2 molar ratio is dependent on the relative thickness of iron and silica bands. Significant clastic input is present in SBIF, whereas CBIF contains no or negligible amount of clastic input. These clastic inputs are reflected in higher Al_2O_3 and TiO_2 content. Most of the CBIF samples have 0.00 to 0.09% TiO_2 with Al_2O_3 values ranging between 0.00 to 0.80%. In SBIF both the TiO_2 and Al_2O_3 values increases from 0.09 to 0.65% and from 3.43 to 33.64% respectively. CBIF and SBIF form separate groups. Linear relationships between Al_2O_3 and TiO_2 has been observed by several workers (Laajoki and Saikkonen, 1977; Trendall and Pepper, 1977; Ewers and Morris, 1981; Khan et al., 1992; Gnaneshwar Rao and Naqvi, 1993; Manikyamba et al., 1993). In BIFs of the present study area a linear relationship is observed between Al_2O_3 and TiO_2 at higher concentration (Fig. 9.2). The exceptionally higher amount of Al_2O_3 in SBIF (upto 33%) due to the presence of kaolinite and muscovite clearly indicate that terrigenous sedimentation in variable amounts continued with chemical precipitation. The alkali content of CBIF is negligible, maximum being 0.08% and in SBIF it ranges from 0.03 to 4.23%. Chemical weathering in the source region has left the clay which was brought to the basin as suspended load and deposited during regression of ocean along with the precipitation of FeO and SiO_2. The samples of high K_2O and Na_2O reflect the incorporation of acid volcaniclastic debris in SBIF. Both the BIFs are extremely depleted in CaO, reflecting absence of calcite. MgO content in CBIF is negligible but in SBIF it goes upto 2% indicating volcaniclastic contribution during the precipitation of BIF.

9.1. High order correlation coefficient between SiO_2 and Fe_2O_3 is illustrated. In CBIF the antipathetic relationship is of very high order as it entirely consists of SiO_2 and Fe_2O_3 whereas this relationship in SBIF is comparatively of lower order as it contain some other major elements also in substantial amount. Solid circle = cherty banded iron formation; open square = shaly banded iron formation. Same symbols are used in all the illustration of BIF.

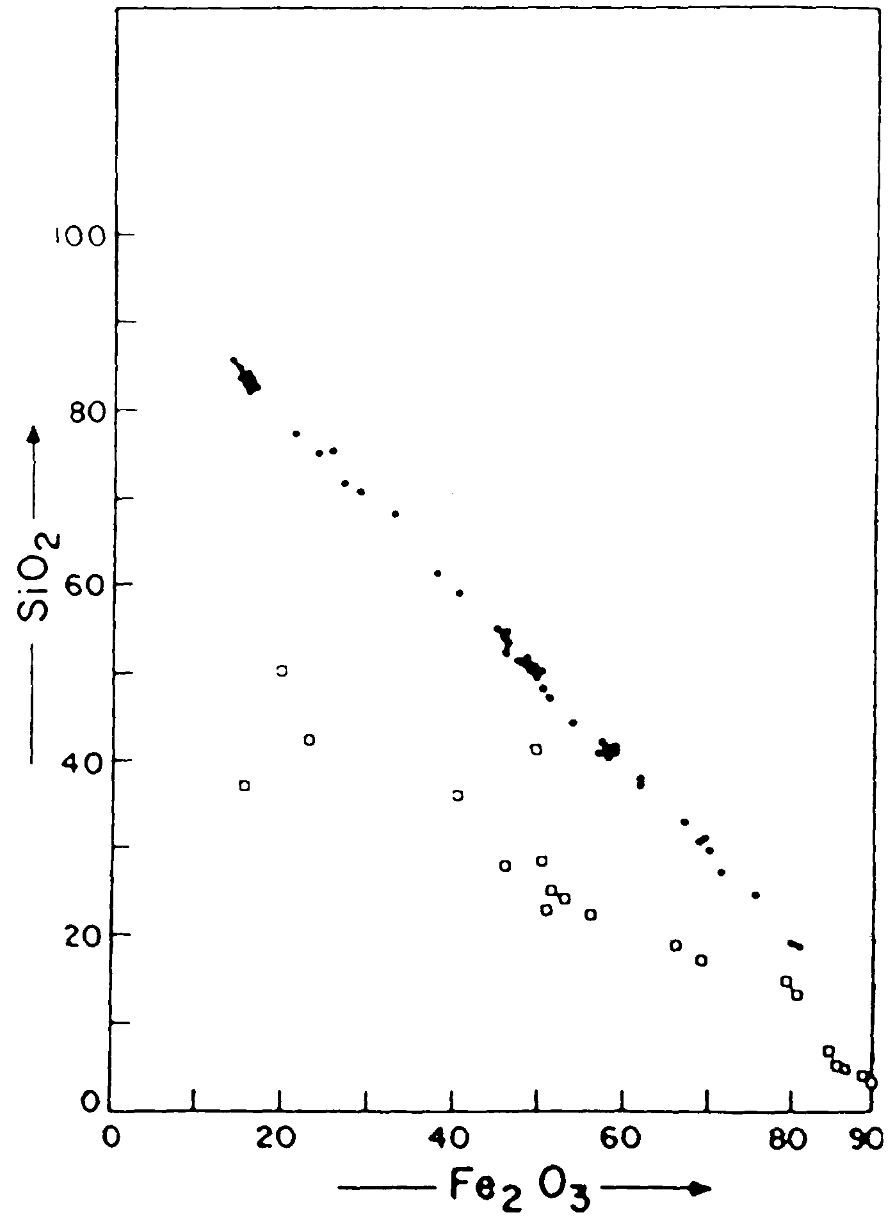

SiO2
100
80
60
40
20
0
0
20
40
60
80
90
Fe2 O3

Figure 9.2. Al_2O_3/TiO_2 variation diagram for BIF of Kushtagi schist compared with BIFs of some other localities. High Al_2O_3 and TiO_2 in SBIFs indicate considerable clastic input.

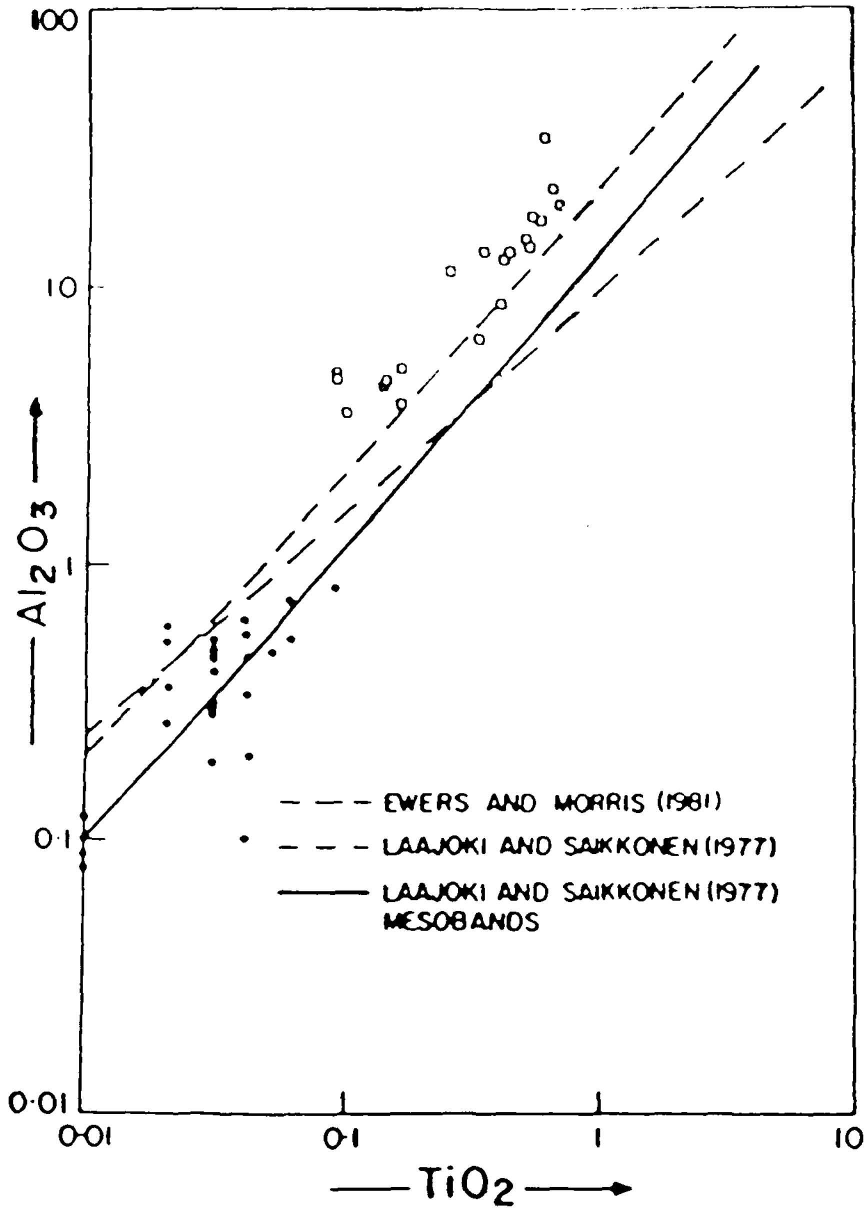

100
10
1
0.1
0.01
0.01
0.1
1
10
Al2O3
TiO2
EWERS AND MORRIS (1981)
LAAJOKI AND SAIKKONEN (1977)
LAAJOKI AND SAIKKONEN (1977) MESOBANDS

9.3 Trace Element Geochemistry

Zr, Hf, Y, Rb, Sr, Ta, U and Th are the few elements brought to the ocean water by the weathering of felsic rocks of the crust. On the other hand the source of ferromagnesian elements namely Cr, Ni, Co, V and Sc are generally mafic rocks. They can be supplied either from the weathering of the exposed land or by the within basin volcanism. The enrichment of Zr, Hf, Y, Rb, Sr, Ta, U and Th in BIF may be considered as indicators for the supply of the terrigenous material to the basin at the time of deposition of BIF sequence. Similarly, enrichment in Ni, Cr, Co, V and Sc probably indicate that basic-ultrabasic clastic material was also supplied to the basin. Since large quantities of volcaniclastic rocks are present in the basin in association with BIF, this enrichment of ferromagnesium traces may be attributed either to basic volcanism or to a basic source outside the basin.

In geochemical processes Rb and Sr generally accompany alkalies. A close examination reveals that CBIF and SBIF both contain Rb below one ppm but in few samples of SBIF, Rb is very high; it goes even upto 233 ppm. Sr content of around 35 CBIF samples (out of 50) is less than 10 ppm but almost all SBIF have Sr more than 10 ppm. The low order positive correlation ($r = 0.59$) between Rb and Sr and their comparatively higher value in SBIF (Fig. 9.3A) reflect the felsic contribution. A perfect sympathetic positive relationship exists between Hf and Zr (Fig. 9.3B), two most diagnostic element for terrigenous contribution. There is no gap between CBIF and SBIF. The concentration of Hf and Zr is low in CBIF in comparison to SBIF. This suggests that a continuous supply of a varying quantity of terrigenous debris has been maintained to the basin and the mixing of hydrothermal solutions with clastics has been quantitatively and qualitatively consistent.

This inference about terrigenous contribution is further strengthened by Y vs V, Y vs Zr and Nb vs Ta diagrams (Fig. 9.3C, D and E). Y-V plot show sympathetic linearity (r = 0.80) and a noticeable distinction between CBIF and SBIF (Fig. 9.3C). Similar distinctive behaviour is seen in Y and Zr distribution (r = 0.80). Zr and Y content is less than 10 ppm in most of the CBIF, whereas they are more than 10 ppm in most of the SBIF. The Zr enrichment in SBIF goes upto 280 ppm and Y upto 37 ppm. A complete gradation of CBIF into SBIF is seen on the Y-Zr plot (Fig. 9.3D). Similar distinctive behaviour is seen in the Nb and Ta plot (Fig. 9.3E; r = 0.87). The Nb and Ta in CBIF is very low in comparison to SBIF. Some of the CBIF have Ta value below detection limit. Sample Nos. RHR-16 and 27 show abnormal behaviour in Nb and Ta. The concentration of Th and U is not the same as those measured in the rocks today and at the time of deposition as both Th and U undergo radioactive decay. The Th/U ratio is also affected as the half lives of Th and various uranium isotopes are different. Both Th and U show two different scattered population in BIFs of Kushtagi schist belt and the total concentration of Th and U in CBIF is lower than that in SBIF (Fig. 9.3F). It clearly indicate that Th and U in BIF have been brought from two different sources and its higher concentration in SBIF reflect the terrigenous contribution.

9.3A. Shows simultaneous increase of Rb and Sr. Rb enrichment in SBIF is due to contribution from terrigenous input.

9.3B. Hf vs Zr plot show a very high order positive correlation in CBIF as well as in SBIF. Hf and Zr are more enriched in SBIF than CBIF, indicating contribution from terrigenous input.

9.3C. Illustrates positive correlation between Y and V.

9.3D. Shows excellent positive relationship between Y and Zr.

9.3E. Shows positive correlation between Nb and Ta.

9.3F. Th-U relationship also indicate that the higher concentration of Th and U in SBIF is a consequence of terrigenous input.

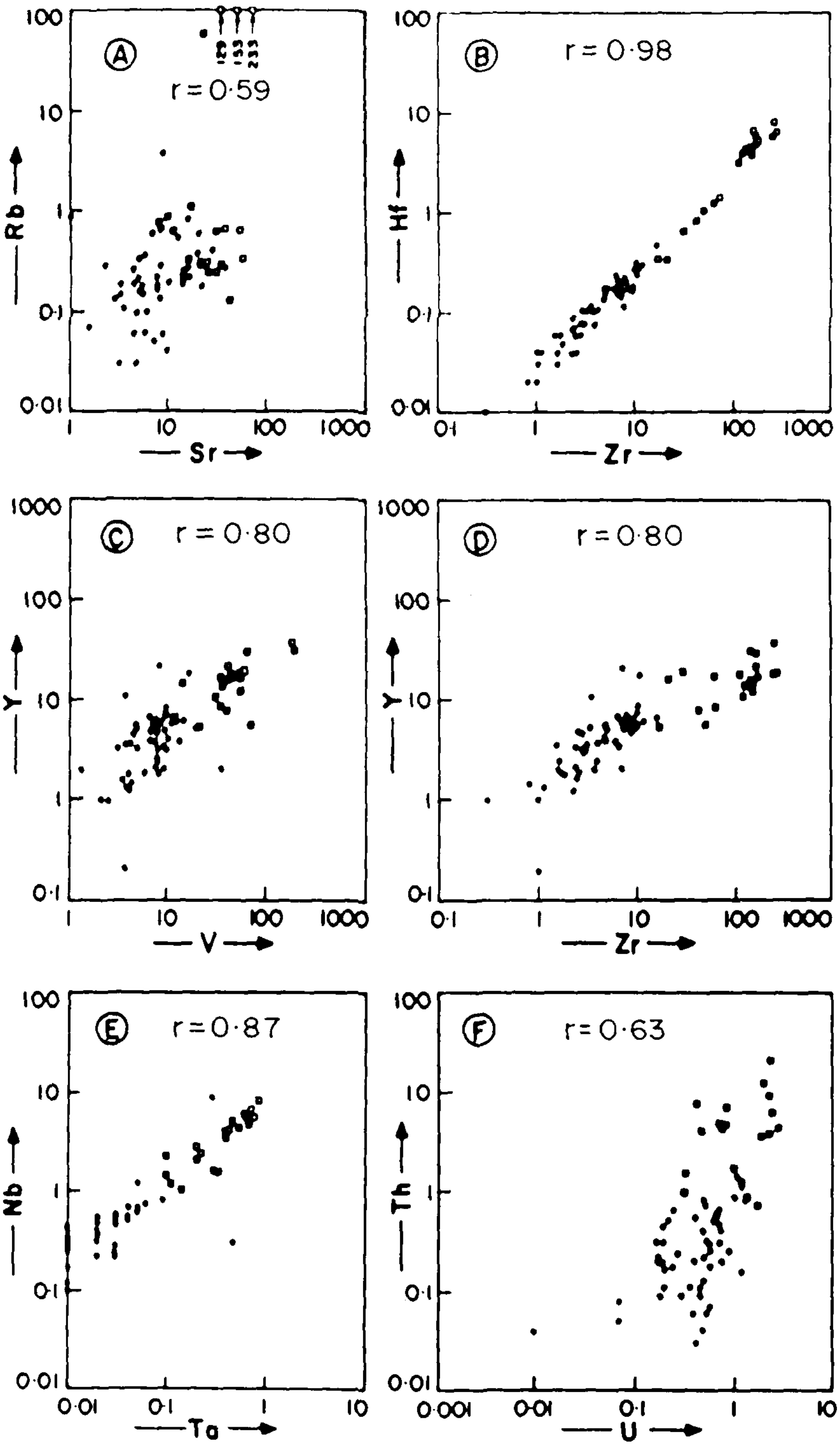

A
r=0·59
Rb
Sr
B
r=0·98
Hf
Zr
C
r=0·80
Y
V
D
r=0·80
Y
Zr
E
r=0·87
Nb
Ta
F
r=0·63
Th
U

Ni and Cr content in both types of BIF show wide variation (r = -0.52). The Cr content in CBIF ranges from 100 ppm to 310 ppm whereas in SBIF it varies between 11 to 85 ppm. Ni show two population in its concentration. In 8 SBIF samples and all the CBIF samples Ni varies from 4 to 15 ppm; in rest of the SBIF it ranges from 25 to 65 ppm. When Cr, Ni and Zr are plotted in various combination they show three different populations, one in CBIF and two in SBIF (Fig. 9.4A, B and C). The highest value of Cr is found in CBIF exhibiting a scatter; these CBIF shows depletion in Ni. One population of SBIF shows depletion in both Ni and Cr whereas the other population shows depletion in Cr but enrichment in Ni (Fig. 9.4A). BIFs formed by chemical precipitation from normal seawater do not have such high concentrations of these elements. Therefore, higher abundances of these elements indicate that enrichment in Cr and Ni contents is probably due to the contribution of volcaniclastic input and cannot be explained satisfactorily unless the fumarolic and explosive volcanic activity, producing ash, is invoked in this basin (Gnaneshwar Rao and Naqvi, 1993; Manikyamba et al., 1993). When Ni and Cr are plotted against Zr, a random behaviour with three different populations is seen. CBIF occupy a distinct place from SBIF as Ni, Cr and Zr concentrations are significantly different. Ni vs Zr (Fig. 9.4B) and Cr vs Zr (Fig. 9.4C) also show three different populations as shown by Ni-Cr plot. Zr and Cr concentrations are higher in SBIF but the Ni concentration is of two different populations, indicating two different types of volcanic activity has contributed to the compositional parameters; one with lower Ni content and the other with higher Ni content. Two types of volcaniclastic and terrigenous debris appears to have been deposited along with the chemical precipitates in highly variable proportions. The Sc and V are also very diagnostic elements. Their increase or decrease simultaneously and their enrichment in a sediment signifies the contribution from a basic-ultrabasic source. Most of the CBIF have very low amount of Sc (<2 ppm) and V (<20 ppm) but the SBIF have more than 2 ppm of Sc and more than 20 ppm of V. Although Sc and V show a positive correlation (r = 0.60); a close observation of Table 9.2 and Sc-V plot (Fig. 9.4D) indicate that SBIF have two different populations. The SBIF samples which show lower amount of Zr, Ni and Cr also show low abundance of Sc and V in comparison to other SBIF of this region. This distinction in population of ferromagnesian trace elements is also reflected in SiO_2-Cr plot. At moderate values of silica in CBIF the Cr is always more than 100 ppm but at a higher silica value it shows slight enrichment in Cr (Fig. 9.4E). Two populations of samples based on abundance of Cr are also seen in SBIF. At very low level of silica the Cr content in SBIF is also very low. The samples of hematite rich layers of SBIF (with the exceptionally enriched Fe_2O_3 of about 75%) are depleted in Cr (Fig. 9.4F); these samples are also depleted in Ni, Zr and Al_2O_3. At 40-55% concentration level of Fe_2O_3 in SBIF Ni enrichment is pronounced. The marked difference in the abundance of Ni ans Cr in different BIF groups appear to be due to similar differences in the volcanic rocks. Ni and Cr content of the associated volcanic rocks varies greatly (Chapter X). One group of volcanic rock

Figure 9.4A. Ni vs Cr diagram showing three different populations. CBIF shows a scatter with enrichment in Cr and depletion in Ni. In SBIF Ni and Cr shows two population. One shows depletion in both Ni and Cr and the other shows depletion in Cr but enrichment in Ni.

Figure 9.4B. Ni-Zr diagram illustrating three different population.

Figure 9.4C. Cr-Zr diagram showing very well defined three population of Cr vs Zr combination.

Figure 9.4D. Illustrates positive correlation between Sc and V, with SBIF having two different population.

Figure 9.4E. SiO_2-Cr plot shows the distinction in population of ferromagnesian mineral indicative of two different types of volcanic activity taking place in the basin.

Figure 9.4F. Fe_2O_3 vs Cr plot also shows three different population. SBIF with exceptionally enriched Fe_2O_3 samples are depleted in Cr. SBIF with moderate Fe_2O_3 content have enriched in Cr. CBIF has higher amount of Cr in comparison to SBIF.

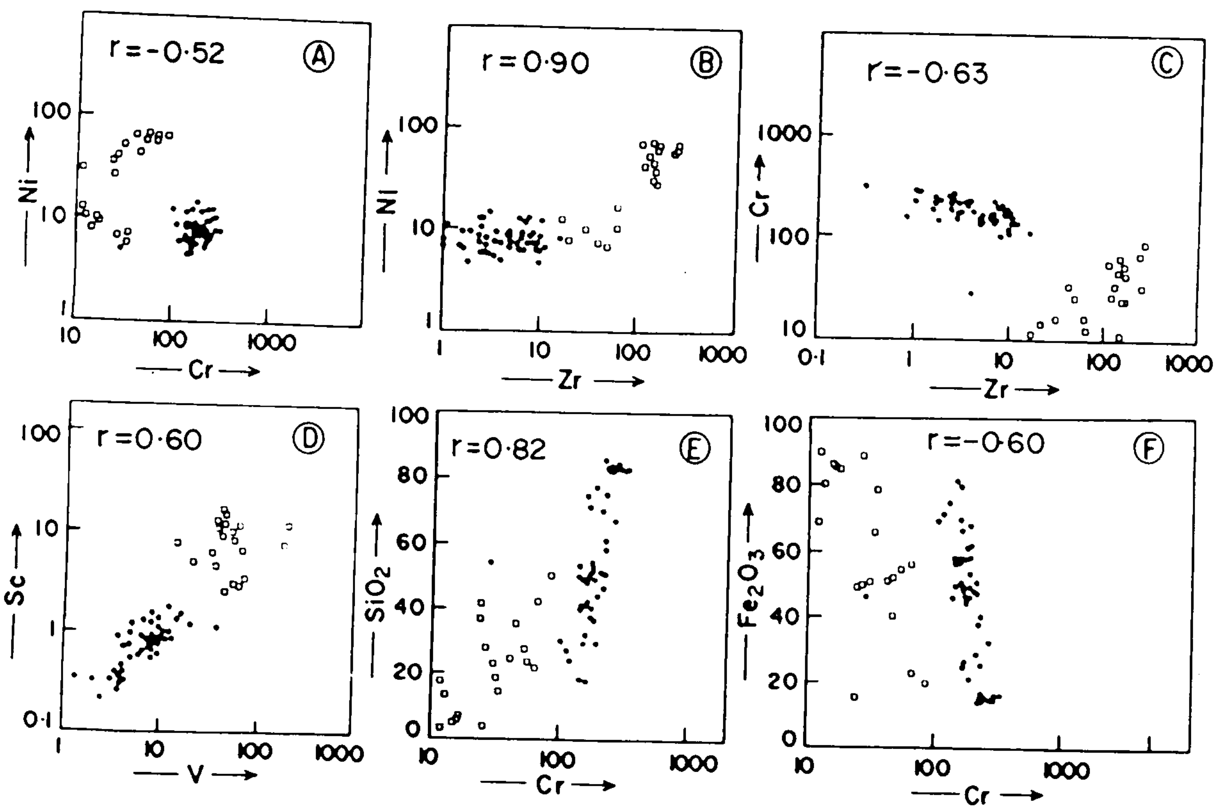

r=-0.52
A
Ni
Cr
r=0.90
B
Ni
Zr
r=-0.63
C
Cr
Zr
r=0.60
D
Sc
V
r=0.82
E
SiO_2
Cr
r=-0.60
F
Fe_2O_3
Cr

samples is highly enriched in Ni and Cr while the other group is depleted, indicating divergent type of magmatic activity in this belt. This variation in the chemical composition of magmatic activity is reflected in the composition of SBIF, thus two population are seen in it. The hematite rich band got deposited by the reaction between FeO and O_2 produced by biological mediation. While FeO is converted into iron-oxides, hydroxides and Fe_2O_3 to precipitate, Cr do not react with O_2, therefore do not precipitate as oxide. Thus Cr appears to have settled down along with SiO_2 rich band. This may be the possible cause for inverse relationship between Cr on one hand and Fe_2O_3/SiO_2 on other. Therefore the hydrothermal characteristic was superimposed and modified during the deposition of BIF.

When Cr:Zr:Y ratios are considered and plotted on a ternary diagram (Fig. 9.5), all the CBIF samples are observed to occupy the Cr apex and the SBIFs show tendancy to converge towards Zr apex. This further substantiate the inference that higher amount of Zr in SBIF and Cr in CBIF were added from a source other than the hydrothermal; possibly terrigenous and volcanic. The data presented above suggest that the type and quantity supplied by the terrigenous and volcaniclastic material to the different BIF suites and layers at different places has been extremely variable. Both volcaniclastic (probably of two type) and terrigenous debris have been deposited along with chemical precipitates in highly variable proportions.

Figure 9.5. Shows Cr:Zr:Y ratios in BIFs. Cr enrichment in CBIF with respect to Zr and Y and Zr enrichment in SBIF with respect to Cr and Y may be noticed.

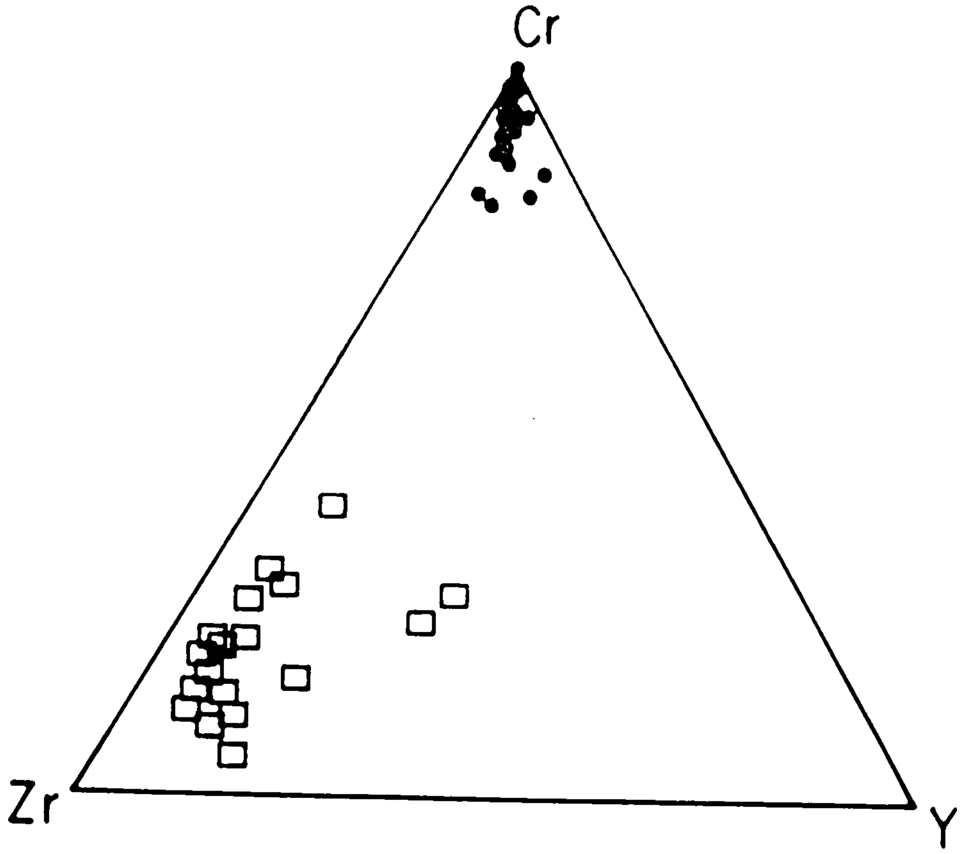
Cr
Zr
Y

9.4 Rare Earth Elements

REE content of CBIF and SBIF show significant variation in their abundance, Ce depletion and nature, magnitude of Eu anomalies (Eu/Eu^*). NASC normalized REE patterns of individual samples of CBIF as a whole show little difference and are almost identical in $LREE_{(N)}/HREE_{(N)}$ <1 and $Nd_{(N)}/Yb_{(N)}$ <1 in most of the samples. The REE patterns of the BIFs are shown in Fig. 9.6A to G. Out of the 50 CBIF samples anlaysed for REE concentration, 47 samples show little difference and are almost identical and have been plotted in 6 different illustrations (Fig. 9.6A to F) as the presentation of 47 samples in one illustration is difficult and confusing. Only 3 CBIF samples out of 47 samples show anomalous behaviour (Fig. 9.6G). Therefore in general most of the CBIF samples contain depleted to moderate ΣREE, $LREE_{(N)}/HREE_{(N)}$ <1, $Nd_{(N)}/Yb_{(N)}$ <1 and strong positive Eu anomalies. Average REE pattern of SBIF are almost identical except the level of ΣREE is elevated. Negative Ce anomaly is also observed in some samples (Fig. 9.7A to D), as a consequence oxidation of Ce^{+3} to Ce^{+4}. The removal of Ce^{+4} from the system was not complete resulting in variable abundance level of Ce in SBIF. This Ce anomaly is not observed in CBIF as probably the abundance of O_2 was less during its deposition whereas at the time of deposition of SBIF abundance level of O_2 has intermittently increased to oxidize Ce^{+3} to Ce^{+4}. The layer which was deposited during relatively higher Eh shows negative Ce anomoly. Cerium thus oxidized was accumulated in another layer producing positive Ce anomaly.

Figure 9.6A-F. 47 samples of CBIF out of 50 samples analysed shows similar REE patterns. All samples show depleted to moderate ΣREE, flat to slightly HREE pattern with strong positive Eu anomaly.

Figure 9.6G. REE pattern of 3 samples of CBIF showing anomalous behaviour in their REE patterns.

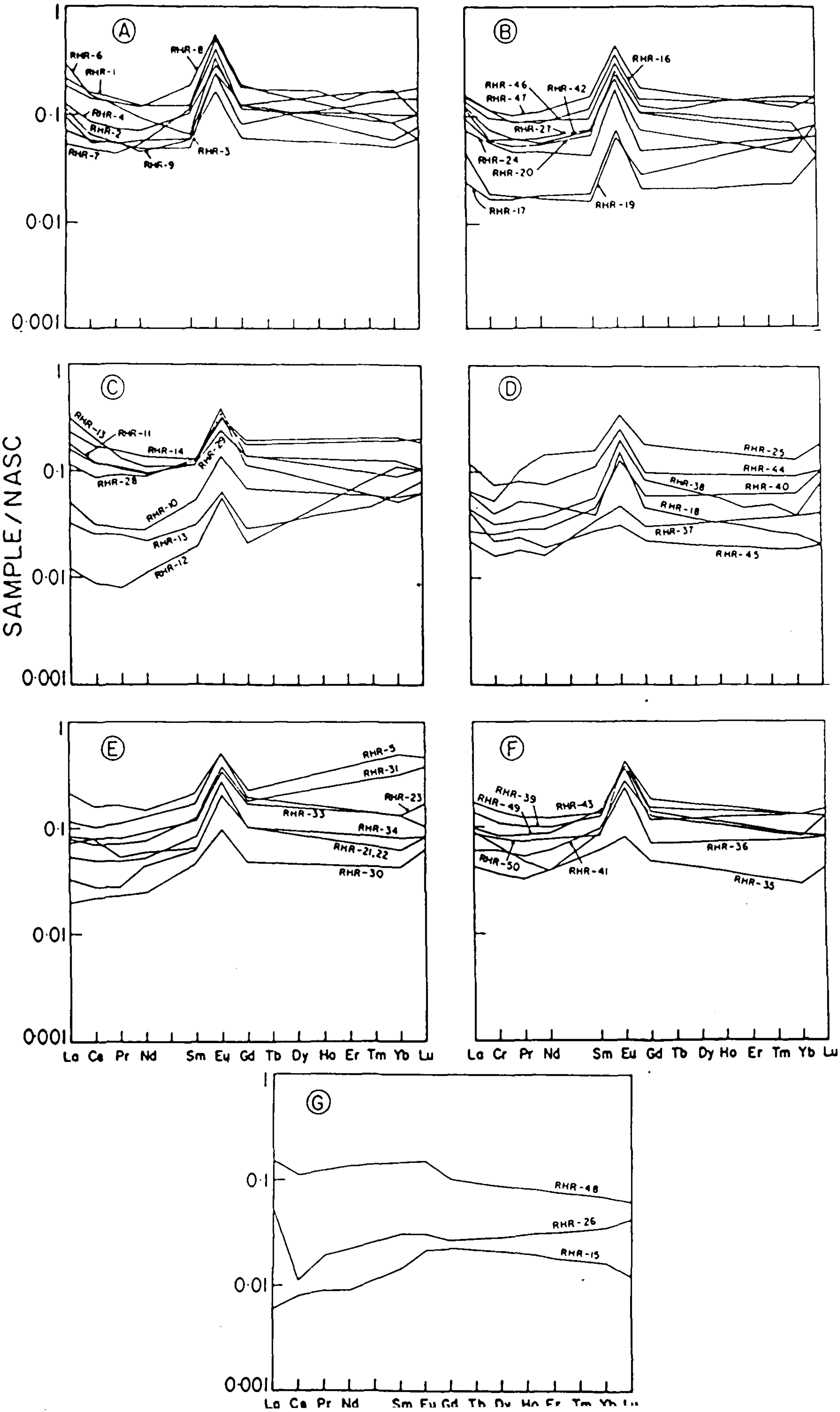
SAMPLE / NASC
1
0·1
0·01
0·001
A
RHR-6
RHR-1
RHR-8
RHR-4
RHR-2
RHR-7
RHR-9
RHR-3
B
RHR-16
RHR-46
RHR-47
RHR-42
RHR-27
RHR-24
RHR-20
RHR-17
RHR-19
C
RHR-13
RHR-11
RHR-14
RHR-29
RHR-28
RHR-10
RHR-13
RHR-12
D
RHR-25
RHR-44
RHR-38
RHR-40
RHR-18
RHR-37
RHR-45
E
RHR-5
RHR-31
RHR-23
RHR-33
RHR-34
RHR-21,22
RHR-30
F
RHR-39
RHR-49
RHR-43
RHR-50
RHR-41
RHR-36
RHR-35
G
RHR-48
RHR-26
RHR-15
La Ce Pr Nd Sm Eu Gd Tb Dy Ho Er Tm Yb Lu

Figure 9.7A-D. REE pattern of 20 SBIF samples showing negative through no to positive Ce anomaly with slightly elevated ΣREE content indicating terrigenous input in variable proportions.

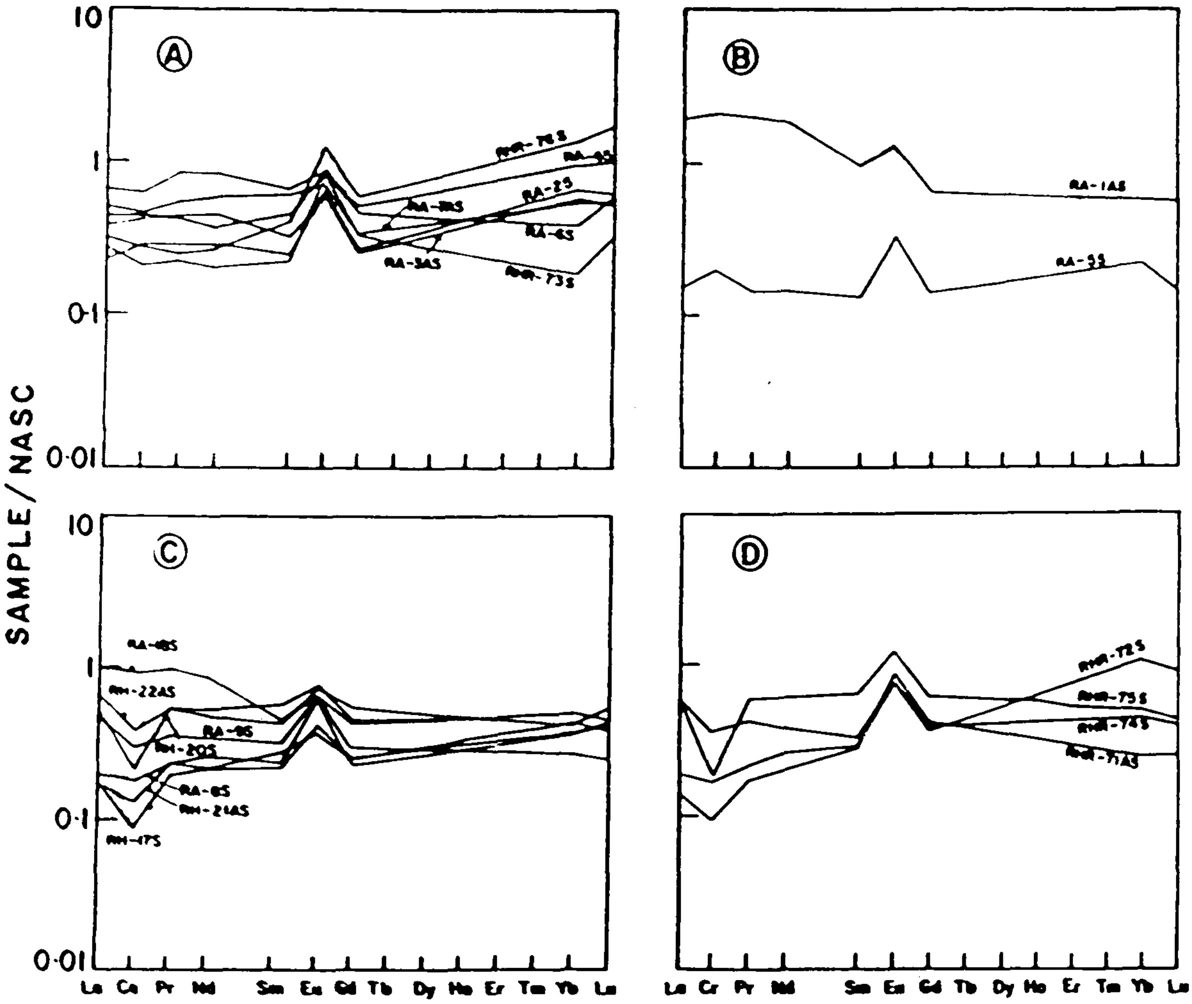
SAMPLE/NASC
10
1
0·1
0·01
A
B
C
D
RA-1AS
RA-5S
RA-3AS
RA-2S
RA-6S
RA-18S
RH-22AS
RH-17S
RHR-72S
RHR-75S
RHR-74S
La Ce Pr Nd Sm Eu Gd Tb Dy Ho Er Tm Yb Lu

In spite of scatter in the HREE/LREE ratios, both LREE and HREE increases simultaneously in CBIF and SBIF (Fig. 9.8A; r = 0.65). The Nd/Yb ratios shows the same scatter and a simultaneous increase of Yb and Nd from pure CBIF to SBIF (Fig. 9.8B; r = 0.53). A complete gradation between these values is seen in HREE/LREE and Yb/Nd plots. If the REE in BIF samples would have been derived from a felsic volcanic source a reverse pattern would be evident because of fractionation which produces the felsic rocks and thus a sloping pattern from La to Lu. The simultaneous increase of Nd and Yb at very low concentration levels indicates that the solution which carried FeO, SiO_2 and REE were not derived from leaching of either a felsic or a basic rock or the sediments deposited at the ocean floor. These low order abundances are similar to those observed in the hydrothermal solutions generated at the MOR. Almost all the BIF samples exhibit positive Eu anomalies. The magnitude of variation in the Eu/Eu^* is high (Fig. 9.8C). Predominance of the positive Eu anomalies in all types of BIF indicate that the solutions which brought FeO and SiO_2 to the ambient ocean were derived from a reducing environment. Such positive Eu anomalies are observed in BIFs irrespective of their age or locality and can only result from the input of Eu enriched hydrothermal fluids into the water column of the oceans (Graf, 1978; Fryer, 1983; Barrett et al., 1988; Khan et al., 1992; Manikyamba et al., 1993). A high Al_2O_3 concentration is believed to elevate the level of ΣREE. The ΣREE and Al_2O_3 plot (Fig. 9.8D) shows a scatter from 3 to 35 ppm at 0.01 to 1% Al_2O_3 level. But at a higher concentration of Al_2O_3 in SBIF the ΣREE also increases

Figure 9.8A. HREE vs LREE plot show sympathetic relationship. This ratio increases from CBIF to SBIF.

Figure 9.8B. Yb vs Nd plot show sympathetic correlation.

Figure 9.8C. Illustrates the relationship between Eu and Eu^*. Predominance of positive Eu anoamlies in both types of BIFs is reflected.

Figure 9.8D. ΣREE vs Al_2O_3 plot show that REE content increases with clastic input as most of SBIF have higher ΣREE than those of CBIF.

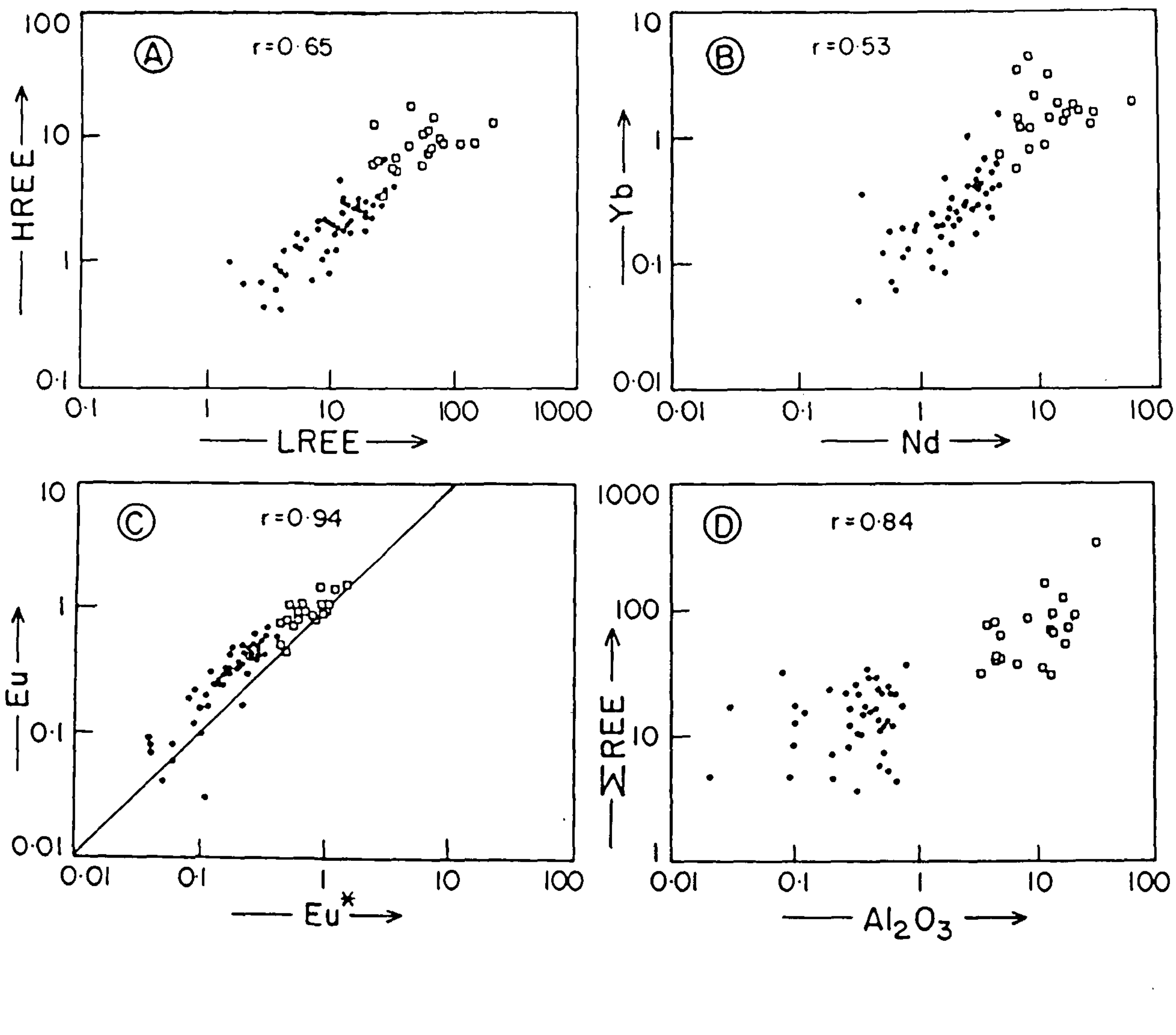

A
r=0·65
HREE
LREE
B
r=0·53
Yb
Nd
C
r=0·94
Eu
Eu*
D
r=0·84
ΣREE
Al_2O_3

from about 30 ppm to 300 ppm. This clearly shows that ΣREE enrichment is caused by clastic input. This is further substantiated by a perfect positive linear relationship between ΣREE-Zr (Fig. 9.9A; r = 0.61) and ΣREE-Hf (Fig. 9.9B; r = 0.69). A high Zr concentration is believed to elevate the level of ΣREE, especially HREE (Taylor and McLennan, 1985), resulting in a slight HREE enriched REE pattern (Fig. 9.6 and 9.7; Derry and Jacobsen, 1990) and higher Hf is also indicative of terrigenous input resulting in enrichment of ΣREE.

When La is deduced from ΣREE and plotted on ΣREE-La vs La plot then a sympathetic correlation is observed between ΣREE-La and La indicating a normal behaviour of La in both CBIF and SBIF samples of Kushtagi schist belt (Fig. 9.9C). The La spiking reported from Canada (Barrett et al., 1988), Sandur (Manikyamba et al., 1993), Chitradurga (Gnaneshwar Rao and Naqvi, 1993) and in few samples of Kudremukh (Khan et al., 1992) is not observed in these samples. When La+Ce is subtracted from ΣREE and ΣREE-(La+Ce) is plotted against Ce, we find that almost all the CBIFs fall on the line of linearity but only few of SBIFs fall on this line. Rest of the SBIF samples fall above this line (Fig. 9.9D). This indicates an anomalous behaviour of Ce in SBIF. This may be attributed to presence of high amount of free O_2 above wave base and photic zone, where SBIF were deposited. In general, pronounced Ce depletion is not seen in samples of Kushtagi as has been found in the BIFs of Chitradurga and Sandur (Gnaneshwar Rao and Naqvi, 1993; Manikyamba et al., 1993). Absence of Ce

Figure 9.9A. ΣREE vs Zr plot show sympathetic relationship both are high in SBIF as compared to CBIF.

Figure 9.9B. Illustrates the positive correlation between ΣREE and Hf.

Figure 9.9C. Show sympathetic correlation between ΣREE-La and La. Normal behaviour of La may be noticed.

Figure 9.9D. Illustrates mutual relationship between ΣREE-(La+Ce) and Ce.

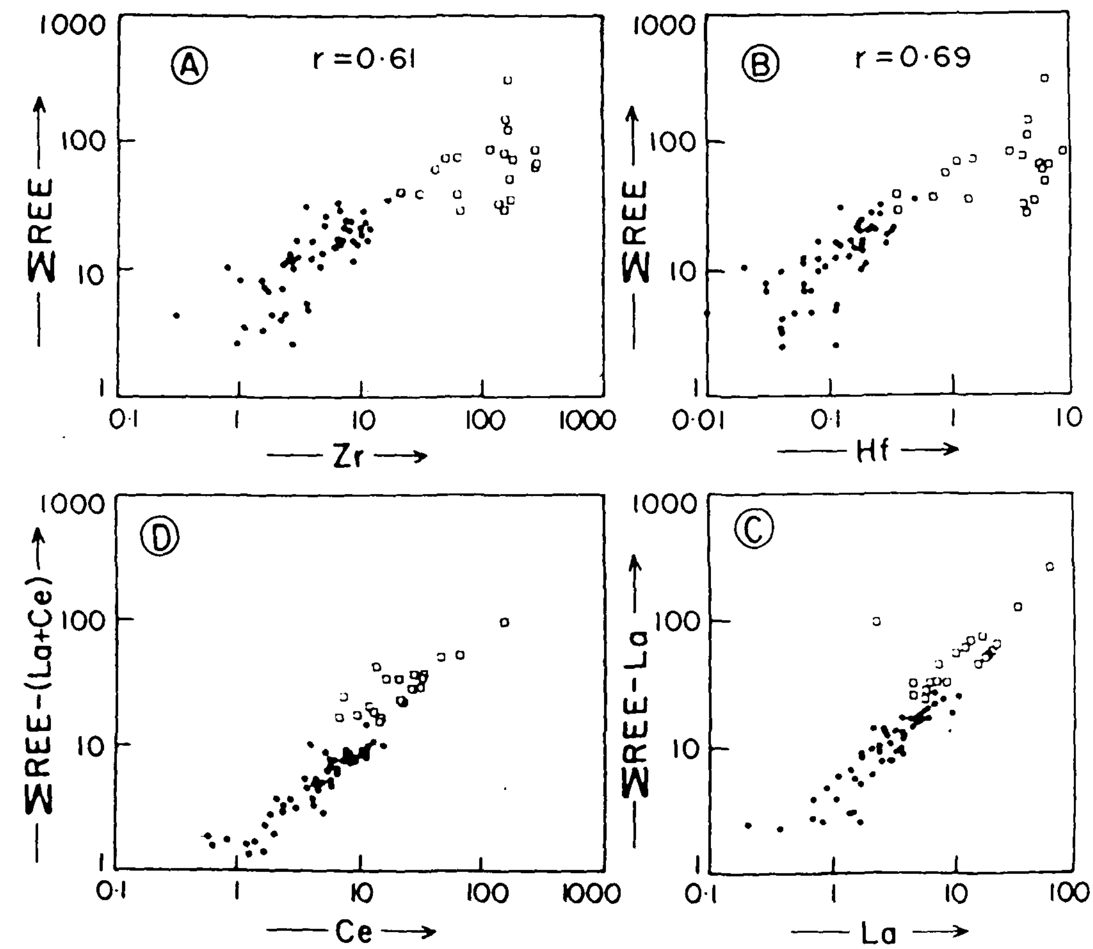

A
r = 0·61
ΣREE
Zr
B
r = 0·69
ΣREE
Hf
D
ΣREE-(La+Ce)
Ce
C
ΣREE-La
La

anomalies has been recorded from other Archaean BIFs (Shimizu et al., 1990; Derry and Jacobsen, 1990; Khan et al., 1992).

Geochemical studies of the hydrothermal solutions coming out of the vents at the Mid Oceanic Ridges (MOR) of modern oceans have provided a great constraint for the understanding of the origin of Precambrian BIF (Jacobsen and Pimentel-Klose, 1988). A binary plot comprising of Cu+Co+Ni against ΣREE of the hydrothermal solution samples from East Pacific Rise (EPR) and metalliferous deposits near the MOR has been prepared by Klein and Beukes (1989). When the present data is plotted on this illustration, some of the samples are observed to fall within the field and most of them fall very close to the field of hydrothermal solution (Fig. 9.10). This strongly substantiates the view that FeO, SiO_2, some of the trace elements and the REEs in BIFs have been added to the Archaean oceans by hydrothermal solutions.

9.5 Oxygen isotopes of Kushtagi BIF

Oxygen isotope ratio of coexisting silica and hematite in the banded iron formations is capable of putting important constraints on the depositional environment and/or subsequent alteration of the BIFs due to diagenesis, metamorphism etc. If silica and hematite are precipitated in a common reservoir, then the isotopic fractionation between the mineral pairs can be used to determine the temperature of formation of these pairs, provided that subsequent to their deposition the system remained closed and no isotopic resetting has taken place. On the other hand, if the original isotopic signature is disturbed due to diagenesis or metamorphism there will be perturbation of the original δ-values

Figure 9.10. (Cu+Co+Ni) vs ΣREE plot show most of the samples fall within well defined field of hydrothermal deposits or very close to it. All the smaples of SBIF lies outside this field indicating mixing of continental debris and volcaniclastic material with hydrothermal solutions, field of hydrothermal deposits and deep sea deposits are after Klein and Beukes (1989).

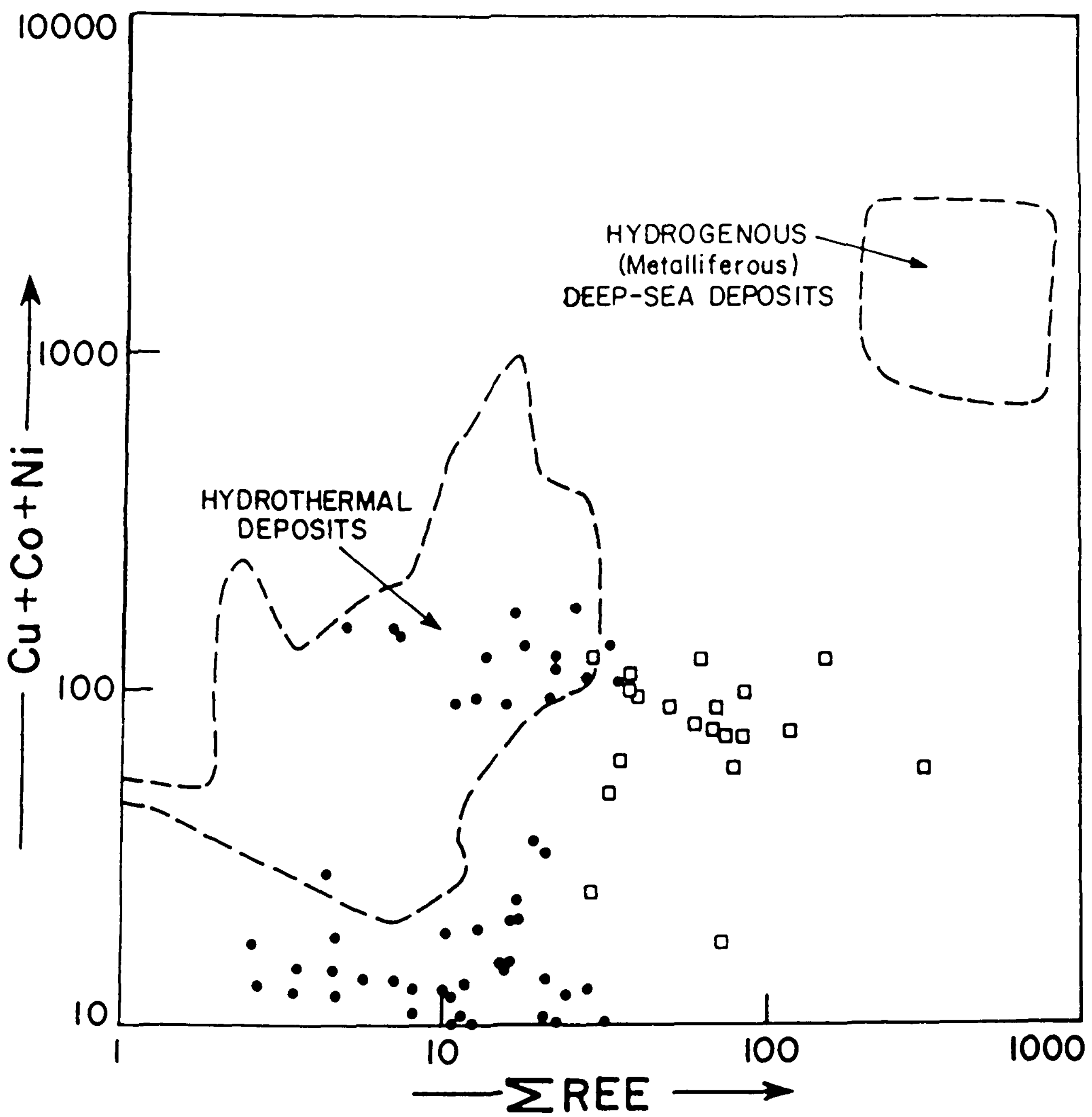

10000
1000
100
10
1
10
100
1000
Cu+Co+Ni
ΣREE
HYDROGENOUS
(Metalliferous)
DEEP-SEA DEPOSITS
HYDROTHERMAL
DEPOSITS

depending upon the temperature and δH_2O (of the interacting fluid) during diagenesis or metamorphism. In this section, the oxygen isotopic compositions of a few chert and hematite separates are reported. Thin section examination reveals that the chert bands are having variable amounts of hematite in them (Fig. 6.1C; Chapter VI) whereas,the hematite bands are mixed with silica. Since these samples are microcrystalline in nature it was not possible to separate pure fraction of the two mineral phases. Similar problem was encountered by Hoefs et al. (1987) for Urucum BIF. Thus the separated bulk chert as well as the hematite fractions were determined for their Fe_2O_3 content before their oxygen extraction and subsequent mass spectrometric analysis. Although, at present oxygen isotopic data is available only on 4 samples, still its provides a significant constraint on the temparature of BIF genesis.

The $\delta^{18}O$ values of the SiO_2 rich fraction and hematite rich fraction along with their Wt% Fe_2O_3 are reported in Table 9.3. The measured $\delta^{18}O$ of the mixtures were corrected for pure end member $\delta^{18}O$ values and are also included in Table 9.3. Since the Wt fraction of hematite in a quartz-hematite system is not equal to the mole fraction of the total system oxygen content in hematite, for the purpose of calculation of pure end member $\delta^{18}O$ values the Wt% Fe_2O_3 were converted to mole fraction of total system oxygen content in hematite in a two component quartz-hematite system. The corrections were applied according to the following equation;

$$\delta^{18}O_{sample} = \delta^{18}O_{silica} + (\delta^{18}O_{Hm} - \delta^{18}O_{silica}).X(O)_{Hm}$$

where,

$\delta^{18}O_{sample}$ represents δ value of the bulk sample (mixture) and,

$$X(O)_{Hm} = \frac{n_{Hm}(O)}{n_{(SiO2)}(O) + n_{Hm}(O)}$$

n(O) represents moles of oxygen

The oxygen isotopic fractionation between SiO_2 and hematite for the four mineral pairs obtained after correction for end member $\delta^{18}O$-values have been used to calculate the temperature using the quartz-hematite fractionation equation

$$1000 \ln \alpha^{SiO_2} = \frac{1.46 \times 10^6}{T^2} + 9.0 \quad \text{(Yapp, 1990)}$$

The calculated temperatures range between 71.4° and 165.2°C. The range of temperature obtained shows that the sample have undergone diagenetic alteration and metamorphism of lower greenschist facies which is corroborated by field observation as well as petrographic study.

TABLE 9.3 OXYGEN ISOTOPE DATA AND TEMPERATURES CALCULATED FROM QUARTZ-HEMATITE FRACTIONATION FACTORS

			Corrected for end member δ-values		
Sample No.	$\delta^{18}O_{(mixture)}$	Wt% Fe_2O_3	$\delta^{18}O_{SiO2}$	$\delta^{18}O_{Hm}$	T°C
RHR-20	15.6	7.55	16.4	-1.8	125.2
	4.0	79.08			
RHR-25	14.9	9.38	16.1	-5.2	71.4
	4.8	66.63			
RHR-34	14.3	10.94	15.7	-5.3	75.7
	3.9	69.36			
RHR-44	14.0	9.06	14.9	-1.7	165.2
	5.3	70.84			

CHAPTER X

GEOCHEMISTRY OF ASSOCIATED METAVOLCANICS

10.1 General Statement

During the 4.6 Ga since the formation of the Earth and its primary fractionation into core, mantle and crust, melting of the more fusible constituents of the upper mantle has produced magmas which rise to the surface and solidify resulting in crustal evolution. Therefore volcanism plays an essential and vital role in all the stages of crustal evolution from Archaean to present. Greenstone belts represent one of the main components of early crustal growth and evolution. A large number of the contemporary earth scientists believe that most greenstone belts formed as a result of sea floor spreading followed by subduction-accretion processes associated with island arcs (Helmstaedf et al., 1986; de Wit et al., 1987; Condie, 1989; Taira et al., 1992). Burke and Kidd (1980) have reviewed the various types of volcanic rocks and their probable tectonic environments. They (ibid) suggest that basalts form at divergent plate boundaries; tholeiitic and calc-alkaline rocks, most characteristically andesites dominate where arcs form above subduction zones; highly potassic volcanics are associated with active continental collision. Burke and Kidd (1980) suggest that these processes along with the intraplate volcanism, appear to have operated at plate margins throughout most of the Earth's history. The geochemical data from volcanic rocks has been of great help to infer the tectonic setting and the processes through which they have formed.

Three sequences of volcanism including ultramafic, mafic and felsic rocks have been recognized in Kushtagi schist belt. The lower volcanic sequence is not well preserved and consists of largely ultramafic rock of komatiitic affinity. It is overlain by a succession of bimodal volcanism. Only overlying bimodal volcanic rocks have been taken up in the present study.

10.2 Major Element Geochemistry

The usefulness of major elements is restricted by element mobility and by the fact that these elements are always correlated in very simple patterns. There is not enough information in the limited number of independent variables to enable major elements to be used for tectonic discrimination. However for rock type definition and elementary petrogenetic classification they are useful.

The chemical data (Table 10) indicate that the volcanic sequence is bimodal in composition with basalts and rhyodacites dominant volumetrically (Fig. 10.1A). The intermediate volcanics are however not encountered in the present study.

Two fundamental magma series generally recognized are alkalic and sub-alkalic series. Each series has a succession of fractionation products ranging from basic to acid in composition. Based on Na_2O+K_2O and SiO_2 content it is evident from Fig. 10.1A that the Kushtagi volcanics are of sub-alkalic magma series. The sub-alkalic Kushtagi volcanics are further plotted on Alkali Index (A.I.) vs Wt.% Al_2O_3 diagram (Fig. 10.1B), which distinguishes between tholeiitic and calc-alkali basalts. As A.I. is less than 2 and Al_2O_3 is less than 16% in both basalts and rhyodacites, the

TABLE 10 CHEMICAL COMPOSITION OF BASIC AND ACIDIC VOLCANICS

Elements	Basic					Acidic				
(Wt.%)	RN-16	RN-25	RM-10	RKY-10	RKY-18	RKL-19	RKL-27	RKL-35	RKL-45	RKL-50
SiO_2	46.99	49.68	48.37	50.17	49.69	69.57	72.73	70.17	70.05	71.10
TiO_2	2.89	3.19	1.51	0.82	0.71	0.25	0.28	0.27	0.22	0.26
Al_2O_3	11.91	11.92	13.62	12.46	12.14	15.08	15.14	14.92	15.87	15.62
Fe_2O_3	5.89	4.19	5.85	3.27	0.97	0.67	0.97	1.28	0.89	1.43
FeO	12.02	11.86	7.84	8.68	9.76	1.32	0.92	1.06	0.92	0.78
MnO	0.23	0.26	0.20	0.19	0.20	0.03	0.03	0.02	0.04	0.02
MgO	5.32	5.56	7.92	10.62	12.64	0.82	0.70	0.80	0.46	0.77
CaO	9.35	7.96	9.65	10.77	11.88	1.91	2.29	1.82	2.45	2.06
Na_2O	1.98	2.24	1.50	1.82	1.68	5.82	4.32	5.92	5.12	5.54
K_2O	0.21	0.29	0.14	0.41	0.16	1.28	0.71	0.83	1.60	0.72
P_2O_5	0.12	0.14	0.07	0.08	0.08	0.07	0.06	0.08	0.07	0.08
LOI	3.00	3.00	2.50	1.00	1.00	2.50	1.50	2.00	2.00	2.00
Total	**99.91**	**100.29**	**99.17**	**100.29**	**100.91**	**99.32**	**99.65**	**99.17**	**99.69**	**100.38**
Sc(ppm)	46.88	38.90	29.54	38.78	41.24	2.66	3.39	2.67	2.26	2.29
V	605.76	186.52	335.09	233.36	251.58	2.99	3.17	21.42	-	-
Cr	5.47	36.54	102.72	728.71	1550.94	20.83	14.28	9.85	9.22	3.87
Co	80.84	80.71	56.27	97.62	99.75	73.13	59.29	44.57	37.87	68.76
Ni	2.00	2.00	67.64	81.34	167.26	2.63	2.03	3.36	1.00	2.00
Cu	25.47	21.43	200.83	128.66	98.43	31.58	24.85	41.99	0.81	5.41
Zn	140.58	140.59	224.93	88.15	82.75	34.14	20.60	43.89	32.35	38.86
Ga	17.05	18.88	19.06	14.43	13.79	22.73	24.77	21.72	19.60	20.70
Rb	4.87	13.20	1.00	26.13	2.96	32.56	21.66	21.78	36.89	19.14
Sr	119.64	132.39	166.39	218.90	99.94	303.41	178.06	220.28	266.04	185.78
Y	33.02	64.36	53.27	22.29	18.98	4.74	6.84	7.21	5.89	4.95
Zr	27.15	69.96	48.78	14.80	15.48	57.90	99.33	60.06	85.73	64.41
Nb	2.58	6.15	4.99	3.11	2.43	2.58	2.49	1.46	1.99	1.82
Ba	26.07	57.59	12.65	38.90	12.07	378.56	441.33	233.16	268.10	153.57
Hf	0.85	1.95	1.07	0.61	0.58	1.85	2.58	1.78	2.22	1.85
Ta	0.31	0.41	0.35	0.41	0.19	0.56	0.53	0.34	0.62	0.62
Th	0.32	0.54	0.56	0.45	0.36	4.45	4.67	3.24	4.22	2.39
U	0.11	0.17	0.20	0.16	0.09	1.44	1.88	0.69	1.59	0.31
La	3.71	6.30	8.66	4.29	3.08	15.04	20.12	12.78	12.63	12.64
Ce	9.11	16.77	21.56	11.13	7.44	27.37	37.76	26.22	23.79	23.98
Pr	1.63	2.99	2.82	1.52	1.10	3.00	3.46	2.70	2.21	2.66
Nd	7.64	13.42	16.66	7.76	5.02	10.90	14.87	12.51	10.17	10.54
Sm	2.20	5.39	5.11	2.40	1.42	1.93	1.87	2.06	1.69	1.79
Eu	1.22	1.65	1.67	0.73	0.48	0.61	0.67	0.62	0.49	0.70
Gd	3.58	5.60	5.92	2.38	1.85	1.68	2.36	1.67	1.39	1.82
Tb	0.74	1.18	1.15	0.46	0.34	0.21	0.29	0.25	0.21	0.22
Dy	5.04	8.05	7.55	2.97	2.17	0.85	1.17	1.27	0.90	0.85
Ho	0.99	1.71	1.62	0.62	0.49	0.17	0.23	0.27	0.19	0.20
Er	2.39	4.46	4.21	1.52	1.37	0.39	0.51	0.70	0.51	0.55
Tm	0.42	0.76	0.66	0.24	0.22	0.06	0.08	0.11	0.09	0.07
Yb	2.86	5.18	4.17	1.64	1.44	0.38	0.53	0.69	0.53	0.34
Lu	0.40	0.60	0.57	0.23	0.21	0.06	0.07	0.07	0.07	0.04
Fe_2O_3/FeO	0.49	0.35	0.75	0.38	0.10	0.51	1.05	1.21	0.97	1.83
Cr/Ni	2.74	18.27	1.52	8.96	9.27	7.92	7.03	2.93	9.22	1.94
Rb/Sr	0.04	0.10	0.01	0.12	0.03	0.11	0.12	0.10	0.14	0.10
$La_{(N)}/Lu_{(N)}$	1.00	1.14	1.64	2.02	1.59	27.10	31.07	19.74	19.51	34.16
ΣREE	41.93	74.06	82.33	37.89	26.63	62.65	83.99	61.92	54.87	56.40

Figure 10.1A. Total Alkali Silica (TAS) diagram show types of metavolcanic present in Kushtagi schist belt (after Le Bas et al., 1986). Solid triangle = Low Mg-basalt; + = High Mg-basalt; Solid circle = rhyodacite. Same symbols are used in all illustrations of this chapter.

Figure 10.1B. A.I. vs Al_2O_3 diagram show tholeiitic nature of metavolcanics (after Middlemost, 1975).

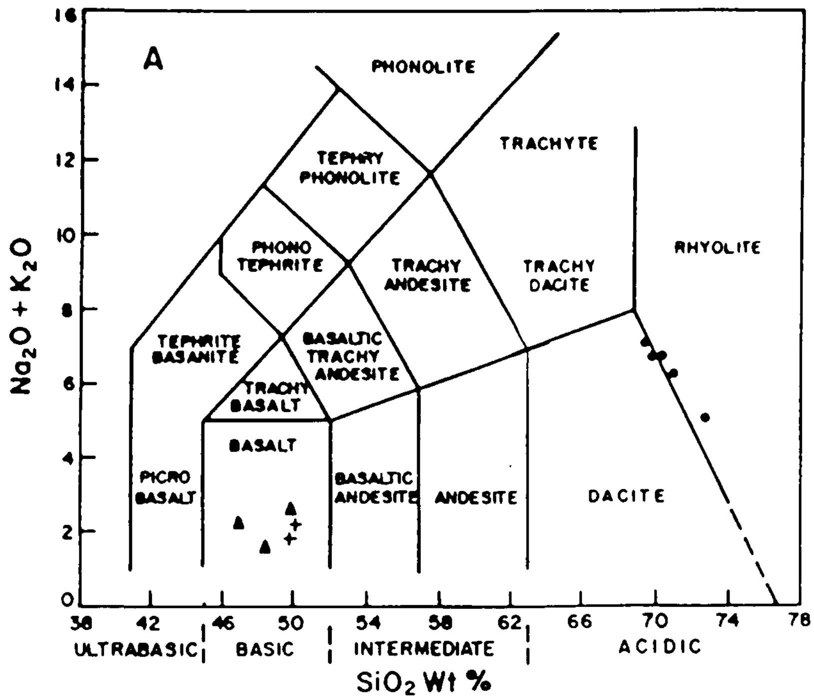

TOTAL ALKALI SILICA (TAS) DIAGRA after Le Bas et. al. 1986)

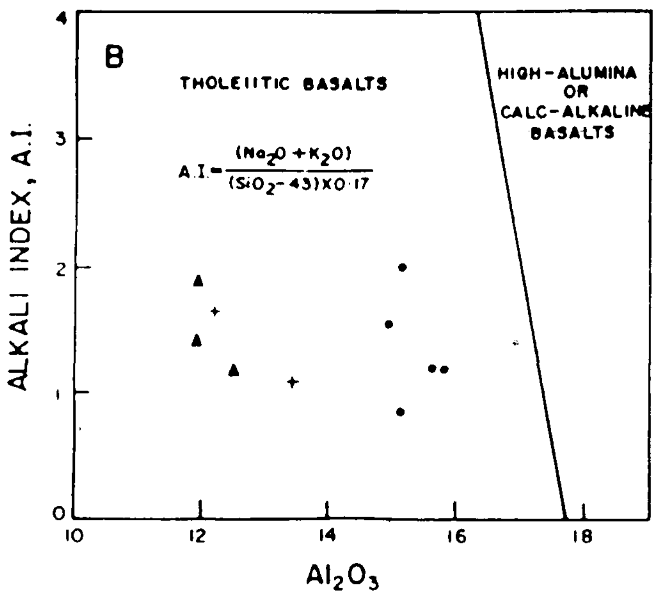

magma series is classified as of tholeiitic basalt characteristic. Based on MgO% two types of basalts are recognized in the belt. The basalts with <8% MgO is enriched in Fe_2O_3(T) and TiO_2 and other variety having MgO>10% is depleted in Fe_2O_3(T) and TiO_2. CaO content in MgO depleted variety is less than 10% whereas in MgO enriched variety it is more than 10%. Alkali content is similar in both the varieties. TiO_2 content in low Mg basalts is very high. It is enriched upto 3.19%., due to the presence of very high amount of sphene and ilmenite. The Al_2O_3 content in basalts ranges from 11.91 to 13.62%, whereas, in rhyodacites it ranges from 14.92 to 15.87%. The CaO in rhyodacites varies between 1.82 to 2.45 and the alkali content ranges from 5.03 to 7.74.

10.3 Trace Element Geochemistry

The concentrations of the compatible elements Ni, Cr and Co are higher in Archaean than modern tholeiitic basalts (Condie, 1985). In Kushtagi belt low Mg-basalts contain very low amount of Ni and Cr (Ni range between 2-68 ppm; Cr ranges between 5-103 ppm) whereas the high-Mg variety contain appreciably higher amount of Ni and Cr (Ni ranges between 81-167 ppm and Cr ranges between 728-1550 ppm). Co content is uniform in both the varieties and varies from 56 to 100 ppm. Zr content in both the varieties ranges between 14.80 to 69.96 which is slightly lower in comparison to Zr content of basalts from other late Archaean schist belts.

In rhyodacites Cr, Ni and Zr content is low as was in the case of low Mg-basalts, indicating a probable common source. Sr ranges from 178-303 ppm, Ba ranges from 153-441 ppm whereas Hf is extremely low (<3 ppm). These trace elements indicate that low-Mg basalts and rhyodacites might have formed by partial melting and fractional crystallization of high Mg basalt and other ultramafic bodies.

Trace element data help to describe and characterize the rocks utilizing comparative diagrams. These data are then used to establish possible tectonic settings. Fairly large number of trace element studies have been made on volcanic rocks of different places and ages, with the aim of identifying their eruptive environment (Bickle and Nisbet, 1972; Pearce and Cann, 1973; Naqvi and Hussain, 1979; Burke and Kidd, 1980; Bhaskar Rao and Drury, 1982; Drury, 1983; Rajamani et al., 1985; Manikyamba and Naqvi, 1993).

10.3.1 Discriminant Diagrams

Volcanic rocks of the Kushtagi schist belt are plotted on TiO_2-Mn-P_2O_5 tectonic discriminant diagram; which was developed by Mullen (1983; Fig. 10.2A). As the TiO_2 content in low Mg basalts is exceptionally high, these samples fall in MORB field whereas other basalts fall in IAT field. The rhyodacites also fall in IAT field or close to it. In general, the Kushtagi schist belt volcanic suite plot as a plate margin sequence with characteristic of both diverging (MORB) and converging (IAT) margins. Two rhyodacitic sample lie in oceanic island alkalic (OIA) setting.

The Zr-(Ti/100)-(Yx3) tectonic discriminant diagram was developed by Pearce and Cann (1973), using data from Cenozoic basaltic rocks that met the criteria of 20% >(CaO+MgO) >12%. The low Mg-basalt sample met the CaO+MgO requirement but the high

Mg-basalt contain slightly higher amount of CaO+MgO (upto 24.52%). Rhyodacites contain very low amount of CaO+MgO (max. 2.99%). Therefore this diagram is not applicable for knowing the tectonic setting of acid volcanics. Due to abnormality in TiO_2 and Zr content none of the basalt sample plots on any of the field but they show affinity towards IAT and MORB (Fig. 10.2B).

Three of the basalt samples plot just at the edge of low-K tholeiite field, while two falls away due to higher amount of TiO_2 content in them on Ti-Zr diagram (Fig. 10.2C). All the samples of rhyodacites fall away from specified fields.

In Zr/Y-Zr plot (Fig. 10.2D) also the basalt samples lie very close to IAT and MORB field. When all the geochemical characteristic are taken into account the Kushtagi volcanics seems to be the product of multiple melting and crystallization with characters of one superimposed on the other.

Nb, Th and La are normalized to primitive mantle values (Hofmann, 1988), and plotted on $Th_{(N)}$-$Nb_{(N)}$-$La_{(N)}$ diagram, developed by Jochum et al. (1991). The samples are displaced slightly away from the Th and Nb apexes as a result of depletion of the more incompatible elements. All the samples seems to follow komatiitic trend indicating their uncontaminated nature.

10.4 <u>REE Geochemistry</u>

The REE content of the Kushtagi basalts are found to be very similar to the low K-tholeiites of island arcs (Arth and Hanson, 1975). The low Mg-basalts have higher amount of ΣREE in comparison to high-Mg basalts. The fact that MgO content decreases as REE content increases is consistent with olivine, 10.2A. TiO_2-MnO-P_2O_5 tectonomagmatic discrimination diagram for oceanic basaltic rocks. OIT= oceanic island tholeiite; OIA= oceanic island alkalic; MORB= mid-ocean ridge basalt; IAT= island arc tholeiite; CAB= island arc calc-alkaline basalt (after Mullen, 1983).

10.2B. Ti/100-Zr-Y.3 tectonomagmatic discrimination diagram for basaltic rocks. WPB= within-plate basalts; IAT= island-arc tholeiites; CAB= calc-alkaline basalts; MORB= mid-ocean ridge basalts (after Pearce and Cann, 1973).

10.2C. Ti-Zr discrimination diagram. Ocean-floor basalts (OFB) plot in fields D and B, low-potassium tholeiites (LKT) in fields A and B, and calc-alkali basalts (CAB) in fields C and B (after Pearce and Cann, 1973).

10.2D. Zr vs Zr/Y plot. WPB = within-plate basalts; MORB= mid-ocean ridge basalts; IAT = island-arc tholeiites (after Pearce, 1980).

10.2E. La-Nb-Th diagram. All data are normalized to primitive mantle values (Hofmann, 1988). The metavolcanics of Kushtagi schist belt show komatiitic trend. OIB= oceanic island basalt; MORB= mid-ocean ridge basalt (after Jochum et al., 1991).

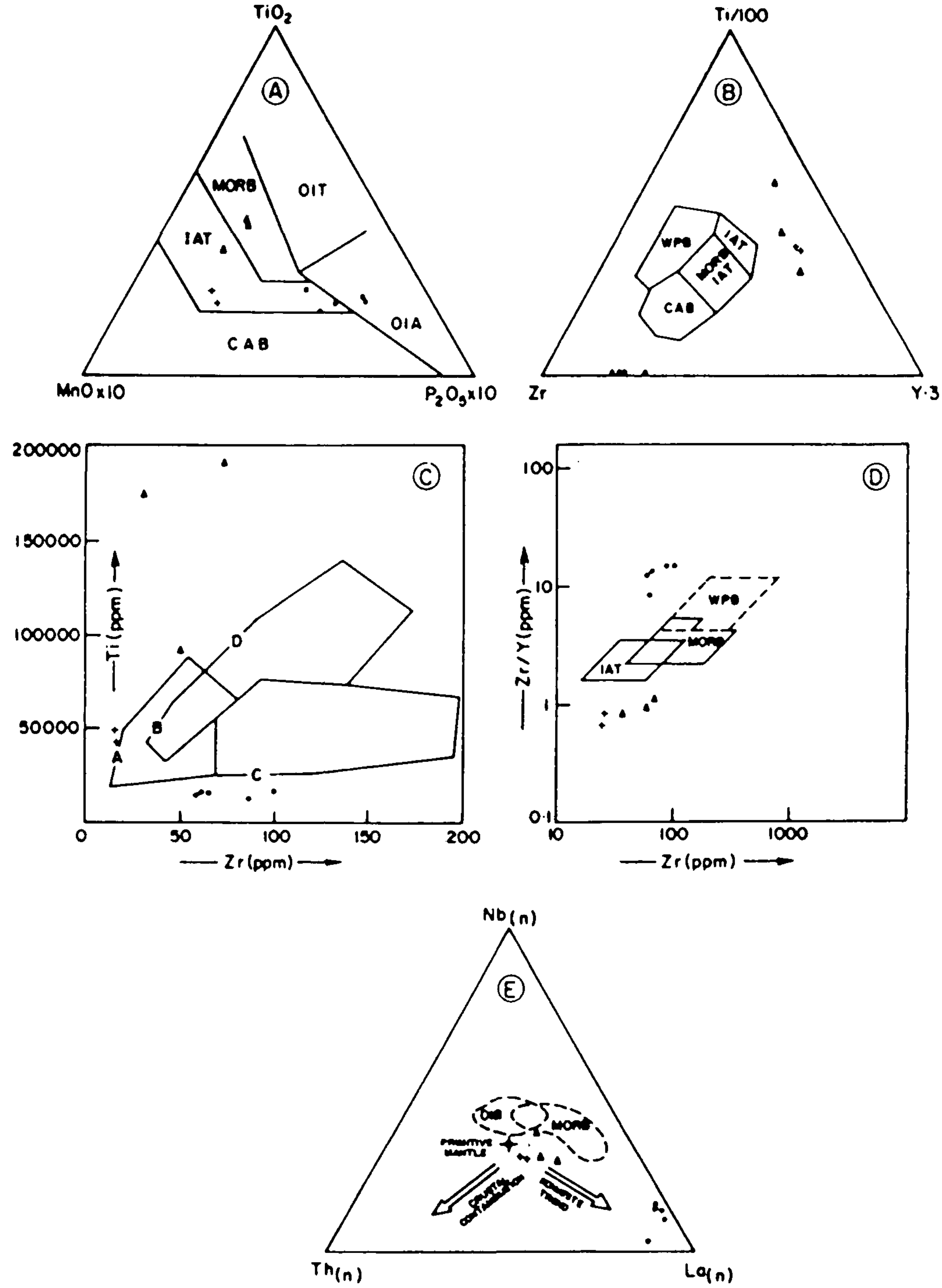

TiO2
A
MORB
OIT
IAT
OIA
CAB
MnO x10
P2O5 x10
Ti/100
B
WPB
IAT
MORB
IAT
CAB
Zr
Y·3
200000
150000
100000
50000
Ti (ppm)
C
D
B
A
C
0
50
100
150
200
Zr (ppm)
100
10
1
0·1
10
100
1000
Zr/Y (ppm)
D
WPB
MORB
IAT
Zr (ppm)
Nb(n)
E
OIB
MORB
PRIMITIVE MANTLE
Th(n)
La(n)

pyroxene and plagioclase fractionation. Both types of basalts show REE patterns confining to a narrow range of chondrite normalized REE abundance with no significant LREE to HREE fractionation with mild negative to positive Eu anomalies (Fig. 10.3). The flat REE pattern with no Eu anomaly in the basalts can be produced by about 25% melting for a magma by direct melting of peridotite source (Arth and Hanson, 1975).

The rhyodacites are interbedded with the depleted basalts and exhibit the distinctive signature of HREE depletion (Fig. 10.4), characteristic of many Archaean dacites (Arth, 1979) and some modern dacites formed at convergent plate margins (Hickey-Vargas et al., 1989).

Presence of basaltic and rhyodacitic volcanics in the belt with significant chemical parameters indicate that they were generated in a regimes of compositional of IAT and tensional setting of MORB as well. Ultramafic rocks along with basalts similar to those of IAT and MORB requires the spreading ridge in the region and the presence of basalts of IAT characteristic and rhyodacites indicate partial melting of the subducting lithosphere. The basalt formed at MOR probably got subsequently subducted and gave rise to basalts and rhyodacites of IAT affinity after partial melting and fractional crystallization. The geochemical data of the BIF as presented earlier and discussed subsequently very clearly demonstrates the existence of a MOR from which FeO and SiO_2 rich solutions were added (Chapter IX). Deformation pattern of greenstone belts and emplacement of IAT

Figure 10.3. REE patterns of basalts show flat REE pattern similar to low-K tholeiites of island arcs.

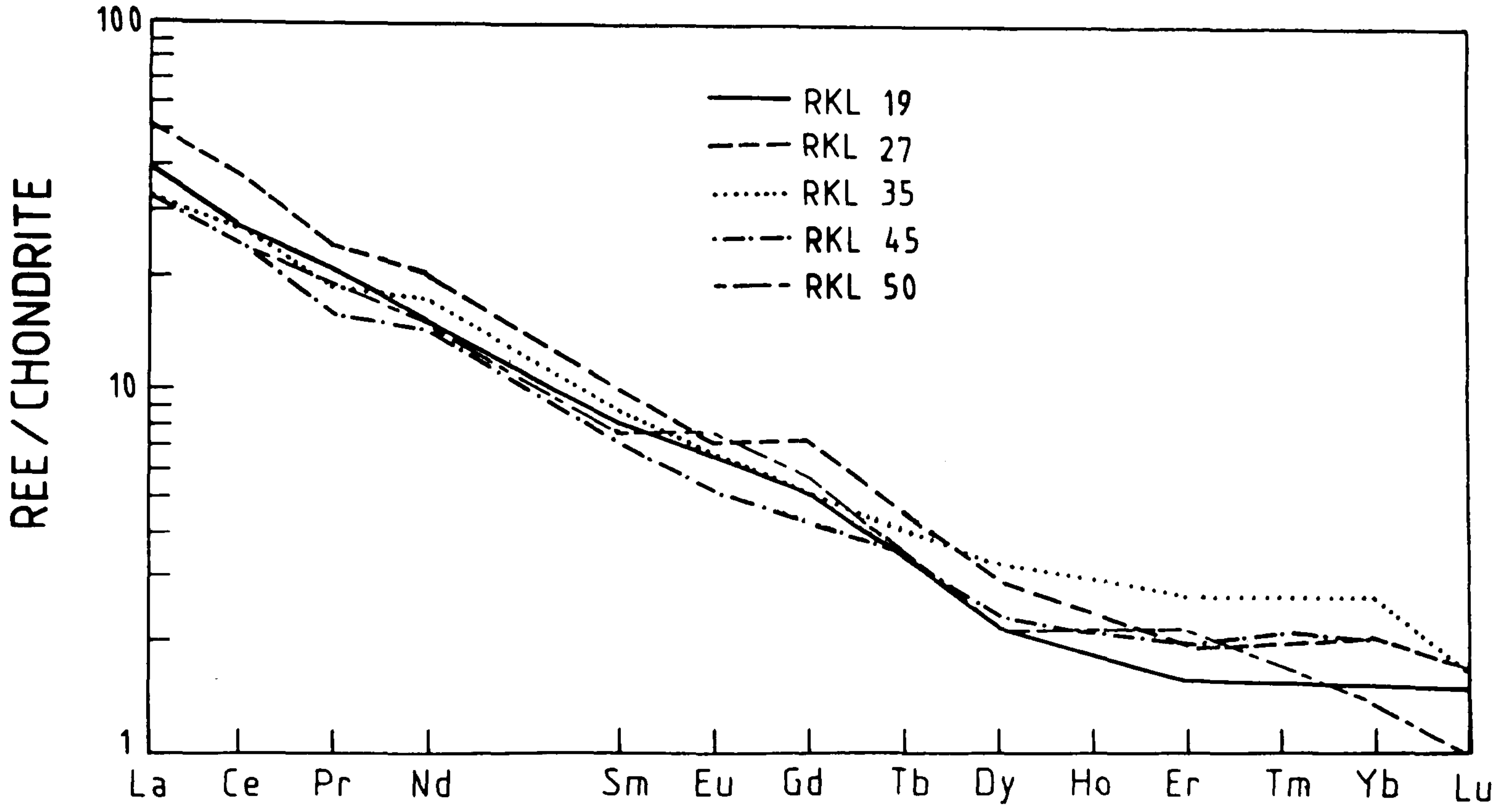
REE / CHONDRITE
100
10
1
RKL 19
RKL 27
RKL 35
RKL 45
RKL 50
La
Ce
Pr
Nd
Sm
Eu
Gd
Tb
Dy
Ho
Er
Tm
Yb
Lu

Figure 10.4. REE pattern of rhyodacites show highly fractionated pattern.

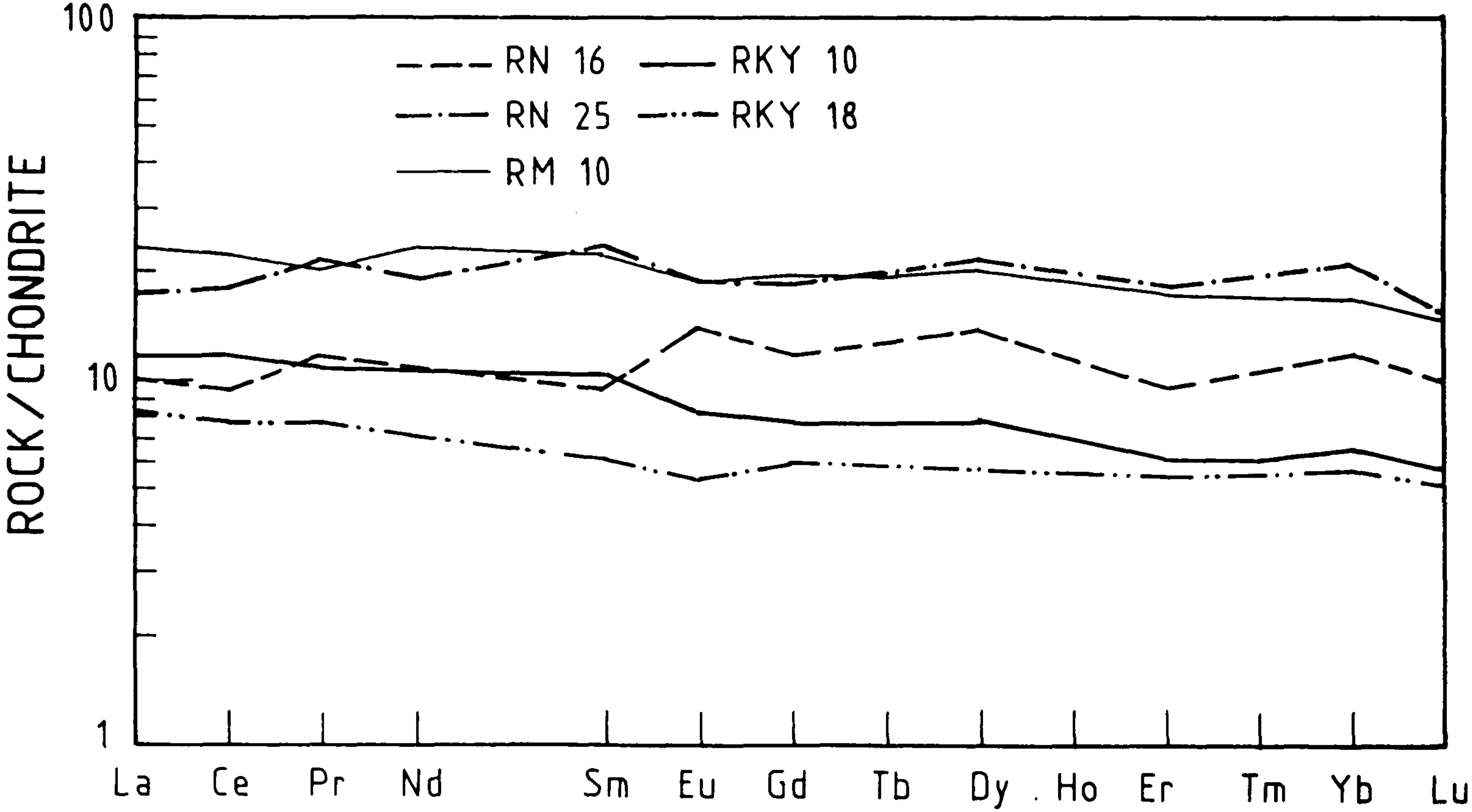
ROCK / CHONDRITE
100
10
1
RN 16
RKY 10
RN 25
RKY 18
RM 10
La
Ce
Pr
Nd
Sm
Eu
Gd
Tb
Dy
Ho
Er
Tm
Yb
Lu

indicates that these regions were converted into subduction related tectonic zones. Hence rocks of different types of tectonic setting were brought together.

CHAPTER - XI

DISCUSSION AND SYNTHESIS

The chemical and petrological characteristics of BIF and associated metavolcanics from Kushtagi schist belt, presented in the preceding chapters, provide insight into the genesis of BIF, which is one of the highly debatable and controversial aspects of Precambrian Geology. In Chapter V, a brief review of the existing information related to the problems of the genesis and evolution of the BIFs has been presented and various questions have been raised which still awaits satisfactory explanation. Based on the present work, a possible model for the genesis of BIF, namely, source of SiO_2, FeO and other constitutents alongwith depositional environment and tectonic setting is proposed.

11.1 Source of FeO and SiO_2

The mineralogy and geochemistry of Kushtagi banded iron formation indicate that the CBIF mainly consists of hematite and microcrystalline quartz (chert), with some clastic contamination in the form of muscovite, whereas, the SBIF, apart from iron and silica, has significant amount of clastic contamination in the form of kaolinite and muscovite, which is reflected in their whole rock chemistry. The salient features of REE in CBIFs which help to model the source of FeO and SiO_2 are , (1) low ΣREE content, (2) prominent positive Eu anomalies and (3) flat REE to HREE enriched pattern. The La spiking observed in Sandur (Manikyamba et al., 1993), Chitradurga (Gnaneshwar Rao and Naqvi, 1993), Lake

Superior region (Barrett et al., 1988) and in some samples of Kudremukh iron formation (Khan et al., 1992) is however, not present in the samples of Kushtagi schist belt. In previous chapters, it has been indicated that there can be three possible sources for iron and silica in BIFs, namely, (a) river water and aeolian storms, (b) detrital sediments deposited in the deeper and reducing part of the basin and (c) hydrothermal exhalation. Presence of low concentration of ΣREE and flat REE to slightly enriched HREE pattern with positive Eu anomaly have ruled out the possibility of continental material and/or detrital sediments deposited in deeper and reducing part of the basin being the only source of FeO and SiO_2 for BIFs of Kushtagi schist belt, as these data remarkably differ from those of the present day ocean water. Present day ocean water shows extreme depletion in ΣREE, absence of positive Eu anomaly and presence of a strong negative Ce anomaly (Fig. 11.1A). Instead, these geochemical characteristics are almost similar to those of hydrothermal fluids and metalliferous deposits near the Mid Oceanic Ridge (MOR). Hydrothermal solutions emplaced in present day oceans of East Pacific Rise, Mid Atlantic Ridge and Red Sea are depleted in ΣREE and have positive Eu anomalies (Edmond et al., 1982; Piepgras and Wasserburg, 1983; Klinkhammer et al., 1983; Michard et al., 1983; DeBaar et al., 1985; Bowers et al., 1985; Michard and Albarede, 1986; Ruhlin and Owen, 1986; Campbell et al., 1988b; Olivarez and Owen, 1989; Derry and Jacobsen, 1990). The REE patterns of the hydrothermal solutions from EPR are shown in Fig. 11.1B. Chemical data on hydrothermal deposits have been used by Dymek and Klein

(1988), and Klein and Beukes (1989) to distinguish between the hydrothermal and hydrogenous deposits. When data from Kushtagi schist belt are plotted on this diagram, most of the CBIF samples fall within or very close to the field of hydrothermal deposits (Fig. 9.10). However, due to presence of clastic contamination, which has elevated the ΣREE content, SBIF samples fall away from this field. Therefore, depleted nature of ΣREE, positive Eu anomalies and flat REE to slightly enriched HREE in the BIFs of Kushtagi schist belt indicate that their metal constituent was added to ambient ocean by hydrothermal solution at Archaean Mid Oceanic Ridge (AMOR). Such hydrothermal source for the FeO of BIF has been suggested by several workers (Simonsen, 1985; Barrett et al., 1988; Klein and Beukes, 1989; Khan et al., 1992; Morris, 1993; Alibert and McCulloch, 1993; Gnaneshwar Rao and Naqvi, 1993; Manikyamba et al., 1993). The REE patterns of Kushtagi iron formation is in general similar to that of many other Archaean BIFs (Fig. 11.1C). Klein and Beukes (1989) have modelled that deposition from an admixture of EPR hydrothermal fluids and North Atlantic sea water in a 1:100 ratio will yield ΣREE and positive Eu anomalies identical to those observed in BIFs (Fig.11.1D).

The ϵ_{Nd} data (ϵ_{Nd} = $^{143}Nd/^{144}Nd$) of the BIF from Hamersley basin (Western Australia) and Michipicoten basin, Ontario, Canada (2.7-2.9 Ga) show that the solutions which provided iron and Nd were derived from the mantle as the ϵ_{Nd} is closer to that of depleted mantle and varies between 0 to +4 (Jacobsen and Pimentel-Klose, 1988). The data from Michipicoten BIF is presented in Fig. 11.2A. The Nd elemental concentration is shown against Al_2O_3 and

Figure 11.1A NASC normalized REE abundances of average river water dissolved material, the effective river flux to the oceans, average hydrothermal water and average sea water. The heavy REE enrichment of average river water and the effective river flux to the oceans is similar to that of average sea water (after Goldstein and Jacobsen, 1988).

Figure 11.1B REE data from 21^{O}N hydrothermal waters (after Derry and Jacobsen, 1990).

Figure 11.1C REE patterns of various Archaean iron formations. closed triangle = Bjornevorn iron formation, open circle = Beartooth iron formation, closed circle = Vermillian iron formation, open triangle = averege of Isua iron formations. Solid lines represents the REE pattern of averege seawater (after Derry and Jacobsen, 1990).

Figure 11.1D NASC normalized REE patterns of the EPR hydrothermal fluid of different dilutions, North Atlantic Seawater and Siderite Rich BIF (after Klein and Beukes, 1989).

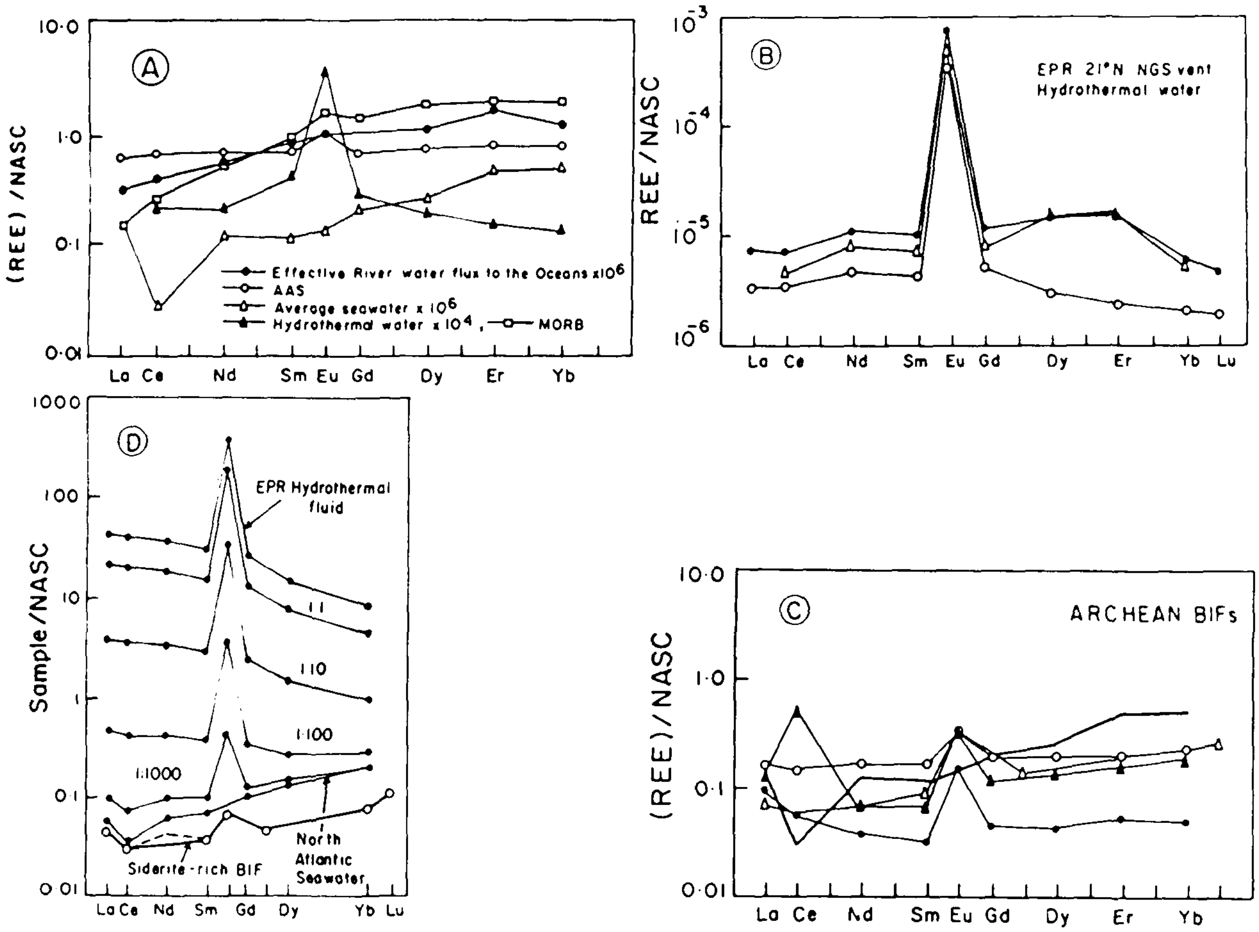

A
(REE)/NASC
Effective River water flux to the Oceans x10^6
AAS
Average seawater x 10^6
Hydrothermal water x 10^4
MORB
B
REE/NASC
EPR 21°N NGS vent
Hydrothermal water
D
Sample/NASC
EPR Hydrothermal fluid
1:1
1:10
1:100
1:1000
Siderite-rich BIF
North Atlantic Seawater
C
(REE)/NASC
ARCHEAN BIFs
La Ce Nd Sm Eu Gd Dy Er Yb Lu

P_2O_5 (Fig. 11.2B). The positive ϵ_{Nd} signature observed in Hamersley and Michipicoten was a global feature of Archaean ocean (Jacobsen and Pimentel-Klose, 1988). Positive values of ϵ_{Nd} indicate that there is a strong depleted mantle contribution for the Nd present in BIFs older than 2.0 Ga. The sediments of younger ages, ocean water and river water yield negative ϵ_{Nd} values. Therefore, the Nd isotopic data rules out the continental source, either as dissolved or suspended load for the Fe of BIFs. However, according to Alibert and McCulloch (1993), all Nd in Hamersley iron-formation does not belong to hydrothermal source. The ϵ_{Nd} of the Marra Mamba and Jeerinah BIFs and shales have negative ϵ_{ND} values and are therefore continental, but the Dales Gorge-Joffne iron-formation in Wittenoom area have positive ϵ_{ND} values similar to that of depleted mantle.

Apart from iron, the second most important constituent in BIF is silica. As the REE patterns of silica enriched samples also show the same character as those of the iron rich samples, the source of silica must be the same as that of iron in BIF. Cherts and ferruginous cherts within, and associated with, BIF having depleted ΣREE, flat patterns with significant positive Eu anomalies have also been reported from other schist belts of DC (Khan et al., 1992; Gnaneshwar Rao and Naqvi, 1993; Manikyamba et al., 1993). These characteristics indicate that the SiO_2 of BIFs is also supplied by the hydrothermal solutions. Probably due to high exit temperature and alkalinity of the Archaean hydrothermal water, higher amount of SiO_2 was dissolved in it and added to the oceans. Mixing with the relatively cold oceanic water and lower

Figure 11.2A Isochron diagram showing the analytical results for Michipicoten BIFs. Reference lines corresponding to the U-Pb zircon age of 2.744 Ga are shown for initial Nd values of 0 and +4 (after Jacobsen and Pimentel-Klose, 1988). Symbols are same as in Fig. 11.1C.

Figure 11.2B Nd vs P_2O_5 and Nd vs Al_2O_3 variation diagrams of Michipicoten BIFs (after Jacobsen and Pimentel-Klose, 1988).

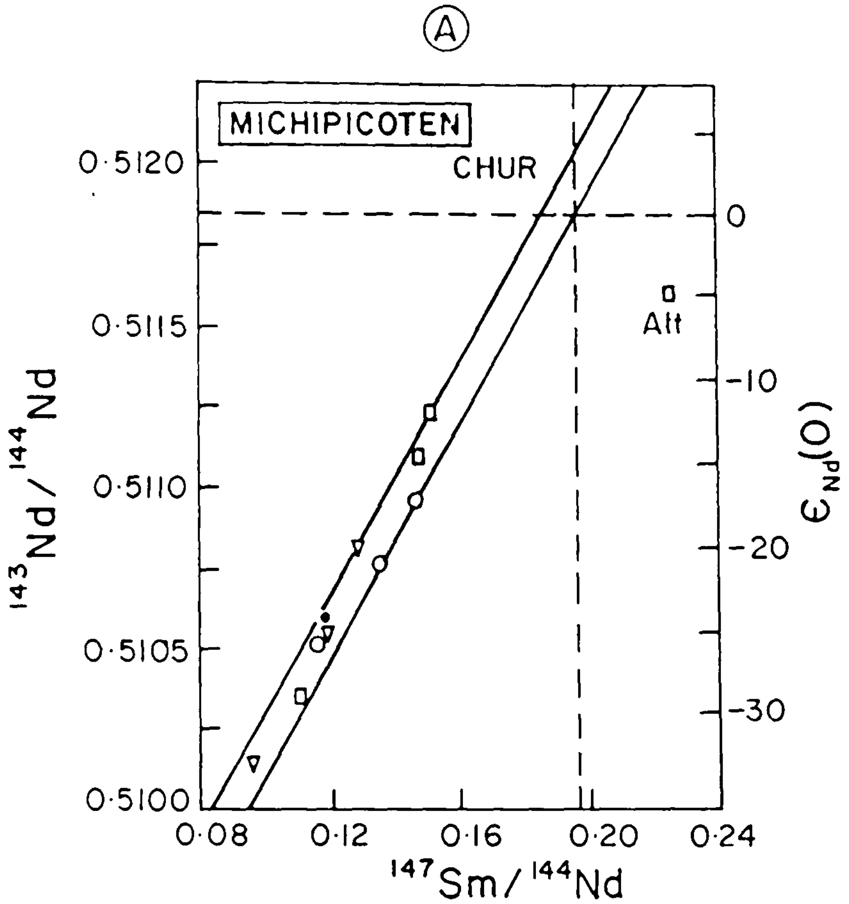
A
MICHIPICOTEN
CHUR
Alt
0·5120
0·5115
0·5110
0·5105
0·5100
0
-10
-20
-30
0·08
0·12
0·16
0·20
0·24
$^{147}Sm/^{144}Nd$
$^{143}Nd/^{144}Nd$
$\epsilon_{Nd}(0)$

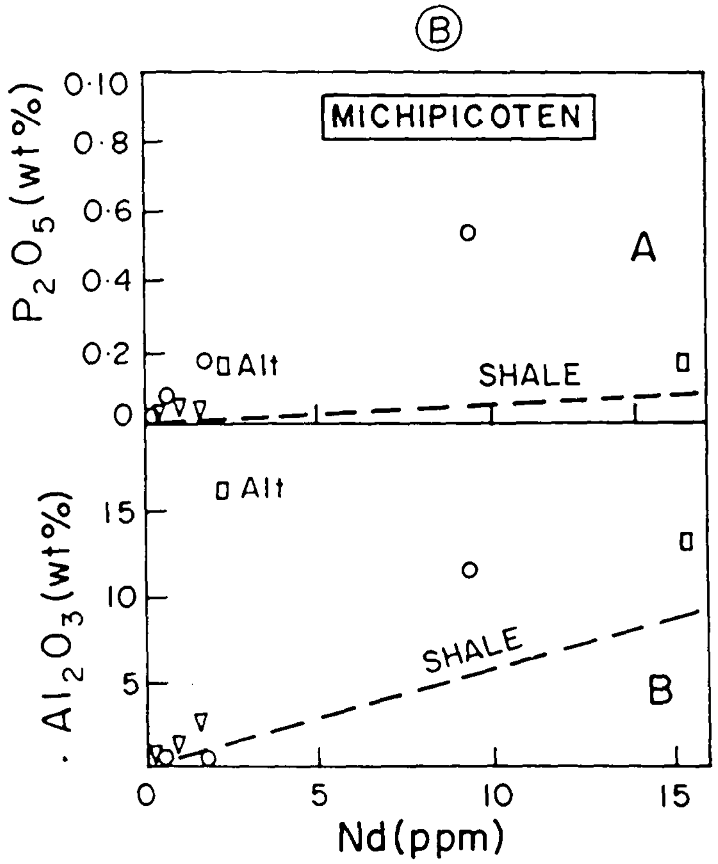
B
MICHIPICOTEN
Alt
SHALE
A
Alt
SHALE
B
0·10
0·8
0·6
0·4
0·2
0
15
10
5
0
5
10
15
P_2O_5 (wt%)
Al_2O_3 (wt%)
Nd(ppm)

alkalinity might have resulted in its precipitation. Hence, continuous supply of high concentration of SiO_2 rich hydrothermal solutions is essential to generate these BIFs. Higher silica concentrations (silica anomalies) associated with hydrothermal solutions of vents of the Guayamas Basin of Gulf of California and other places have been observed (Campbell and Gieskes, 1984; Campbell et al., 1988a). Cloud like features are formed from numerous hydrothermal plumes at modern MOR, which spread laterally as they approach density equilibrium with ambient water. These hydrothermal clouds show enrichment in dissolved SiO_2 and other elements and show depletion in dissolved oxygen relative to areas away from the vents (Campbell and Gieskes, 1984; Campbell, 1985; Campbell et al., 1988b).

11.2 Source of O_2

The source of O_2 has to be consistent with the rate of oxidation of FeO to Fe_2O_3 within a short time. So far, neither stromatolites nor microfossils have been discovered in Kushtagi region, but bands of dolomite are present at various places in the belt in association with chlorite schist and BIF. As Kushtagi schist belt is a truncated one, it is possible that the stromatolitic horizon has been eroded and destroyed or preserved elsewhere. Although stromatolites were not observed during reconnaissance survey, the lithological association and tectonic setting indicate that a detailed search may reveal a stromatolitic horizon. Transitional sequences from stromatolites through carbonates to BIFs have been reported from Chitradurga, Shimoga and Sandur schist belt (Gnaneshwar Rao, 1992). This phenomena is very rare in the Archaean as well as in early Proterozoic iron bearing basin except the Transvaal basin in South Africa (Klein and Beukes, 1989). This transition from stromatolitic carbonates to BIF is a very important constraint in the genesis of microfossils. In some of the greenstone belts of India, the O_2 level was high enough to allow MnO_2 precipitation, which is associated with organic matter, stromatolites and a few bands of cherts containing cyanobacteria (Manikyamba and Naqvi, 1993a). Microfossils and pseudo-microfossils are found in Chitradurga schist belt (Suresh, 1982) and the $\delta^{13}C$ values (-16.5%. MSW) of the carbon present in it provide the basic data to infer the relationship between the deposition of BIF and biogenic activity (Gnaneshwar Rao and Naqvi, 1993). Stromatolitic structures have been recognized in BIF of Sandur schist belt (Naqvi et al., 1987), Michipicoten (Hofmann et al., 1991) and Transvaal region (Klein et al., 1987). Moreover, Morris (1993) has also argued in favour of widespread organic carbon productivity and photosynthetic activity to produce O_2, needed for the precipitation of Fe oxides and hydroxides. Therefore, the most probable source of O_2 needed for the precipitation of Kushtagi iron-formation appears to be the cyanobacterial/stromatolitic colony present in the shallow shelf region, above wave base and photic zone.

11.3 Formation of Banding in BIF

One of the highly debated and controversial aspects of BIF is the formation of the mesoband of iron and chert. In previous sections, it has been inferred that the source for FeO and SiO_2 of the Kushtagi iron-formation is hydrothermal exhalatives produced near AMOR. The FeO and SiO_2 were supplied continuously in ambient ocean in a reducing environment. These FeO and SiO_2 under the affect of thermocline and chemocline moved towards shallow shelf region of the basin where O_2 was being generated by photosynthetic activity. Iron oxides and hydroxides were formed by reaction between FeO and O_2. As there is no apparent relation between the presence of free O_2 and the deposition of SiO_2, it is possible that precipitation of chert was a continuous phenomena. The production of free O_2 was episodic, which was required to react with Fe^{3+}. This episodic production of O_2 seems to be mainly responsible for the formation of rhythmic iron and silica rich layers. However, discontinuity in supply of FeO cannot be ruled out. Trendall (1983) and Garrels (1987) have proposed evaporatic model for the formation of bands in BIF. This possibility is ruled out for the lack of presence of anhydrite and gypsum along with BIF. It is difficult to assume a restricted basin where hydrothermally produced FeO and SiO_2 were being continuously supplied. Morris (1993) has advocated that chert rich band was formed under seasonal meteorological influence by precipitation of silica from the surface currents, saturated with silica, whereas, the iron rich band precipitated from convection driven upwelling from MOR or hot-spot activity. This model is also not applicable to Kushtagi iron-formation, as, the source of iron and silica is the same. Both chert and CBIF have identical ΣREE and Eu anomalies. The chert precipitated from sea water does not have positive Eu anomalies (Rangin et al., 1981). Therefore it is suggested that both iron and silica upwelled from MOR and reached the shallow shelf of the basin where they got precipitated. Silica was precipitated due to change in the alkalinity and temperature of the ocean water, whereas, FeO was precipitated as iron-oxides and -hydroxides after reacting with photosynthetically produced O_2. For the lack of presence of iron and/or silica secreting bacteria in BIFs of Kushtagi, the direct involvement of microorganisms for the production of iron and chert bands, as suggested by LaBerge (1973, 1986) and Nealson and Myers (1990) is not substantiated. Thus, it is possible that the precipitation of silica rich layers was a continuous phenomenon while the deposition of iron rich layers was rhythmic, dependent on the availability of O_2 or FeO or both. Since the FeO content in the ocean water reservoir has been accumulated from the beginning as a consequence of reducing environment, it is likely that intermittent availability of O_2 may be the main reason for the formation of banding in BIF.

11.4 Palaeoenvironment of Deposition of BIF

Geochemical studies of BIF from the Kushtagi schist belt indicate that FeO, SiO_2 and REE were provided through AMOR. The huge BIF deposit implies a higher amount of contribution of these elements into the basin. Three factors might have combined to add a large amount of FeO and SiO_2 namely (1) very high amount of hydrothermal flux into the basin, (2) fairly higher exit temperature of the hydrothermal solutions than those of the present to bring large amount of FeO and SiO_2 into solution and (3) higher ridge length and shorter duration of Wilson Cycle.

The FeO, SiO_2 and REE provided by hydrothermal exhalation got upwelled and reached the site of deposition, i.e., shelf region. To understand the mechanism of upwelling and transportation of FeO, SiO_2 and REE, the composition of ancient ocean has to be known. The present day temperature of the hydrothermal solutions added at MOR is estimated to be around 350°C (Campbell et al., 1988b). Therefore, the temperature of Archaean hydrothermal solutions should be same or even more. Oxygen isotopic data for the Archaean cherts indicate a mean temperature of around 80°C for the ocean at that time (Costa et al., 1981). Based on these observations, Holland (1984) suggested that thermal upwelling of ocean water takes place due to temperature differences between the ocean water at depth and that at the continental shelf. This has been termed as thermocline (Jacobsen and Pimentel-Klose, 1988). The other major difference between the deep ocean water and that of shelf region is chemocline. The deep ocean is highly reducing whereas the shelf region is oxidizing. Thus, these thermal and chemical differences at two sites are responsible for transportation of FeO, SiO_2 and REE from ridge to the site of deposition.

Ferric iron is virtually insoluble in the pH range of most natural waters (pH 3-9) and it is accepted that it is normally transported in the ferrous state (Fe^{2+}, $Fe(OH)^{+}$) (Morris, 1993), with its solubility controlled by both pH and redox conditions, as well as by the activities of carbonate, silicate and sulphide (Ewers, 1983). Although number of mechanisms for precipitation of BIF have been proposed (Morris, 1993), oxidation of soluble Fe^{2+}

to insoluble Fe^{3+} seems to be more acceptable. The solubility of amorphous silica in normal sea-water is independent of pH and unaffected by oceanic salinities (Ewers, 1983). However, it is presumed that the enormous quantity of SiO_2 present as chert in the Archaean BIFs can be explained, if the solubility of silica, at higher temperature and alkalinity, is greatly increased. The precipitation of silica in BIF is still being greatly debated from biological (LaBerge, 1986) through evaporative concentration (Garrels, 1987) co-precipitation with Fe^{3+} (Ewers, 1983) and polymerisation (Iler, 1979) to supersaturation (Morris, 1993).

The fluctuation in Kushtagi basin is indicated by the presence of continental derived clayey material within the SBIF band (Fig. 3.6B and C). This SBIF is in turn interbedded with CBIF. It indicates that, during transgression, CBIF was deposited below wave base and photic zone and during regression SBIF got deposited above photic zone and wave base. During transgression when wave base was raised up deposition of most of the BIF has taken place. When regressive stage setsin, these chemical sediments were buried by terrigenous sediments in which dissipited FeO were precipitated. When terrigenous or volcaniclastic material reaches the relatively deeper part of the shelf, deposition of SBIF has taken place. Such transgressive-regressive cycles have been proposed to explain BIF-shale interbedding in other areas also (Klein and Beukes, 1989; Gnaneshwar Rao and Naqvi, 1993).

There are two possibilities for the evolution of the basin in which Kushtagi schist belt might has been formed (1) during early stage a rifted basin was formed on a fairly stable continental crust or (2) an oceanic basin existed between the continental nuclei. None of the two possibilities can be ruled out with the existing knowledge and data. The chlorite schist-carbonate-BIF sequence could have been deposited on a trailing edge margin of a continental crust or on a rifted and newly opening ocean basin margin. In view of the Nd isotopic and other data, the BIFs of Hamersley basin are also viewed as shelf deposits in a newly formed ocean, possibly of an evolving rift (Alibert and McCulloch, 1993).

11.5 Archaean Plate Motions and Evolution of Greenstone Belts

Perhaps the most debatable of the implications discussed here is the style of plate motion during late Archaean. According to Abbott and Hoffman (1984), plate tectonics "have evolved over time due to a gradually decreasing rate of creation of lithosphere; meaning that Archaean tectonics and Phanerozoic tectonics are but two points of an evolutionary continuum". Now it is possible to visualize a form of plate motion - sea floor spreading, subduction and terrain accretion responsible for continental growth. Greenstone deformation was originally thought to be product of dominance of vertical tectonics (Anhaeusser, 1975), but recent work suggests horizontal shortening and thrusting in most belts (Abbott, 1984; Hargraves, 1986; Gnaneshwar Rao and Naqvi, 1993). The original depositional environment of greenstone belts is still disputed, and models range from entirely intraoceanic to oceanic ridge-forearc basins, marginal basins, island arcs, active continental margins, continental platforms, and continental rifts (Kroner, 1991). The main reason for all these disputes is presence of rock types characteristic of more than one environment of deposition. Therefore, it is very difficult to apply a single model for the deposition of greenstone belts. The Earth's oldest known *in situ* crustal units, namely, Isua (Baadsgaard et al., 1984), Acasta (Bowring et al., 1989), Nulliak-Uivak (Collerson et al., 1991), Mt. Sones (Black et al., 1986) and Anshan (Liu et al., 1992) are all 3.8-4.0 Ga old. The only known material older than 4.0 Ga is a sedimentary component in western Australia having an age of 4.2 Ga (Compston and Pidgeon, 1986). Thus, it appears that there is no record of the crust older than 4.0 Ga. What happened to this crust? It was probably destroyed by early impact and later erosion, and was recycled as subducted plates into the mantle by tectonic processes. The preservation of the ^{142}Nd anomaly in the Isua source suggests that the crust of Hadean time enriched in LREE was static, and recycling (plate tectonic process) did not start before ~4 Ga ago. Since then, tectonic processes have destroyed all but isotopic vestiges of these "lost terrains" of the early Earth (Harper and Jacobsen, 1992).

Archaean sea floor production and spreading rates are generally believed to be high on the basis of thermal evolution of the Earth (Bickle, 1978; Turcott, 1980; Abbott, 1984; Abbott and Hoffman, 1984; Hargraves, 1986). Bulk of the high heat production of the early Archaean mantle is thought to have been dissipated at constructive plate margins via a greater role of production of mafic rocks (including komatiite), as a consequence of thinner oceanic crust, a faster spreading rate, a greater ridge-trench length (Sleep and Windley, 1982; Arndt, 1983; Nisbet and Fowler, 1983; Hargraves, 1986; Jacobsen and Pimentel-Klose, 1988; Gnaneshwar Rao and Naqvi, 1993; Manikyamba et al., 1993) or more intense hot-spot/plume activity (Fyfe, 1978). It implies that Archaean oceanic crust had very less resident time, was warmer and more buoyant than that in modern subduction zones. With passage of time, geotherms fell at subduction zones and as the Archaean oceanic crust resisted subduction, shallow subduction zones and accretion complexes formed by arc collisions, which led to rapid growths of cratons. Because of high mantle temperature, relatively fast mantle convection, and high rates of surface impact, most pre-3.5 Ga continental crust was recycled into the mantle (Condie, 1992).

11.6 Tectonic Settings of Late Archaean Greenstone Belts

The greenstone belts of India have a very large and widespread horizon of BIF, extensively thick sequences of greywacke, quartzites, conglomerate and volcanic rocks. The interpretation of tectonic setting from the geochemical data available on these belts indicate that most probably plate tectonic theory in modified form can be applied to these rock types (Fyfe, 1990; Manikyamba et al., 1993). With the variety of models and the explanations as available for the different set of greenstone belts of KN, the most important factor is presence of both rock types, characteristics of tensional and compressional regime. Understanding of this process requires the understanding of heat transport process. To decipate the three times higher heat flow in the Archaean time, a ridge length of 27 times of present time is required (Hargraves, 1986). Therefore, plate tectonics at Archaean time would require the ridge length equal to 27 x 50000 = 1.35 x 10^6 km. with a maximum age of subducting lithosphere at trench of ~20 Ma and an average distance from ridge to trench of about ~215 km (maximum ~770 km). Widespread "shallow subduction" in the Archaean is a tectonic style suggested by Dewey and Windley (1981), Sleep and Windley (1982), Abbott, (1984) and Abbott and Hoffman (1984) to the extent that dominant force driving the plates is considered to be "slab pull". It has also been proposed that a greater rate of accretion and subduction could have been achieved by faster spreading, by increasing ridge length (equivalent to subduction zone) or by both (Burke and Kidd, 1978; Burke et al., 1981). Minimum relative plate motion of about six times faster during late Archaean than today is suggested by Dewey and Windley (1981). Nisbet and Fowler (1983) has assumed a spreading rate of 40 cm/yr. Increased ridge length will consequently result in increased trench length. This geometry of the ridge-trench length will divide the globe into a large number of mini plates and will create a large shelf area. The configuration and distribution of BIF in DC can probably be explained through these inferences (Gnaneshwar Rao and Naqvi, 1993).

11.7 Evolution of Late Archaean Greenstone Belts of Dharwar Craton: Constraints from Metavolcanics

There is still no satisfactory model for the evolution of late Archaean greenstone belts of Dharwar craton, but recent work indicates a plate tectonic model for their evolution (Naqvi, 1985; Rajamani et al., 1985; Naqvi et al., 1988; Arora, 1991; Manikyamba, 1992; Gnaneshwar Rao and Naqvi, 1993). The greenstone belts consist of varying proportions of predominantly mafic, dark to green volcanic rocks tuffs and a variety of metasedimentary rocks, including banded iron formation. The volcanic sequence is frequently bimodal. It consists of Mg rich mafic to ultramafic varieties known as komatiite to komatiitic basalt and of minor felsic varieties generally of dacitic to rhyolitic composition. The komatiites probably reflect large degrees of partial melting in the upper mantle, from which these rocks are derived, and this mantle was probably 200^{o} to 400^{o}C hotter than it is today (Kroner and Layer, 1992 and ref. therein). Burke and Kidd (1980) have reviewed the various types of volcanic rocks and their probable tectonic environments. They suggest that basalt forms at divergent plate boundaries, tholeiitic and calc alkaline rocks, most characteristically andesite dominate where arcs form above subduction zones; highly potassic volcanics are associated with active continental collision. These processes along with the intraplate volcanism, appear to have operated at plate margins throughout most of the Earth's history (Burke and Kidd, 1980) and the rate and type of magmatism in constructive and destructive plate margins and in intraplate environment differ considerably (Wilson, 1989).

Detailed geochemical studies carried out on the metavolcanic rocks of Chitradurga, Kudremukh, Bababudan, Kolar, Shimoga, Sandur and other greenstone belts indicate that all these belts have metavolcanic suites which are characteristic of continental intra plate, constructive margins and destructive plate margins (Manikyamba and Naqvi, 1993b; Gnaneshwar Rao and Naqvi, 1993). In initial stages of rifting, within plate type of magmatism (basalts of tholeiitic affinites) occurred which was succeeded by emplacement of basalt and other rock types of MOR and finally during compression, volcanism characteristic of destructive plate margins took place (Manikyamba and Naqvi, 1993b). Naqvi (1985) has demonstrated this variation from within plate volcanism to active plate margin volcanism through a MOR stage in case of Chitradurga schist belt. Similar observation has been made by Rajamani (1990) in the Kolar schist belt. Bababudan, Kudremukh and Sandur bimodal volcanics believed to be equivalent to those of Kushtagi schist belt show similar characteristics of WPB, MOR and OIA (Bhaskar Rao and Naqvi, 1978; Drury, 1981, 1983; Arora, 1991; Manikyamba and Naqvi, 1993b). Geochemistry of metavolcanic rocks from Kushtagi schist belt has already been discussed in Chapter X. Presence of ultramafic to mafic and rhyodacitic volcanics in the belt indicate compositional characteristic of IAT to MORB. Presence of basalts similar to those of MORB requires the spreading ridge in the region and the presence of basalts of IAT characteristic and rhyodacites indicate partial melting of the subducting lithosphere. Most probably the basalt formed at MOR got subducted and gave rise to basalt and rhyodacites of IAT affinity after partial melting and fractional crystallization.

11.8 Proposed Model for the Genesis of BIF and Evolution of Kushtagi Schist Belt

Similar studies have been carried out on the origin and evolution of the BIFs present in various Precambrian basins. Simonson (1985) has given a set of sedimentological constraints on the origin of iron formations and suggested that (a) iron formation were deposited in marine environments, which were highly variable but exclusively or largely subtidal, (b) surface waters were sufficiently oxidizing to preclude transportation of ferrous iron in true solution, (c) the source of iron and silica was located to basinward of the depositional environment, and (d) BIF deposition was superimposed on existing physical environments.

According to Simonson (1985) most BIFs described in the literature appear to have characteristics that are compatible with these constraints, although some of the iron-formations of the Transvaal Basin of South Africa are notable exceptions.

Beukes and Klein (1990) have suggested a model for the BIF of Transvaal basin on the basis of local characteristics and field association. In this model an interaction between, (a) near-shore water column for which the physico-chemical characteristics are largely determined by primary organic activity, and (b) open marine system in which the deep water incorporates an hydrothermal input. In this model the importance of interaction between oxygen and carbon supply has been stressed, which occurred in the shallower mixed surface water. Oxygen was supplied from atmosphere and carbon from benthic organisms. FeO and SiO_2 are envisaged to be supplied from deeper water by hydrothermal source. In contrast, the surface waters (upto a depth of about 100m) must have been essentially devoid of iron in solution. The rate of supply of oxygen and carbon to the interface between the surface and the deeper waters was probably responsible for the various types of iron-formation. In Fig. 11.3A, they depict a regressive stage with an abundant supply of carbon to the zone of mixing above the chemocline. The depth of thermocline is arbitrarily set at 100 m (Fig. 11.3A and B) since this is the depth of mixing in the present day oceans. In Fig. 11.3B, the photic zone reaches down to the floor of the deep shelf. This is the region of precipitation of the cryptalgal-limestones for which the depth limit may have been about 45 to 50 m (Klein et al., 1987). In this regressive stage of Klein and Beukes (1989) model, considerable precipitation of pyrite is expected. However, as pointed out by Cameron (1982) and Melezhik (1987) if the early Proterozoic ocean SO_4 content were low and/of if SO_4 reducing bateria were not abundantly present, a source of H_2S might not have been available for pyrite precipitation. Instead, Fe^{2+} in solution might have precipitated as silicates which were subsequently converted to Fe-rich chlorites found in many of the shales of Transvaal basin and also in western part of Sandur schist belt (Manikyamba, 1992). In Fig. 11.3B they have illustrated a transgressive stage in which the supply of carbon to the interface was much reduced, such that O_2 became available.

Figure 11.3 Schematic depositional enviromnent for iron-formation deposition and that of associated lithofacies in a marine system with a stratified water column in (A) a regressive stage and in (B) a transgressive stage are shown. (A) The photic zone reaches the floor of the deep shelf, allowing for cryptalgalaminated limestone deposition. (B) The photic zone is considerably above the floor of the deep shelf, causing the deposition of various iron formation facies and chert. The thick arrow labelled C (carbon) in (A), represent high carbon productivity and supply, and the narrow arrow in (B), represent much less carbon productivity and supply. The vertical depth scale is based upon the basinal reconstruction of Klein et al., 1987 (after Klein and Beukes, 1989).

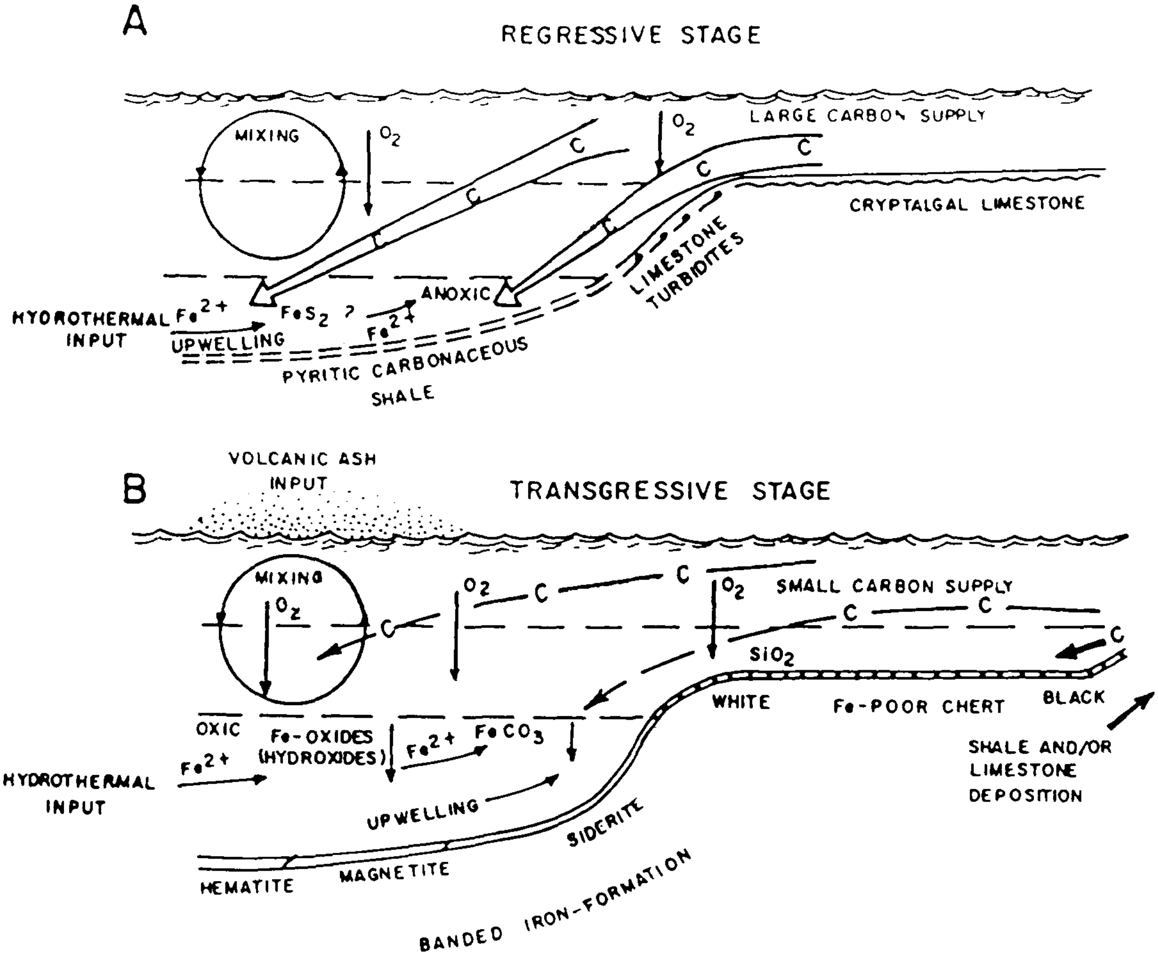
A
REGRESSIVE STAGE
MIXING
O_2
C
LARGE CARBON SUPPLY
CRYPTALGAL LIMESTONE
LIMESTONE TURBIDITES
ANOXIC
HYDROTHERMAL INPUT
Fe^{2+}
FeS_2 ?
UPWELLING
PYRITIC CARBONACEOUS SHALE
B
VOLCANIC ASH INPUT
TRANSGRESSIVE STAGE
SMALL CARBON SUPPLY
SiO_2
WHITE
Fe-POOR CHERT
BLACK
SHALE AND/OR LIMESTONE DEPOSITION
OXIC
Fe-OXIDES (HYDROXIDES)
$FeCO_3$
UPWELLING
SIDERITE
HEMATITE
MAGNETITE
BANDED IRON-FORMATION

Here the photic zone does not reach the bottom and is shifted landward and the input of siliciclastic material is less. This would have resulted in oxic conditions and the deposition of hematite and magnetite rich iron-formation, as there was little or nothing in the water column to reduce the primary Fe-oxides and-hydroxides. When, on the other hand O_2 was in short supply at the water interface (chemocline) and some carbon was available, Fe^{2+} and CO_2 would have been built upto saturation levels, resulting in the primary precipitation of $FeCO_3$ instead of FeS_2. The various types of iron formation probably resulted from variations in the supply of oxygen to the chemocline and may not reflect realistically the changes in water depth. As such variations in carbon productivity and the concomitant oxygen supply may well have resulted in siderite rich iron formation in one locale and oxide rich formation in another, but both appear to have formed at essentially similar water depths.

Jacobsen and Pimentel-Klose (1988) envisage that the Archaean oceans like the present, are represented by a three-layer model (Fig. 11.4) incorporating (a) a surface layer, (b) the thermocline and (c) deep water. The strong hydrothermal component in the BIFs indicated by Nd isotope data, is reflective of hydrothermal activity along the Archaean Mid Ocean Ridge Systems, with the deeper waters having the largest hydrothermal component. Through upwelling under the affect of thermocline and chemocline these solutions moved towards the shallow shelf region resulting in deposition of Lake Superior type BIF and if they moved towards the island arcs, Algoma type BIF got deposited. In this model, it is

Figure 11.4 Model for BIF deposition. Deep water enriched in Fe^{2} from hydrothermal sources moves up onto a shallow shelf and precipitates Fe and Si as a result of oxidation and evaporation. Algoma type BIFs are deposited in shallow waters surrounding island arcs while Lake Superior type BIFs are deposited on Atlantic type continental shelves (Jacobsen and Pimentel-Klose, 1988).

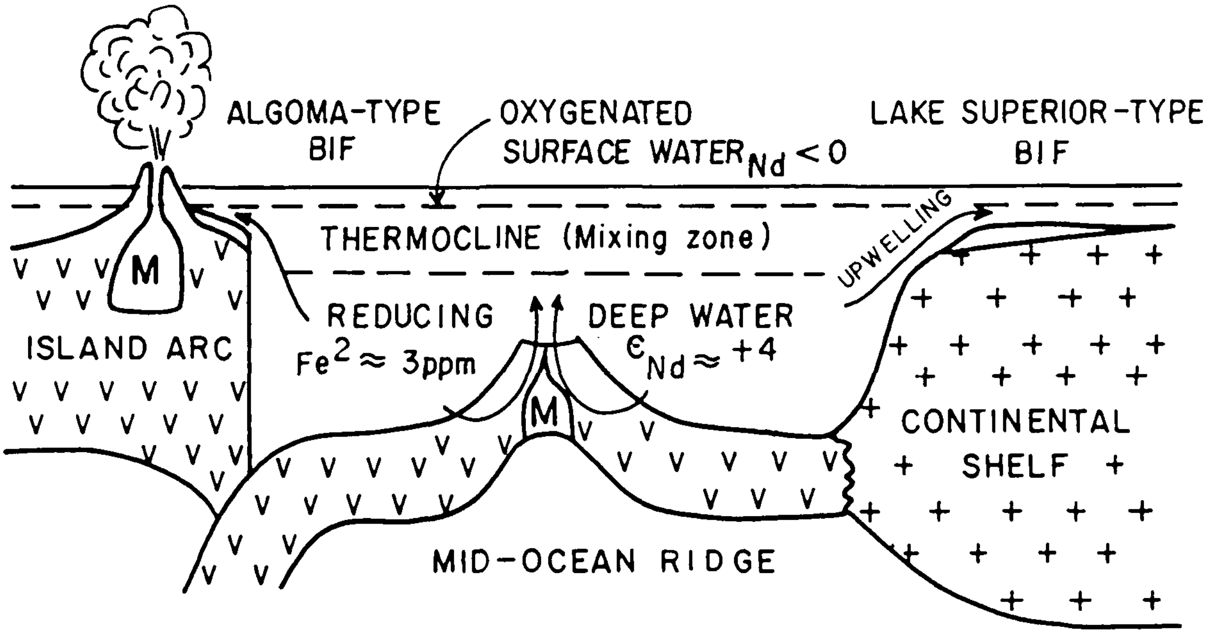

ALGOMA-TYPE
BIF
OXYGENATED
SURFACE WATER$_{Nd}$ < 0
LAKE SUPERIOR-TYPE
BIF
THERMOCLINE (Mixing zone)
UPWELLING
M
REDUCING
DEEP WATER
$Fe^2 \approx$ 3ppm
$\epsilon_{Nd} \approx +4$
ISLAND ARC
M
CONTINENTAL
SHELF
MID-OCEAN RIDGE

assumed that the O_2 level during late Archaean was sufficient to generate an oxygenated surface water. Their (ibid) argument is substantiated by the evidence from the widespread occurrence of stromatolites (Hofmann et al., 1991), microbiota and isotopic information (Goodwin et al., 1985). Becuase of the large quantities of Fe^{+3} in BIFs, it is necessary to have an oxidizing agent to precipitate Fe^{+2} as Fe^{+3}. One possibility is the dissolved photosynthetic oxygen produced by micro organisms near the surface waters. In upwelling regions, the Fe^{+2} rich deeper waters would mix with the oxygenated surface waters. In such a scenario, different portions of the reducing Fe^{2+} rich deep ocean waters characterised by positive $\epsilon_{Nd(T)}$ are mixed in upwelling zones with oxidising water. Consequently, since much of the Nd in BIFs appears to be of hydrothermal origin, essentially all of the Fe in BIFs must be of hydrothermal origin. In contrat to the models of Drever (1974) and Holland (1984) in which Fe^{2+} is thought to be produced as a porewater flux from reduced oceanic sediments, Jacobsen and Pimentel-Klose (1988) believe that most of the Fe in BIF is of hydrothermal origin. This is in agreement with the proposal of Veizer et al. (1982) stating that the Archaean oceans were buffered to a large extent by hydrothermal circulation. Since clastic sediments have a continental ϵ_{Nd} signature (<O), these sediments cannot be the major source of Nd, Fe and SiO_2 present in the BIFs.

Morris (1993) has proposed that iron and silica in the oxide facies BIF can be accommodated by the interaction of two major oceanic supply systems : (1) surface currents and (2) convective upwelling from mid-oceanic ridge (MOR) or hot-spot activity, both modified by varied input of pyroclastic material. (1) The surface currents were saturated in silica and carried minimal iron due to photic precipitation, but were periodically recharged by storm mixing. Precipitation from them gave rise to the banded chert-rich horizons, including the varves, whose regular and finely laminated iron/silica distribution resulted from seasonal meteorological influences. (2) Precipitation from convection driven upwelling of high iron solutions from MOR or hot-spot activity periodically overwhelmed the delicate seasonal patterns to produce the iron-dominated mesobands. During these periods of oxide-dominated BIF, silica was deposited from saturated solution mainly by evaporative concentration, and iron by oxidation due to protolysis and phtosynthetically produced oxygen.

Meteorological and depositional conditions were modified by varying effect of fine aluminous ash from volcanic sources. During volcanic periods, the normally high capacity of sunlight to precipitate ferric iron directly by photolytic oxidation of ferrous iron, and by photosynthetic production of oxygen, was modified by turbidity in the atmosphere (aerosols and dust) and in the water (colloids from reactive ash). Surface-precipitated ferric hydroxide redissolved in the presence of decaying organic matter in the sub-photic zone, augmenting the iron content of the zone. Precursor ferrous carbonates and silicates were precipitated when the iron concentration of this sub-photic zone exceeded their respective solubilities. During volcanism, the increased availability of nutrients, particularly phosphorous, to surface waters increased the organic contribution despite lower light values, leading to an almost total absence of ferric iron oxides. Cooling to warm, silica-saturated sea-water during the periods of "volcanic winter" increased the ratio of precipitation of silica to iron, which however, was still controlled by seasonal conditions. Intermediate concentrations of organic matter, insufficient to totally convert the ferric compounds either during precipitation or diagenesis, resulted in overgrowths of magnetite on hematite, and eventually in the substantial conversion of hematite to magentite, where higher temperatures were achieved during low-grade regional metamorphism.

A model is proposed for the genesis of BIF and evolution of Kushtagi schist belt, based on the data of the present work and the available information on various other belts. It is envisaged that the presence of BIF in this belt represents a stage where volcanism and hydrothermal activity along the Archaean Mid Oceanic Ridge was predominant in the region. A graphical hypothetical model for the origin and evolution of BIF of Kushtagi schist belt is shown in Fig. 11.5. It is emphasized that Kushtagi schist belt is a truncated part of the original belt. All components of a greenstone belt as present in Chitradurga and Sandur schist belts are not present, as a large part has been destroyed and dismembered by the early Proterozoic acid magmatism. Therefore, some of the assumed characteristics of the model are not discovered in the field as yet. Iron and silica-rich hydrothermal solutions, ultramafics of komatiitic affinity and high Mg-basalts were provided by MOR. The ocean was compositionally layered both

Figure 11.5 Schematic cross-section of the proposed model depicting the deposition of BIF and associated rocks in the Kushtagi basin. (A) Show the hydrothermal activity at MOR, stratified water column, suspected and assumed stromatolites and the zones of BIF deposition and photosynthetic production of O_2. (B) Show the closing of Kushtagi basin, marked by dacitic volcanism. Thickness for the supracrustal rocks are exaggerated to depict the observed associations. Thickness of the lithosphere reduces and represents only the conceptual aspect.

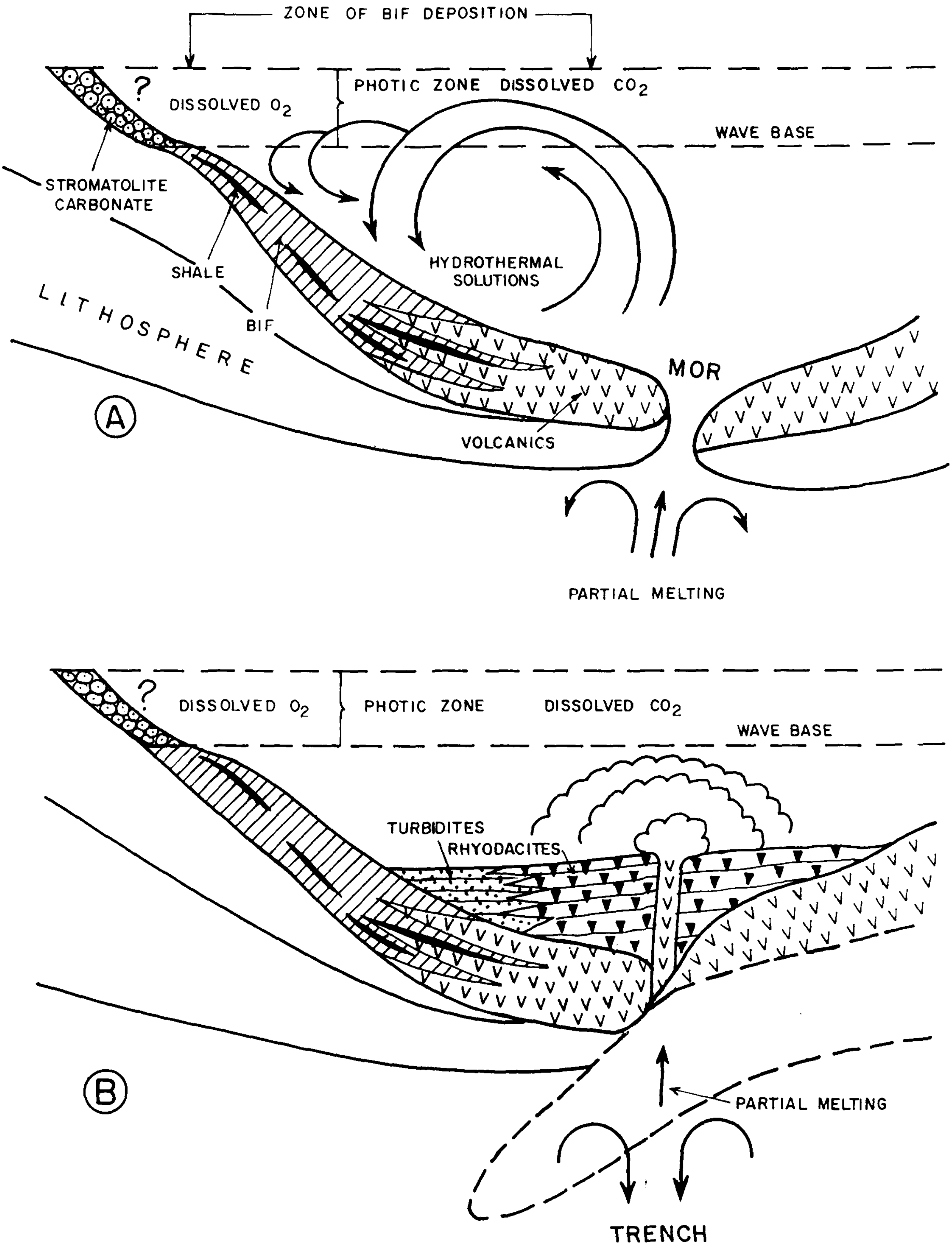

ZONE OF BIF DEPOSITION
?
DISSOLVED O_2
PHOTIC ZONE
DISSOLVED CO_2
WAVE BASE
STROMATOLITE CARBONATE
SHALE
BIF
LITHOSPHERE
HYDROTHERMAL SOLUTIONS
MOR
VOLCANICS
A
PARTIAL MELTING
?
DISSOLVED O_2
PHOTIC ZONE
DISSOLVED CO_2
WAVE BASE
TURBIDITES
RHYODACITES
B
PARTIAL MELTING
TRENCH

vertically and horizontally in respect of O_2 and CO_2. The ocean was reducing but the shore-lines where the stromatolites (?) were producing O_2 through photosynthesis was oxidizing. The FeO and SiO_2 were added at MOR in a reducing environment. These FeO and SiO_2 under the affect of thermocline and chemocline upwelled and reached the shallow shelf region of the basin. FeO combined with O_2 and precipitated in the form of iron-oxides and -hydroxides below wave base and photic zone and thus gave rise to the oxide facies BIF of the Kushtagi schist belt. In addition to contribution from hydrothermal source, detrital fine grained sedimentation in the basin gave rise to the observed variability in the composition. Since the endogenic and exogenic processes were rapid and vigorous during the Archaean time, continuous generation and inflow of terrigenous material to the basin from a juvenile crust of the proto-continent was prevalent. During transgression when wave base is raised up, deposition of most of the BIF takes place. When regressive stage setsin these chemical sediments are buried by tterrigenous sediments in which dissipited FeO are precipitated. When terrigenous or volcaniclastic material reaches the relatively deeper part of the shelf, deposition of SBIF takes place.

With the smaller size of the plates and a predominantly reducing environment in the oceans coupled with the shorter distance between the hydrothermal vents and the shallow shelves being prevalent, it does not appear to be a major problem for transportation of FeO from the vent site through a thermocline and chemocline to the shallower shelf region where O_2 was being photosynthetically produced. With an increasing ridge length and faster construction as well as destruction of the then ocean floor, the hydrothermal exhalative hypothesis is capable of explaining most of the characteristics observed in the oxide facies BIF of the Kushtagi schist belt.

The presence of ultramafic rocks of komatiitic affinity in patches at a few places in the Kushtagi belt along with a broad band of pillow basalts and chemical sediments could possibly indicate the presence of ophiolite sequence in this belt. Portions of some Archaean greenstone sequences have recently been described as possible ophiolites (Naqvi, 1985; Helmstaedt et al., 1986; de Wit et al., 1987; Rajamani, 1990). Interpreted as fragments of ancient oceanic lithosphere, ophiolites have become a "standard part of the plate tectonic paradigm" (Coleman, 1977). Their widespread occurrence in Phanerozoic mountain belts is regarded as evidence that the Wilson cycle, involving the opening and closing of ocean basins (Wilson, 1968), has operated in geological past. Because well preserved ophiolites are rare in the Archaean, no consensus on the role of plate tecotnics in the evolution of Archaean crust has emerged (Helmstaedt et al., 1986). However, Burke et al. (1976) have suggested that dismembered ophiolites should exist in Archaean greenstone belts.

In Kushtagi schist belt the ultramafic rocks of komatiitic affinity, pillow basalts and rhyodacites are not genetically related with each other. However, the low Mg-basalt and rhyodacite may be cogenetic, formed by partial melting and fractional crystallization of high Mg-oceanic crust. All these features along with the presence of chemical sediments indicate that the Kushtagi schist belt may represent a possible ophiolite zone.

Based on the field evidences present in Kushtagi schist belt and several geochemical evidences presented in previous chapters, a tectonic model suggesting a faster completion of Wilson Cycle, is proposed. The whole spectrum of tectonic activity starting from opening to closing of the basin is responsible for the evolution of Kushtagi schist belt in general and deposition of BIF in particular. In this model it is envisaged that chlorite schist-carbonate-BIF and high Mg-basalt represent the AMOR associated volcanism and hydrothermal activity, whereas the closing stage of the basin is represented by low Mg-basalt and rhyodacite. Multiple compressive deformation of the belt has brought rocks of different setting juxtaposed. Since Kushtagi schist belt is only a truncated arm of a greenstone belt, all the components of the belt and part of this proposed and speculative model are not preserved. However, the remnants preserved in the belt strongly favour this model.

CHAPTER - XII

SUMMARY AND CONCLUSIONS

BIFs (Banded Iron Formations) are the most important and significant rock suites of Precambrian terrains and are mainly confined to the early and middle Precambrian era. Their origin, confinement in time-space and environment of deposition are not clearly understood as yet. In these rocks, enormous amount of Fe and Si have been chemically precipitated in the form of rhythmic layers of varying dimensions within 600 million years of early history of the Earth. The source of Fe and Si as well as oxygen in these iron formations is debated. The nature of the process(es) by which these Fe-rhythmites have developed is still speculated. A relation between the BIF and the biogeochemical processes has been proposed by several workers during last few years. Change from anoxic to an oxygenated atmosphere is reflected by the distribution of BIFs and red beds.

In India, occurrence of BIF is confined to the late Archaean greenstone belts (2.9-2.6 Ga) whereas Proterozoic sedimentary basins/mobile belts are completely devoid of these interesting and enigmatic rock types. In the DC (Dharwar Craton) of India, BIFs are found in three associations namely (1) with quartzites-shales-volcanics (Bababudan, Kudremukh, Kushtagi belts), (2) with quartzites-carbonatic stromatolites-Mn-formations-shales-volcanics (Sandur, Chitradurga, Shimoga belts) and (3) with greywackes-acid- intermediate volcanics, a deep water facies (Chitradurga, Sandur, Shimoga belts). The genesis, depositional environment and tectonic setting of these BIFs of different rock assemblages is not understood. Keeping these aspects and other exciting but unresolved questions regarding the origin of BIF in view, a detailed geochemical study of the BIF of Kushtagi schist belt was taken up. This belt was chosen as it is one of the least metamorphosed belts of DC where the original mineralogy of the BIFs is presumed to be better preserved. The main objective of this work is to understsand the genesis of the BIF of Kushtagi schist belt and its bearing on the Archaean depositional environment and tectonic processes. With these objectives, detailed geological and geochemical studies on the BIFs and associated volcanic rocks have been carried out and the results of these studies are presented in this thesis.

Based on their Al_2O_3 content the Banded Iron Formation of Kushtagi schist belt are classified into two type namely cherty and shaly BIFs. They are found in association with shallow shelf and platformal chloritic shale-carbonate-volcanic rock assemblages. They are mostly of oxide facies. At several places, oxide facies BIF bands are hosted in pillowed and spherulitic volcanic rocks of basaltic composition. In these oxide facies BIF, interbedded SBIF and shales of thickness varying from a few cm to a few meters are present. The strata have been folded and deformed by atleast three phases of deformation. Isoclinal, recumbent and tight of first as well as second generation are commonly well exhibited by these BIFs.

About 200 samples of the cherty and shaly BIFs and the associated volcanic rocks were collected from working mines. Special care was taken to collect relatively unweathered samples from freshly blasted surfaces of the mines. Thin section and ore microscopic studies were carried out for characterizing various mineral phases present. Composition of the minerals was determined with the help of an Electron Probe Micro Analyser. Major, trace and rare earth element analysis for about 42 elements in each sample, was carried out with the help of XRF and ICP-MS using international standard reference materials. Oxygen isotopic estimation by using the SIMS were carried out on the hematite-chert pairs.

Mineralogy of these BIFs is simple as they are metamorphosed to lower grade of greenschist facies only. Many layers of BIF have just undergone diagenesis. The interbeddded clays have not been recrystallized and the detrital micas are preserved. The interbedded shaly BIF in addition to hematite and chert contains kaolinite and muscovite. Shales also exhibit similar mineralogy. The oxide facies cherty and shaly BIFs show large scale compositional varitions as reflected by their major and trace elemental abundance. Oxide facies BIF samples exhibit a large scatter in the Fe_2O_3-SiO_2 molar ratio, which is mainly dependent on the relative thickness of the hematite rich bands in the samples analysed. Primarily, the pure oxide facies BIFs which are constituted by Fe_2O_3 and SiO_2, exhibit a distinct linear antipathetic relationship between the two components. They are extremely depleted in Al_2O_3, TiO_2, Zr, Hf and other trace elements like Cr, Ni, Co, Rb, Sr, V, Y and REE. MnO content of these rocks is generally less than 0.01% indicating that effective Fe-Mn fractionation had taken place in this zone as the Eh values had not reached such a level where Mn could be precipitated while the oxide facies BIFs were deposited. Extremely depleted ΣREE, positive Eu anomalies and HREE enrichment are distinctive and essential features of these pure oxide facies BIF. Negative Ce anomalies are seen in a few samples of SBIF which indicate the oxidation of Ce^{+3} to Ce^{+4} and hence its separation from the system. Depletion in REE in proportion to the abundance levels of Co, Cu and Ni and the observed Eu anomaly strongly indicates that the source of FeO, and SiO_2 for these BIFs was the hydrothermal solutions released at the AMOR vent sites. FeO and Ce present in these solutions were oxidized by photsynthetically generated oxygen produced by the blue-green algae present at the shallow shelf regions. This oxygen, through ocean circulation, was dissolved in the ocean waters and reached below the wave base and photic zone, where due to a thermocline and chemocline effect, FeO was transported and reacted with this oxygen to produce the Fe-rhythmites. The aftband and mesobands of Fe-rich layers were produced due to the intermittent (seasonal) availability of either oxygen and/or FeO.

The $\delta^{18}O$ values of coexisting silica and hematite in the CBIF of Kushtagi schist belt give a temperature range between 71.4^{o} and 165.2^{o}C. It indicates that samples have undergone diagenetic alteration and metamorphism of lower greenschist facies which is corroborated by field observation as well as petrographic study.

SBIF interbedded with the oxide facies CBIF show entirely different geochemical characters as a result of modification by detrital processes. Both terrigenous and volcaniclastic processes have exerted control on the composition of the SBIF, in addition to chemical precipitation. SBIF have been deposited as a result of change in the physico-chemical conditions of the watermass at two different times, namely the time of deposition of oxide facies CBIF and the time of deposition of SBIF. Large variation is observed in most of the elements, all trace elements (including REE) are relatively high in these rock types. The magnitude of Eu anomalies show variation. The signatures of hydrothermal processes are modified by those of the clastic processes.

The volcanic rocks of the Kushtagi schist belt are of basaltic and rhyodacitic types. Basalts can be subdivided into high and low MgO types. High MgO basalts show geochemical characters resembling to those of MORB. The dacitic rocks are characterized by geochemical parameters of the island arc volcanics. REE patterns of these two types are distinct from each other. High Mg basalts are depleted in REE with almost flat patterns. Dacites show differentiated patterns with slight negative Eu anomalies in some samples. It is proposed that the partial melting of the MORB has given rise to the rhyodacitic rocks. The melting is suggested to have taken place when the tensional regime was converted to compressional regime.

REE and other geochemical characteristics of the BIF indicate that FeO and SiO_2 of the BIFs was added to ambient Archaean ocean at the AMOR. The Nd isotopic data from elsewhere has demonstrated that the main source of FeO of BIF is the hydrothermal and fumarolic activity at the vent sites on the MORB. Therefore existance of a MOR is evidenced by the REE patterns of the BIFs and Eu anomalies. This inference is further substantiated by interlayering of BIFs with the high Mg basalt which have geochemical parameters resembling with that of MORB. Subsquent deposition of sediments and volcanism related with the active plate margins and deformational patterns of greenstone belts indicate that the closure of the basins of greenstone belts as a whole and Kushtagi schist belt in particular is a subduction related phenomenon. The basin was probably initiated by opening of a rift. Spreading along a newly formed ocean along this rift-AMOR widened the basin. Hydrothermal solutions at this AMOR enriched the ocean water in FeO and SiO_2 moved towards the trailing edge due to thermal and chemical differences. The encounter of these solutions with oxygen, produced by photosynthesis, caused precipitation of oxides and hydroxides of iron below wave base and photic zone. FeO was precipitated to the extent of the availability of O_2. Rest of it remained within the ocean reservoir. When again oxygen become available it was precipitated and layered with the rhyodacitic subduction related volcanic and sedimentary rocks.

Thus the studies presented in previous pages help to identify two stages of the tectonic setting through which the BIF and greenstone belts were formed. First stage was an opening and spreading of ocean, where extensive volcanism and hydrothermal fumarolic activity added large amount of FeO and SiO_2 to the ocean waters. The exit temperature of these hydrothermal water was probably very high so that higher quantity of FeO was dissolved. To explain the enormous quantity of Fe present in BIFs it is essential to assume that hydrothermal flux itself was very high at that time. Therefore large quantity of hydrothermal waters with higher amount of dissolved FeO was added to the Archaean oceans. To dissipate the higher heat flow of Archaean era a larger ridge length, faster creation and destruction of oceanic lithosphere is essential. Thus the combination of higher hydrothermal flux, its high exit temperature, larger ridge length and faster completion of Wilson Cycle explain not only the source of the constituents of BIF but also the tectonic setting and lithological assemblages of greenstone belts. The second stage was due to change in the direction of convection current. This resulted in the conversion of the basin area from a spreading basin to a converging margin. At this time the turbidites and rhyodacites were formed.

The supply of the O_2 for the precipitation of ferrous iron to ferric state is not directly demonstrated by the field occurrence of stromatolite or the microbiota, as has been shown in case of Chitradurga and Sandur belts. However, there are significant bands of carbonate present in the viscinity of BIF which may contain stromatolites as some of them appear to be stratifera type but convincing forms and morphologies have not been discovered as yet. This process of biogenic suply of O_2 is very much evidenced in the other greenstone belts of the DC and since Kushtagi schist belt is only a truncated arm of the original belt, it can be safely assumed that similar biogenic process might have supplied O_2 for the BIF precipitation in the Kushtagi schist belt also. The banding of BIF is also related with the availability of O_2. Seasonal variations in the rainfall and the suply of the clastic debris to the ocean margin where biogenic activity was taking place has affected the growth of bacteria and production of O_2. During high rainfall, larger quantity of clastic debris was brought to the margin which burried the algae and hence the organism and oxygen productivity was reduced. During this period, only silica precipitation continued and very little ferric-hydroxide was deposited. When rain fall reduced, the bacteria/algae emerged above the sedimentary layer, received more sunlight and produced more oxygen, which reacted with FeO and hence iron rich layers were deposited. The production of oxygen at the shallow shelf has created a partially layered ocean water mass. At depth and away from the margin the ocean water had higher amount of dissolved CO_2. Primary prcipitation and/or diagenic reaction between Fe_2O_3 and organic matter (degradation of organic carbon) resulted in the formation of interstitial siderite. It is proposed that formation of BIF is not a simple chemical process. Instead it is a result of combination of (1) hydrothermal activity, (2) terrigenous and volcaniclastic sedimentation (3) biogeochemical processes, (4) chemical precipitation and diagenetic reactions and (5) the physico-chemical conditions prevailing at the vent sites and depositional shelf. Mini plate model and faster completion of Wilson Cycle with shorter distance between the constructive and destructive margins, and the conversion of constructive margins to the destructive one are able to explain most of the above mentioned processes and the observations. The studies on the BIF and volcanic rocks of the Kushtagi schist belt lead to the following conclusions.

1. Iron, silica and the REE of the BIF were mainly provided by the hydrothermal solutions emplaced at the vent sites of the Archaean Mid Oceanic Ridges (AMOR). These hydrothermal solutions enriched in iron and silica were subsequently mixed with the ambient sea water. It is proposed that the hydrothermal flux of higher exit temperature was quite significantly elevated during Archaean. This higher quantity of hydrothermal flux was able to bring large quantity of dissolved FeO and SIO_2 to the ocean water.

2. Due to thermal and chemical potential differences and upwelling, this iron and silica enriched ocean water was transported to the site of deposition in the shallow shelf region where it reacted with oxygen resulting in the precipitation of iron oxide and hydroxide. Oxygen was most probably generated photosynthetically.

3. On burial these oxides and hydroxides reacted with organic carbon of the bacteria and most probably the Fe-carbonates were produced by this diagenetic reaction. It is also possible that

some of the Fe-carbonates were directly precipitated by reaction with atmospheric CO_2 dissolved in the ocean water.

4. Oxide facies BIFs were deposited below the wave base and photic zone at the shallow shelf regions of low organic productivity.

5. During the deposition of BIF, terrigenous and volcaniclastic sedimentation also took place resulting in compositional variation in cherts, CBIF to SBIF and the shales. Deposition of the BIF of oxide facies is dependent on the supply of O_2, CO_2 and C to various parts of the basin and on the compositional layering of the ocean with respect to the dissolved quantity of O_2 and CO_2.

6. Petrological and geochemical data suggest that the BIF sequence in the Kushtagi schist belt is formed by an interaction of hydrothermal, biogenic-photosynthetic and sedimentary processes in a compositionally layered ocean.

7. The banding of BIF is probably a result of seasonal changes in the availability of O_2 and/or FeO.

8. A Mini plate model with shorter duration of the completion of Wilson Cycle, large ridge length, higher rate of generation and consumption of oceanic lithosphere is able to explain most of the observed facts of BIF and the greenstone belts.

9. Late Archaean greenstone belts were initiated as a MOR related basins and were closed as subduction related active margins.

REFERENCES

Abbott, D.H. (1984) Archaean Plate Tectonics revisited 2. Paleosea level changes, Continental area, oceanic heat loss and the area age distribution of the ocean basins. Tectonics, V. 3, pp. 709-722.

Abbott, D.H. and Hoffman, S.E. (1984) Archaean Plate tectonics revisited. 1. Heat flow, spreading rate and their age of subducting lithosphere and their effects on the origin and evolution of continents. Tectonics, V. 3, pp. 429-448.

Ahn, J.H. and Buseck, P.R. (1990) Hematite nanospheres of possible colloidal origin from a Precambrian banded iron formation. Science, V. 250, pp. 111-113.

Alibert, C. and McCulloch, M.T. (1993) Rare earth element and neodymium isotope composition of the banded iron formation and associated shales from Hamersley, Western Australia. Geochim. Cosmochim. Acta. V. 57, pp. 187-204.

Allaart, J.H. (1976) The pre-3760 m.y. old supracrustal rocks of the Isua area, central west Greenland, and the associated occurrence of quartz - banded ironstone. In : B.F. Windley (Ed.), The Early History of the Earth. John Wiley and Sons, New York, N.J., pp. 177-190.

Allen, P., Condie, K.C. and Narayana, B.L. (1983) The Archaean low-to high-grade transition in the Krishnagiri-Dharmapuri area, Tamil Nadu, Southern India. In : S.M. Naqvi and J.J.W. Rogers (Eds.), Precambrian of South India, Geol. Soc. of India, Mem. 4, pp. 450-461.

Anantha Iyer, G.V. and Vasudev, V.N. (1979) Geochemistry of the Archaean metavolcanic rocks of Kolar and Hutti gold fields, Karnataka, India. Jour. Geol. Soc. India, V. 20, pp. 419-432.

Anantha Iyer, G.V., Vasudev, V.N. and Jayaram, S. (1980) Rare earth element geochemistry of metabasalts from Kolar and Hutti gold-bearing volcanic belts, Karnataka craton, India. Jour. Geol. Soc. India, V. 21, pp. 603-608.

Ananthanarayana, R., Duraisamy, K. and Khan, R. (1989) Geology of parts of Yelbarga, Khustagi, Koppal, Gangavati and Lingsugur taluks of Raichur district and parts of Ron taluk of Dharwar district, Karnataka. Rec. Geol. Surv. India, V. 122, Pt. 5, pp. 87-94.

Anhaeusser, C.R. (1975) Precambrian tectonic environments. Annu. Rev. Earth Planet. Sci., V. 3, pp. 31-53.

Anhaeusser, C.R. (1990) Precambrian crustal evolution and metallogeny of South Africa. In : S.M. Naqvi (Ed.), Precambrian Continental Crust and its Economic Resources, Elsevier Amsterdam, pp. 123-156.

Appel, P.W.U. (1983) Rare Earth Elements in the early Archaean Isua Iron Formation, West Greenland. Precamb. Res., V. 20, pp. 243-258.

Appel, P.W.U. and Mahabaleswar, B. (1988) Secular trends in rare earth element patterns of Precambrian iron-formation from India and Greenland. Jour. Geol. Soc. India, V. 32, pp. 214-226.

Arndt, N.T.(1983) Role of a thin, komatiite-rich oceanic crust in the Archaean plate-tectonic process. Geology, V. 11, pp. 372-375.

Arora, M. (1991) Geology, geochemistry and tectonic setting of Conglomerates and Quartzites of the Bababudan Schist Belt, Karnataka Nucleus, India. Unpub. Ph.D. thesis, Aligarh Muslim University, Aligarh, 311pp.

Arora, M. and Naqvi, S.M. (1993) Geochemistry of Archaean arenites formed by anoxic exogenic processes : an example from Bababudan schist belt, India. Jour. Geol. Soc. India (in press).

Arora, M., Khan, R.M.K. and Naqvi, S.M. (1993) Composition of the early and middle Archaean upper continental crust as sampled by the Kaldurga conglomerate, Karnataka Nucleus, India. Precamb. Res. (communicated).

Arth, J.G. (1979) Some trace elements in trondhjemites- their implications to magma genesis and plate tectonic setting. In: F. Barker (Ed.), Trondhjemites, Dacites and related rocks, Elsevier, Amsterdam, pp.123-132.

Arth, J.G. and Hanson, G.N. (1975) Geochemistry and origin of the early Precambrian crust of northeastern Minnesota. Geochim. Cosmochim. Acta, V. 39, pp. 325-362.

Ayers, D.E. (1972) Genesis of Iron-bearing minerals in Banded Iron Formation mesobands in the Dales Gorge Member, Hamersley Group, Western Australia. Econ. Geol., V. 67, pp. 1214-1233.

Baadsgaard, H., Nutman, A.P., Bridgwater, D., Rosing, M., McGregor, V.R. and Allaart, J.H. (1984) The zircon geochronology of the Akilia association and Isua supracrustal belt, West Greenland. Earth Planet. Sci. Lett., V. 68, pp. 221-228.

Balaram, V., Saxena, V.K., Manikyamba, C., Ramesh, S.L. and Anjaiah, K.V. (1988) Determination of selected trace elements in geological samples by inductively coupled plasma mass spectrometry. Proc. National Symposium on Analytical Applications in Earth Sciences, Shillong, pp. 72-81.

Balaram, V., Manikyamba, C., Ramesh, S.L. and Saxena, V.K. (1990) Determination of rare earth elements in Japanese rock standards by Inductively Coupled Plasma-Mass Spectrometry. Atomic Spectroscopy, V. 11, pp. 19-23.

Baral, M.C. (1986) Archaean stromatolites from Dodguni belt, Karnataka craton, India. Jour. Geol. Soc. India, V. 28, pp. 328-333.

Barghoorn, E.S. and Tyler, S.A. (1965) Microorganisms from the Gunflint Chert. Science, V. 147, pp. 563-577.

Barrett, T.J., Fralick, P.W. and Jarvis, I. (1988) Rare-earth-element geochemistry of some Archean iron formations north of Lake Superior, Ontario. Can. J. Earth Sci., V. 25, pp. 570-580.

Basavanna, M. and Mahabaleswar, B. (1988) Rare-earth elements in banded iron formation of Halaguru Area, high-grade metamorphic terrain of Southern Karnataka. India Jour. of Earth Sci., V. 15, pp. 58-64.

Beckinsale, R.D., Drury, S.A. and Holt, R.W. (1980) 3360 m.y. old gneisses from the South Indian Craton. Nature, V. 283, pp. 469-470.

Berkner, L.V. and Marshall, L.C. (1965) On the origin and rise of oxygen concentration in the Earth's atmosphere. J. Atmos. Sci., V. 22, pp. 225-261.

Beukes, N.J. (1973) Precambrian banded iron formations of Southern Africa. Econ. Geol., V. 68, pp. 960-1004.

Beukes, N.J. (1980) Suggestion towards a classification of and nomenclature for iron formation. Trans. Geol. Soc. S. Africa, V. 83, pp. 285-290.

Beukes, N.J. (1983) Palaeoenvironmental setting of iron-formations in the depositional basin of the Transvaal Supergroup, South Africa. In : A.F. Trendall and R.C. Morris (Eds.), Iron-formation : Facts and Problems, Elsevier, Amsterdam, pp. 131-209.

Beukes, N.J. (1984). Sedimentology of the Kuruman and Griquatown Iron Formations : Transvaal Supergroup, Griqualand west, South Africa. Precamb. Res., V. 24, pp. 47-84.

Beukes, N.J. and Klein, C. (1990) Geochemistry and sedimentology of a facies transition from microbanded to granular iron formation in the early Proterozoic Transvaal Supergroup, South Africa. Precamb. Res., V. 47, pp. 99-139.

Beukes, N.J., Klein, C., Kaufman, A.J. and Hayes, J.M. (1990) Carbonate petrography, kerogen distribution and carbon and oxygen isotope variations in an early Proterozoic transition from limestone to iron formation deposition, Transvaal Supergroup, South Africa. Econ. Geol., V. 85, pp. 663-690.

Bhaskar Rao, Y.J. (1980) Geology and geochemistry of metavolcanics and associated rock types from Bababudan belt and the late Archaean crustal evolution in Karnataka Craton. Unpub. Ph.D. thesis, Osmania University, Hyderabad, 258pp.

Bhaskar Rao, Y.J. and Naqvi, S.M. (1978) Geochemistry of metavolcanics from the Bababudan schist belt; A late Archaean-early Proterozoic volcanosedimentary pile from India. In : B.F. Windley and S.M. Naqvi (Eds.), Archaean Geochemistry Proc. First Int. Symp. on Archaean Geochemistry. The origin and evolution of Archaean continental crust. Elsevier, Amsterdam, 325-341.

Bhaskar Rao, Y.J. and Drury, S.A. (1982) Incompatible trace element geochemistry of Archaean metavolcanic rocks from the Bababudan volcanic-sedimentary belt, Karnataka. Jour. Geol. Soc. India, V. 23, pp. 1-12.

Bhaskar Rao, Y.J., Sivaraman, T.V., Pantulu, G.V.C., Gopalan, K. and Naqvi, S.M. (1992) Rb-Sr ages of late-Archaean metavolcanics and granites, Dharwar Craton, South India and evidence for early Proterozoic thermotectonic event(s). Precamb. Res., V. 59, pp. 145-170.

Bickle, M.J. (1978) Heat loss from the earth : a Constraint on Archaean tectonics from the relation between geothermal gradients and the rate of plate production. Earth Planet. Sci. Lett., V. 40, pp. 301-315.

Bickle, M.J. and Nisbet, E.G. (1972) The oceanic affinities of some alpine mafic rocks based on their Ti-Zr-Y contents. Jour. Geol. Soc., V. 128, pp. 267-271.

Black, L.P., Williams, I.S. and Compston, W. (1986) Four zircon ages from one rock : the history of a 3930 Ma-old granulite from Mt. Sones, Antarctica. Contrib. Mineral. Petrol., V. 94, pp. 427-437.

Bowering, S.A., Williams, I.S. and Compston, W. (1989) 3.96 Ga gneisses from the Slave province, Northwest territories, Canada. Geology, V. 17, pp. 971-975.

Bowers, T.S., Von Damm, K.L. and Edmond, J.M. (1985) Chemical evolution of mid-ocean ridge hot springs. Geochim. Cosmochim. Acta, V. 49, pp. 2239-2252.

Bruce Foote, R. (1886) Notes on the geology of parts of Bellary and Anantapur districts. Rec. Geol. Surv. India, V. 19(2), pp. 97-111.

Burke, K. and Kidd, W.S.F. (1978) Were Archaean Continental geothermal gradients much steeper than those of today ? Nature, V. 272, pp. 240-241.

Burke, K. and Kidd, W.S.F. (1980) Volcanism on Earth through time. In The Continental Crust and its Mineral Deposits. Edited by D.W. Strangway. The Geological Association of Canada, Special Paper, V. 20, pp. 503-522.

Burke, K., Dewey, J.F. and Kidd, W.S.F. (1976) Dominance of horizontal movements, arc and microcontinental collisions during the later per-mobile regime. In : B.F. Windley (Ed.), The Early history of the Earth, Wiley, London, pp. 113-129.

Burke, K.C., Kidd, W.S.F., Turcotte, D.L., Dewey, J.F., Mouginis-Mark, P.J., Parmentier, E.M., Sengor, A.M.C. and Topponnier, P.E. (1981). Tectonics and basaltic volcanism of the terrestrial planets. New York, Pargamon Press, p. 804-898.

Campbell, A.C. (1985) Geochemistry of hydrothermal clouds in the Guaymas Basin, Gulf of California, Ph.D. dissertation, Univ. of California, San Diego.

Cameron, E.M. (1982) Sulphate and sulphate reduction in early Precambrian oceans. Nature, V. 296, pp. 145-148.

Campbell, A.C. and Gieskes, J.M. (1984) Water column anomalies associated with hydrothermal activity in the Guaymas Basin, Gulf of California. Earth. Planet. Sci. Lett., V. 68, pp. 57-72.

Campbell, A.C., Gieskes, J.M., Lupton, J.E. and Lousdale, P.E. (1988a) Manganese geochemistry in the Guaymas basin, Gulf of California. Geochim. Cosmochim. Acta, V. 52, pp. 345-357.

Campbell, A.C., Palmer, M.R., Klinkhammer, G.P., Bowers, T.S., Edmond, J.M., Lawrence, J.R., Casey, J.F., Thompson, G., Humphris, S., Rona, P. and Karson, J.A. (1988b) Chemistry of hot springs on the Mid-Atlantic Ridge. Nature, V. 335, pp. 514-519.

Canuto, V.M., Levine, J.S., Augustrson, T.R., Imhoff, C.L. and Giampapa, M.S. (1983) The young Sun and the Photochemistry of the early Earth. Nature, V. 305, pp. 281-286.

Carey, S.W. (1986) Genesis of Proterozoic Banded Iron Formations. Jour. Geol. Soc. India, V. 28, pp. 223-226.

Carrigan, W.J. and Cameron, E.M. (1991) Petrological and stable isotope studies of carbonate and sulfide minerals from the Gunflint Formation, Ontario: evidence for the origin of early Proterozoic iron-formation. Precamb. Res., V. 52, pp. 347-380.

Chadwick, B., Ramakrishnan, M., Viswanatha, M.N. and Murthy, V.S. (1978) Structural studies in the Archaean Sargur and Dharwar supracrustal rocks of the Karnataka Craton. Jour. Geol. Soc. of India, V. 19, pp. 531-542.

Chadwick, B., Ramakrishnan, M. and Viswanatha, M.N. (1981a) The stratigraphy and structure of the Chitradurga region : An illustration of cover-basement interaction in the late Archaean evolution of the Karnataka Craton, southern India. Precamb. Res., V. 16, pp. 31-54.

Chadwick, B., Ramakrishnan, M. and Viswanatha, M.N. (1981b) Structural and metamorphic relations between Sargur and Dharwar supracrustal rocks and Peninsular Gneiss in Central Karnataka. Jour. Geol. Soc. India, V. 22, pp. 557-569.

Chadwick, B., Gorrioch, N.H.G., Ramakrishnan, M. and Viswanatha, M.N. (1986) Mineral composition, textures and deformation in late Archaean banded iron formation rich in magnesioriebeckite and aegirine, Bababudan, Karnataka, Southern India. Jour. Geol. Soc. India, V. 28, pp. 189-200.

Chadwick, B., Vasudev, V.N. and Jayaram, S. (1988) Stratigraphy and structure of late Archaean, Dharwar volcanic and sedimentary rocks and their basement in a part of the Shimoga Basin east of Bhadravathi, Karnataka. Jour. Geol. Soc. India, V. 32, pp. 1-19.

Chakraborty, K.L. and Majumder, T. (1986) Geological aspects of the Banded Iron-Formation of Bihar and Orissa. Jour. Geol. Soc. india, V. 28, pp. 109-133.

Chapman, D.J. and Schopf, W.J. (1983) Biological and biochemical effects of the development of an aerobic environment. In : J.W. Schopf (Ed.) Earth's earliest biosphere. Its origin and evolution. Princeton University Press, Princeton, N.J., p. 632-635.

Christie, A.T. (1836) Madras J. Lit. Sci. 457pp.

Clayton, R.N. and Mayeda, T.K. (1963) The use of bromine pentafluoride in the extraction of oxygen from oxides and silicates for isotopic analysis. Geochim. Cosmochim. Acta., V. 27, pp. 43-52.

Cloud, P. (1973) Paleoecological significance of the banded iron formation. Econ. Geol., V. 68, pp. 1135-1143.

Cloud, P. (1976) Major features of crustal evolution. Geol. Soc. S. Africa, Annexure to volume 79, pp. 1-33.

Cloud, P. (1983) Banded Iron-Formation - A Gradualist's Dilemma. In : A.F. Trendall and R.C. Morris (Eds.). Iron-Formation : Facts and Problems. Elsevier, Amsterdam, pp. 401-416.

Coleman, R.G. (1977) Ophiolites. Springer-Verlag, New York, 229p.

Collerson, K.D., Campbell, L.M., Weaver, B.L. and Palacz, Z.A. (1991) Evidence for extreme mantle fractionation in early Archaean ultramafic rocks from northern Labrador. Nature, V. 349, pp. 209-214.

Compston, W. and Pidgeon, R.T. (1986) Jack Hill evidence of more very old detrital zircon in western Australia. Nature, V. 321, pp. 766-769.

Condie, K.C. (1981) Archaean Greenstone Belts. Elsevier, Amsterdam, 434pp.

Condie, K.C. (1985) Secular variation in the composition of basalts: an index to mantle evolution. Jour. Petrol., V. 26, pp. 545-563.

Condie, K.C. (1989) Plate Tectonics and Crustal Evolution, 3rd ed., Pergamon Press, New York, 476pp.

Condie, K.C. (1992) Evolutionary changes at the Archaean-Proterozoic boundary. In : J.E. Glober and S.E. Ho (Eds.), The Archaean: Terrains, Processes and Metallogeny, Proceeding Volume for the 3rd Int. Archaean Symp., Perth, Australia pp. 177-189.

Costa, U.R., Fyfe, W.S., Kerrich, R. and Nesbitt, H.W. (1981). Is Ocean formation synchronus with first preservation of crust ? In : J.E. Glover and D.I. Groves (Eds.), Archaean Geology, Second International Symposium, Perth, 1980, pp. 453-456.

Crawford, A.R. (1969) Reconnaissance Rb-Sr dating of the Precambrian rocks of the Southern Peninsular India. Jour. Geol. Soc. India, V. 10, pp. 117-167.

Crookshank, H. (1963) Geology of southern Bastar and Jeypore from the Bailadila Range to the Eastern Ghats. Geol. Surv. India, Mem. 87, 150pp.

Cullen, D.T. (1963) Tectonic implications of banded ironstone formations. Jour. Sed. Petrol., V. 33, pp. 387-392.

Curtis, L.C., Radhakrishna, B.P. and Naidu, G.K. (1990) Hutti-Gold Mine With a Future. Goel. Soc. India, Bangalore, 123 pp.

Das Sharma, S., Patil, D.J. and Gopalan, K. (1993) A system for the extraction of oxygen from oxides and silicates for isotopic analysis. ISMAS Bulletin, pp. 14-19.

Davy, R. (1983) A contribution on the chemical composition of Precambrian iron-formations. In : A.F. Trendall and R.C. Morris (Eds.). Iron Formation : Facts and Problems, Elsevier, Amsterdam, ppp. 325-343.

De Baar, H.J.W., Michael, P., Brewer, P.G. and Bruland, K.W. (1985) Rare earth elements in the Pacific and Atlantic Oceans Geochim. Cosmochim. Acta, V. 49, pp. 1943-1959.

Deer, W.A., Howie, R.A. and Zussman, J. (1979) An introduction to the rock forming minerals. ELBS and Longman Group Limited, London, 528 p.

Derry, L.A. and Jacobsen, S.B. (1990) The chemical evolution of Precambrian seawater: Evidence from REEs in banded iron formations. Geochim. Cosmochim. Acta, V. 54, pp. 2965-2977.

Devaraju, T.C. and Laajoki, K. (1986) Mineralogy and mineral chemistry of the manganese-poor and manganiferous iron-formations from the high-grade metamorphic terrain of Southern Karnataka, India. Jour. Geol. Soc. India, V. 28, pp. 134-164.

Devaraju, T.C., Anantha Murthy, K.S. and Khanadali, S.D. (1986) Iron-Formation of the Chiknayakanhalli Greenstone Belt, Karnataka, India. Jour. Geol. Soc. India, V. 28, pp. 201-217.

Devaraju, T.C., Rajshekhar, N., Srikantappa, C., Khanadali, S.D. and Subba Rao, G. (1990) Lithium pegmatites of Amareshwar, Raichur district, Karnataka, India. In : S.M. Naqvi (Ed.), Precambrian Continental Crust and its Economic Resources, Elsevier, Amsterdam, pp. 653-669.

Dewey, J.F. and Windley, B.F. (1981) Growth and differentiation of continental crust. Royal Society London, Philosophical Transactions. Ser. A., V. 301, pp. 189-206.

de Wit, M.J., Hart, R. and Hart, R.J. (1987) The Jamestown ophiolite complex, Barberton mountain belt : a section through 3.5 Ga oceanic crust. Jour. Afr. Earth Sci., V. 6, pp. 681-730.

Dhoundial, D.P., Paul, D.K., Sarkar, A., Trivedi, J.R., Gopalan, K. and Potts, P.J. (1987) Geochronology and geochemistry of Precambrian granitic rocks of Goa, SW India. Precamb. Res., V. 36, pp. 287-302.

Dia, A., Allegre, C.J. and Erlank, A. (1990) The development of continental crust through geological time : the South African case. Earth Planet. Sci. Lett., V. 98, pp. 74-89.

Dimroth, E. (1975) Paleo-environment of iron-rich sedimentary rocks. Geol. Rundsch., V. 64(3), pp. 751-767.

Dimroth, E.(1977) Diagenetic facies of Iron-Formation. Geosci. Canada, V. 4, pp. 83-88.

Dimroth, E. (1986) Depositional environments and tectonic settings of cherty iron formations of the Canadian shield. Jour. Geol. Soc. India, V. 28, pp. 239-250.

Dimroth, E. and Chauvel, J.J. (1973) Petrography of the Sokoman Iron Formation in part of the Central Labrador Trough, Quebec, Canada. Geol. Soc. Amer. Bull., V. 84, pp. 111-134.

Dimroth, E. and Kimberley, M.K. (1976) Precambrian atmospheric oxygen : evidence in the sedimentary distributions of carbon, sulfur, uranium and iron. Can. Jour. Earth Sci., V. 13, pp. 1161-1185.

Divakara Rao, V. and Rama Rao, P. (1982) Granitic activity and crustal growth in the Indian shield. Precamb. Res., V. 16, pp. 257-271.

Divakara Rao, V., Rama Rao, P., Subba Rao, M.V., Govil, P.K., Rao, R.U.M., Walsh, J.N., Thompson, N. and Reddy, G.R. (1990) Trace and rare earth element geochemistry and origin of the Closepet granite, Dharwar Craton, India. In : S.M. Naqvi (Ed.) Precambrian Continental Crust and its Economic Resource, pp. 203-222.

Divakara Rao, V., Rama Rao, P., Subba Rao, M.V. and Murthy, N.N. (1991) Terminal report on the project "Geochemical and isotopic studies on acid plutonic rocks and evolution of continental lithosphere". NGRI Tech. Report (Unpub.), 100pp.

Draganic, I.G., Bjergbakke, E., Draganic, Z.D. and Sehested, K. (1991) Decomposition of ocean water by potassium - 40 radiation 3800 Ma ago as a source of oxygen and oxidizing species. Precamb. Res., V. 52, pp. 337-345.

Drever, J.I. (1974) Geochemical model for the origin of Precambrian banded iron formations. Geol. Soc. Am. Bull., V. 85, pp. 1099-1106.

Drury, S.A. (1981) Geochemistry of Archaean metavolcanic rocks from the Kudremukh area, Karnataka. J. Geol. Soc. India, V. 22, pp. 405-416.

Drury, S.A. (1983) The petrogenesis and setting of Archaean metavolcanics from Karnataka State, South India. Geochim. Cosmochim. Acta, V. 47, pp. 317-329.

Drury, S.A. and Holt, R.W. (1980) The tectonic framework of the South Indian craton : A reconnaissance involving LANDSAT imagery. Tectonophysics, V. 65, pp. T1-T15.

Drury, S.A., Holt, R.W., Calsteren, P.C.V. and Beckinsale, R.D. (1983) Sm-Nd and Rb-Sr ages for Archaean rocks in Western Karnataka, South India. Jour. Geol. Soc. India, V. 24, pp. 454-459.

Drury, S.A., Holt, R.W., Reeves-Smith, G.J. and Weightman, R.T. (1984) Precambrian tectonics and crustal evolution in south India. Jour. Geol., V. 92, pp. 3-20.

Dymek, R.F. and Klein, C. (1988) Chemistry, petrology and origin of banded iron formation lithologies from the 3800 Ma Isua supracrustal belt, West Greenland. Precamb. Res., V. 39, pp. 247-302.

Edmond, J.M., Von Damm, K.L., McDuff, R.E. and Measures, C.T. (1982) Chemistry of hot springs on the East Pacific Rise and their effluent dispersal. Science, V. 297, pp. 187-191.

Eugster, H.P. and Chou, I-Ming (1973) The depositional environments of Precambrian banded iron-formations. Econ. Geol., V. 68, pp. 1144-1168.

Ewers, W.E. (1983) Chemical factors in the deposition and diagenesis of banded iron-formation. In : A.F. Trendall and R.C. Morris (Eds.), Iron Formation : Facts and Problems. Elsevier, Amsterdam, pp. 491-512.

Ewers, W.E. and Morris, R.C. (1981) Studies of the Dales Gorge member of the Brockman Iron Formation, Western Australia. Econ. Geol., V. 76, pp. 1929-1953.

Feng, R. and Kerrich, R. (1990) Geochemistry of fine grained clastic sediments in the Archaean Abitibi greenstone belt, Canada : Implications for Provenance and tectonic setting. Geochem. Cosmochim. Acta, V. 54, pp. 1061-1081.

Floran, R.J. and Papike, J.J. (1978) Mineralogy and petrology of the Gunflint Iron Formation, Minnesota-Ontario : Correlation of compositional and assemblage variations at low to moderate grade. Jour. Petrol., V. 19, pp. 215-288.

Folk, R.L. (1962) Spectral subdivision of limestone types. In : Classification of carbonate rocks. Amer. Assoc. Petroleum Geologists, Mem. 1, pp. 62-84.

Fralick, P.W., Barrett, T.J., Jarvis, K.E., Jarvis, I., Schnieders, B.R. and Kemp, R.V. (1989) Sulfide-facies iron formation at the Archaean Morley occurrence, Northwestern Ontario : Contrasts with oceanic hydrothermal deposits. Can. Mineral., V. 27, pp. 601-616.

Friend, C.R.L. and Nutman, A.P. (1991) SHRIMP U-Pb geochronology of the Clospet granite and peninsular gneiss, Karnataka, South India. Jour. Geol. Soc. of India, V. 38, pp. 357-368.

Fryer, B.J. (1983) Part B : Rare earth elements in iron-formation. In : A.F. Trendall and R.C. Morris (Eds.), Iron-Formation : Facts and Problems, Elsevier, Amsterdam, pp. 345-358.

Fyfe, W.S. (1978) The evolution of the earth's crust: modern plate tectonics to ancient hot spot tectonics ? Chem. Geol., V. 23, pp. 89-114.

Fyfe, W.S. (1980) Crust formation and destruction. In : D.W. Strangway (Ed.), The Continental Crust and its Mineral Deposits. Geological Association of Canada, Sp. paper, V. 20, pp. 77-88.

Fyfe, W.S. (1990) Reflections on the Archaean. In : S.M. Naqvi (Ed.) Precambrian Continental Crust and its Economic Resources. Elsevier, Amsterdam, pp. 1-11.

Garrels, R.M. (1987) A model for the deposition of the microbanded Precambrian iron formations. Amer. Jour. Sci., V. 287, pp. 81-106.

Gera, N.L. (1989) Geology of parts of Raichur, Bijapur and Dharwar districts, Karnataka. Rec. Geol. Surv. India, V. 122, Pt. 5, pp. 83-85.

Ghosh, S.K. and Sengupta, S. (1985) Superposed folding and shearing in the western quartzite of Kolar Gold Field. Ind. Jour. of Earth Sci., V. 12, pp. 1-8.

Glikson, A.Y (1979) Comment on the paper by Chadwick et al. (1978) Jour. Geol. Soc. India, V 20, pp. 248-251.

Gnaneshwar Rao, T. (1992) Geochemistry and genesis of Banded Iron Formations from central part of Chitradurga schist belt, Karnakata Nucleus, India. Unpub. Ph.D. thesis, Osmania University, Hyderabad, 350pp.

Gnaneshwar Rao, T. and Naqvi, S.M. (1993) Geochemistry, depositional environment and tectonic setting of the BIF of late Archaean Chitradurga schist belt, India - Evidence of opening and closing of an ocean basin. Chem. Geol. (communicated).

Goldstein, S.J. and Jacobsen, S.B. (1988) Rare earth elements in river waters. Earth Planet. Sci. Lett., V. 89, pp. 35-47.

Gole, M.J. and Klein, C. (1981) Banded iron formation through much of time. Jour. Geol., V. 89, pp. 169-183.

Goode, A.D.J., Hall, N.D.M., Bunting, J.A. (1983) The Nabberu basin of Western Australia. In : A.F. Trendall and R.C. Morris (Eds.) Iron Formations : Facts and Problems. Elsevier, Amsterdam, pp. 295-324.

Goodwin, A.M. (1956) Facies relations in the Gunflint Iron Formation. Econ. Geol. V. 51, pp. 565-595.

Goodwin, A.M. (1973) Archaean iron-formations and tectonic basins of the Canadian Shield. Econ. Geol., V. 68, pp. 915-933.

Goodwin, A.M. (1977) Archaean basin-craton complexes and the growth of Precambrian shields. Can. Jour. Earth Sci., V. 14, pp. 2737-2759.

Goodwin, A.M. (1981) Archean plates and greenstone belts. In : A. Kroner (Ed.), Precambrian Plate Tectonics, Elsevier, Amsterdam, pp. 105-135.

Goodwin, A.M. (1991) Precambrian Geology, Academic Press Limited. London, 666 pp.

Goodwin, A.M., Thode, H.G., Chou, C.L. and Karkhansis, S.N. (1985) Chemostratigraphy and origin of the late Archaean siderite-pyrite-rich Helen Iron Formation, Michipicoten belt, Canada. Can. Jour. Earth. Sci., V. 22, pp. 72-84.

Gopal Rao, B., Venkatasubba, R., Venkata Dasu, S.P., Manjunatha, Kumanan, C.J., Mahalakshmamma, A.P., Deepak Bellur and Mohieddin, K.R. (1989) Geology and evolution of Nagamangala, Yediyur-Karighatta schist belts and adjoining Gneissic Terrain in parts of Mandya and Tumkur dists., Karnataka. 28th International Geological Congress, Washington D.C., Abs. V. 2 of 3, pp. 2-610.

Govil, P.K. (1985) X-ray fluorescence analysis of major, minor and selected trace elements in new IWG reference rock samples. Jour. Geol. Soc. India, V. 26, pp. 38-42.

Govil, P.K. and Gnaneshwar Rao, T. (1991) Determination of trace elements in iron formations by XRF spectrometry. National

Symposium on Modern analytical techniques in material science, BARC, Dec. 9-11, 1991. Preprint volume, pp. 70-72.

Graf, J.L. (1978) Rare earth elements, iron-formations and seawater. Geochim. Cosmochim. Acta., V. 42, pp. 1845-1850.

Gross, G.A. (1965) The geology of iron deposits in Canada: 1. General geology and evaluation of Iron Deposits. Geol. Surv. Canada. Econ. Geol. Ser. Rep., No. 22(1), 181 pp.

Gross, G.A. (1980) A classification of iron-formation based on depositional environments. Can. Mineral., V. 18, pp. 223-229.

Gross, G.A. (1983) Tectonic systems and the deposition of iron-formation. Precamb. Res., V. 20, pp. 171-187.

Gross, G.A. (1986) The metallogenetic significance of Iron Formation and related stratafer rocks. Jour. Geol. Soc. India, V. 28, pp. 92-108.

Guidotti, C.V. (1984) Micas in metamorphic rocks. In : S.W. Bailey (Ed.), Micas. Reviews in Mineralogy, V. 13, pp. 357-467.

Gururaja Rao, T.P. and Devadu, G.R. (1975) Molybdenite occurrence near Malatgud, Raichur district, Karnataka. Indian Minerals, V. 29, pp. 85-88.

Haase, C.S. (1982) Metamorphic petrology of the Negaunee Iron Formation, Marquette district, northern Michigan : Mineralogy, metamorphic reactions and phase equilibria. Econ. Geol., V. 77, pp. 60-81.

Hackett, J.P. and Bischoff, J.L. (1973). New data on the stratigraphy, extent and geologic history of the Red Sea geothermal deposits. Econ. Geol., V. 68, pp. 553-564.

Hargraves, R.B. (1986) Faster spreading of greater ridge length in the Archaean ? Geology., V. 14, pp. 750-752.

Harper, C.L. (Jr.) and Jacobsen, S.B. (1992) Evidence from coupled ^{147}Sm-^{143}Nd and ^{146}Sm-^{142}Nd systematics for very early (4.5 Gyr) differentiation of the Earth's mantle. Nature, V. 360, pp. 728-732.

Harris, N.B.W. and Jayaram, S. (1982) Metamorphism of cordierite gneisses from the Bangalore region of the Indian Archaean. Lithos, V. 15, pp. 89-98.

Hawthorne, C.I. (1981) Crystal chemistry of the amphiboles. In : D.R. Veblen (Ed.), Amphiboles and other hydrous pyriboles - Mineralogy, Review in Mineralogy, V. 9A, pp. 1-102.

Heaney, P.J. and Veblen, D.R. (1991) An examination of spherulitic dubiomicrofossils in Precambrian banded iron formations using the transmission electron microscope. Precamb. Res., V. 49, pp. 355-372.

Helmstaedt, H., Padgham, W.A. and Brophy, J.A. (1986) Multiple dikes in Lower Kam Group, Yellow knife greenstone belt : Evidence for Archaean sea-floor spreading. Geology, V. 14, pp. 562-566.

Henoc, J. and Maurice, F. (1978) Micro-analyses and scanning electron microscopy. In : F. Maurice, L. Meny and R. Tixier (Eds.) Les Editors des Physique, Orgay, pp. 281-307.

Hey, M.H. (1954) A new review of the chlorites. Mineral. Mag., V. 30, pp. 277-292.

Hickey-Vargas, R., Roa, H.M., Lopez Escobar, L. and Frey, F.A. (1989) Geochemical variations in Andean basaltic and silicic lavas from the Villarrica-Lanin volcanic chain (39.5^{o}S): an evaluation of source heterogeneity, fractional crystallization and crustal assimilation. Contrib. Mineral. Petrol., V. 103, pp. 361-386.

Hoefs, J., Muller, G., Schuster, K.A. and Walde, D. (1987) The Fe-Mn ore deposits of Urucum, Brazil: An oxygen isotope study. In: N. Clauer and S. Chaudhuri (Eds.), Isotopes in the Sedimentary Cycle. Chem. Geol., (Isot. Geosci. Sect.), V. 65, pp. 311-319.

Hofmann, A.W. (1988) Chemical differentiation of the Earth: the relationship between mantle, continental crust, and oceanic crust. Earth Planet. Sci. Lett., V. 90, pp. 297-314.

Hofmann, H.J., Sage, R.P. and Berdusco, E.N. (1991) Archaean stromatolites in Michipicoten Group Siderite Ore at Wawa, Ontario. Econ. Geol., V. 86, pp. 1023-1030.

Holland, H.D. (1973) The oceans, a possible source of iron in iron formations. Econ. Geol., V. 68, pp. 1169-1172.

Holland, H.D. (1984) The chemical evolution of the atmosphere and the oceans. Princeton University Press, Princeton, N.J., 582pp.

Hough, J.L. (1958) Fresh-water environment of deposition of Precambrian banded iron formations. Jour. Sed. Pet., V. 28, pp. 414-430.

Hussain, S.M. and Naqvi, S.M. (1983) Geological, geophysical and geochemical studies over the Holenarasipur schist belt, Dharwar craton, India. In : S.M. Naqvi and J.J.W. Rogers

(Eds.), Precambrian of South India, Geol. Soc. India, Mem. 4, pp. 73-94.

Iler, R.K. (1979) The chemistry of Silica. Wiley, New York, 866pp.

Immage, I.P. and Klein, C. (1976) Mineralogy and petrology of some metamorphic Precambrian iron-formations in south western Montana. Amer. Mineral., V. 61, pp. 1117-1144.

Iyengar, S.V.P. (1976) The stratigraphy, structure and correlation of the Dharwar Supergroup. Geol. Surv. India, Misc. Publ. 23, Part 2, pp. 415-455.

Jackson, E.D. and Thayer, T.P. (1972) Some criteria for distinguishing between stratiform, concentric and alpine-peridotite gabbro complexes. Proc. 24th Int. Geol. Congr., Sec. 2, pp. 289-296.

Jacobsen, S.B. (1988) Isotopic and chemical constraints on mantle-crust evolution. Geochem. Cosmochim. Acta, V. 52, pp. 1341-1350.

Jacobsen, S.B. and Pimentel-Klose, M.R. (1988) A Nd isotopic study of the Hamersley and Michipicoten banded iron formations : The source of REE and Fe in Archaean Oceans. Earth Planet. Sci. Lett., V. 87, pp. 29-44.

Jagannathachar, L.G. and Madusudanan (1989) Preliminary investigation for tin in Mangalur schist belt, Gulbarga district, Karnataka, Rec. Geol. Surv. India, V. 122, Pt. 5, pp. 133-134.

James, H.J. (1954) Sedimentary facies iron-formation. Econ. Geol., V. 49, pp. 253-293.

James, H.J. (1983) Distribution of banded iron formation in space and time. In : A.F. Trendall and R.C. Morris (Eds.) Iron-Formation Facts and Problems. Elsevier, Amsterdam, pp. 471-490.

Janardhan, A.S. and Vidal, PH. (1982) Rb-Sr dating of the Gundlupet gneiss around Gundlupet, Southern Karnataka. Jour. Geol. Soc. India, V. 23, pp. 578-580.

Jayaram, B. (1922) Report on the work done during the field season 1917-18. Rec. Mysore Geol. Dept., V. 18, pp. 43-87.

Jochum, K.P., Arndt, N.T. and Hofmann, A.W. (1991) Nb-Th-La in komatiites and basalts: constraints on komatiite petrogenesis and mantle evolution. Earth Planet. Sci. Lett., V. 107, pp. 272-289.

Kaila, K.L. and 10 others (1979) Crustal structure along the Kavali-Udipi profile in the Indian Peninsular shield from deep seismic sounding. Jour. Geol. Soc. India, V. 20, pp. 307-333.

Kalugin, A.S. (1973) Geology and genesis of the Devonian banded iron-formation in Altai, Western Siberia and eastern Kazakhstan. In : Genesis of Precambrian Iron and Manganese Deposits. UNESCO Press, Earth Science, No. 9, pp. 159-166.

Kasting, J.F. (1987) Theoretical Constraints on Oxygen and Carbondioxide concentrations in the Precambrian atmosphere. Precamb. Res., V. 34, pp. 205-229.

Kasting, J.F. (1993) Earth's Early Atmosphere. Science, V. 259, pp. 920-926.

Kaufman, A.J., Hayes, J.M., Knoll, A.H. and Germs, G.J.B. (1991) Isotopic compositions of carbonates and organic carbon from upper Proterozoic successions in Namibia : stratigraphic variation and the effects of diagenesis and metamorphism. Precamb. Res., V. 49, pp. 301-327.

Khan, R.M.K., Govil, P.K. and Naqvi, S.M. (1992) Geochemistry and genesis of banded iron formation from Kudremukh schist belt, Karnataka Nucleus, India. Jour. Geol. Soc. India, V. 40, pp. 311-328.

Khan, R.M.K., Nirmal Charan, S., Arora, M. and Naqvi, S.M. (1993) Mineral composition and its bearing on depositional history of banded iron formation from Kudremukh schist belt, Karnataka Nucleus, India. Jour. Geol. Soc. India (communicated).

Klein, C. (1973) Changes in mineral assemblages with metamorphism of some banded Precambrian iron formations. Econ. Geol., V. 68, pp. 1075-1088.

Klein, C. (1983) Diagenesis and metamorphism of Precambrian banded iron formations. In : A.F. Trendall and R.C. Morris (Eds.), Iron-Formation: Facts and Problems, Elsevier, Amsterdam, pp. 417-469.

Klein, C. and Gole, M.J. (1981) Mineralogy and petrology of parts of the Marra Mamba Iron Formation, Hamersley Basin, Western Australia. Amer. Mineral., V. 66, pp. 507-525.

Klein, C. and Beukes, N.J. (1989) Geochemistry and sedimentology of a facies transition from limestone to iron-formation deposition in the early Proterozoic Transvaal Supergroup, South Africa. Econ. Geol., V. 84, pp. 1733-1774.

Klein, C., Beukes, N.J. and Schopf, J.W. (1987) Filamentous microfossils in the early Proterozoic Transvaal Supergroup, their morphology, significance and palaeo-environmental setting. Precamb. Res., V. 36, pp. 81-94.

Klinkhammer, G., Elderfield, H. and Hudson, A. (1983) Rare earth elements in seawater near hydrothermal vents. Nature. V. 305, pp. 185-188.

Krishna Murthy, M. (1974) Tectonomagmatic history of the Precambrians in Bellary district, Mysore State. Jour. Geol. Soc. India, V. 15, pp. 37-47.

Kroner, A. (1991) Tectonic evolution in the Archaean and Proterozoic. Tectonophysics, V. 187, pp. 393-410.

Kroner, A. and Layer, P.W. (1992) Crust Formation and Plate Motion in the Early Archaean. Science, V. 256, pp. 1405-1411.

Kumar, B., Venkatasubramanian, V.S. and Rama Saxena, (1983) Carbon and oxygen isotopic composition of the carbonates from greenstone belts of Dharwar craton, India. In : S.M. Naqvi and J.J.W. Rogers (Eds.), Precambrian of South India. Geol. Soc. India, Mem. 4, pp. 260-266.

Kump, L.R. and Holland, H.D. (1992) Iron in Precambrian rocks: Implications for the global oxygen budget of the ancient Earth. Geochim. Cosmochim. Acta., V. 56, pp. 3217-3223.

Laajoki, K. and Devaraju, T.C. (1989) Fe-chlorite, Grunerite, Stilpnomelane, Ankerite and Siderite occurrence in the iron-formation of Chiknayakanahalli schist belt, Karnataka. Jour. Geol. Soc. India, V. 33, pp. 175-182.

Laajoki, K. and Saikkonen, R. (1977) On the geology and geochemistry of the Precambrian iron-formations in Vayrylankyla, South Puolanka area, Finland. Bull. Geol. Surv. Finland, V. 293, 137 pp.

LaBerge, G.L. (1973) Possible biological origin of Precambrian iron-formation. Econ. Geol., V. 68, pp. 1098-1109.

LaBerge, G.L. (1986) A model for the biological precipitation of Precambrian iron formation. LPI Technical report : Lunar and Planetary Institute, Houston, p. 71-75.

Le Bas, M.J., Le Maitre, R.W., Streckeisen, A. and Zanettin, B. (1986) A chemical classification of volcanic rocks based on the Total Alkali Silica Diagrams. Jour. Petrol., V. 27, pp. 745-750.

Lesher, C.M. (1978) Mineralogy and petrology of the Sokoman Iron Formation near Ardua Lake, Quebec. Can. Jour. Earth Sci., V. 15, pp. 480-500.

Liu, D.Y., Nutman, A.P., Compston, W., Wu, J.S. and Shen, Q.H. (1992) Remnants of $\geq$ 3800 Ma crust in the Chinese part of the Sino-Korean craton. Geology, V. 20, pp. 339-342.

Mahabaleswar, B. (1986) Mineral chemistry of the silicate mineral phases of Banded Iron-Formation of high-grade region, Karnataka. Jour. Geol. Soc. India, V. 28, pp. 165-178.

Majumder, T. and Chakraborty, K.L. (1979) Petrography and petrology of the Precambrian banded iron-formation of Orissa, India and reformation of the bands. Sed. Geol., V. 19, pp. 287-300.

Majumder, T., Whitley, J.E. and Chakraborty, K.L. (1984) Rare Earth Elements in the Indian Banded Iron-Formation. Chem. Geol., V. 45, pp. 203-211.

Mallikarjuna, C., Devapriyan, G.V., Balachandran, V. and Harinadha Babu. (1987) Archaean stromatolites near Bhimasamudra, Karnataka. Jour. Geol. Soc. India, V. 13, pp. 159-161.

Manikyamba, B. (1992) Geochemistry of Iron and Manganese Formations of Sandur Schist Belt, Dharwar Craton, India. Unpub. Ph.D. thesis, Osmania University, Hyderabad, 327pp.

Manikyamba, C. and Naqvi, S.M. (1993a) Geochemistry of Fe-Mn formations of Archaean Sandur schist belt, India -- Mixing of clastic and chemical processes at a shallow shelf. (communicated)

Manikyamba, C. and Naqvi, S.M. (1993b) Geochemistry of volcanic rocks from Sandur schist belt and its significance in greenstone belt tectonics (under preparation).

Manikyamba, C., Balaram, V. and Naqvi, S.M. (1993) Geochemical signatures of polygenecity of Banded Iron Formations of Archaean Sandur greenstone belt (schist belt) Karnataka Nucleus, India. Precamb. Res., V. 61, pp. 137-164.

Matin, A. and Mukhopadhyay, D. (1987) Structural interpretation of the north western termination of the Sandur schist belt. Ind. Jour. Earth Sci., V. 14, pp. 214-216.

McLennan, S.M. and Taylor, S.R. (1991) Sedimentary rocks and crustal evolution : Tectonic setting and secular trends. Jour. Geol., V. 99, pp. 1-22.

Melezhik, V.A. (1987) Composition of waters of Precambrian basins as indicated by geochemical data: Internat. Geol. Rev., V. 29, pp. 1188-1199.

Mel'nik, Y.P. (1982) Precambrian banded Iron-Formation, Physico-chemical conditions of Formation. Elsevier, Amsterdam, 310pp.

Menon, A.G., Venkatasubramanian, V.S., Vasudev, V.N. and Anantha Iyer, G.V. (1981) Sulphur isotope abundance variations in sulphides of the Dharwar Craton - Part III : Hutti. Jour. Geol. Soc. India, V. 22, pp. 448-450.

Michard, A. and Albarede, F. (1986) The REE content of some hydrothermal fluids. Chem. Geol., V. 55, pp. 51-60.

Michard, A., Albarede, F., Michard, G., Minster, J.F. and Charlou, J.L. (1983) Rare earth elements and uranium in high temperature solutions from the East Pacific Rise hydrothermal vent fields (13°N). Nature, V. 303, pp. 795-797.

Middlemost, E.A.K. (1975) The basalt clan. Earth Sci. Rev., V. 11, pp. 337-364.

Mishra, R.N. (1990) Precambrian Banded Iron Formations of Karnataka. In: Studies in Earth Sciences, Prof. C. Naganna felicitation volume, Deptt. of Geology, Bangalore University, pp. 33-48.

Mook, W.G. (1968) Geochemistry of the stable carbon and oxygen isotopes of natural waters in the Netherlands. Unpub. Ph.D. thesis, Rijksuniversiteit, Gronniggen, Netherlands.

Morris, R.C. (1986) The cycling redox state of iron in the genesis of Banded Iron-Formations and their associated enrichment iron ores. Jour. Geol. Soc. India, V. 28, pp. 227-236.

Morris, R.C. (1993) Genetic modelling for banded iron-formation of the Hamersley Group, Pilbara Craton, Western Australia. Precamb. Res., V. 60, pp. 243-286.

Mukhopadhyay, D. (1986) Structural pattern in the Dharwar craton. Jour. Geol., V. 94, pp.

Mukhopadhyay, D. and Matin, A. (1993) The structural anatomy of the Sandur schist belt - a greenstone belt in the Dharwar craton of South India. Jour. Struct. Geol., V. 15, pp. 309-322.

Mullen, E.D. (1983) $MnO/TiO_2/P_2O_5$: a minor element discriminant for basaltic rocks of oceanic environments and its implica tions for petrogenesis. Earth. Planet. Sci. Lett., V. 62, pp. 53-62.

Murthy, P.S.N. and Reddy, K.R. (1984) 2900 m.y. old stromatolite from Sandur Greenstone belt of Karnataka craton, India. Jour. Geol. Soc. India, V. 25, pp. 263-266.

Nagy, B., Weber, R., Guerrero, J.C. and Schidlowski, M. (1983) (Eds.) Developments and Interactions of the Precambrian Atmosphere, Lithosphere and Biosphere. Elsevier, 475pp.

Naha, K. and Mukhopadhyay, D. (1990) Structural styles in the Precambrian metamorphic terranes of Peninsular India : A synthesis. In : S.M. Naqvi (Ed.) Precambrian Continental Crust and its Economic Resource. Elsevier, Amsterdam, pp. 157-178.

Naha, K., Srinivasan, R. and Naqvi, S.M. (1986) Structural unity in the Early Precambrian Dharwar Tectonic Province, Peninsular India. Quart. Jour. Geol. Min. Metal. Soc. India, V. 58, pp. 219-243.

Naha, K., Srinivasan, R. and Jayaram, S. (1991) Sedimentational, structural and migmatitic history of the Archaean Dharwar tectonic province, southern India. Proc. Indian Acad. Sci. (Earth Planet. Sci.), V. 100, pp. 413-433.

Naqvi, S.M. (1973) Geological structure and aeromagnetic and gravity anomalies in the central part of the Chitaldurg schist belt, Mysore. India. Geol. Soc. of Amer. Bull., V. 84, pp. 1721-1732.

Naqvi, S.M. (1976) Physico-chemical conditions during the Archaean as indicated by Dharwar Geochemistry. In : B.F. Windley (Ed.), Early History of the Earth, John Wiley and Sons, London, pp. 289-298.

Naqvi, S.M. (1978) Geochemistry of Archaean metasediments; evidence for prominent anorthosite-norite-troctolite (ANT) in the Archaean basaltic primordial crust. In : B.F. Windley and S.M. Naqvi (Eds.), Archaean Geochemistry, Proc. First Internat. Symp. on Archaean Geochem. The Origin and Evolution of Archaean Continental Crust, Elsevier, Amsterdam, pp. 343-360.

Naqvi, S.M. (1981) The oldest supracrustals of the Dharwar Craton. Jour. Geol. Soc. India, Vol. 22, pp. 458-469.

Naqvi, S.M. (1983) Early Precambrian clastic metasediments of Dharwar greenstone belts : implications to SIMA-SIAL transformation processes. In : S.M. Naqvi and J.J.W. Rogers (Eds.), Precambrian of South India, Geol. Soc. of India, Mem. 4, pp. 220-236.

Naqvi, S.M. (1985) Chitradurga schist belt - An Archaean suture (?). Jour. Geol. Soc. India, V. 26, pp. 511-525.

Naqvi, S.M. (1990) (Ed.) Precambrian Continental Crust and its Economic Resources. Elsevier, Amsterdam, 669pp.

Naqvi, S.M. and Hussain, S.M. (1972) Petrochemistry of some early Precambrian metasediments from the central part of the Chitradurga schist belt, Mysore, India. Chem. Geol., V. 10, pp. 109-135.

Naqvi, S.M. and Hussain, S.M. (1979) Goechemistry of metaanorthosites from a greenstone belt in Karnataka, India. Can. Jour. Earth Sci., V. 16, pp. 1254-1264.

Naqvi, S.M. and Rogers, J.J.W. (1983) (Eds.) Precambrian of South India. Geol. Soc. India, Mem. 4, 575pp.

Naqvi, S.M. and Rogers, J.J.W. (1987) Precambrian Geology of India. Oxford Monographs on Geology and Geophysics. No. 6, Oxford University Press, Oxford. 223pp.

Naqvi, S.M., Divakara Rao, V., Hussain, S.M., Narayana, B.L., Rogers, J.J.W. and Satyanarayana, K. (1978) The petrochemical and geological implications of conglomerates from Archaean geosynclinal piles of Southern India. Can. Jour. Earth Sci., V. 15, pp. 1085-1100.

Naqvi, S.M., Govil, P.K. and Rogers, J.J.W. (1981) Chemical sedimentation in Archaean-early Proterozoic greenschist belts of the Dharwar craton, India. In : J.E. Glover and D.I. Groves (Eds.), Second Internat. Symposium on Archaean Geology, Geol. Soc. of Aust., Sp. Publ., V. 7, pp. 245-253.

Naqvi, S.M. and 13 others (1983) Geochemistry of gneisses from Hassan district and adjoining areas, Karnataka, India. In : S.M. Naqvi and J.J.W. Rogers (Eds.), Precambrian of South India, Geol. Soc. India, Mem. , pp. 401-413.

Naqvi, S.M., Venkatachala, B.S., Manoj Shukla, Kumar, B., Natarajan, R. and Mukund Sharma (1987) Silicified cyanobacteria from the cherts of Archaean Sandur schist belt, Karnataka, India. Jour. Geol. Soc. India, V. 29, pp. 535-539.

Naqvi, S.M., Sawkar, R.H., Subba Rao, D.V., Govil, P.K. and Gnaneshwar Rao, T. (1988) Geology, geochemistry and tectonic setting of greywackes from Karnataka Nucleus, India. Precamb. Res., V. 39, pp. 193-216.

Narain, H. and Subrahmanyam, C. (1986) Precambrian tectonics of the south Indian shield inferred from geophysical data. Jour. Geol. V. 94, pp. 187-195.

Narasimha, S. and Hans, S.K. (1983) Geology of the Gurgunta schist belt, Raichur district, Karnataka. Jour. Geol. Soc. India, V. 24, pp. 299-302.

Nealson, K.H. and Myers, C.R., (1990) Iron reduction by bacteria: A potential role in the genesis of banded iron formations. Am. Jour. Sci., V. 290-A, pp. 35-45.

Newbold, T.J. (1844) Summary of the geology of south India. Jour. Royal Asiatic Society. V. 8, pp. 138-11, V. 9, pp. 1-42, V. 12, pp. 78-96.

Nisbet, E.G. and Fowler, C.M.R. (1983) Model for Archaean plate tectonics. Geology, V. 11, pp. 376-379.

Nutman, A.P., Chadwick, B., Ramakrishnan, M. and Viswanatha, M.N. (1992) SHRIMP. U-Pb ages of detrital zircon in Sargur supracrustal rocks in western Karnataka, South India. Jour. Geol. Soc. India, V. 39, pp. 367-374.

Olivarez, A.M. and Owen, R.M. (1989) REE/Fe variations in hydrothermal sediments; implications for REE content of seawater. Geochim. Cosmochim. Acta, V. 53, PP. 757-762.

O'Rourke, J.E. (1961) Paleozoic banded iron-formations. Econ. Geol., V. 56, pp.331-361.

Pearce, J.A. (1980) Geochemical evidence for the genesis and eruptive setting of lavas from Tellyan ophiolites. In: Proc. Int. Ophiolite Symposium , Cyprus, 1979. Geol Surv. Dept., Nicosia, 261pp.

Pearce, J.A. and Cann, J.R. (1973) Tectonic setting of basic volcanic rocks determined using trace element analysis. Earth Planet. Sci. Lett., V. 19, pp. 290-300.

Perraju, P. and Natarajan, V. (1977) "Peninsular Gneiss" in the northern parts of Andhra Pradesh. Jour. Geol. Soc. India, V. 18, pp. 224-232.

Pichamuthu, C.S. (1945) Algal structures in the cherts from Dodguni, Tumkur District. Ind. Sci. Congr. 32nd Session, pp. 60.

Pichamuthu, C.S. (1967) The Precambrian in India. In : K. Rankama (Ed.), The geological systems - The Precambrian. Wiley Interscience, New York, 3, pp. 1-96.

Pichamuthu, C.S. (1974) On the Banded Iron-Formation of Precambrian age in India. Jour. Geol. Soc. India, V. 15, pp. 1-30.

Pichamuthu, C.S. and Srinivasan, R. (1983) A billion year history of the Dharwar craton (3200 to 2100 m.y. ago). Mem. Geol. Soc. India, V. 4, pp. 121-142.

Pichamuthu, C.S. and Srinivasan, R. (1984) The Dharwar craton - A Golden Jubilee Publication. Ind. Natl. Sci. Acad., New Delhi, 34pp.

Piepgras, D.J. and Wasserburg, G.J. (1983) Influence of the Mediterranean outflow on the isotopic composition of neodymium in waters of the North Atlantic. Jour. Geophys. Res., V. 88, pp. 5997-6006.

Prasad, C.V.R.K., Subba Reddy, N. and Windley, B.F. (1982) Iron-formations in Archaean granulite gneiss belts with special reference to Southern India. Jour. Geol. Soc. India, V. 23, pp. 112-122.

Raase, P., Raith, M., Ackermand, D. and Lal, R.K. (1986) Progressive metamorphism of mafic rocks from greenschist to granulite facies in the Dharwar craton of South India. Jour. Geol., V. 94, pp. 261-282.

Radhakrishna, B.P. (1967) Reconsideration of some problems in the Archaean complex of Mysore. Jour. Geol. Soc. India., V. 18, pp. 102-110.

Radhakrishna, B.P. (1983) Archaean granite greenstone terrain of the South Indian sheild. In : S.M. Naqvi and J.J.W. Rogers (Eds.), Precambrian of South India. Geol. Soc. India., Mem. 4, pp. 1-46.

Radhakrishna, B.P. (1987) Introduction. In Purana Basins of Peninsular India (Middle to Late Proterozoic). Geol. Soc. of India, Mem. 6, I-XV.

Radhakrishna, B.P. and Vasudev, V.N. (1977) The early Precambrian of the southern Indian shield. Jour. Geol. Soc. India., V. 18, pp. 525-541.

Radhakrishna, B.P. and Naqvi, S.M. (1986) Precambrian continental crust of India and its evolution. Jour. Geol., V. 94, pp. 145-166.

Radhakrishna, B.P. and Ramakrishnan, M. (1988) Archaean-Proterozoic boundary in India. Jour. Geol. Soc. India, V. 32, pp. 263-278.

Radhakrishna, B.P. and Ramakrishnan, M. (1990) (Eds.) Archaean Greenstone belts of South India. Geol. Soc. India, Mem. 20, 481pp.

Radhakrishna, B.P., Devaraju, T.C. and Mahabaleswar, B. (1986) Banded iron formation of India. Jour. Geol. Soc. India., V. 28, pp. 71-91.

Rajamani, V. (1990) Petrogenesis of metabasites from the schist belts of the Dharwar craton. Implications to Archaean mafic magmatism. Jour. Geol. Soc. India, V. 36, pp. 565-587.

Rajamani, V., Shivkumar, K., Hanson, G.N. and Shirey, S.B. (1985) Geochemistry and petrogenesis of amphibolites, Kolar schist belt, south India. Evidence for komatiitic magma derived by low percentage of melting of mantle. Jour. Petrol., V. 96, pp. 92-123.

Ramakrishnan, M. (1980) Geology of the Javanahalli, Holenarsipur and Sargur schist belts of Karnataka Craton and the geochemistry of mafic rocks. Unpub. Ph.D. thesis, Indian Institute of Science, Bangalore.

Ramakrishnan, M. and Viswanatha, M.N. (1981) Holenarasipur belt. In : J. Swami Nath and M. Ramakrishnan (Eds.), Early Precambrian Supracrustals of Southern Karnataka. Mem. Geol. Surv. India., V. 112, pp. 115-141.

Ramakrishnan, M., Viswanatha, M.N. and Swami Nath, J. (1976) Basement-cover relationships of Peninsular Gneiss with high grade schist and greenstone belts of southern Karnataka. Jour. Geol. Soc. of India, V. 7, pp. 97-111.

Rama Rao, B. (1940) Remarks on the mode of occurrence and origin of the Peninsular Gneiss of Mysore. Records Mysore Geology Department, V. 38, pp. 52-72.

Rama Rao, P., Naqvi, S.M., Govil, P.K. and Balaram, V. (1991) Geochemistry of trondhjemites from Sigegudda, Hassan district, Karnataka. Jour. Geol. Soc. of India, V. 37, pp. 351-358.

Rangin, C., Steinberg, M. and Bannot-Courtois, C. (1981) Geochemistry of the Mesozoic bedded cherts of central Baja California (Vizcaino-Cedros-San Benito); implications for paleogeographic reconstruction of an old oceanic basin. Earth Planet. Sci. Lett., V. 54, pp. 313-322.

Rao, K.S. (1989) Preliminary investigation for diamond in the Hagari river basin, Bellary district, Karnataka. Rec. Geol. Surv. India, V. 122, Pt. 5, pp. 139-140.

Rogers, J.J.W. (1986) The Dharwar craton and the assembly of Peninsular India. Jour. Geol., V. 94, pp. 129-144.

Rogers, J.J.W. (1990) Comparison of the Indian and Nubian-Arabian shields. In: S.M. Naqvi (Ed.), Precambrian Continental Crust and Its Economic Resources. Elsevier, Amsterdam, pp. 223-243.

Rogers, J.J.W. (1992) Contrast between an old and a young Gondwana shield. Jour. Geodynamics, V. 16, pp. 211-214.

Roy, A. (1979) Polyphase folding deformation in the Hutti-Maski schist belt, Karnataka. Jour. Geol. Soc. India, V. 20, pp. 598-607.

Roy, A. (1983) Structure and tectonics of the cratonic areas of North Karnataka. Recent Res. Geol., V. 10, pp. 81-97.

Roy, A. and Biswas, S.K. (1979) Metamorphic history of the Sandur schist belt, Karnataka. Jour. Geol. Soc. India, V. 20, pp. 179-187.

Roy, A. and Biswas, S.K. (1983) Stratigraphy and structure of the Sandur schist belt, Karnataka. Jour. Geol. Soc. India, V. 24, pp. 19-29.

Ruhlin, D.E. and Owen, R.M. (1986) The rare earth element geochemistry of hydrothermal sediments from the East Pacific Rise: Examination of a seawater scavenging mechanism. Geochim. Cosmochim. Acta, V. 50, pp. 393-400.

Sampath Iyengar, P. (1905) Report on the survey work in the Chitaldurg district. Records Mysore Geology Department, V. 6, pp. 57-116.

Sarkar, S.N. and Saha, A.K. (1977) The present status of the Precambrian stratigraphy, tectonics and geochronology of the Singhbhum - Keonjhar - Mayurbhanj region, Eastern India. Indian Jour. Earth Sci., S. Ray Volume, pp. 37-66.

Sarkar, S.N., Saha, A.K. and Miller, J.A. (1969) Geochronology of Precambrian rocks of Singhbhum and adjacent regions, Eastern India. Geol. Mag. V. 106, pp. 15-45.

Sarvothaman, H. and Leelanandam, C. (1992) Peraluminous, Metaaluminous and Alkaline Granites from parts of Andhra Pradesh and Karnataka in the Dharwar Craton. Jour. Geol. Soc. India, V. 39, pp. 279-291.

Schidlowski, M. (1989) A 3,800 million year isotopic record of life from carbon in sedimentary rocks. Nature, V. 333, pp. 313-318.

Schidlowski, M. (1990) Early evolution of life and economic mineral and hydrocarbon resources. In : S.M. Naqvi (Ed.) Precambrian Continental Crust and its economic resources, Elsevier, Amsterdam, pp. 605-606.

Schopf, J.W. (1983) Earth's Earliest Biosphere. Its origin and evolution. Princeton Univ. Press, Princeton, N.J., 544 pp.

Schopf, J.W. (1993) Microfossils of the Early Archaean Apex Chert: New Evidence of the Antiquity of Life. Science, V. 260, pp. 640-646.

Schopf, J.W. and Walter, M.R. (1983) Archaean microfossils : new evidence of ancient microbes. In : J.W. Schopf (Ed.) The Earth's Earliest Biosphere : Its Origin and Evolution. Princeton Univ. Press, Princeton, N.J., pp. 214-239.

Seshadri, T., Chaudhuri, A., Harinadha Babu, P. and Chayapathi, N. (1981) Shimoga belt. In : J. Swami Nath and M. Ramakrishnan (Eds.), Early Precambrian supracrustals of Southern Karnataka, Geol. Surv. India, Mem., 112, pp. 163-198.

Seyfried, W.E. and Janecky, D.R. (1985) Heavy metal and sulfer transport during subcritical and supercritical hydrothermal alteration of basalt: Influence of fluid pressure and basalt composition and crystallinity. Geochim. Cosmochim. Acta., V. 49, pp. 2545-2560.

Shaw, D.M. (1980) Evolutionary tectonics of the earth in the light of early crustal structures. In : D.W. Strangway (Ed.), The Continental Crust and its Mineral Deposits, Geol. Assoc. of Canada, Sp. paper, 20, pp. 65-76.

Shimizu, H., Umemoto, N., Masuda, A. and Appel, P.W.U. (1990) Sources of iron-formations in the Archean Isua and Malene supracrustals, West Greenland: Evidence from La-Ce and Sm-Nd isotopic data and REE abundances. Geochim. Cosmochim. Acta, V. 54, pp. 1147-1154.

Simonsen, B.M. (1985) Sedimentological constraints on the origins of Precambrian iron formations. Geol. Soc. Am. Bull., V.96, pp.244-252.

Sleep, N.H. and Windley, B.F. (1982) Archaean Plate tectonics constraints and inferences. Jour. Geol., V. 90, pp. 363-379.

Smeeth, W.F. (1916) Outline of the geological history of Mysore. Bull. Mysore Geol. Dept. No. 6, 22pp.

Srinivasan, R. (1985) Stratigraphical and geochemical characterization of the type sections of the Early Precambrian Rock Formations of Karnataka. Unpub. Ph.D. thesis, University of Mysore, Mysore 215pp.

Srinivasan, R. (1988) Present status of the Sargur Group of the Archaean Dharwar Craton, South India. Indian Jour. Earth Sci., V. 60, pp. 57-72.

Srinivasan, R. and Sreenivas, B.L. (1972) Dharwar stratigraphy. Jour. Geol. Soc. of India, V. 13, pp. 72-83.

Srinivasan, R. and Naqvi, S.M. (1990) Some distinctive trends in the evolution of the early Precambrian (Archaean) Dharwar craton, South India. In : S.M. Naqvi (Ed.), Precambrian Continental Crust and its Economic Resources. Elsevier, Amsterdam, pp. 245-266.

Srinivasan, R., Manoj Shukla, Naqvi, S.M., Yadav, V.K., Venkatachala, B.S., Uday Raj, B. and Subba Rao, D.V. (1989) Archaean stromatolites from the Chitradurga schist belt, Dharwar Craton, South India. Precamb. Res., V. 43, pp. 239-250.

Srinivasan, R., Naqvi, S.M. and Vasantha Kumar, B. (1990) Archaean self-facies and stromatolite proliferation in Dharwar Supergroup, North Kanara district, Karnataka. Jour. Geol. Soc. India, V. 35, pp. 203-212.

Srinivasan, R., Subba Rao, D.V., Pantulu, G.V.C., Sivaraman, T.V., Balaram, V. and Gopalan, K. (1992) Negative Europium anomalies and reset Rb-SR ages of Archaean detrital metasedimentary rocks of the low grade supracrustal belts of the Dharwar Craton, South India. In : J.E. Glover and S.E. Ho (Eds.), The Archaean : Terrains, Processes and Metallogeny, Proceedings Volume for the 3rd Int. Archaean Symp., Perth, Australia, pp. 295-304.

Stanton, R.L. (1989) The precursor principle and the possible significance of stratiform ores and related chemical sediments in the elucidation of processes of regional metamorphic mineral formation. Phil. Trans. R. Soc., London, Ser. A, 328, pp. 529-646.

Stroh, P.T., Monrad, J.R., Fullagar, P.D., Naqvi, S.M. and Rogers, J.J.W. (1983) 3,000 m.y. old Holekote trondhjemite, a record of stabilization of the Dharwar craton. In : S.M. Naqvi and J.J.W. Rogers (Eds.) Precambrian of South India. Geological Society of India, Memoir 4, pp. 365-376.

Suresh, R. (1982) Further evidence of biogenic nature of Dodguni microbiota, Dharwar craton, India. Jour. Geol. Soc. India, V. 23, pp. 567-574.

Swami Nath, J. and Ramakrishnan, M. (1981) (Eds.) Early Precambrian supracrustals of southern Karnataka, Mem. Geol. Surv. India, V. 112, 350pp.

Swami Nath, J., Ramakrishnan, M. and Viswanatha, M.N. (1976) Dharwar stratigraphic model and Karnataka craton evolution. Geol. Surv. of India Records, V. 107(2), pp. 149-175.

Taira, A., Pickering, K.T., Windley, B.F. and Soh, W. (1992) Accretion of Japanese island arcs and implications for the origin of Archean greenstone belts. Tectonics, V. 11, pp. 1224-1244.

Taylor, S.R. and McLennan, S.M. (1985) The Continental Crust : Its Composition And Evolution. Geoscience Texts, Blackwell, Oxford, 307pp.

Taylor, P.N., Moorbath, S., Chadwick, B., Ramakrishnan, M. and Viswanatha, M.N. (1984) Petrography, chemistry and isotopic ages of Peninsular gneiss, Dharwar acid volcanic rocks and the Chitradurga granite with special reference to the Late Archaean evolution of the Karnataka craton, South India, Precamb. Res., V. 23, pp. 349-375.

Taylor, P.N., Chadwick, B., Friend, C.R.L., Ramakrishnan, M., Moorbath, S. and Viswanatha, M.N. (1988) New age data on the geological evolution of southern India. In : L.D. Ashwal (Ed.), Workshop on the Deep Continental Crust of South India, Lunar Planet. Inst. Tech. Rept., V. 88-06, pp. 181-183.

Towe, K.M. (1978) Early Precambrian Oxygen : a case against photosynthesis. Nature, V. 274, pp. 657-661.

Towe, K.M. (1983) Precambrian atmospheric oxygen and banded iron formations : A delayed ocean model. Precamb. Res., V. 20, pp. 161-170.

Towe, K.M. (1988) Environmental implications of Banded Iron-formations. An abstract printed from : The Proterozoic Biosphere: A multidisciplinary study. pp. 54-55.

Towe, K.M. (1990) Aerobic respiration in the Archaean ? Nature, V. 348, pp. 54-56.

Trendall, A.F. (1968) Three great basins of Precambrian banded iron formation deposition : a systematic comparison. Geol. Soc. Amer. Bull., V. 79, pp. 1527-1544.

Trendall, A.F. (1973) Iron-Formations of the Hamersley Group of Western Australia : type examples of varved Precambrian evaporites. In: Genesis of Precambrian Iron and Manganese Deposits, UNESCO, Paris, Earth Sciences, No. 9, pp. 257-268.

Trendall, A.F. (1983) The Hamersley basin. In : A.F. Trendall and R.C. Morris (Eds.), Iron Formation: Facts and Problems, Elsevier, Amsterdam, pp. 69-129.

Trendall, A.F. and Blockley, J.G. (1970) The iron formations of the Precambrian Hamersley Group, Western Australia, with special reference to the associated crocidolite. West. Aust., Geol. Surv., Bull. 119.

Trendall, A.F. and Pepper, R.S. (1977) Chemical composition of the Brockman Iron Formation. Geol. Surv. West. Aust., Rec. No. 1976/25

Trendall, A.F. and Morris, R.C. (1983) (Eds). Iron-Formation : Facts and Problems, Elsevier, Amsterdam, 558 pp.

Turcotte, D.L. (1980) On the thermal evolution of the earth. Earth Planet. Sci. Lett., V. 48, pp. 53-58.

Udas, G.R., Narayana, B.L., Das, D.R. and Sharma, C.V. (1979) Carbonatites of India in relation to structural setting. Geol. Surv. India. Misc. Publ., 35, pt. 2, pp. 77-94.

Uday Raj, B. (1991) Geology and geochemistry of the Melukote belt, Mandya District, Karnataka. Unpub. Ph.D. thesis, Osmania University, 261pp.

Vasudev, V.N. and Naganna, C. (1973) Mineragraphy of gold-quartz-sulphide reefs of Hutti gold mines of Raichur district, Mysore State. Jour. Geol. Soc. India, v. 14, pp. 378-383.

Vasudev, V.N., Naqvi, S.M., Shukla, M. and Uday Raj, B. (1989) Stromatolites from the chert-dolomite of Archaean Shimoga schist belt, Dharwar Craton, India. Jour. Geol. Soc. India, V. 33, pp. 201-205.

Veizer, J., Compston, W., Hoefs, J. and Nielsen, H. (1982) Mantle buffering of the early oceans. Naturwissenchaften, V. 69, pp. 173-180.

Venkatachala, B.S., Naqvi, S.M., Chadha, M.S. and 13 others (1989) Paleobiology and geochemistry of the Precambrian stromatolites and associated sedimentary rocks from the Dharwar craton : constraints on Archaean biogenic processes. Himalayan Geology, V. 13, pp. 1-20.

Venkatachala, B.S., Shukla, M., Sharma, M., Naqvi, S.M., Srinivasan, R. and Uday Raj, B. (1990) Archaean microbiota from the Donimalai Formation, Dharwar Supergroup, India. Precamb. Res., V. 47, pp. 27-34.

Venkata Dasu, S.P., Ramakrishnan, M. and Mahabaleswar, B. (1991) Sargur-Dharwar relationship around the komatiite-rich Jayachamarajapura greenstone belt in Karnataka. Jour. Geol. Soc. India, V. 38, pp. 577-592.

Venkatasubramanian, V.S. and Narayanaswamy, R. (1974) Studies in the Rb-Sr geochronology and trace element geochemistry in granitoids of Mysore craton, India. Jour. Ind. Inst. Sci. (Bangalore), V. 56, pp. 19-42.

Venkatasubramanian, V.S., Iyer, S.S. and Pal, S. (1971) Studies on the Rb-Sr geochronology of the Precambrian formations of Mysore State. Am. Jour. Sci., V. 270, pp. 43-53.

Verma, R.K. and Subramanyam, C. (1984) Gravity anomalies and the Indian lithosphere : Review and analysis of existing gravity data. Tectonophysics, V. 105, pp. 141-161.

Viswanatha, M.N. and Ramakrishnan, M. (1975) The pre-Dharwar supracrustal rocks of Sargur schist complex in southern Karnataka and their tectonic-metamorphic significance. Indian Mineral., V. 16, pp. 48-65.

Viswanathiah, M.N. and Sathyanarayan, S. (1968) Banded ferruginous quartzites near Bagalkot and Amingarh, Bijapur district, Mysore State. Indian Min., V. 9, pp. 68-75.

Walker, J.C.G. (1987) Was the Archaean biosphere upside down? Nature, V. 329, pp. 710-712.

Walker, J.C.G., Klein, C., Schidlowski, M., Schopf, J.W., Stevenson, D.J. and Walter, M.R. (1983) Environmental evolution of the Archaean-Early Proterozoic Earth. In : J.W. Schopf (Ed.), Earth's Earliest Biosphere : Its Origin and Evolution, Princeton Univ. Press, Princeton, N.J., pp. 260-290.

Walsh, M.M. (1992) Microfossils and possible microfossils from the Early Archaean Onverwacht Group, Barberton Mountain Land, South Africa. Precamb. Res., V. 54, pp. 271-293.

Walter, M.R. and Hofmann, H.J. (1983) The Palaentology and Palaeoecology of Precambrian Iron-Formations. In : A.F. Trendall and R.C. Morris (Eds.) Iron Formation : Facts and Problems. Elsevier, Amsterdam, pp. 373-400.

West, W.S. (1980) Formation of continental crust. In : D.W. Strangway (Ed.), The Continental Crust and its Mineral Deposits, Geol. Assoc. of Canada, Sp. paper, V. 20, pp. 117-148.

Widdel, F., Schnell, S., Heising, S., Ehrenreich, A., Assmus, B. and Schink, B. (1993) Ferrous iron oxidation by anoxygenic phototrophic bacteria. Nature, V. 362, pp. 834-836.

Wilson, J.T. (1968) Static or mobile Earth : The current scientific revolution. In : Gondwanaland revisited. American Philosophical Society Proceedings, V. 112, pp. 309-320.

Wilson, J.T. (1989) Continental drift and a theory of convection. Terra Review, pp. 519-539.

Winkler, H.G.F. (1976) Petrogenesis of metamorphic rocks. IV Ed. Springer International.

Yapp, C.J. (1990) Oxygen isotopes in iron (III) oxides 2. Possible constraints on the depositional environment of a Precambrian quartz-hematite banded iron formation. Chem. Geol., V. 85, pp. 337-344.

GEOLOGY, GEOCHEMISTRY AND PALAEOENVIRONMENT OF DEPOSITION OF BANDED IRON FORMATION OF THE KUSHTAGI SCHIST BELT, KARNATAKA NUCLEUS, INDIA

ABSTRACT OF THE
Thesis Submitted in Partial Fulfilment of the Requirement
For the Award of the Degree of
Doctor of Philosophy
IN GEOLOGY

BY
RIYAZ MD. KAMARUDDIN KHAN

FACULTY OF SCIENCE
DEPARTMENT OF GEOLOGY
ALIGARH MUSLIM UNIVERSITY
ALIGARH

1993

ABSTRACT

Banded Iron Formations (BIFs) are the most important and significant rock suites of Precambrian terrains and are mainly confined to the early and middle Precambrian era. Their origin, confinement in time and space and environment of deposition are not clearly understood as yet. In these rocks, enormous amount of FeO and SiO_2 have been chemically precipitated in the form of rhythmic layers of varying dimensions within 600 million years of early history of the Earth. The source of FeO and SiO_2 as well as in these iron formations is debated. The nature of the process(es) by which these Fe-rhythmites have developed is still speculated. A relation between the BIF and the biogeochemical processes has been proposed by several workers during last few years. Change from anoxic to an oxygenated atmosphere is reflected by the distribution of BIFs and red beds.

In India, occurrence of BIF is confined to the late Archaean greenstone belts (2.9-2.6 Ga) whereas Proterozoic sedimentary basins/mobile belts are completely devoid of these interesting and enigmatic rock types. In the Dharwar Craton (DC) of India, BIFs are found in three associations namely (1) with quartzites-shales-volcanics (Bababudan, Kudremukh, Kushtagi belts), (2) with quartzites-carbonatic stromatolites-Mn-formations shales-volcanics (Sandur, Chitradurga, Shimoga belts) and (3) with greywackes-acid-intermediate volcanics, a deep water facies (Chitradurga, Sandur, Shimoga belts). The genesis, depositional environment and tectonic setting of these BIFs of

different rock assemblages is not understood. Keeping these aspects and other exciting but unresolved questions regarding the origin of BIF in view, a detailed geochemical study of the BIF of Kushtagi schist belt was taken up. Kushtagi schist belt is located in the northern part of the KN. This belt has been referrred as Hungund schist belt in goelogical literature. The field investigation of the belt suggests that this belt is a remnant of some Archaean orogenic belt. Part of the original belt is present as an enclave within gneisses and has been intruded by granites. The BIFs present in the belt directly overlie the metavolcanics. It is bounded on either side by the Closepet Granite and on SE part of eastern flank by Peninsular Gneiss Complex. The northwestern tip of the belt is covered by the sediments of Kaladgi Group. The oxide facies BIF present in the NW tip of the belt, once blanketed by the Kaladgi, now stands exposed after the erosion and subsequent removal of the cover of Kaladgi sediments. The BIFs are associated with basic and acidic metavolcanics; in the mining area, they are absolutely fresh. Therefore this belt was chosen as it is one of the least metamorphosed belts of DC where the original mineralogy of the BIFs is presumed to be better preserved. The main objective of this work is to understand the genesis of the BIF of Kushtagi schist belt and its bearing on the Archaean depositional environment and tectonic processes. With these objectives, detailed geological and geochemical studies on the BIF and associated volcanic rocks have been carried out and the results of these studies are presented in this thesis.

Based on their Al_2O_3 content the Banded Iron Formation of Kushtagi schist belt are classified into two type namely Cherty Banded Iron Formation (CBIF) and Shaly Banded Iron Formation (SBIF). They are found in association with shallow shelf and platformal chloritic shale-carbonate-volcanic rock assemblages. They are mostly of oxide facies. At several places, oxide facies BIF bands are hosted in pillowed and spherulitic volcanic rocks of basaltic composition. In these oxide facies BIF, interbedded SBIF and shales of thickness varying from a few cm to a few meters are present. The strata have been folded and deformed by atleast three phases of deformation. Isoclinal, recumbent and tight of first as well as second generation are commonly well exhibited by these BIFs.

About 200 samples of the cherty and shaly BIFs and the associated volcanic rocks were collected from working mines. Special care was taken to collect relatively unweathered samples from freshly blasted surfaces of the mines. Thin section and ore microscopic studies were carried out for characterizing various mineral phases present. Composition of the minerals was determined with the help of an Electron Probe Micro Analyser. Major, trace and rare earth element analysis for about 42 elements in each sample, was carried out with the help of XRF and ICP-MS using international standard reference materials. Oxygen isotopic estimation by using the VG Mass Spectrometer were carried out on the hematite-chert pairs.

Mineralogy of these BIFs is simple as they are metamorphosed to lower grade of greenschist facies only. Many layers of BIF have just undergone diagenesis. The interbeddded clays have not been recrystallized and the detrital micas are preserved. The interbedded SBIF in addition to hematite and chert contains kaolinite and muscovite. Shales also exhibit similar mineralogy.

The oxide facies cherty and shaly BIFs show large scale compositional variations as reflected by their major and trace elemental abundance. Oxide facies BIF samples exhibit a large scatter in the Fe_2O_3-SiO_2 molar ratio, which is mainly dependent on the relative thickness of the hematite rich bands in the samples analysed. Primarily, the pure oxide facies BIFs which are constituted by Fe_2O_3 and SiO_2, exhibit a distinct linear antipathetic relationship between the two components. They are extremely depleted in Al_2O_3, TiO_2, Zr, Hf and other trace elements like Cr, Ni, Co, Rb, Sr, V, Y and REE. MnO content of these rocks is generally less than 0.01% indicating that effective Fe-Mn fractionation had taken place in this zone as the Eh values had not reached such a level where Mn could be precipitated while the oxide facies BIFs were deposited. Extremely depleted ΣREE, positive Eu anomalies and HREE enrichment are distinctive and essential features of these pure oxide facies BIF. Negative Ce anomalies are seen in a few samples of SBIF which indicate the oxidation of Ce^{+3} to Ce^{+4} and hence its separation from the system. Depletion in REE in proportion to the abundance levels of Co, Cu and Ni and the observed Eu anomaly strongly indicates that the source of FeO, and SiO_2 for these BIFs was the hydrothermal solutions released at the AMOR vent sites. FeO and Ce present in these solutions were oxidized by photsynthetically generated O_2 produced by the blue-green algae present at the shallow shelf regions. This O_2, through ocean circulation, was dissolved in the ocean waters and reached below the wave base and photic zone, where due to a thermocline and chemocline effect, FeO was transported, and reacted with this O_2 to produce the Fe-rhythmites. The aftband and mesobands of Fe-rich layers were produced due to the intermittent (seasonal) availability of either oxygen and/or FeO.

The $\delta^{18}O$ values of coexisting silica and hematite in the CBIF of Kushtagi schist belt give a temperature range between 71.4^0 and 165.2^0C. It indicates that samples have undergone diagenetic alteration and metamorphism of lower greenschist facies which is corroborated by field observation as well as petrographic study.

SBIF interbedded with the CBIF show entirely different geochemical characters as a result of modification by detrital processes. Both terrigenous and volcaniclastic processes have exerted control on the composition of the SBIF, in addition to chemical precipitation. SBIF have been deposited as a result of change in the physico-chemical conditions of the watermass at two different times, namely the time of deposition of oxide facies CBIF and the time of deposition of SBIF. Large variation is observed in most of the elements, all trace elements (including REE) are relatively high in these rock types. The magnitude of Eu anomalies show variation. The signatures of hydrothermal processes are modified by those of the clastic processes.

The volcanic rocks of the Kushtagi schist belt are of basaltic and rhyodacitic types. Basalts can be subdivided into high and low MgO types. High MgO basalts show geochemical characters resembling to those of MORB. The dacitic rocks are characterized by geochemical parameters of the island arc volcanics. REE patterns of these two types are distinct from each other. High Mg basalts are depleted in REE with almost flat patterns. Dacites show differentiated patterns with slight negative Eu anomalies in some samples. It is proposed that the partial melting of the MORB has given rise to the rhyodacitic rocks. The melting is suggested to have taken place when the tensional regime was converted to compressional regime.

REE and other geochemical characteristics of the BIF indicate that FeO and SiO_2 of the BIFs were added to ambient Archaean ocean at the AMOR. The Nd isotopic data from elsewhere has demonstrated that the main source of FeO of BIF is the hydrothermal and fumarolic activity at the vent sites on the MORB. Therefore existance of a MOR is evidenced by the REE patterns of the BIFs and Eu anomalies. This inference is further substantiated by interlayering of BIFs with the high Mg basalt which have geochemical parameters resembling with that of MORB. Subsquent deposition of sediments and volcanism related with the active plate margins and deformational patterns of greenstone belts indicate that the closure of the basins of greenstone belts as a whole and Kushtagi schist belt in particular is a subduction related phenomenon. The basin was probably initiated by opening of a rift. Spreading along a newly formed ocean along this rift-AMOR widened the basin. Hydrothermal solutions at this AMOR enriched the ocean water in FeO and SiO_2 moved towards the trailing edge due to thermal and chemical differences. The encounter of these solutions with oxygen, produced by photosynthesis, caused precipitation of oxides and hydroxides of iron below wave base and photic zone. FeO was precipitated to the extent of the availability of O_2. Rest of it remained within the ocean reservoir. When again oxygen become available it was precipitated and layered with the rhyodacitic subduction related volcanic and sedimentary rocks.

Thus the studies presented in previous pages help to identify two stages of the tectonic setting through which the BIFs and greenstone belts were formed. First stage was an opening and spreading of ocean, where extensive volcanism and hydrothermal fumarolic activity added large amount of FeO and SiO_2 to the ocean waters. The exit temperature of these hydrothermal water was probably very high so that higher quantity of FeO was dissolved. To explain the enormous quantity of Fe present in BIFs it is essential to assume that hydrothermal flux itself was very high at that time. Therefore large quantity of hydrothermal waters with higher amount of dissolved FeO was added to the Archaean oceans. To dissipate the higher heat flow of Archaean era a larger ridge length, faster creation and destruction of oceanic lithosphere is essential. Thus the combination of higher hydrothermal flux, its high exit temperature, larger ridge length and faster completion of Wilson Cycle explain not only the source of the constituents of BIF but also the tectonic setting and lithological assemblages of greenstone belts. The second stage was due to change in the direction of convection current. This resulted in the conversion of the basin from a spreading basin to a converging margin. At this time the turbidites and rhyodacites were formed.

The supply of the O_2 for the precipitation of ferrous iron to ferric state is not directly demonstrated by the field occurrence of stromatolite or the microbiota, as has been shown in case of Chitradurga and Sandur belts. However, there are significant bands of carbonate present in the viscinity of BIF which may contain stromatolites as some of them appear to be stratifera type but convincing forms and morphologies have not been discovered as yet. This process of biogenic supply of O_2 is very much evidenced in the other greenstone belts of the DC and since Kushtagi schist belt is only a truncated arm of the original belt, it can be safely assumed that similar biogenic process might have supplied O_2 for the BIF precipitation in the Kushtagi schist belt also. The banding of BIF is also related with the availability of O_2. Seasonal variations in the rainfall and the suply of the clastic debris to the ocean margin where biogenic activity was taking place has affected the growth of bacteria and production of O_2. During high rainfall, larger quantity of clastic debris was brought to the margin which burried the algae and hence the organism and oxygen productivity was reduced. During this period, only silica precipitation continued and very little ferric-hydroxide was deposited. When rain fall reduced, the bacteria/algae emerged above the sedimentary layer, received more sunlight and produced more O_2 which reacted with FeO and hence iron rich layers were deposited. The production of O_2 at the shallow shelf has created a partially layered ocean water mass. At depth and away from the margin the ocean water had higher amount of dissolved CO_2. Primary precipitation and/or diagenetic reaction between Fe_2O_3 and organic matter (degradation of organic carbon) resulted in the formation of interstitial siderite. It is proposed that formation of BIF is not a simple chemical process. Instead it is a result of combination of (1) hydrothermal activity, (2) terrigenous and volcaniclastic sedimentation (3) biogeochemical processes, (4) chemical precipitation and diagenetic reactions and (5) the physico-chemical conditions prevailing at the vent sites and depositional shelf. Mini plate model and faster completion of Wilson Cycle with shorter distance between the constructive and destructive margins, and the conversion of constructive margins to the destructive one are able to explain most of the above mentioned processes and the observations. The studies on the BIF and volcanic rocks of the Kushtagi schist belt lead to the following conclusions :

* Iron, silica and the REE of the BIF were mainly provided by the hydrothermal solutions emplaced at the vent sites of the Archaean Mid Oceanic Ridges (AMOR). These hydrothermal solutions enriched in iron and silica were subsequently mixed with the ambient sea water. It is proposed that the hydrothermal flux of higher exit temperature was quite significantly elevated during Archaean. This higher quantity of hydrothermal flux was able to bring large quantity of dissolved FeO and SiO_2 to the ocean water.

* Due to thermal and chemical potential differences and upwelling, this FeO and SiO_2 enriched ocean water was transported to the site of deposition in the shallow shelf region where it reacted with O_2 resulting in the precipitation of iron oxide and hydroxide. Oxygen was most probably generated photosynthetically.
* On burial these oxides and hydroxides reacted with organic carbon of the bacteria and most probably the Fe-carbonates were produced by this diagenetic reaction. It is also possible that some of the Fe-carbonates were directly precipitated by reaction with atmospheric CO_2 dissolved in the ocean water.
* Oxide facies BIFs were deposited below the wave base and photic zone at the shallow shelf regions of low organic productivity.
* During the deposition of BIF, terrigenous and volcaniclastic sedimentation also took place resulting in compositional variation in cherts, CBIF to SBIF and the shales. Deposition of the BIF of oxide facies is dependent on the supply of O_2, CO_2 and C to various parts of the basin and on the compositional layering of the ocean with respect to the dissolved quantity of O_2 and CO_2.
* Petrological and geochemical data suggest that the BIF sequence in the Kushtagi schist belt is formed by an interaction of hydrothermal, biogenic-photosynthetic and sedimentary processes in a compositionally layered ocean.

* The banding of BIF is probably a result of seasonal changes in the availability of O_2 and/or FeO.
* A Mini plate model with shorter duration of the completion of Wilson Cycle, large ridge length, higher rate of generation and consumption of oceanic lithosphere is able to explain most of the observed facts of BIF and the greenstone belts.
* Late Archaean greenstone belts were initiated as a MOR related basins and were closed as subduction related active margins.